THÈSE POUR OBTENIR LE GRADE DE DOCTEUR DE L'UNIVERSITÉ DE MONTPELLIER

Écologie Fonctionnelle et Sciences Agronomiques

École doctorale : GAIA

Unité de recherche : CIRAD-PHIM , PRISM-FORISK
in collaboration with
Rockwinds LBMS

IMPORTANCE DES COMPOSANTES DE LA SÉCHERESSE SUR LA PRODUCTIVITÉ DE THEOBROMA CACAO ET MOYENS D'AMÉLIORER LA CAPACITÉ DE PRÉVISION SAISONNIÈRE DE L'INDUSTRIE.

Présentée par Pietro DELLA SALA
Le 13 Décembre 2021

Sous la direction de Christian CILAS,
Fabienne RIBEYRE et Alina GAINUSA - BOGDAN

Devant le jury composé de

Evelyne COSTE, Directrice de recherche, INRAE UMR AGAP, Montpellier, France	PRESIDENT DU JURY
Nicolas MARRON, Chargé de recherche, INRAE, UMR 1434 SILVA, Nancy, France	RAPPORTEUR
Michel GENARD Directeur de recherche, INRAE, UMR PSH, Avignon, France	RAPPORTEUR
Fiona LAHIVE, Chargé de recherche, University of Reading,Reading, Angleterre	EXAMINATRICE
Frédéric DO, Chargé de recherche, IRD, UMR ECO&SOLS, Montpellier, France	EXAMINATEUR
Claire DAMESIN, Professeure, Université de Paris Saclay, UMR 8079, Paris, France	EXAMINATRICE
Christian CILAS, Directeur de recherche, CIRAD, DGDRS, Abidjan, Côte d'Ivoire	DIRECTEUR DE THESE

UNIVERSITÉ DE MONTPELLIER

Résumé général du manuscrit en français

Cette thèse répond au besoin de recherche appliquée de l'industrie mondiale du cacao pour mieux comprendre et prévoir les changements saisonniers de la productivité en Afrique de l'Ouest. Pour répondre à cette nécessité, il était crucial de faire progresser l'état de l'art sur la physiologie du cacao dans les conditions climatiques de l'Afrique de l'Ouest. En prenant comme référence un modèle mécaniste de cacao existant (CASE 2), le projet a abordé toutes les questions pratiques pour concevoir un modèle dédié mieux adapté à l'environnement de culture ouest-africain, qui présente plus de défis pour les cacaoyers par rapport à leur zone d'origine. Pour comprendre et modéliser correctement la production ouest-africaine, ce projet a principalement étudié l'importance du stress dû à la sécheresse chez le cacaoyer. Il s'est plus particulièrement intéressé à la sécheresse atmosphérique qui est propre à la longue saison sèche de l'Harmattan, lorsque les précipitations sont absentes, que les températures augmentent et que l'humidité relative de l'air diminue.
Le cacaoyer (Theobroma cacao, L.) est un arbuste de sous-bois appartenant à la famille des Malvaceae, surtout connu pour ses fèves, dont on fait le chocolat, et dont on extrait le beurre de cacao, une graisse végétale utilisée dans l'industrie pharmaceutique et cosmétique. Comme la plupart des espèces du genre Theobroma, le cacao a ses origines botaniques dans la forêt tropicale de l'Amérique tropicale, le lieu d'origine le plus important est le bassin supérieur de l'Amazone. Trois sous-familles de cultivars de cacao sont documentées comme ayant évolué dans le monde, toutes issues de la grande diversité morphologique observée en Amérique centrale et du Sud : Criollo, Forestero et Trinitario, un croisement des deux premières sous-familles. Bien qu'il soit connu de l'homme depuis l'époque maya, sa domestication pour une culture extensive est assez récente, de sorte que le processus de sélection de variétés améliorées est encore un domaine en développement et le matériel génétique actuellement planté dans les champs n'est pas si éloigné du type sauvage.
Le cacaoyer pousse à une latitude de 20° de l'équateur mais il ne prospère réellement que dans des conditions climatiques extrêmement stables à moins de 10° de l'équateur où la gamme de température est stable tout au long de l'année, l'humidité relative de l'air élevée et les pluies abondantes. Plus précisément, le cacao a besoin de précipitations annuelles supérieures à 1250 mm mais ne dépassant pas 3000 mm, idéalement entre 1500 et 2000 mm, ne descendant pas en dessous de 100 mm/mois pendant plus de trois mois consécutifs au cours d'une année de production, et d'une humidité de l'air supérieure à 70% et d'une température moyenne d'environ 25°C avec des minima supérieurs à 15°C et une faible différence de température jour-nuit. Depuis son foyer d'origine, le cacaoyer a été introduit par l'homme d'abord, au 19^{eme} siècle, sur le continent africain et ensuite en Asie. Ainsi, le cacaoyer est aujourd'hui cultivé dans de nombreux pays de la ceinture intertropicale comprise entre $\pm 10°$N de l'équateur.
La demande du marché pour le cacao a presque triplé au cours des quarante dernières années et la production mondiale de cacao a doublé au cours des trente dernières années, principalement en raison de la croissance de l'importance de quatre pays d'Afrique de l'Ouest qui représentent environ trois quarts de la production mondiale : la Côte d'Ivoire, le Ghana, le Cameroun et le Nigeria. La dépendance mondiale en cacao d'Afrique de l'Ouest est encore plus importante que ces chiffres ne le suggèrent. En fait, il a été estimé que les importations mondiales cumulées de fèves de cacao en provenance d'Afrique de l'Ouest dépassent largement les 80%. Plus important encore, dans des pays comme la Côte d'Ivoire et le Ghana, l'importance du cacao est telle que les exportations sont fortement réglementées par le gouvernement, car elles représentent un élément majeur et omniprésent du produit intérieur brut de ces pays et peuvent représenter jusqu'à 70-100% du revenu des ménages de près de deux millions de petits exploitants agricoles de la région.

Malgré la grande importance de la culture du cacao en Afrique de l'Ouest, le climat de pays comme la Côte d'Ivoire, le Ghana et le Nigeria présente des différences majeures avec celui de la zone d'origine du cacao. Les précipitations annuelles diffèrent du bassin amazonien et, souvent, ne correspondent pas aux exigences du cacao. Les précipitations varient entre 1100 et 2100 mm en moyenne selon les macro zones de production de cacao d'Afrique de l'Ouest. Une autre différence essentielle avec la zone d'origine du cacao est qu'en Côte d'Ivoire, au Ghana et au Nigeria, il y a chaque année deux saisons sèches, séparées par deux saisons humides avec des précipitations mensuelles supérieures à 100 mm/mois. La saison sèche principale, longue, a lieu entre la mi-novembre et la mi-mars, tandis que la deuxième saison sèche, plus courte (mineure), a lieu entre fin juillet et septembre. Les saisons des pluies et sèches sont liées au mouvement saisonnier du Front Intertropical (ITF) qui traverse l'Afrique de l'Ouest. Le ITF est l'endroit où la masse d'air saharienne sèche rencontre le flux d'air humide de la mousson provenant du Golfe de Guinée. Au nord du ITF, il n'y a pratiquement aucune possibilité de précipitations en raison de l'air extrêmement sec. Les pluies sont également inhibées dans certaines zones au sud de l'ITF. Pendant la longue saison sèche (mi-novembre à mi-mars), l'ITF induit un vent sec sur les régions cacaoyères, l'Harmattan. L'Harmattan est un alizé continental de nord-est qui souffle sur l'Afrique saharienne, centrale et occidentale. Il apporte des conditions extrêmement chaudes et sèches pendant la journée, plus fraîches la nuit et il est généralement poussiéreux. La présence de l'Harmattan annule non seulement les chances de précipitations, mais fait chuter rapidement l'humidité relative de l'air, réduisant ainsi la capacité thermique globale de l'atmosphère et entraînant de grandes oscillations quotidiennes de la température de l'air. Pendant la saison où les vents d'Harmattan investissent les régions cacaoyères, la température peut monter jusqu'à 44°C pendant la journée et descendre jusqu'à 12-14°C la nuit. Tant les valeurs absolues de ces températures extrêmes que leur large différentiel de température quotidien sont responsables de graves dysfonctionnements physiologiques chez le cacaoyer. En outre, la faible humidité relative de l'air est considérée comme un facteur de stress supplémentaire. En bref, chaque fois que les vents d'Harmattan atteignent une région cacaoyère, les plantes subissent à la fois un stress atmosphérique et un stress hydrique du sol. En plus de la sécheresse du sol causée par l'absence de précipitations pendant de longues périodes, le cacaoyer doit faire face à un déficit croissant de la pression de vapeur de l'atmosphère induit par les températures élevées et les faibles valeurs de l'humidité de l'air. La longue saison sèche devrait s'intensifier avec le changement climatique, il est donc crucial d'étudier comment le cacaoyer interagit avec l'environnement en cas de stress.

Sur le papier, le cacaoyer est très sensible à la sécheresse en raison de nombreux traits morphologiques. Il a de grandes feuilles larges avec peu de cire et une forte densité stomatique. Cela entraîne une forte transpiration et peu de contrôle sur la perte d'eau dans des conditions d'irradiation élevée, de déficit de pression de vapeur (VDP) élevé ou de vent. De plus, les vaisseaux du xylème dans la tige sont larges et peuvent pomper l'eau efficacement mais comportent un grand risque d'embolie ou de cavitation sous une pression trop forte, liée à l'atmosphère ou au sol. En outre, le système racinaire du cacaoyer est relativement peu profond, avec une forte densité de racines fines dans les 0.2 à 0.6 m supérieurs du sol et seulement quelques-unes dans les couches plus profondes, et il ne peut donc pas accéder à l'eau profonde.

D'un point de vue physiologique, le cacao présente donc une prédisposition à souffrir de la sécheresse, bien que des études supplémentaires soient nécessaires pour éclaircir complètement le sujet. Les feuilles de cacao ont un point de saturation relativement bas pour la photosynthèse (400 $\mu mol * s^{-1} * m^{-2}$), par conséquent, le système photosynthétique peut être facilement mis sous pression par un rayonnement excessif. Cette capacité limitée à faire face à une irradiation élevée peut exacerber les effets d'une limitation en eau qui conduit à une perturbation de la chaîne des électrons, en particulier dans le cadre de la culture sans

ombre ou à faible ombre, largement adoptée en Afrique de l'Ouest. Chaque fois que le cacao est contraint de réduire sa transpiration sous un niveau d'irradiation moyen ou élevé, la photorespiration sera aggravée par la faible capacité photosynthétique du cacao. Afin d'avoir une compréhension globale des mécanismes qui entourent le cacao sous la sécheresse, et potentiellement guider des études de terrain ciblées, un outil approprié est la modélisation de l'ensemble sol-plante-atmosphère. Actuellement, le seul modèle de physiologie du cacao existant est CASE 2, un modèle mécaniste physiologique développé pour comparer la capacité de production de différentes régions du monde, à la fois pour des scénarios idéaux et limités en eau. Ce modèle ne peut pas être utilisé dans sa version actuelle 4 pour étudier les effets de la sécheresse à une échelle de temps saisonnière ou sous-saisonnière en raison de l'objectif très général du modèle CASE 2 et de l'indisponibilité d'informations fiables pour paramétrer des mécanismes spécifiques au moment de son développement qui a conduit à plusieurs approximations, qui ne sont plus acceptables aux échelles de temps saisonnières et sous-saisonnières. L'objectif principal du projet était donc de concevoir un modèle mécaniste pour la croissance et la production du cacao à l'échelle de temps sous-saisonnière afin d'étudier les effets des conditions atmosphériques et de stress du sol sur la productivité du cacao dans les conditions actuelles et futures de l'Harmattan en Afrique de l'Ouest.
Afin d'atteindre l'objectif de concevoir un nouveau modèle conceptuel pour le cacao dans les conditions de culture en Afrique de l'Ouest, les effets du stress hydrique atmosphérique et du sol sur la transpiration du cacaoyer pendant la saison sèche de l'Harmattan ont été étudiés pendant la longue saison sèche 2019/2020, avec et sans irrigation. L'étude a été menée à la station expérimentale de l'Institut de recherche sur le cacao du Ghana (CRIG) située à New Tafo Akyem, dans la région de l'Est, au Ghana. Deux parcelles de cacaoyers, avec et sans irrigation, ont été suivies pendant toute la durée de l'expérience (3^{me} décembre 2019 au 16^{me} mars 2020) et leur réponse au climat suivie. Les variables environnementales mesurées étaient : la teneur en eau volumétrique du sol à quatre profondeurs de 10 à 60 cm, la température de l'air, l'humidité relative de l'air et le rayonnement photosynthétiquement actif. De plus, pendant toute la durée de l'expérience, la transpiration des arbres a été estimée à partir des mesures de la vitesse de sève en utilisant l'approche de la méthode double, qui combine la méthode de la ration thermique et la méthode Tmax. Enfin, l'état de la canopée des deux parcelles a été suivi en calculant chaque jour le LAI moyen.
Le climat mesuré de la saison sèche 2019-2020 était représentatif des conditions rencontrées par le cacaoyer à cette période de l'année dans la région orientale du Ghana. Alors que l'humidité du sol s'approchait du point de flétrissement permanent dans la parcelle témoin, l'humidité de l'air a chuté en dessous de 20% et les températures quotidiennes étaient sous-optimales. En réponse à ce stress, la parcelle témoin (non irriguée) a perdu les deux tiers de son feuillage, soit deux fois plus que la parcelle irriguée. En outre, on a constaté que la transpiration du cacao répondait fortement à un VDP élevé pendant la longue saison sèche de l'Harmattan, ce qui peut fragiliser encore davantage l'arbre en épuisant plus rapidement les réservoirs d'eau du sol et en aggravant finalement le stress lié au sol. L'étude a montré que même sous irrigation constante, les cacaoyers étaient stressés par les conditions atmosphériques difficiles de l'Harmattan. Un ensemble de deux modèles BRT (Boosted Regression Trees) créés pour expliquer la transpiration du cacao a montré que l'impact de la sécheresse atmosphérique sur la canopée et la transpiration de l'arbre est d'une importance comparable à la sécheresse du sol, plus étudiée. La sécheresse du sol a un rôle prédominant à l'échelle de la saison tandis que la sécheresse atmosphérique est responsable de pics de stress aigus sur un ou quelques jours mais avec des effets potentiellement durables, par exemple sur la fructification et la saisonnalité de la production.
Pour étudier les effets sur la production saisonnière des conditions environnementales subies par le cacao, nous avons défini cinq indicateurs de stress et utilisé une classification hiérarchique pour définir quatre types de climat sur la saison de production 2019/2020. Les quatre

types de climat ont ensuite été utilisés pour définir sept saisons ultérieures. Les sept saisons comprenaient deux saisons sèches majeures (1_Main_Dry et 7_Main_Dry), deux saisons sèches mineures (4_Minor_Dry et 6_Minor_Dry) précédées d'autant de saisons humides (3_Humid et 5_Humid) et une saison intermédiaire entre la très stressante 1_Main_Dry et la 3_Humid (2_Transition). Les effets des conditions environnementales (saisons et irrigation) sur la dynamique des différents stades phénologiques (fleurs, nouaisons, cabosses, cabosses mûres, jeunes fruits flétries) ont été étudiés au moyen d'un modèle linéaire généralisé mixte avec une distribution binomiale négative (GLMM.NB) en raison de la surdispersion des distributions. Tous les modèles ont été construits en intégrant l'interaction entre la saison et le traitement (irrigué ou témoin) comme effet fixe et l'arbre comme effet aléatoire.
Cette étude présentée au Chapitre 3 a révélé que, sous le climat ouest-africain, les fortes contraintes atmosphériques et pédologiques subies lorsque les vents d'Harmattan soufflent sur l'Afrique de l'Ouest ont tendance à concentrer la production pendant la période sans contrainte, indépendamment de l'irrigation. Comme les arbres ont concentré leur production au cours de la première période humide, il est possible que leurs puits totaux aient saturé la production totale d'assimilats (source), empêchant une fructification supplémentaire plus tard dans la saison, malgré les conditions favorables. L'irrigation n'évite pas le stress lorsque la saison de l'Harmattan est très sèche, mais elle aide les arbres à répartir plus uniformément la fructification, ce qui rend la production globale plus résiliente aux événements extrêmes. De plus, l'irrigation n'a pas influencé de manière significative le taux de flétrissement des chérelles (jeunes fruits) par rapport au contrôle, contrairement à ce qui était attendu.
Parallèlement aux progrès réalisés dans la compréhension des effets sur la phénologie de l'occurrence saisonnière des sécheresses en Afrique de l'Ouest, le projet s'est penché sur le fonctionnement du flétrissement des chérelles (wilt), un mécanisme d'auto-éclaircissement important chez le cacaoyer qui était absent du modèle de référence (CASE 2) et devait être inclus dans le modèle pour viser des applications pratiques dans le monde industriel. Les analyses se sont appuyées sur deux expériences de terrain pour étudier le moment et les mécanismes physiologiques du flétrissement des chérelles, avec une attention particulière sur la compétition pour les ressources entre les fruits. La première expérimentation, étudiant le timing du flétrissement de la chérelle, a été réalisée à la station expérimentale du CIRAD de Combi (5°20'N-52°55'W), en Guyane française. Sur trois années (2016-2018), 441 cabosses issues de dix clones différents ont été pollinisées manuellement et suivies toutes les semaines. Leur taille a été modélisée en fonction de leur devenir (flétrissement ou non) et de leur âge à partir du jour de pollinisation. Les analyses ont mis en évidence un pic principal de flétrissement des chérelles entre la troisième et la cinquième semaine après la pollinisation. Ce pic principal a été suivi pour certains clones par un ou plusieurs pics considérablement plus faibles, commençant neuf semaines après la pollinisation. Cette étude a également confirmé que le risque de flétrissement d'une chérelle est limité par son âge. Même si l'on a constaté que les chérelles pouvaient flétrir jusqu'à 15 semaines après la pollinisation, le risque a sensiblement diminué après les sept premières semaines de croissance. De plus, en utilisant une nouvelle approche, il a été découvert que le processus de flétrissement est visible trois semaines avant l'apparition des symptômes sur le fruit. Pendant ces trois semaines, le taux de croissance relatif a chuté de façon quasi linéaire. Cette étude a également confirmé que, dans la plupart des cas, le flétrissement concernait des chérelles qui avaient déjà connu une croissance lente par rapport à d'autres chérelles d'âge similaire. La deuxième expérience de terrain a eu lieu à la ferme expérimentale La Lola du CATIE (Centro Agronómico Tropical de Investigación y Enseñanza) dans la forêt tropicale humide du Costa Rica (10°06'N 83°23'W, 40 m asl). Pour l'expérience, 91 arbres matures de trois clones de cacaoyers ($CATIER4$, $CC137$, $Pound7$) ont été suivis. Entre le 29 mai 2012 (la première génération) et le 12 de juin 2013 (la 55^{eme} génération), toutes les nouvelles cabosses émergentes de moins de 10 cm ont été suivies dans le temps jusqu'au moment où elles ont été enlevées soit à cause de la récolte, soit à cause

du flétrissement ou d'autres causes (i.e. maladies). Au total, l'étude a porté sur 8796 cabosses dont la position sur l'arbre (branches ou tronc principal) a été notée. Chaque semaine, l'état des fruits marqués a été enregistré en utilisant cinq catégories : (1) saine, (2) attaquée par la moniliose, (3) flétrie, (4) récoltée et (5) "autre", une catégorie comprenant toutes les possibilités restantes (endommagés par des rongeurs, dommages mécaniques, pourriture brune, etc.). Un modèle basé sur les arbres de régression (BRT) a permis d'étudier la probabilité de flétrissement en fonction avec notamment de l'âge de la chérelle, de sa position sur l'arbre, de la charge en fruits de l'arbre dans les semaines précédant le flétrissement. Ces analyses ont quantifié l'importance de la compétition intra et intergénérationnelle pour les ressources. La compétition intergénérationnelle pour les assimilats s'est avéré être un prédicteur clé du flétrissement, principalement imputable aux cabosses âgées de 10 à 16 semaines. Ces fruits sont les concurrents les plus importants car ils sont dans la phase linéaire de croissance et leur taux de croissance relatif est maximisé. On a constaté que la compétition intragénérationnelle favorisait le flétrissement pour les cohortes de fruits qui étaient très abondantes. Enfin, contrairement à ce qui était attendu, la position du fruit sur l'arbre n'a eu qu'une importance négligeable. Cette question nécessite donc plus d'investigations pour être pleinement clarifiée. La conclusion de l'ensemble du projet a été la conceptualisation d'un modèle de physiologie du cacao qui a le potentiel de capturer une grande partie de la complexité du système de production du cacao en Afrique de l'Ouest. La modélisation proposée s'appuie les nouvelles connaissances sur l'influence de la sécheresse (atmosphérique et du sol) sur 1) la physiologie du cacaoyer (Chapitre 2), 2) le rôle des types de climat dans le façonnement de l'évolution saisonnière de la production (Chapitre 3) et 3) le flétrissement (Chapitre 4). En s'appuyant sur l'expérience de modèles précédents plus généralistes dans la littérature (par exemple, GECROS), le chapitre 5 résume les connaissances actuelles en matière de modélisation des processus physiologiques tels que la photosynthèse, l'utilisation de l'eau et la transpiration, tout en les combinant avec les résultats des analyses discutées. Le modèle conceptuel proposé (Chapitre 5) est adapté pour prendre en compte tous les processus pertinents à une échelle de temps sous-saisonnière. Par rapport au précédent "modèle de référence" de la physiologie du cacao, CASE2, cette étude a proposé des solutions innovantes pour : (1) inclure l'effet direct du stress atmosphérique sur l'utilisation de l'eau par la plante, (2) augmenter la plasticité de la plante modélisée dans son adaptation à une situation de stress hydrique du sol, (3) augmenter le réalisme de la fructification et (4) du développement et de la croissance des fruits, et (5) inclure le mécanisme d'avortement des fruits connu sous le nom de " flétrissement des chérelles ".

UNIVERSITÉ DE MONTPELLIER

DOCTORAL THESIS

Importance of drought components on the productivity of Theobroma cacao and ways to improve the industry's seasonal forecasting capacity.

Author:
Pietro DELLA SALA

Supervisor:
Dr. Christian CILAS,
Dr. Fabienne RIBEYRE,
Dr. Alina GĂINUŞĂ-BOGDAN

A thesis submitted in fulfillment of the requirements
for the degree of Doctor of Philosophy
by the PhD school GAIA

in Functional Ecology and Agronomic Sciences

under the joint coordination of
CIRAD-PHIM *and* Rockwinds LBMS

February 22, 2022

Declaration of Authorship

I, Pietro DELLA SALA, declare that this thesis titled, "Importance of drought components on the productivity of Theobroma cacao and ways to improve the industry's seasonal forecasting capacity." and the work presented in it are my own. I confirm that:

- This work was done wholly or mainly while in candidature for a research degree at this University.
- Where any part of this thesis has previously been submitted for a degree or any other qualification at this University or any other institution, this has been clearly stated.
- Where I have consulted the published work of others, this is always clearly attributed.
- Where I have quoted from the work of others, the source is always given. With the exception of such quotations, this thesis is entirely my own work.
- I have acknowledged all main sources of help.
- Where the thesis is based on work done by myself jointly with others, I have made clear exactly what was done by others and what I have contributed myself.

Signed:

Date:February 22, 2022

"Try and leave this world a little better than you found it, and when your turn comes to die, you can die happy in feeling that at any rate, you have not wasted your time but have done your best."

Robert Baden-Powell, Lord of Gilwell

Résumé

Le cacaoyer (*Theobroma cacoyer L.*) a son centre d'origine dans le bassin amazonien, au climat stable et humide, mais est cultivé en Afrique de l'Ouest, où les sécheresses atmosphériques et du sol sont des risques saisonniers récurrents dus aux vents de l'Harmattan. L'Harmattan modifie les précipitations, l'humidité et la température de l'air atteignent des niveaux stressants. En outre, le changement climatique entraîne une augmentation de la température qui accroîtra le pouvoir d'évaporation de l'atmosphère, augmentant potentiellement le stress sur le sol et l'atmosphère. Cela menacerait davantage la viabilité de la cacaoculture dans cette région. Pour toutes les parties prenantes de l'industrie cacaoyère, il est vital d'évaluer la viabilité et le potentiel de la culture du cacao par rapport aux événements de sécheresse à une échelle sous-saisonnière et en vue de l'adaptation au changement climatique. Afin d'évaluer la variation sous-saisonnière de la production, le stress hydrique (atmosphérique et du sol) et le flétrissement des cherelles ont été étudiés en utilisant des techniques de modélisation statistique telles que le BRT, le GAMM, le GLM et la classification hiérarchique des données. Nous avons suivi deux sous-parcelles de cacao, avec et sans irrigation, tout au long d'une saison d'Harmattan (2019 - 2020) et mesuré : (1) leur environnement (rayonnement (PAR) au-dessus et en dessous de la canopée, humidité du sol, température, humidité de l'air et précipitations) et (2) la santé et la productivité des arbres (vitesse de la sève, LAI et fructification). Les causes du flétrissement des cherelles ont été étudiées sur différents matériels génétiques au Costa Rica, en Guyane française et au Ghana. Cette étude a confirmé l'importance de la sécheresse du sol mais a également mis en évidence le rôle crucial du stress atmosphérique dans la transpiration du cacao. En dehors de leur effet direct sur la transpiration, les stress hydriques du sol et de l'atmosphère n'ont pas un effet synergique sur la transpiration, mais ils ont un effet synergique sur la densité de la canopée, qui à son tour réduit la transpiration. Ainsi, l'augmentation de la sécheresse atmosphérique est susceptible d'avoir un impact négatif sur le cacaoyer en Afrique de l'Ouest, actuellement sous l'effet des vents d'Harmattan et dans le futur pour le changement climatique. En réponse au stress atmosphérique et au stress du sol pendant l'Harmattan, le cacaoyer a concentré sa production pendant la période sans stress. En conséquence, il est possible que leurs puits totaux aient saturé la production totale d'assimilats (source) et n'ont pas répondu à un climat favorable par une fructification abondante. L'irrigation n'a pas annulé les effets du stress, mais a permis aux arbres de mieux répartir la nouaison sur la saison, rendant la production plus résiliente aux événements extrêmes. Pour tous les clones, un pic principal de flétrissement a été trouvé entre la 3e et la 5e semaine après la pollinisation, suivi d'un déclin régulier, contrairement aux études précédentes qui ont trouvé un second pic d'une ampleur similaire autour de la 9e et de la 11e semaine. Le flétrissement commence 3 semaines avant les symptomes, avec une baisse du taux de croissance relatif de la chérelle. Les cherelles avec la croissance la plus lente étaient les plus susceptibles de se flétrir. De plus, la compétition entre les fruits s'est avérée être un facteur prédictif clé du flétrissement, notamment en raison des cabosses en phase linéaire de croissance. De la même manière, la concurrence intergénérationnelle a augmenté le flétrissement total. Enfin, l'étude n'a pas trouvé de différence de flétrissement en fonction de la position des chérelles sur l'arbre. Le rôle de l'irrigation dans le flétrissement ne s'est pas non plus avéré significatif, probablement en raison du manque de données. Tous les résultats de l'étude ont été utilisés pour concevoir un modèle de physiologie du cacao capable de capturer le système de culture ouest-africain.

Abstract

Cacao (*Theobroma cacao L.*) has its centre of origin in the Amazon basin, with a stable and humid climate, but is cultivated in West Africa, where atmospheric and soil droughts are recurrent seasonal hazards due to the Harmattan winds. The Harmattan hinders rainfall and makes air temperature and relative humidity reach stressful levels. In addition, climate change is causing an increase in temperature which will increase the evaporative power of the atmosphere, potentially increasing soil and atmospheric stress and further threatening the viability of cocoa farming in this region. For all stakeholders in the cocoa industry, it is vital to assess the viability and potential of cocoa cultivation in relation to drought events on a sub-seasonal scale and with a view to adaptation to climate change. In order to assess the sub-seasonal variation in production, water stress (atmospheric and soil) and cherelle wilt were studied using statistical modelling techniques such as BRT, GAMM, GLM and hierarchical clustering of data. Two cocoa subplots, with and without irrigation, were followed throughout a Harmattan season (2019 - 2020) simulateously measuring: (1) their environment (radiation (PAR) above and below the canopy, soil moisture, temperature, air humidity and rainfall) and (2) tree health and productivity (sap flow, LAI and fruiting). Moreover, the causes of cherelle wilt were studied on different genetic material in Costa Rica, French Guiana and Ghana. This study confirmed the importance of soil drought but also highlighted the crucial role of atmospheric stress for cocoa transpiration. Soil and atmospheric water stresses do not have a synergistic effect on transpiration, but they do have an effect on canopy density, which in turn reduces transpiration. Thus, increasing atmospheric drought is likely to have a negative impact on the cocoa tree in West Africa, presently under Harmattan winds and in the future due to climate change. The cocoa tree concentrated its production during the unstressed period in response to atmospheric stress and soil stress during the Harmattan. As a result, the trees saturated the source-sink capacity and did not respond to a favourable climate with abundant fruit set. Irrigation did not negate the stressful effects, but allowed the trees to better distribute fruit set over the season, making production more resilient to extreme events. For all clones a main wilt peak was found between the 3rd and 5th week after pollination, followed by a steady decline, in contrast to previous studies which found a second peak of similar magnitude around the 9th and 11th week. Wilt begins 3 weeks before symptomatology, with a drop in the relative growth rate of the cherry. The slowest growing cherries were the most likely to wilt. In addition, competition between fruits was found to be a key predictor of wilting, especially due to pods in the linear phase of growth. In addition, intergenerational competition increased total wilt. Finally, the study did not find a difference in wilting depending on the position of the cherelles on the tree. The role of irrigation in wilting was also not found to be significant, probably due to the lack of data. All the results of the study were used to design a cocoa physiology model capable of capturing the West African cropping system.

Contents

List of Figures

List of Tables

Chapter 1

General introduction

1.1 Cacao: an introduction to the species

1.1.1 Botanical overview

The cacao tree (*Theobroma cacao*, L.) is an understory shrub that belongs to the Malvaceae family, of which it is one of the prominent species cultivated for commercial purposes. Cacao commerce revolves around mostly the sale of its beans, from which chocolate is made, and from which cacao butter, a vegetable fat used in the pharmaceutical and cosmetics industry, is extracted. The 22 species of the *Theobroma* genus have their botanical origins in the rainforests of tropical America where some are still used for human consumption nowadays but only *T. cacao*, L. is cultivated extensively [202]. Cacao, the 'food of the gods' (from the Greek theos = gods, and broma = food), has several botanical foci located in tropical America, the most important of which is in the upper Amazon River [163, 250]. Three subfamilies of cacao cultivars are documented to have evolved in the world, all originated from the great morphological diversity observed in Central and South America. Cuatrecasas (1964) [49] proposed that initially only two distinct cacao populations evolved in America separated by the Isthmus of Panama. These two populations evolved independently into two distinct subspecies with their own morphology and geographical distribution (*T. cacao ssp. Cacao* and *T. cacao ssp. Sphaerocarpum*) [49]. *T. cacao ssp. Cacao* and *T. cacao ssp. Sphaerocarpum* are respectively known as "Criollo" and "Forastero". The third subfamily originated from the natural crossing of Criollos and Forasteros varieties that took place in the Republic of Trinidad and Tobago, where the two subfamilies happen to coexist. This third subfamily is called Trinitario, from its geographical origin, and has traits intermediate between the Criollo and Forestero subfamilies. Despite there are proves of cacao being known to humans since the Mayan times, its domestication for extensive cultivation is quite recent, thus the breeding process for improved varieties is still a developing field in cacao research and the genetic material currently planted in the field is not so distant from the wild type [163].
Cacao was found to grow within 20° latitude from the equator but it really thrives only under extremely stable climatic conditions within 10°C of the equator where the temperature range is stable throughout the year, there is high air relative humidity and abundant rainfalls[180, 202, 245]. To thrive, it needs:

- annual rainfalls above 1250 mm but not exceeding 3000 mm, ideally between 1500 and 2000 mm and not falling below 100 mm/month for longer than three months in a row over the course of a production year. [39, 132, 245];
- the need for stable conditions restricts the altitude of its cultivation between sea level and 1250 m asl [245];
- an annual relative humidity above 70% is recommendable and above 90%, optimal;

- an average temperature around 25°C with minima above 15°C [132, 245] and narrow day-night temperature difference. Large temperature oscillations can induce serious enzymatic dysfunctions that inhibit photosynthesis and require several days to recover [167].
- a minimal occurrence of extreme temperatures beyond 33°C or below 20°C. Otherwise, above 33°C the efficiency of photosynthesis drops. Below 20°C many genotypes greatly reduce or completely stop vegetative growth [132].

In its wild, natural habitat, the cacao tree reaches 10 to 15 m in height and it occupies the lower canopy strata of the tropical American rainforest ecosystem [163, 245]. This is because cacao needs a vegetation cover that protects it from direct radiation and that limits evaporation, which makes it a shade plant [118, 124, 135, 161, 199, 227]. In its natural growing environment, the cacao tree architecture is very peculiar. In the first 18 months, the growth is only orthotropic (along the vertical axis) and forms the main trunk. Then, the plant emits 3 - 5 plagiotropic (main axis along the horizontal plan) branches, referred to as a "jorquette". Once the lateral branches are fully grown, the tree starts growing orthotropically again through the emission of secondary stems, or suckers (Spanish: chupones, French: drageon), that in turn will branch laterally (Fig. 1.1 A). The emission of suckers occurs both in correspondence of branching and at the base of the main trunk [58]. The vegetative growth in cacao is particular as well because the elongation of new phytomers (plant's structural unit consisting in a leaf, an internode and a node) is not continuous on a branch but happens in flushes [58, 173]. Each branch elongates independently by flushing approximately 4 to 10 new phytomers simultaneously. The most accredited theory is that vegetative growth is triggered, in flushes, when the plant has enough resources locally to sustain the growth of all the new organs at once [58, 173, 226]. Therefore, new phytomers are produced constantly but are expanded simultaneously only when the plant has sufficient resources to sustain their growth. When cacao is cultivated, the suckers are often removed and the architecture is forced toward a plagiotropic growth, mostly because it is widely thought that suckers reduce the yielding capacity of the tree by competing for resources. Furthermore, limiting the orthotropic growth in favour of the plagiotropic growth limits the height to 1.5-3 metres, facilitating most field operations [237] (Fig. 1.1 B).
On the other end, underground, the cacao tree develops an orthotropic taproot system, which

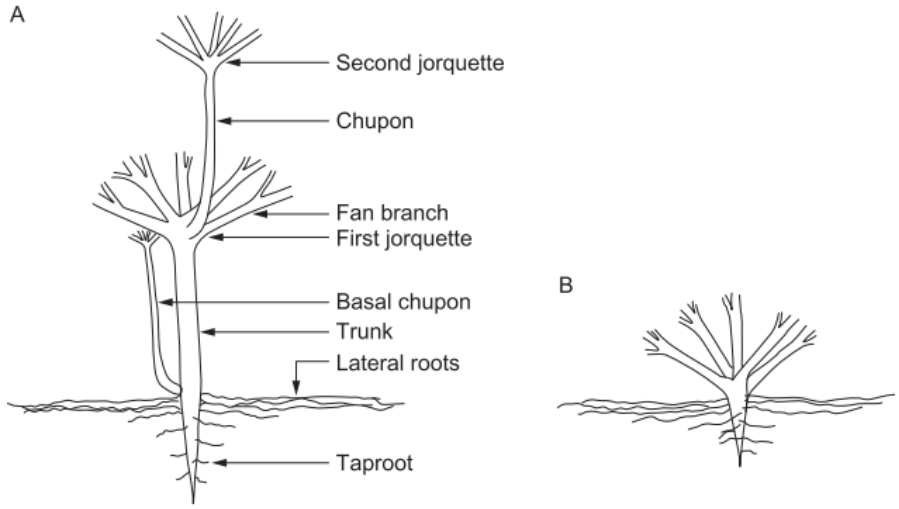

FIGURE 1.1: A schematic representation of the cacao tree main architecture, excluding further order of branching and leaves. A = Natural "Nozeran" cacao tree architecture. B = Plagiotropic cacao tree architecture, typical when it is cultivated. The original image is from Van Vliet et al. (2017)[237].

goes as deep as 2 m, from which a network of lateral roots with subsequent plagiotropic ramifications of fine roots (<2 mm in diameter) develops. This root mass of secondary ramifications and fine roots is concentrated mostly in the 0-20 cm depth horizon and extends up to 5 to 6 m around the foot of the mature tree trunk [39, 162, 177, 191].
The reproductive organs of cacao present some peculiarities as well. Its hermaphroditic flowers are produced in inflorescences grouped on floral cushions. The floral cushions are the result of the final differentiation, in the form of bark blisters, of axillary buds after leaf fall. At each period of floral induction, flower production is simultaneous on all flower cushions of the same tree. Flowering occurs all year round but presents some seasonal peaks that are synchronous for all cacao trees in the same region. Thus, in the different production areas across the globe, there are seasonal flowering peaks, more or less marked depending on the individual, genetics, the tree's age and the surrounding environment - especially the occurrence of high temperatures and the abundance of rainfalls. The pollination of flowers is carried out by small midges and more than one passage is required for a complete pollination of the flower, which otherwise is shed within 36 hours from opening. As a consequence, only 2% of the total flowering leads to fruitlets, initially called cherelles [58, 77, 98, 173]. A second peculiarity of the reproductive phase of cacao is the wilting of young cherelles during the first 4 to 10 weeks after pollination for physiological reasons. This self-trimming mechanism is responsible for a drop in the number of initially set cherelles, often of around 60-70% [14, 112, 155, 226]. Finally, when they ripen, cacao pods do not fall off, but remain anchored to the tree. It has been proposed that this is an adaptation to facilitate a zoochorous mode of dissemination [250]. Other authors advanced the hypothesis that, due to competition with other rainforest species, cacao's preferential way of survival is through the production of suckers rather than by seed dissemination [Christian Cilas, personal communication, January 2020]. More research is certainly required before understanding cacao's evolutionary reasons to firmly retain the fruits from falling.

Cacao trees are grown from seed. Each plant can grow to a height of 12-15 metres when mature, which can take up to three years. Trees under 3-5 years old do not produce pods. Peak production is reached when the tree is 10 years old. When the trees start producing, the cacao trees produce thousands of small white or pink flowers. These are pollinated by tiny insects called midges. However, only 0.5 to 5% of these flowers will develop into cacao pods. The pods take five to six months to reach full maturity [58].

1.1.2 Cultivation and spreading

From its geographical origins, cacao has spread by human introduction first, in the 19^{th} century, to the African continent and then to Asia as well. Therefore, cacao is now cultivated in many countries of the inter-tropical belt comprised between $\pm 10^{\circ}$N of the equator (Fig. 1.2). The market volume of cacao almost tripled in the last forty years, driven by a steady compounded annual growth rate, which reached a value of 3.1% in the last decade [21, 180]. Consequently, world cacao production has doubled in the last thirty years, mostly due to the growth in importance of four West African countries that account for roughly three fourths of the world production: Ivory Coast, Ghana, Cameroon and Nigeria. During the past three decades, production in West Africa almost tripled from 1.37 million tonnes to 3.47 million tonnes, while the production in the rest of the world remained stable [80, 180]. Consequently, the world market share of the big four West African cacao producers increased from 55% to 74% in these years (Fig. 1.2) [80, 180]. The world dependence on cacao from West Africa is even greater than these figures suggest. In fact, in Latin America and Asia, many countries have an internal demand for cacao that is greater than their own internal production, thus are driven toward importing cacao as well. The magnitude of the imports is greater than

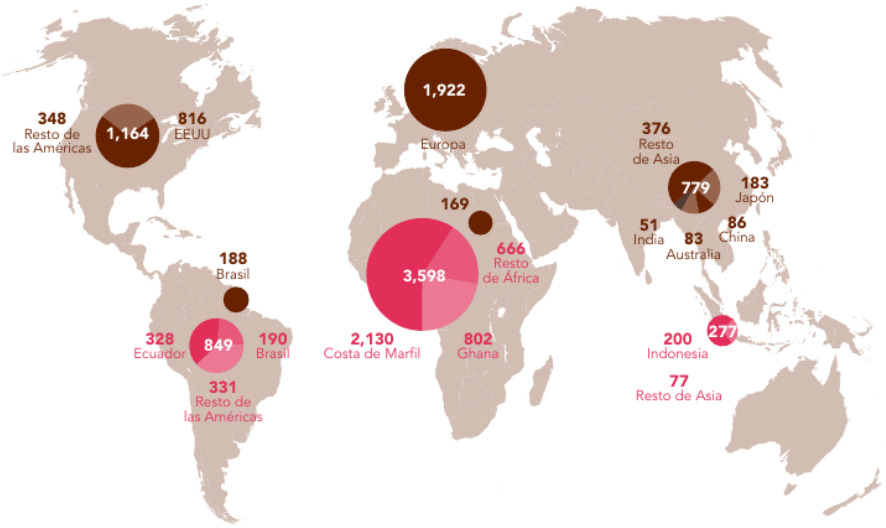

FIGURE 1.2: Worldwide cacao production per country in kTon for 2019/20 (pink) and cacao consumption in kTon for 2018/19 (brown). Source: VOICE Network [86] with data from ICCO (International cacao Organisation) (2020) [180].

the internal deficit in production. This is because, in particular in Latin America, cacao production is mostly fine flavor cacao (about 10% of world cacao production), which is traded and priced differently from the ordinary bulk cacao from West Africa and it is mostly used in fine chocolate, while the cheaper bulk cacao is used not only for chocolate production but for cosmetics and pharmaceutics as well. As an example, domestic consumption in Central and South American countries totals about 450 KTon [80, 180], with only a fraction of that cacao that is fine or flavor cacao, thus sourced locally, and a great share that it is imported. As such, the dependence of the world on the West African "regular cacao" is not only limited to those countries that are only importers but it extends to many producing countries as well. Overall, it was estimated that the world aggregated import of cacao beans from West Africa is well above 80% [80, 86, 180].

1.1.3 Cacao in West Africa

The West African cacao production is dominated by Ivory Coast as the top producer at 39% of global production, followed by Ghana at 21% [80, 180]. Thus, West Africa has a paramount influence on a worldwide market worth 7 billion USD.
In countries such as Ivory Coast and Ghana, cacao's importance is such that exports are strongly regulated by the government, as they represent an omnipresent, major item of these countries' gross domestic product and can represent up to 70-100% of the household income of almost two million of smallholder farmers in the region [8, 216, 230, 237].
Despite cacao being a steady source of income for many smallholder farmers across West Africa, particularly in Ghana and Ivory Coast [8, 216, 230], the yields obtained in the West African cacao belt are merely 10-20% of the estimated potential bean yield [76, 257]. The difference between attained and potential production in some West African countries may be partly explained by the fact that the habitat of commercial cacao trees here is often markedly different from its natural one, with cacao being exposed to much drier conditions throughout the year and predominantly grown in unshaded or lightly shaded environments [220, 241]. Furthermore, in most of the West African cacao belt, cacao farming is done with little or even no investment in terms of field management. The old average age of farmers together with a low farm gate price and a not always complete knowledge of cacao have led to three main

causes for low yields: (1) high incidence of pests and diseases (mirids, mealybugs, black pod disease (*Phythophtora spp.*), swollen shoot disease (CSSV) are the main ones), (2) old average tree age in most farms and (3) lack of proper soil nutrition [237, 241].
In the last two decades, the average investment on cacao by farmers has been insufficient, nonetheless, cacao was considered a cash crop and farmers continued to increase their cacao production establishing new farms elsewhere in the primary or secondary forests, slowly eroding the forest zones [38, 197, 241]. This phenomenon has led to large-scale deforestation in both Ghana and Ivory Coast, but has slowed down recently, partly due to regulations and partly because the areas available for expansion are limited [38, 80, 197]. Therefore, production in West Africa can now mainly be boosted by increasing the yield of existing mature trees and/or by replanting unproductive old cacao farms. Both options are likely to depend on governmental intervention, as farmers alone cannot pay for it [237, 241].

1.2 Climate of West Africa

The lack of inputs and improper field management make the present and future cacao cultivation more sensitive to weather and climate anomalies. Variations in temperature and precipitation constitute one of the main drivers of African cacao crop variations, and thus of uncertainty in crop yields, both at the level of one season or when looking at long-term production trends [257].

1.2.1 General overview

The climate over the West African cacao belt presents very different situations, ranging from stable wet and warm conditions in coastal Cameroon to much drier conditions in the northern parts of Nigeria, Ghana and Ivory Coast [**GPCC**, 209]. If we limit the analysis to the cacao producing areas (Fig. 1.3; [209]), in particular of the three largest producers (Ivory Coast, Ghana, Nigeria), the climate presents some important differences from the one in cacao's zone of origin. Like in the Amazon basin, the West African lowlands where cacao is mostly cultivated have a uniform daylight and solar irradiation over the year. The average temperature over a year is 26°C, with a monthly variation from the mean of 1.7-2.8°C (Fig. 1.3)[106]. The usual diurnal temperature excursion varies between 5.6 and 8.3°C depending on the period [48, 209]. The annual precipitations are a first climatic element that differs from the Amazonian basin and, often barely meet cacao's requirements. Precipitations span between 1100 and 2100 mm across six West African macro areas defined for internal use at Rockwinds (the company supporting the project) in collaboration with Dr. Alina Gainusa-Bogdan (Fig 1.3). In Ivory Coast, Ghana and Nigeria, every year there are two wet seasons with monthly precipitations above 100 mm/month separated by two dry seasons, another key difference with cacao's zone of origin. The long main dry season occurs between mid-November and mid-March while the second, shorter dry season (minor) occurs between late July and September. The alternation of dry and wet seasons shapes cacao's production cycle into a main crop between October and March and a minor crop the rest of the year (Fig 1.3), while the harshness of these two dry seasons is a major cause of inter-annual yield variability [46].

The rainy and dry seasons are tied to the seasonal movement of the Inter-tropical Front (ITF) across West Africa. The ITF is where the dry Saharan air mass meets the moist monsoon air flow coming form the Gulf of Guinea. North of the ITF there is virtually no possibility of rainfall due to the extremely dry air. Rainfalls are inhibited south of the ITF as well until the rain band, which has the northern edge at 100-250 km from the ITF and the main core that lags more than 400 km south of the ITF. The ITF movement determines the seasonality of

rainfall [4, 130, 208]. In late boreal summer (July - September), the ITF and rain-band advance so far north that some of the cacao regions are left on the southern flank of the rainbelt, where they experience significantly less precipitation (Fig. 1.4). This is the above-mentioned little dry season. This is felt throughout the cacao regions in Ivory Coast, Ghana and west Nigeria, especially on the coast. East Nigeria and Cameroon, on the other hand, do not suffer a little dry season because of a volcanic mountain range, the Cameroon Line, that always retains humidity coming from the Gulf of Guinea through the triggering of orographic precipitations [4, 130, 182, 208]. Between November and March, the ITF moves south, pushing the rain-band often far from the cacao growing regions and causing the long main dry season. Most of the time, the ITF lingers north of the cacao regions, only inhibiting precipitations for a few hundreds kilometres south of it. Occasionally the ITF reaches a position south enough to leave part of the cacao regions north of it (Fig. 1.4, 1.5). In such cases, the plants are invested by the mass of dry air north of the ITF and undergo stressful atmospheric conditions as well [130, 182, 208].

1.2.2 The Harmattan wind

The Harmattan is a continental north-easterly trade wind blowing in the Saharan, Central and West Africa. The Harmattan conveys extremely hot and dry conditions during the day, cooler conditions at night and it is usually dusty [208]. The southward movement of the ITF brings the Harmattan - and, with it, the dry Saharan air mass - close to the cacao regions during the main dry season. The southernmost reach of the Harmattan is, on average, around the northern edge of the West African cacao regions. Variations around this average southernmost position of the ITF mean that sometimes the Harmattan reached further south, directly affecting the cacao regions [208]. The presence of the Harmattan wind not only nullifies the chances for precipitations, but causes the air relative humidity to drop rapidly (Fig. 1.4, 1.5). The low air relative humidity reduces the overall heat capacity of the atmosphere, leading to large daily oscillations in air temperature. During the season when the Harmattan winds invest the cacao regions, temperature may rise as high as 44°C during the day [2, 13] and drop as low as 12-14°C at night [102, 117].
Both the absolute values of such extreme temperatures and their wide daily temperature differential are responsible for severe physiological dysfunctions in cacao [132, 167]. Furthermore, the low air relative humidity in itself is thought of as an additional stressor. As a matter of fact, in tropical environments relative air humidity is considered a hard constraint to biomass production whenever it goes below 40%, especially in combination with high temperatures [154, 178]. This is a recurrent scenario under the influence of the Harmattan winds during the long dry season in the cacao belt of West Africa. Cacao, a tropical species, is negatively affected by such stressful air humidity conditions. This falls in line with cases described in literature [93] and with the results that emerged from the present study in Ghana (Chapter 2, 3). In short, whenever the Harmattan winds reach a cacao region, the plants undergo both atmospheric and soil hydric stress (Fig. 1.5, 1.4). In addition to the soil drought caused by the absence of rainfalls for long periods, cacao has to deal with increasing vapour pressure deficit of the atmosphere induced by the high temperatures and the low values of air humidity.

1.2.3 Future evolution of the West African climate

Zooming out of the seasonal time scale, an additional challenge to cacao production in West Africa is climate change. Climate in West Africa is predicted to change drastically by 2050 [129, 209]. Temperatures are likely to increase by 2°C; a small, insignificant change in the total annual precipitations is expected, but the number of consecutive dry months in a season is

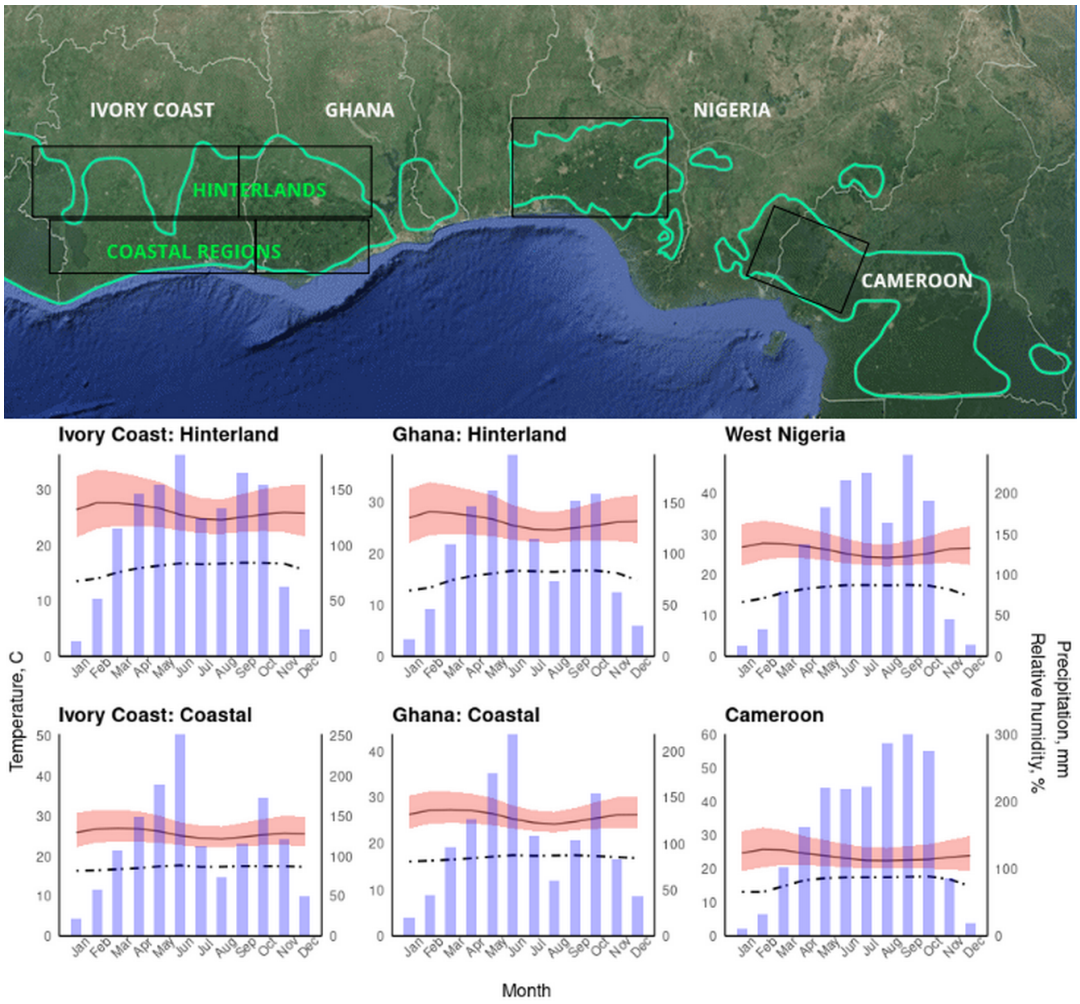

FIGURE 1.3: Above: Map of West Africa with the contours of the cacao producing regions in light blue [209]. The black squares mark six major macro regions for cacao production based on the cacao regions' contours [209]. The macro regions are: (1)Ivory Coast coast and (2) hinterland, (3) Ghana coast and (4) hinterland, (5) Western Nigeria and (6) North Cameroon. Below: Climatographical description of the six major macro regions where cacao is grown in West Africa. The solid lines represent the climatological monthly average temperature with its maxima and minima (red shaded area), the dashed lines represent the climatological monthly value of air relative humidity and the blue bars are the climatological monthly precipitations. The analyses were based on monthly data from the ERA5 and GPCC databases from 1987 to 2016 [**GPCC**, 106].

supposed to slightly decrease on average [129, 209]. Because many regions are characterized by sub-optimal watering (Fig 1.3), the small variations in annual rainfalls ($\pm$ 40 mm) are of little interest in themselves. If, instead, the temperature increase is factored in, it is evident that more stressing conditions are to be expected. The increase in temperatures will drive up the potential evapotranspiration and plant water requirement as well, making hydric stress potentially more frequent and/or more intense. Schroth et al. (2016) [209] modeled the suitability for cacao production in West Africa using an intermediate emission scenario, RCP 6 [115]. This study predicted that in the future many farmers may be forced to abandon farms, intensify cultivation or change crop due to the change in climate. Despite the fact that some currently marginal areas will become more suitable for cacao production, the overall outlook for West Africa is negative, even factoring in the global higher availability for CO_2 [131, 209].

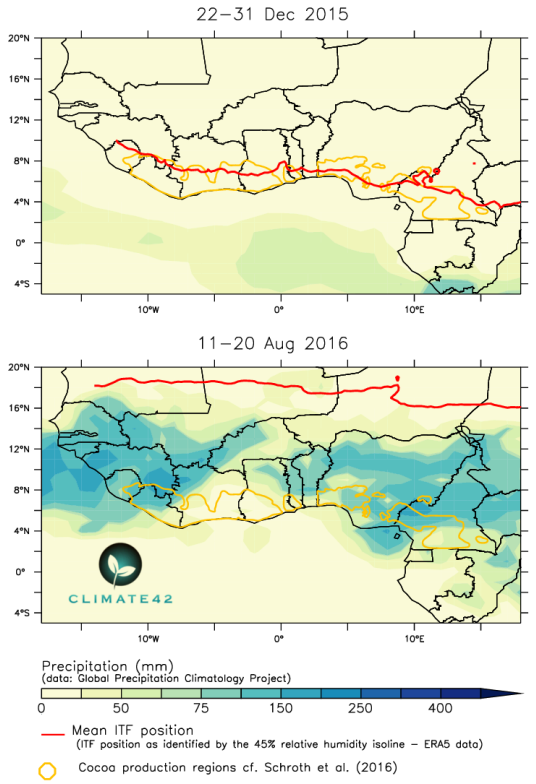

FIGURE 1.4: Cumulative precipitations over West Africa at contrasting positions of the inter-tropical front (ITF). Above it is show a common southern position of the ITF during the Harmattan season (22^{nd} - 31^{st} of December 2015). Below it is presented an extremely north position of the ITF during the summer little dry season (11^{th} - 20^{th} of August 2016). The chances of precipitations change drastically with the movement of the ITF because the rain band is roughly 200 - 400 km south of it. Whenever the position of the ITF is extremely south, rainfalls are virtually zeroed. But also an extremely north position can lead to a lack of rainfalls on the coasts as the rain band goes north as well, leaving the southern corners of West Africa dry. Graphical representation realised by Dr. Alina Găinuşă-Bogdan (Climate42 agroclimatic research department).

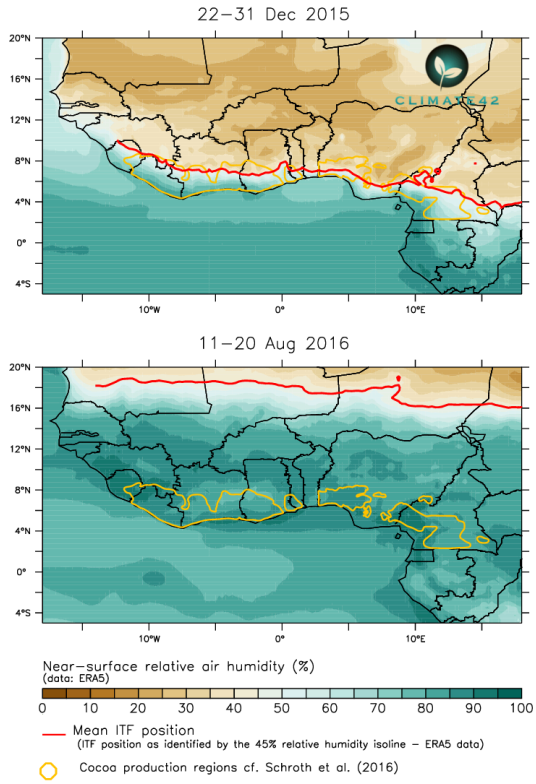

FIGURE 1.5: Mean air relative humidity over West Africa caused by contrasting positions of the inter-tropical front (ITF). Above it is show a common southern position of the ITF during the Harmattan season (22^{nd} - 31^{st} of December 2015). Below it is presented an extremely north position of the ITF during the summer little dry season (11^{th} - 20^{th} of August 2016). The air humidity changes drastically when a region is north or south of the ITF. Graphical representation made by Dr. Alina Găinuşă-Bogdan (Climate42 agroclimatic research department).

1.3 Drought in plants

1.3.1 Plant response to drought

Plants have four strategies of response to drought stress, namely: drought avoidance, drought tolerance, drought escape and drought recovery. The first two, drought tolerance and drought avoidance, are common to many species, as these are the main strategies to cope with water stress for plants [78, 114]:

- Drought tolerance consists in the ability of a plant to endure desiccation through physiological adaptations that can enhance, even temporarily, the resistance of the plant without avoiding the drought.
- Drought avoidance, instead, consists in the over or under-regulation of morpho-physiological and developmental traits to mitigate the drought itself. A common example of drought avoidance are the members of the *Cactaceae* family, which do not have leaves and photosynthesise with the stems to limit the surface from which water can be lost [78, 114].
- Drought escape is the plant's ability to adapt its life cycle to the environmental conditions in order to avoid having to deal with stressing drought conditions in the first place. Good examples are plants with a short life cycle or the production of seeds that only germinate when certain humidity conditions are met.
- Finally, drought recovery is the intrinsic capacity of a plant to recover after exposure to extreme hydric stress and resume growth. A curious, marvelous example are the so-called "resurrection plants" that can recover from months of harsh drought in a matter of hours or days [179, 255].

The last two strategies, as much as they are interesting, go beyond the scope of this dissertation because they are purely evolutionary niche traits, while drought avoidance and drought tolerance are mostly phenotypic processes that are expressed as a strong response component to drought [78, 114].
Whenever a plant is pressured by drought, the first strategy to resist it is to reduce transpiration, to limit water loss at the leaf level. To achieve that, a first option is to reduce the overall area from which water can be lost. Consistently, under water deficit, plants reduce the canopy surface area by shedding old leaves and reducing new leaf size [70]. Arguably the most widespread way to reduce transpiration, though, is to dampen the gas and water exchange rate through stomatal closure. Drought tolerance is inversely correlated to stomatal conductance: the tighter the control on stomata opening, the higher the species drought tolerance [18, 70, 78, 137, 221]. It is established that atmospheric drought negatively affect plant biomass in terms of growth and productivity [44, 138, 158, 236, 240]. In fact, extreme VPD values triggers the closure of leaf stomata, the fastest and more common way for a plant to reduce water loss due to transpiration, but this also entails a reduction in CO_2 uptake to supply photosynthesis, thus a reduced growth and production of reproductive structures [153, 247]. Beyond stomatal closure, high VPD also increases non-stomatal water losses, for example through the cuticle, further increasing the risk of hydraulic failure [59, 125, 141].
A second way to reduce the transpiration rate while maintaining the canopy photosynthetic surface area is to reduce the number of stomata on the leaf or their size. It has been found that mild drought has an additive effect on the number of stomata, whereas under harsh drought, the number of stomata decreases [131, 253]. Other ways plants adapt to hydric stress is by forming a thick layer of waxy cuticle to limit the loss of water through the mesophyll [78, 221], produce thick palisade tissues (trichomes) or produce thicker and smaller leaves [78, 114].
Far from the leaves, the root system, the first to experience drought in most cases, plays a critical role in drought stress response. In addition to reducing transpiration, an opposite but compatible strategy plants can use is to increase water uptake. In the short term, plants will invest in expanding their root systems to explore more soil volume. But, more importantly, at an evolutionary level, deeper rooting systems with longer roots are important traits for drought tolerance. Adaptive root systems in drought-tolerant plants are characterized by long tap roots and high density fine root systems in deep soil layers. A more extensive root system allows a greater number of roots to come into contact with more water, maximizing the absorption surface area [70, 78, 114].

1.3.2 Environmental stress in cacao

Many physiological responses to aerial or soil drought have been described in relation to other plant species [18, 44, 108, 253], but with regards to Theobroma cacao's responses to such conditions, our knowledge is not complete [59]. Several authors have already worked on the relation between drought and cacao (relative humidity [93], temperature [55, 56, 167], soil water content [87, 162, 210]) but they highlighted as well the need to investigate the water relations of cacao under drought in the field [39, 132].
On paper, cacao is very sensitive to drought due to many morphological traits. Cacao has large, broad leaves with minimal waxing and high stomatal density that cause strong transpiration and little control over water loss under high irradiance, high vapor pressure deficit (VPD) or windy conditions [155]. Furthermore, the xylem vessels in the stem are large and can pump water efficiently but carry a great risk of embolism or cavitation under too much pressure from the atmosphere or the soil [125, 132]. This characteristic of the xylem demonstrates that the hydraulic system of cacao is not designed to cope with low water availability. Moreover, the cacao root system is relatively shallow, with a high density of fine roots in the top 0.2-0.6 m of the soil and only a few in the deeper layers, and hence it cannot access deep water [162, 210]. The shallow root system is the opposite of what is usually found in plants' drought tolerance strategy and corroborates the idea that cacao is not made for undergoing drought.
Besides the morphological reasons, cacao shows a predisposition to suffer from drought from the physiological point of view as well, although more studies are needed to unravel the subject completely. Cacao leaves have a relatively low saturation point for photosynthesis (400 $\mu mol * s^{-1} * m^{-2}$) and an overall reduction in photosynthesis was documented after long exposure to irradiance of 200 $\mu mol * s^{-1} * m^{-2}$, with the decline accelerating above 500 $\mu mol * s^{-1} * m^{-2}$ [17, 132, 199]. Therefore, the photosynthetic system can be pressured easily by excessive radiation compared to what the photosystems and the electrons' chain can handle. This limited capacity to deal with high irradiance may exacerbate the effects of a water limitation that leads to a disruption in the electrons' chain, especially under no-shade or low shade cultivation, widely adopted in West Africa. Whenever cacao is forced to reduce transpiration under mid or high level of irradiance, the photorespiration will be worsened by the low photosynthetic capacity of cacao. This happens, for example when relative humidity drops, causing the VPD to rise. In response to high VPD, cacao triggers reduces stomata openness, and with it CO_2 for photosynthesis [153, 247]. This ends up directly reducing cacao effectiveness in fixing incoming radiation to produce assimilates.
Moreover, under atmospheric drought due to low relative air humidity, for example induced by the presence of the Harmattan wind, cacao is also confronted with the side effects of the low atmospheric heat capacity caused by the low air water vapor content. The low heat capacity of the atmosphere allows temperatures to reach values as high as 44°C [2, 13] during the day and as low as 12-14°C at night [102, 117]. Whenever the temperature goes above cacao's optimal range of temperatures (> 33°C), the increased evaporative power of the atmosphere induces partial stomatal closure and at the same time reduces the overall efficiency of photosynthesis due to enzymatic lower efficiency that leads to higher photorespiration. Whenever temperature drops below the minimum for photosynthetic efficiency, the enzymatic efficiency drops. In both cases, the net growth and physiological performance of cacao it is strongly and negatively affected [167].
On the other end of the cacao plant, soil drought pressures the conductivity of the soil-plant-atmosphere continuum, leading to the same end result as for atmospheric drought: stomatal closure and everything that it entails. The latter is necessary to protect the hydraulic system of the plant from embolism [108, 148]. Soil drought also reduces xylem and phloem transport and, hence, export of carbohydrates from the leaves to reproductive organs for flower and

fruit production [44, 69].
Once established that cacao is sensible to water stress, either atmospheric or edaphic, due to its morphological and physiological traits, it remains to be studied how drought translates into a reduction in transpiration and total biomass production and bean productivity in the field in the short, mid and long term [132]. In particular, to our knowledge no study has ever investigated the effect of a co-occurrence of soil and atmospheric drought, less so their interaction [2, 162, 210]. The simultaneous presence and effect of both soil and atmospheric water stress has been neglected because in most cacao growing areas the atmospheric drought is not a concern, as VPD and air temperature rarely reach stressful conditions for the trees (Brazil [87] and Indonesia [162, 210]). This is not the case for West Africa, where the long dry Harmattan season is characterized by the occurrence of both types of drought. To really understand the susceptibility of cacao to drought, research has to not only progress with studies targetted at either type of drought, but also to their interaction.

1.4 Modelling of cacao trees

In order to have an holistic understanding of the mechanisms around cacao under drought, and potentially guide targeted field studies, a fitting tool is model the entire soil-plant-atmosphere. A model for simulating cacao and its environment would be particularly necessary because (1) cacao is a perennial crop and field experiments require several years and considerable resources and (2) secondly because the model would be a useful tool to not only accelerate research but that could help decision-making for the industry as well.
Modelling aims to simplify a part of reality, containing the interacting components we want to study, called a system. Consequently a model can be used to study dynamic systems such as a growing plant and its interaction with the growing environment. Depending on the type of processes that the model aims to study, the level of complexity of the modelled growing environment can vary. To the extent to which the description of the growing environment and of its interactions with the plant is complete for the question at hand, this can allow to study the effects of individual environmental factors on the plant in isolation. For example, in order to study the competition for light among plants in a growing wheat field, it could be chosen not to consider fertilization or even to model the entire soil system as well [75, 254].
Plant modelling is a powerful tool that allows to extrapolate information on the behaviour of the actors of the system in time and space and to determine variables which cannot be measured directly [231].

1.4.1 A brief introduction to plant modelling

Modelling in crop science was initially used to understand and describe basic physiological processes of crop growth and development that were impossible to capture in field experiments. Examples are the ELCROS (Elementary CROp growth Simulator, [193]), BACROS (Basic CROp Simulator, [73, 193]) and SUCROS (Simple and Universal CROp growth Simulator [127, 232]. In the years, many approaches have been taken to describe the same processes, depending on the purpose of the model, the available input data and level of complexity desired [193]. For clarity, it is reported a scheme by Wang et al. (2002) (Fig. 1.6, [239]) that delineates a general crop model in all its essential components.
In the last decades, modelling techniques have been applied more broadly to study and include more applied processes such as the yielding capacity of a crop in different growth conditions [193]. Relevant examples are ORYZA2000 [28] for rice, GOSSYM for cotton [109], SOYGRO for soy bean [29] and GECROS for other annual crops [248]. All these models were

designed to answer practical questions mainly on water and nutrients deficiencies in the field [193], but are being modified in recent years to study the effects of climate change on the various crops [54, 184, 249, 252].

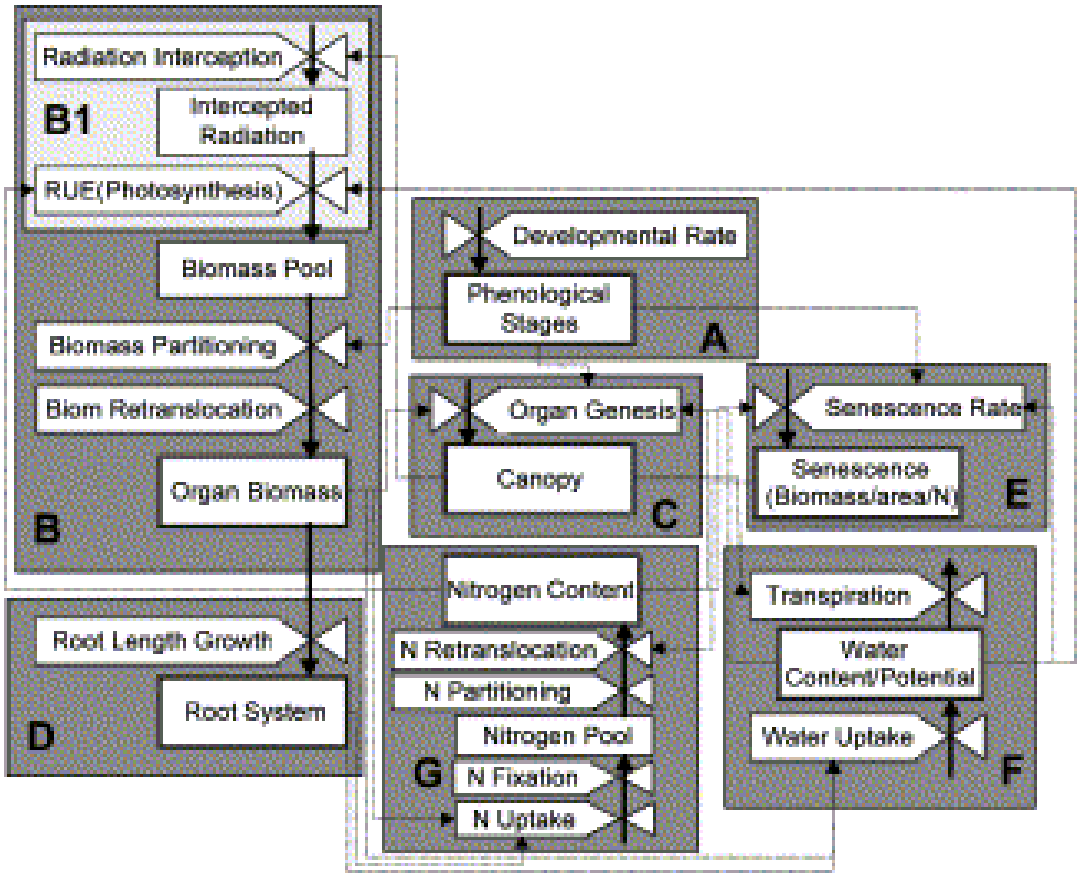

FIGURE 1.6: Simplified diagram of the main components and essential processes of a generic crop model template. Seven components are shown: A, phenology; B, biomass; C, canopy; D, root system; E, senescence pools; F, water; G, nitrogen. Squares represent state variables, valves processes. The dotted lines indicate communications between components. For simplicity, nutrients other than N are not considered [239].

1.4.2 Cacao modelling: state of the art

Currently, the only existing cacao physiology model is CASE 2 [256, 257], a physiological mechanistic model from the SUCROS (Simple and Universal Crop growth Simulator) family [27, 95, 231], developed for production capability comparison of different areas in the world, both for ideal and water limited scenarios [256, 257]. This model would constitute a solid basis to start our investigation, although it cannot be used in its current version to study the effects of drought at a seasonal or sub-seasonal time scale [256, 257]. This is due to the very general purpose of the CASE 2 model and the unavailability of reliable information to parametrize specific mechanisms at the time of its development that led to several approximations, which become highly relevant at the seasonal and sub-seasonal time scales.

More into details, CASE 2 is a cacao simulation model developed for both potential and water-limited production. The model simulates cacao growth and yields for different weather and soil conditions as well as for different cropping systems [256, 257]. CASE 2 uses several data sets as the input, such as weather information (daily precipitations, incoming radiation,

temperature, relative humidity), location, soil type, cropping systems and plant characteristics (physiology and morphology). Output of the model includes bean yield, biomass for different plant parts, leaf area index, water loss and butter hardness of the cacao. The main underlying assumptions in the model are: no nutrient shortage, no incidence of pests and diseases, closed and homogeneous crop canopy, no tree senescence, no pruning and, when included, homogeneous shading.
CASE 2 computes the functioning of cacao trees on a daily basis with inputs of weather (daily precipitations, temperatures, incoming radiation), soil and plant data. In the model, growth of cacao tree starts with photosynthesis. All the carbohydrates assimilated in photosynthesis flow through a series of reservoirs, from where part of them is pulled for maintaining existing organs and replacing lost ones (leaves, fruits, fine roots). After meeting all maintenance and replacement requirements, the surplus of assimilation products is the source of further organ growth.
In CASE 2, a set of statistical allometric relationships between tree and organs weight is used to calculate the potential biomass for leaf, wood, fine roots, taproot and pods. These relationships dictate specific organ-plant biomass ratios. Once the weight of an organ falls below its reference ratio, partitioning of the assimilates to this organ takes place. Instantaneous organ-plant weight ratio of organs that have large turnover rates (such as fine roots, leaves and pods) will drop below the allometric ratios more frequently, therefore, the model trees will thus allocate assimilates more often to organs with a fast turnover to maintain the predetermined organ-plant biomass ratio.
Major physiological processes included in CASE 2 are photosynthesis, transpiration, respiration and pod development. Photosynthetic assimilation is computed based on photosynthesis rate, cacao canopy condition, and leaf condition. CASE 2 adopts a linear, positive relationship to calculate photosynthetic rate at different temperatures up to an optimum between 31 and 33°C, while temperatures above this threshold lead to a rapid, linear decline in photosynthesis rate. The determinants of canopy photosynthesis are cacao canopy thickness, amount of absorbed photosynthetically available radiation (PAR) and leaf area density (LAD). Calculation of light absorption, LAD and leaf area index (LAI) greatly depends on shade level from external sources, though no canopy self-shading is considered. In nature, CO_2 availability is another key factor in determining photosynthesis productivity and depends on stomatal conductance. CASE 2 does not have an input parameter of atmospheric or internal CO_2 concentration, and there is no parameter of stomatal conductance, either. Instead, a water extraction power reducing factor (PCEW), calculated as the ratio between actual and potential transpiration, is used to account for stomatal closure, thus minor gas exchange, an applied to modulate many processes. Notably, photosynthesis is scaled by a factor PCEW to account for the lesser gross CO_2 fixation following the stomata closure. The PCEW modifier depends on and represents stressing atmospheric conditions as temperature and does not only directly affect the photosynthetic rate, but also, indirectly, net growth and resource allocation.

For example, the indirect effect of the high temperatures on net growth is through a lower photosynthetic efficiency coupled to a higher respiration rate. Respiration is also temperature dependent, and its rate increases exponentially with increasing temperatures. In CASE 2, when temperature exceeds 25°C, for every 10°C increase in temperature, cacao respiration rate doubles. If average daily temperature continues to rise, respiration will accelerate, and the rate of respiration will eventually exceed rate of photosynthesis at a high temperature. This is likely above 33°C when photosynthesis rate starts to reduce. Beyond this temperature threshold, simulated cacao tree growth will slow down due to enhanced respiration cost and limited assimilation. In extreme cases where photosynthesis rate and PCEW are largely reduced by high temperature, all assimilates will be used for respiration, and no net growth will occur. The indirect effect of the atmospheric conditions on resource allocation, instead,

pass through the leaf lifespan as PCEW is also used to modify the function for leaf turnover. To be more precise, a reduced PCEW means in CASE 2 that leaves will incur into earlier leaf senescence, thus to faster turnover. The faster leaf turnover translates in a higher need for assimilates to be demanded for leaf biomass.
CASE 2 simulates pod development by creating a series of "boxcars" each representing a stage of pod development. At each stage the pod drains biomass from the reserve depending on a fixed bell shaped function for sink strength, dependent on the developmental stage. At maturity, biomass is removed from the tree as the pods are harvested. Therefore, the fruiting cycle adopted in CASE 2 is continuous and do not fully account for seasonality [256, 257]. The seasonality of climate reflect on production only through the lesser availability of assimilates when conditions are stressing. In this sense, it overlooks the difference between producing less fruits and develop smaller fruits on average. For example, in nature the flowering and setting are almost halted sometimes to deal with the lesser availability of assimilates and maintain the already developing fruits. Therefore, the seasonality of production might result realistic but not necessarily accurate [256, 257].
CASE 2 currently has a module dedicated to water balance with the purpose of simulating soil water limitation, if wanted. The only input data required for the water balance in CASE 2 are the daily precipitations from the weather file. Before the input precipitation reaches the soil, a part of the water is intercepted by the canopy and evaporated, the rest is used to fill the soil layers, from the most superficial to the last layer considered. Whenever a soil layer is filled, the surplus is distributed within a time step (one day) to the soil layer underneath, and so on until the last layer hosting the tap root, after which, the excess water is considered lost. Evaporation involves only the first layer of soil and takes place on leaves surface too after rain. The available water for transpiration is calculated in each soil layer based on the potential transpiration divided by the area of fine roots and corrected with a linear reduction factor between a critical threshold and the permanent wilting point, which is dependent on the Scofield coefficient (pF) corresponding to the relative water content. The actual water uptake determines the actual transpiration and, through PCEW, the degree of stomatal closure and, consequently, the assimilates production decrease. In addition to affecting assimilate production, water limitation also affects leaf lifespan, as water stress causes extra leaf shedding in addition to normal leaf senescence. Overall, most of the mechanisms important for our analysis are already considered. However, some processes have been sometimes approximated or simplified (i.e. stomatal regulation), calibrated (i.e. change of partitioning under stress) and validated (i.e. fructification) due to the lack of data when the model was implemented and due the general purpose of the model [256]. CASE 2 was meant to make broad comparisons among different producing areas, better inform the scientific community on the most important factors for cacao's successful cultivation and be a useful tool to guide research [257]. Some of the simplifications or choices made in CASE 2 are acceptable when looking at a broad scale but make it not adapted to answer questions at medium-to-short timescales. It was stated above that CASE 2 might prove to be an excellent base to develop a mechanistic cacao model for the sub-seasonal timescale but a model dedicated to this purpose address the following limitations of CASE 2:

- The leaf life span dependency on environmental conditions was assumed to be linear but this must be verified as, during very long drought periods, the plant sheds many leaves and the remaining ones partly compensate by increasing the photosynthetic rate, which might impact their life span in a non-linear way [160, 161, 199, 256]. The importance of precisely quantifying this effect is that it impacts the recovery of production after a period of hydric stress, and, therefore, might influence the production on a sub-seasonal time scale. Furthermore, it would be useful to quantify in the field the effect of the soil and atmospheric water stresses on leaf shedding, in order to improve the

accuracy of this process' description.

- The dependence of the PCEW of cacao on the soil water content is currently modelled as linear. This should be revised. From literature it is known that the transpiration decreases not linearly in relation to the soil water content [108, 235]. Because PCEW has a predominant role in modelling the answer of cacao to soil drought, it should be verified if the linear reduction is a legitimate approximation to adopt or not.

- The stomatal closure in CASE 2 is not really considered. A master thesis study highlighted that transpiration in CASE 2 does not respond to extremely high VPD values (i.e. relative humidity set to zero) [82]. This unrealistic behaviour of transpiration arises because the model assumes a perfect regulation of stomata that adapts to transpire what the soil water content can sustain. Because stomatal opening is dependent on both soil and atmospheric drought, a sub-seasonal model to study the effect of the Harmattan on cacao must include a mechanistic description or, at the very least, an empirical relation with the stressors.

- An additional issue of CASE 2 when used for sub-seasonal simulations is how fruiting is modelled. The "boxcar" production modelling, based on an allometric relation, might not allow the due flexibility to include the effects of climate and drought events on production. Flower introduction in the model might not be necessary but different ways of modelling production should be investigated to try to have a more flexible description of fruiting in a dedicated model. In particular, at the sub-seasonal level it is important to not consider fruits of the same generation as one "boxcar" but as individual fruits competing among themselves. This would allow to account for fruit mortality (wilting) and output single fruit dimension and bean weight instead of the properties of an average fruit. The advantage at the sub-seasonal level is to verify how, under stress, the cacao tree partitions assimilates among fruits of the same age and opens the door to introduce fruit wilting based on the single fruit properties.

- The last point above would also permit to include a cacao specific trimming mechanism for young fruits (cherelles) called cherelle wilt [155]. If, for the original purposes of CASE 2, this process could be neglected, this is crucial in a model meant to study the effects of drought on cacao production. In fact, cherelle wilt is responsible for major losses in the field and appears to be tied both to the environment and the competition among fruits.

- More attention might be paid to the modelling of root distribution in the soil. The current distribution, an exponential decay relation with increasing depths that leads to 50% of the fine roots in the first layer, should be revised and updated in light of the recent results from the field [162, 165, 191]. Furthermore, for sub-seasonal analyses involving drought it would be preferable to include the plasticity of root growth to foster root expansion in the moister soil layers.

1.4.3 Project's main objective

The project's main objective, was to conceive a mechanistic model for cacao growth and production at the sub-seasonal time-scale to study the effects of atmospheric and soil stressing conditions on cacao productivity under present and future Harmattan conditions in West Africa. Such model would allow to study the impact of drought on production based on aerial or soil drought intensity and duration. To achieve this goal, it was necessary to fill the gaps of knowledge on the physiological consequences of drought on cacao's health and

production and address the problems evidenced for CASE 2 to conceive a more suited model for the task. The project's main objective needed three sub-objectives.

Project's sub-objective 1

A first sub-objective of this project was to capture the effects of atmospheric and soil water stress on cacao tree transpiration during the dry Harmattan season and shed light on the drivers of transpiration under such circumstances. This sub-objective is necessary to reason on the relations to include in the mechanistic cacao model to be conceived. A first hypothesis was that cacao trees responded strongly both to the soil and atmospheric water limitations. A second hypothesis was that VPD was a key transpiration limiting factor during the Harmattan season because of the extremely low relative humidities and large temperature oscillations that are reported to be harmful for cacao [167]. A third hypothesis was that the co-occurrence of soil and atmospheric drought led to harsher effects on transpiration than the two combined, implying the existence of a synergy between soil and atmospheric drought.

Project's sub-objective 2

Most of the studies on cacao water relations are focused on direct effects of a drought event in the short. It remains to study if a specific drought event has rippling effects on the medium-long term, in particular when it comes to pod growth and production that have a long cycle. Consequently, a second sub-objective for this project was to unravel and quantify the effects of different environmental conditions on the reproductive production and what effects a drought event has on the present and future generations of pods. The first hypothesis was that the type of climate over a season determines the evolution of the crop profile for that season. A second hypothesis was that the soil drought impacted production more than the aerial drought because the former impinges on the root extraction power of cacao as well as on stomatal closure. Furthermore, by answering to this object we would improve the understanding of the ripple effects of a drought on the seasonal production months after the drought episode. Finally, the results from a field study addressing this object would prove useful in a later stage to validate the realism of conceived model when used to simulate the field study conditions.

Project's sub-objective 3

Starting from the good modelling example represented by CASE 2, a third objective was to conceive a model suited to answer the main objective of this study. A first step was to review the literature on mechanistic modelling of perennial crops. This was useful to explore different modelling approaches for drought related processes in perennial crops. To serve the purpose of conceiving a mechanistic model for cacao physiology to be used for sub-seasonal analyses (main objective), a key process that had to be studies was cherelle wilt. This was necessary because the literature on wilting is scarce and very often quite old, thus required to extract relations to be used in the model [155]. Thus, the fourth sub-objective for the project was to better understand:

- at what stage of development the cherelles are most likely to wilt. For over 50 years cherelle wilt has been characterized as having two peaks in the fruit development [151] but a recent thread of research found a single peak followed by a progressive decline in incidence ("Daymond, 2000" in [103]);
- whether the total fruit load of cacao influences the wilting rate, and in case how. The role of competition among fruits has already been acknowledged but not quantified [155];

- gather information on the direct effect of drought on cacao cherelle wilt. Because drought reduces the amount of assimilates produced through photosynthesis, it leads often to competition for resources that can increase the wilting rate [155, 226]. Part of this sub-objective about cherelle wilt is aimed at quantifying such effect, possibly linking it to the harshness of the drought event.

Chapter 2

Short-term effects of a drought episode on cacao transpiration with or without irrigation

From a modelling perspective the most basic and important process to tackle may be the assimilate production through photosynthesis. Under stress, the enzymatic efficiency in harvesting energy of the photosynthetic apparatus may be impaired [10, 59] and the gross CO_2 harvested from the atmosphere is reduced as well due to a lower gas exchange through transpiration. When drought occurs, the reduced water potential in the soil–plant-atmosphere continuum causes reduced stomatal aperture, which is the dominant limitation for transpiration (and photosynthesis) under mild and moderate drought stress [44, 148, 253]. If drought-induced stomatal closure directly reduces the CO_2 harvest from the atmosphere per unit of leaf area, an equally important aspect to consider in a model is the total leaf area available to photosynthesise. A side effect of water stress is that induces the shedding of leaves as well, effectively reducing the plant total CO_2 harvesting capacity. As it was discussed in section 1.4.2, a key limitation of the only currently available cacao model (CASE 2; [257]) is its capacity to capture the effects of soil water stress on transpiration and plant's canopy density in a realistic way. According to the authors their modelling approach may require a field validation and calibration of the stomatal closure and the higher leaf mortality under stress [256]. Moreover, in CASE 2 and in the literature in general lacked a study on the effects of the atmospheric drought on mature cacao trees, a scenario of increasing likelihood with the current change of climate. Thus, the objective of this chapter is to highlight and discuss the relationships between sap velocity, a proxy for transpiration, and several environmental variables, with a focus on when they assume stressing values. This chapter presents and discusses the results of a recent publication in *Agricultural and Forest Meteorology*.

2.1 Introduction

The global climate has changed over the past century and is projected to continue to change in the next decades at a higher pace than in the past [115]. Global general circulation models (GCMs) agree that, except for an unlikely low emissions scenario, by the end of this century, global mean temperatures will rise by at least another 1.5°C and precipitation regimes over large areas worldwide will experience profound changes. In the tropical band (23°3'N-23°3'S), climate change is expected to have a negative impact on agriculture, ultimately threatening the economic stability of countries that rely heavily on this sector. This is particularly true for West Africa where agricultural systems are among the most vulnerable worldwide due to the economic constraints limiting access to agricultural technological advances, among other reasons [216, 230, 237]. West Africa's most famous exported crop, cacao (*Theobroma cacao* L.), will experience a severe reduction of its agro-pedo-climatic zone of cultivation [129, 142, 209]. Recent model predictions based on the SRES-A2 greenhouse gas emission scenario [169] project a continued rise in mean temperatures over the West African cocoa belt in the future and, while cumulative annual precipitations are not expected to change significantly, their distribution over the course of the year is. The period with no precipitations whatsoever may slightly shorten or remain unchanged in the coming decades across West Africa but, due to the aforementioned increase in temperatures, this region is expected to experience longer periods under greater evaporative demand. Ultimately, this will result into increased frequency, severity and duration of episodes of both soil and atmospheric water stress at the plant level. Consequently, a large share of cocoa-producing regions in West Africa will become unsuitable for production in the future [129, 142, 209], leaving millions of smallholder farmers without a reliable source of income [1].

The West African long dry season is characterized by the co-occurrence of low precipitation and a dry wind, the Harmattan. The Harmattan is a north-easterly trade wind blowing over North Africa that results from the continental-scale pressure gradient between the subtropical subsidence zone and the Intertropical Convergence Zone (ITCZ) [208]. During the West

African dry season, corresponding to the boreal winter, the Harmattan advances to the southern part of West Africa conveying a dry air mass from the Sahara to the south which lingers around the northern edge of the cacao belt, along the Gulf of Guinea [208]. The presence of the Harmattan hinders moist convection and suppresses any chance of precipitations, only allowing for sporadic weak rains for hundreds of kilometers south of the Intertropical Front, that marks the southern Harmattan extent at ground level [130]. The Harmattan further enhances soil and air water stress as the evaporative demand increases due to higher wind speed and reduced air humidity, ultimately leading to wide temperature differentials from day to night. Hence, under the influence of the Harmattan, soil water content decreases due to the lack of precipitation together with increased evaporative demand at the leaf level.
Cacao is original from the Amazon basin, where water limitation is virtually inexistent [59, 87, 245]. The morphological traits of cacao are not adapted to deal with water limitation: for example, cacao has large, broad leaves with minimal waxing and high stomatal density that cause strong transpiration and evaporation rates under high irradiance or high vapor pressure deficit (VPD) [155]. The hydraulic system of cacao is also poorly adapted to low water availability: the main stem has wide xylem vessels [125] to pump water more efficiently from the soil to the leaves, but this implies a greater risk of functionality loss due to cavitation under water stress [132]. Moreover, the cacao root system is relatively shallow, with high density of fine roots in the top 0.2-0.6 m of the soil, and hence it cannot access deep water [162, 210]. The physiological performance of cacao is also adapted to its native climatic conditions. Cacao optimum growth temperature is 24°C at night and 30°C during the day [167]. Cacao photosynthetic efficiency starts declining at temperatures above 33°C, while night temperatures below 15.8°C suffice to observe a decline in photosynthesis and stomatal conductance [132]. Additionally, for cacao trees of the Amelonado family, genetically the most representative in West Africa, the reported base temperature for vegetative growth is 19.7°C [56]. In West Africa, during the dry season and under the influence of the Harmattan, air humidity is not sufficient to buffer large daily thermal oscillations and air temperature can reach values as high as 44°C [2, 13] and as low as 12-14°C at night [102, 117]. These large daily temperature oscillations strongly inhibit the net growth and physiological performance of cacao [167]. In addition, reduced air humidity due to the influence of the Harmattan has a direct, negative effect on growth and physiological performance. Indeed, in tropical environments it has been shown that 60% is the air humidity threshold below which tree physiological performance starts to decrease and below 40%, in combination with high temperatures, it is considered that trees are exposed to high atmospheric water stress [154, 178]. It can be assumed that such conditions would be stressful for cacao as well, in line with [93]. Overall, it is clear that cacao lacks high tolerance to drought or extreme temperatures. Thus, the viability of cultivation of this crop outside its native range, in West Africa, is severely threatened by future climate change. The future threats to cacao cultivation are further exacerbated in full sun or lightly shaded monocoltural systems, preferred by farmers across West Africa for the higher yields in the short term but more exposed to atmospheric stress [2].
Both soil and atmospheric drought impact negatively on plant growth and productivity [44, 138]. Plants first respond to increasing vapour pressure deficit (VPD) by closing their pores on their leaf surfaces, the stomata, to reduce transpiration water loss, but this also entails a reduction in CO_2 uptake to supply photosynthesis and, eventually, reduced growth and production of reproductive structures [153, 247]. On the other hand, soil drought reduces the conductivity of the soil-plant-atmosphere continuum, ultimately inducing stomatal closure to protect the hydraulic system of the plant from embolism [108, 148]. Beyond stomatal closure, high VPD also increases non-stomatal water losses, for example through the cuticle, further increasing risk of hydraulic failure [59, 125, 141]. Besides reducing photosynthesis, soil drought also reduces xylem and phloem transport and, hence, export of carbohydrates from the leaves to reproductive organs for flower and fruit production [44, 69].

Several authors have already highlighted the need to better study the water relations of cacao under field conditions [39], but we still lack a detailed characterization of how drought stress influences cacao physiology and reproduction [132]. The effects of relative humidity [93] and temperature have been addressed [55, 56, 167] and a few field trials have addressed soil drought stress but, to our knowledge, no previous study has assessed the simultaneous effect of soil and atmospheric drought, and their interaction [2, 162, 210]. The reduction of transpiration in response to soil water stress has been characterized in Brazil [87] and Indonesia [162, 210], but in these locations VPD and air temperature rarely reach stressful conditions for the trees. Such effects have not been addressed in the West African cacao belt, where radically different atmospheric conditions due to the influence of the Harmattan will likely impose drought stress levels beyond those previously studied. The objective of this study is to clarify the effects of atmospheric and soil water stress on cacao tree transpiration during the dry Harmattan season and shed light on the drivers of transpiration under such circumstances. Our hypothesis is that cacao trees will respond strongly to both types of stresses but we expect VPD to be more influential, due to the extremely low relative humidities and large temperature oscillations experienced under the influence of the Harmattan.

2.2 Materials and methods

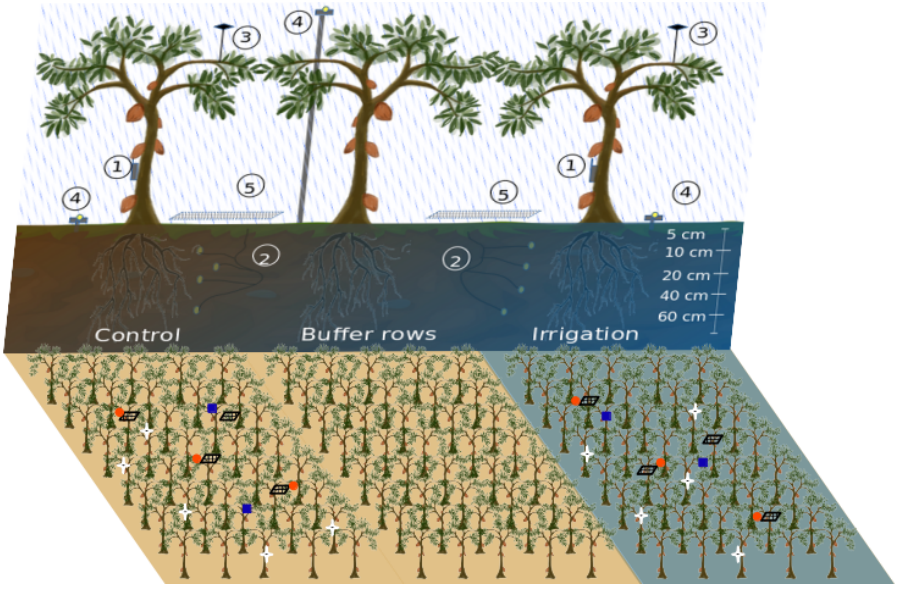

FIGURE 2.1: Schematic representation of the field experimental plan with an overview of the measurements taken. The experiment compared an irrigated plot (5 rows of 8 trees) to a control rain-fed one. The experimental plots were separated by a buffer of ten rows of trees. In each plot we measured 1) sap velocity (crosses), 2) soil moisture (squares), 3) temperature and air relative humidity, 4) photosynthetically active radiation (PAR) above and below the canopy (dots) and 5) litterfall production (hatched parallelograms). Position of the sensors reflect their real position in the field experiment. Graphics by Pietro Della Sala, drawing of the cacao tree by Estelle Ribeyre.

2.2.1 Study site and experimental design

Two plots of cacao trees, with and without irrigation, were monitored throughout the duration of the experiment (3^{rd} December 2019 to 16^{th} March 2020) and their response to climate tracked closely by means of various sensors. The measured environmental variables were: soil volumetric water content at four depths from 10 to 60 cm, air temperature, air relative humidity and photosynthetically active radiation (Fig. 2.1).
The study was conducted at the experimental station of the Cacao Research Institute of Ghana (CRIG) located in New Tafo Akyem, Eastern Region, Ghana (6°13'53.7"N; 0°21'01.6"W; 203 m a.s.l.). At this location, the climate is warm and humid all year round except for two dry seasons. The main dry season has its core between December and February, but the onset can be as early as mid November and lasts until sometime in March. The second dry season occurs between the second half of July and the beginning of September and is typically much less severe than the main dry season.
Throughout the year, temperature in Tafo oscillates between a monthly average minimum of 20 to 22°C and a monthly average maximum of 29 to 33°C [8]. Annual rainfall ranges between 1150 and 1800 mm with a mean value of 1565 mm per year [8, 15].
At the study site, a 2 ha cacao plantation was established in June 2013. Cacao trees (*Theobroma cacao* L.), of homogeneous genetic origin, were planted with a 2.5 x 2.5 m spacing (1600 trees ha^{-1}), underneath *Gliricidia sepium* Jacq. previously planted at a density of 10 trees ha^{-1}. The plantation consisted of four blocks with 10 plots each. Each plot contained 40 trees planted in five rows with eight trees per row. In November 2019, two plots of 40 hybrid Amelonado trees with mean canopy height of 3 meters were selected for the study. The selected plots were located at least 20 m away from the nearest shading tree and, therefore, were considered

as a "typical West African full sun system". The two study plots were separated by ten rows of cacao trees to avoid any edge effect or interaction between the two (Fig. 2.1). From the 26^{th} of November 2019 to the 16^{th} of March 2020, trees in one plot (irrigation treatment) were irrigated with 60 L per tree (equivalent to approximately 9.6 mm per tree) on alternating dates using a hose, whereas trees in the second plot (control) only received ambient precipitation. The irrigation was evenly applied within 50 cm from the trunk, where most of the roots were believed to be distributed [39]. Irrigation close to the trunk was not reduced by losses due to canopy interception, thus its efficacy was higher than a rainfall of 9.6 mm.

2.2.2 Soil properties

According to a soil analysis of the experimental site conducted in March 2020, the upper soil (0-15 cm) was a eutric fluvisol with sandy-loam texture and below 15 cm of depth the soil texture was sandy clay loam. The pH was 6.5 across the entire profile. The upper soil was poor: organic matter content was 1.36%, magnesium was 2.06 $me * 100g^{-1}$, total nitrogen was 0.15 %, ammonium was 14.2 ppm, phosphorus was 12.96 ppm, potassium was 0.049 $me * 100g^{-1}$ and exchangeable calcium was 3.72 $me * 100g^{-1}$. Based on the soil texture at a depth of 30 cm, the bulk density (BD), field capacity (FC) and permanent wilting point (PWP) were estimated in 1.45 $g * cm^{-3}$, 34% and 13%, respectively. Below 30 cm, the values of BD, FC and PWP were 1.55 $g * cm^{-3}$, 35 and 16%, respectively.

2.2.3 Transpiration measurements

For the entire duration of the experiment, tree transpiration was estimated from measurements of sap velocity using the Heat Ratio Method (HRM: [146]). Five trees in each plot were selected, with mean$\pm$sd diameters (measured 20 cm below the main branching) of 11.31$\pm$1.84 and 12.23$\pm$1.34 cm in the control and irrigated plots, respectively (Fig. 2.1, (1)). Within each plot, the trees were selected based on a visual scoring system of overall condition (canopy density, leaf greenness, number and diameter of jorquette branches etc.) and avoiding spatial clustering of monitored trees. In November 2019, we installed one heat probe sensor (SF-3, East30sensors, USA) on each selected tree. Each sensor consisted of three probes, 35 mm in length, 1.3 mm in diameter, and 6 mm axial distance apart. The central probe contained an evanohm heater, and the lateral two probes, one upstream and one downstream with respect to the heater, contained 3 thermistors placed at 5 mm, 17.5 mm, and 30 mm from the sensor tip to monitor sap flow across the entire depth of the sapwood. The thermistor temperature sensor consisted of a 10K precision resistor and a 10K thermistor wired through a three wire half bridge connected to a datalogger per irrigation treatment (CR800, Campbell Scientific, Logan, UT, USA). The accuracy of the thermistors was $\pm$0.2 °C, and the resolution was 0.001 °C. The central needle was heated by a 12V pulse of 3 seconds powered by the datalogger and reduced to 5V through a heat control board (East30sensors, USA).
Sensors were installed on the trunk following the xylem direction, at a minimum distance of 20 cm from any node or branching and at a minimum height from the soil of 50 cm. Bark thickness was 0.3$\pm$0.15 cm (n = 10 trees) and was kept in place to protect the wound from dryness and fungal attacks. The probes were programmed in accordance with the Dual Method Approach (DMA: [84, 85]). The DMA combines the traditional approach to calculate sap velocity from heat pulse velocity [146] with the Tmax method [47]. The latter allows to capture high and low flow rates both upward and downward along the stem [84, 85]. The DMA calculated sap velocity with both methods but the algorithm returned the value calculated with the Tmax method when sap velocity was higher than a critical value (Vh_crit) and the value from the heat pulse velocity method while below Vh_crit. The calculations ex-ante of Vh_crit is described in Forester (2020, 2019) [84, 85] and was found to be 14.36 cm/h for cacao under

Variable	Symbol	Value	Units	Source
Wound tyloses layer diameter	$WoundDiam$	0.2	cm	measured
Wood matrix specific heat capacity	cw	1230	$J/kg/C$ at 25 C	[84, 85]
Sap heat capacity (water)	cs	4182	$J/kg/C$ at 25 C	[84, 85]
Wood water content at FSP	mc_FSP	0.26		[84, 85]
Sap density (water)	ps	1000	kg/m^{-3}	[84, 85]
Cell wall density	pcw	1530	kg/m^{-3}	[84, 85]
Cacao wood density (dry)	δ_{dry}	351.31	kg/m^{-3}	measured
Cacao wood density (fresh)	δ	848.75	kg/m^{-3}	measured
Wood water content	mc	1.416	$kg[water]/kg[drywood]$	calculated
Void fraction of wood at FSP	Fv_FSP	$6.79*10^{-1}$		calculated
Fresh wood specific heat capacity	c	2960.13	$J/kg/C$ at 20 C	measured
Dry wood thermal conductivity	K_Van	$5.58*10^{-1}$	$J/kg/C$ at 20 C	calculated
Dry wood thermal diffusivity	k_Van	$2.22*10^{-3}$	cm^2/s	calculated

TABLE 2.1: List of variables and constants used in the calculation of sap velocity according to the Dual Method Approach [84]. FSP: Fibre saturation point (wood).

the considered experimental conditions of this study.

Three values of heat pulse velocity were recorded every 30 minutes per sensor. Each value was calculated from the temperature difference between each pair of up- and down-flow thermistors located at three depths within the sapwood (5, 17.5 and 30 mm from the bark). Sap velocity was calculated for each of the three positions and then upscaled to an integrated value of sap flux for each tree through a weighted sum based on the sapwood area, estimated through wood coring, associated to the specific radial position [84, 85]. Before upscaling to a single value per tree, each couples of thermocouples was calibrated to have the zero for sap velocity when night potential evapotranspiration was zero (S. 2.2.6) [25, 32]. In this study it was assumed that during the three months of dry season the sapwood area increment is negligible, therefore, changes in transpiration are approximated to variations in sap flux.

The parametrization of DMA calculations for sap velocity used the cacao wood physical properties measured in the field to obtain the fresh (δ) and dry (δ_{dry}) wood density, wood water content (mc) and the fresh wood specific heat capacity(c). At the end of the study period, the average diameter of the tyloses around the wound caused by the needles of the sap flow sensors ($WoundDiam$) was measured with a caliper. The $WoundDiam$ was found to be in line with several other tree species [85] and used to correct the sap velocity calculations [85]. Additional constants that were not possible to measure in the field were adopted from Forester (2019) [84]. These constants were: the wood matrix specific heat capacity (cw), the water content of wood at fibre saturation point (mc_FSP) and the cell wall density (pcw). The density (ps) and heat capacity (cs) of the sap were assimilated to the ones of water.

$$FV\_FSP = 1 - (\frac{\delta_{dry}}{ps}) * ((\frac{ps}{pcw} + mc\_FSP) \tag{2.1}$$

$$K\_Van = Ks * (mc - mc\_FSP) * (\frac{\delta_{dry}}{ps}) + 0.04186 * (21 - 20 * Fv\_FSP) \tag{2.2}$$

$$k\_Van = (\frac{K\_Van}{p * c})) * 10000 \tag{2.3}$$

The previous variables were all used to calculate the void fraction of wood at fibre saturation

point (*Fv_FSP*; Eq. 2.1), the dry wood thermal conductivity (*K_Vand*; Eq. 2.2) and diffusivity (*k_Vand*; Eq. 2.3) as described in [234]. In Equation 2.2 *Ks* is the thermal conductivity of water at 20°C (0.6096 $J/m*s*C$). All relevant variables and constants are summarized in Table 2.1.

2.2.4 Soil VWC

Soil volumetric water content (VWC) was monitored in two flat locations per plot, equidistant (170 cm) to all surrounding trees, at four depths (10, 20, 40, and 60 cm), with TEROS 10 capacitance probes (METER group, Pullman,WA, USA) (Fig. 2.1, (2)). The chosen distance allowed to capture the average VWC of both the irrigated and the non-irrigated plots, avoiding potential biases due to uneven irrigation in the former. Despite their distance from the trees, the locations for VWC monitoring were shaded by the plots' closed canopy, effectively limiting quick evaporation of water after a watering event, be it rainfall or irrigation. The TEROS 10 sensors estimate soil VWC from measurements of the apparent dielectric permittivity in the 430 mL of surrounding medium. For this study, the manufacturer's calibration for a generic mineral soil was used. A value of soil VWC per probe was recorded on a CR800 datalogger every 30 minutes from November 26^{th} 2019 to March 16^{th} 2020. In one instance, the soil VWC was transformed into water potential to compare our results with other reported results. To obtain the pedotransfer function it was adopted the model by Van Genuchten [229]. The parametrization of the model was done with the R package *soilphysics 4.0* [211] and the soil properties measured with the soil analysis.

2.2.5 Leaf area index

Leaf Area Index (LAI) was estimated from measurements of photosynthetically active radiation (PAR) above (I) and below (I_0) the canopy (Fig. 2.1, (4)) in an inverted form of Beer's law (Eq. (2.4)). Measurements of PAR were collected from November 26^{th} 2019 to March 16^{th} 2020, with a brief interruption from December 27^{th} 2019 to January 8^{th} 2020. Incoming photosynthetic active radiation (PAR; $\mu mol * s^{-1} * m^{-2}$) above the canopy was measured every 30 minutes at one position in the irrigated plot. The PAR sensor (SQ110, Apogee instruments, Santa Monica, CA, USA) was mounted on top of a 5 m levelled iron pipe planted in the soil, i.e., 2 m above the canopy. Additionally, PAR was monitored under the canopy at three locations in each plot with three sensors mounted on levelled poles at 20 cm height. The extinction coefficient (K), necessary to calculate LAI from PAR data (Eq. (2.4)), depends on the solar angle (ϕ) and a leaf angle distribution coefficient (x) and was calculated applying Eq. (2.5) [37]. The parameter x was calculated as the ratio of vertical to horizontal projections of the canopy [37]. Based on field measurements, x was evaluated at 1.2, corresponding to an ellipsoid leaf angle distribution. A reliable estimation of K is possible only when the solar angle is close to the zenith [83, 218], therefore, we estimated LAI from PAR measurements collected between 10:30 and 14:30 (solar time). Furthermore, to avoid overestimation of LAI due to excess direct radiation reaching the sensors under the canopy, data from each sensor were smoothed and interpolated with the *Daniell* modified Fourier method [30, 213] and the three resulting curves averaged to get a final LAI value for the entire plot.

$$\frac{I}{I_0} = e^{-K*LAI} \tag{2.4}$$

$$K = \frac{\sqrt{x^2 + 1/tan^2\phi}}{1.47 + 0.45x + 0.1223x^2 - 0.013x^3 + 0.000509x^4} \tag{2.5}$$

LAI change due to defoliation was also monitored through the same monitoring period with a set of four litter traps per treatment (Fig. 2.1, (5)). Each trap consisted on a suspended

fine net of 1.2 m^2 that was positioned in randomized locations within each plot. The litter production was collected every 15 days and oven-dried at 100 °C for 36 hours to obtain the dry weight. To convert the leaf dry weight in LAI, in the beginning of the experiment the mean specific leaf area (SLA $cm^2 * g[dryleaf]^{-1}$) was calculated. A sample of 30 leaves (10 from the lower, middle and top canopy) for each treatment plot was scanned on a reference surface (an A4 sheet). The total area was estimated as the percentage of the images that was not white with ImageJ 1.53a [192]. To obtain the SLA, the average leaf area was divided by its oven-dry weight.

2.2.6 Atmospheric conditions

Air temperature and relative humidity were logged hourly in each plot, with two iButtons (DS1923-F5: Hygrochron, iButtonLink LLC, Whitewater, WI,USA) above the canopy at c.a. 5 m height. To protect the sensors from direct radiation and precipitation, these were installed facing the ground, glued to the internal part of bottle caps (Fig. 2.1, (3)). As temperature and relative humidity were logged hourly and as they represent continuous variables, a linear interpolation was applied in order to obtain half-hourly time series that matched those of the other measured variables in the data set. The vapour pressure deficit (VPD) and night-time potential evapotranspiration (required to calibrate the zero for sap velocity) were calculated following the FAO-56 Penman-Monteith method [6] by means of the Python package *'opencroplib==0.1.5'* [116]. For the calculation of the night-time potential evapotranspiration was considered a wind velocity above the canopy of 0.77 $m * s^{-1}$ at 5 m, in compliance with the average night-time value from a weather station at less than 1 km from the site. Daily precipitation data between October 1^{st}, 2019 and March 16^{th}, 2020 were retrieved from the Unified Gauge-Based Analysis of Daily Precipitation of the NOAA Climate Prediction Center (CPC; [15]).

2.2.7 Statistical analysis

Outliers' detection

Prior to analysis, we checked for sensor glitches, numerical artefacts of the sensor raw signal and measurement errors caused by faulty sensors. All measured variables but sap velocity were treated as continuous, with the hypothesis that they cannot abruptly change over half an hour. For this reason, it was decided to study the evolution of their first derivative in time and consider as outliers the points whose absolute value lied outside the two standard deviations confidence interval. A graphical evaluation of the data points flagged as outliers was carried out before they were discarded.

GAMM analysis

A generalized additive mixed model (GAMM) was used to model and assess the differences between the irrigated and non-irrigated plot dynamics of LAI over time. The GAM family of models was chosen primary because LAI was expected to exhibit a complex non-linear relationship with the environment. Secondly, it was necessary to use a GAMM because LAI measures in time were not completely independent as they were taken from the same sensors. The built GAMM model fitted a gaussian distribution for LAI (continuous variable) using the treatment (irrigated or control) as fixed effects and taking into account the random sensor-to-sensor variability. The effect of time was fitted by a smooth term using Duchon splines, allowing the predictions to take into account the differential in water availability due to irrigation. The GAMM-modeled LAI for both watering treatments was plotted and we interpreted non-overlapping 95% confidence intervals as a significant difference between treatment levels for

a given period. All these analyses were performed in the R environment v3.6.1 [189] using packages plyr [242], tidyverse v1.3.0 [243], mgcv [246] and itsadug v2.3 [233].

Boosted Regression Tree analysis

We used Boosted Regression Trees analysis (BRT) modelling to predict transpiration from climatic variables [71]. BRT uses two algorithms: regression tree and boosting. Tree-based regression models, described for use in ecology by [62], partition the solutions space with a set of rules, identifying the most homogeneous regions in terms of response to predictors. They then fit a constant to each region, fitting the average response in that region with the assumption of normally distributed errors. With each iteration the tree grows by repeatedly applying the analysis of the predictors space to its own output until a user-defined stopping criterion is reached. Tree-based models are intuitive, easy to visualize and are fairly insensitive to outliers, missing data and data types (numeric, binary, categorical etc.) but they lack the accuracy of other methods, such as GLM and GAMM. To compensate for this downside it is convenient to combine tree-based models with boosting. The idea behind the boosting methods is that it is more probable to find many rules of thumb, than to find a single, highly accurate prediction rule [206]. It is, therefore, more convenient to approximate the solution by averaging the results of a large number of rules of thumb rather than aiming for a unique highly accurate one. The BRT uses boosting as a way to evaluate the gradient of the predictors space by focusing on the variation in the response not explained yet by the model at a given step and fitting a new tree to its residuals [72]. Through boosting, decision trees are fitted iteratively to the training data, increasingly emphasising the still poorly modelled observations. As the boosting process is stage-wise, existing trees are left unchanged as the model is enlarged but the fitted value is estimated at each step to reflect the contribution of the newly added tree. The final BRT model is a linear regression model where each term is a tree.
In order to ensure the stability of the models' results and avert over-fitting, the evaluation looked at the difference between the training data coefficient of correlation and the coefficient of correlation for the 100-fold cross-validation. The skill of the models, instead, was assessed by plotting the predicted values against the measured ones [71, 72].
The BRT analyses were carried out using R v3.6.1 [189] and the gbm [97] and dismo [107] packages. The parameterization of the two models can be found in Tab. 2.C.1.

Two BRT models were built using 75% of the dataset to explain the relative importance of the potential drivers of transpiration during the dry Harmattan season. The remaining 25% was used to fit the models and evaluate them against the measured values. The two BRT models considered soil volumetric water content (VWC), photosynthetic active radiation above the canopy (PAR) and the vapour pressure deficit of the atmosphere (VPD) as environmental predictors, the leaf area index (LAI) of the two plots as indicator of the general state of the canopy and the diameter of individual trees as a proxy for their dimension. The first model (model 1) used the half-hourly daytime data ($PAR > 15 \mu mol * s^{-1} * m^{-2}$) to investigate the importance of each aforementioned predictors in determining the daily daytime cycle of sap velocity. The second model (model 2) investigated the role of the same predictors at the time scale of one day; for this, the input variables as well as sap velocity were averaged over the period of the day with a PAR above 15 $\mu mol * s^{-1} * m^{-2}$.

To avoid possible co-variations due to a common daily cycle, for the first model it was decided to remove the daily pattern from the vapor pressure deficit and radiation, maintaining only the effects due to the variation from the average daily cycle. The global daily pattern was maintained as a separate variable, i.e., the hour of the day (Hour), and included among the predictors.
The two models were based on the assumption of a normal distribution of the data (family = "Gaussian") and parameterized to avoid over-fitting (Tab. 2.C.1) [71, 72].

2.3 Results

2.3.1 Climatic conditions

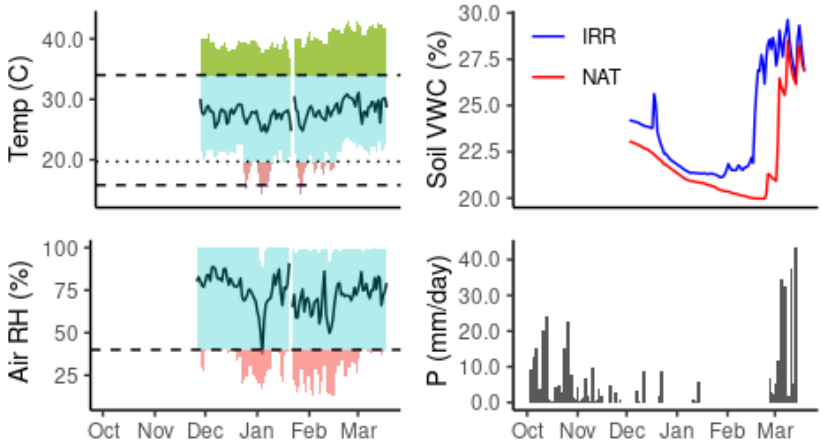

FIGURE 2.2: Climatic conditions during the study period. Left top: mean daily air temperature (solid black line), the thresholds for photosynthetic decline (34 and 15.8°C) and observed base temperature for vegetative growth (19.7°C) [132] (dashed lines) and the range of values (shaded area) are depicted. Left bottom: mean daily relative air humidity (solid black line) with the threshold of 40% (dashed line) and its range of observed values (shaded area). Right top: average soil VWC for the entire profile (10 to 60 cm) for the irrigated (blue line) and non irrigated (red line) plots. Right bottom: daily precipitation.

The average daily temperature during the experiment (26^{th} of November, 2019 -18^{th} of March, 2020) was 27.8 $\pm$ 1.5 °C, and the maximum and minimum recorded temperatures were 43.1 °C and 13.6 °C respectively (Fig. 2.2). Between January and February, the site experienced the hottest temperatures and the largest daily thermal oscillations, surpassing both the upper and lower thresholds for maintaining photosynthesis for several hours. Temperatures above the threshold at which photosynthesis declines (34 °C), were recorded throughout the entire period under analysis on average for 6.5 $\pm$ 1.5 hours a day (Fig. 2.A.1). Temperatures below the lower threshold for photosynthetic efficiency (19.7 °C), instead, occurred only in January and February when the Harmattan winds reached the site. Relative humidity fell below 40% for the first time in early December and, from late December until March, the site experience several hours with RH below 40% almost daily (Fig. 2.A.1), reaching up to fifteen hours per day below 40% in January. During our study period, the total precipitation was 116 mm, of which 92 mm fell in March while the remaining 24 mm were distributed in sporadic events from December to February. Prior to the onset of our study, in October and November 2019, the site received 222 mm of precipitation. The average soil VWC across the entire 10 - 60 cm profile was always higher in the irrigated treatment than in the control throughout the experiment. Soil VWC was above 21% in January and February in the irrigated plot, while in the non-irrigated (control) plot, VWC continued to decline below 20% over the same period. VWC quickly recovered in both treatments in March, when rains resumed.

2.3.2 Leaf area index (LAI)

Overall, LAI declined steadily throughout the experiment both in the irrigated and in the control plot. Throughout December, the LAI remained constant and started to decrease in January, in both treatment plots, at the same time as the number of days with RH < 40%

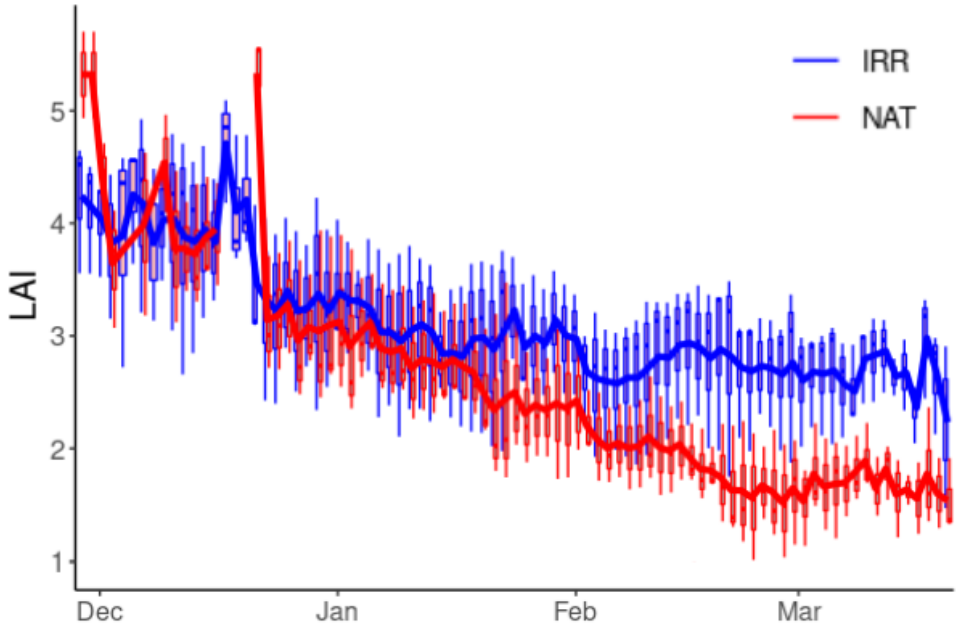

FIGURE 2.3: Leaf area index (LAI: $m^2[leaf] * m^{-2}[soil]$) in the two watering treatments: irrigated (blue) and control (red), throughout the observed dry season. The lines represent the three day-moving averages of the LAI times series. Box-plots represent the variability between the three sensors in each plot for every date.

started to increase (Fig. 2.3, Fig. 2.A.1). In February, LAI continued to decrease, faster in the non-irrigated (control) plot than in the irrigated one. At the end of the study, the estimated LAI was 2.7 $m^2[leaf] * m^{-2}[soil]$ at the irrigated plot and 1.5 $m^2[leaf] * m^{-2}[soil]$ at the non-irrigated plot compared to an estimated 4 $m^2[leaf] * m^{-2}[soil]$ in the beginning of the study for both treatments (Fig. 2.3). The LAI, thus, dropped by approximately 32.5% in the irrigated plot and by approximately 62.5% in the control. According to the GAMM, from mid-February onwards, LAI in the irrigated plot was significantly higher than in the control plot (Fig. 2.B.1). The total litter collected throughout the entire experiment was greater in the control (309 $g[dry] * m^{-2}$) than in the irrigated (247 $g[dry] * m^{-2}$) treatment. Most of the shedding appears to have occurred in late December for both treatments, while in March, with the resumption of rain, the litterfall went to zero (Fig. 2.B.2). The average litterfall was lower in the irrigated plot, notably in the first week of January (Fig. 2.B.2), when air humidity dropped below 40% for the first time. (Fig. 2.2). This is in agreement with the results of LAI dynamic that evidenced a difference in LAI between plots at the end of the season resulting from a steadily larger foliage loss in the non-irrigated plot (Fig. 2.3, Fig. 2.B.2).

2.3.3 Sub-daily patterns of sap velocity in response to climatic drivers

Figure 2.4 shows the response of sap velocity to VPD under different levels of PAR above the canopy in the two treatments. At low VPD values (<1 kPa) trees in the control plot seem to have transpired more than those in the irrigated plot. Under high VPD (> 4 kPa), measurements of sap flow velocity from trees from both treatments presented a high dispersion regardless of the PAR level. Under intermediate VPD (2-4 kPa), sap velocity appeared to respond more to PAR in trees from the irrigated plot. In Figure 2.5 is reported the average daily cycle of sap velocity during the 25% most and least stressing days over the study period. Sap velocity at low VPD followed the same cycle in the two plots without significant differences (Fig. 2.5 B). Although, at low VPD the control trees presented a tendency to reach a higher

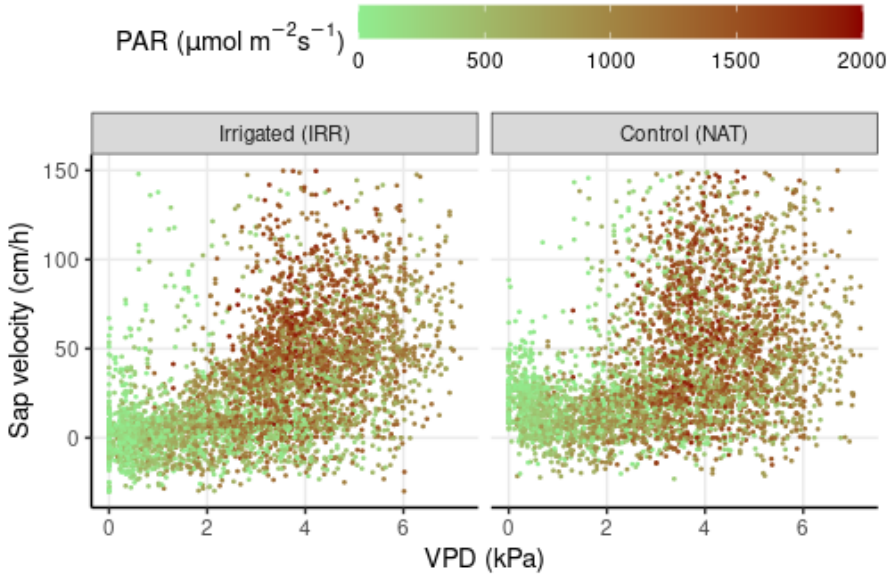

FIGURE 2.4: Sub-daily daytime measurements of cacao trees sap velocity in response to varying VPD: in the irrigated plot (left) and in the control plot (right) during the dry Harmattan season. Symbol colours depict PAR levels measured above the canopy (in $\mu mol * s^{-1} * m^{-2}$).

midday sap velocity. In days when VPD was high the average sap velocity peaked around 70 cm/h for both treatments but the irrigated plot presented on average a sap velocity higher than the control during the late mornings while the control tended to maintain a higher sap velocity in the late afternoon (Fig. 2.5 A). In the morning the control presented a peak in sap velocity around 6 a.m. (20 cm/h), regardless of the level of VPD. A similar phenomenon was found for the irrigated plot in days when VPD was high. Both Figure 2.4 and 2.5 hinted to some behaviours that were not always easy to grasp, thus the importance of the study with the two BRT models.

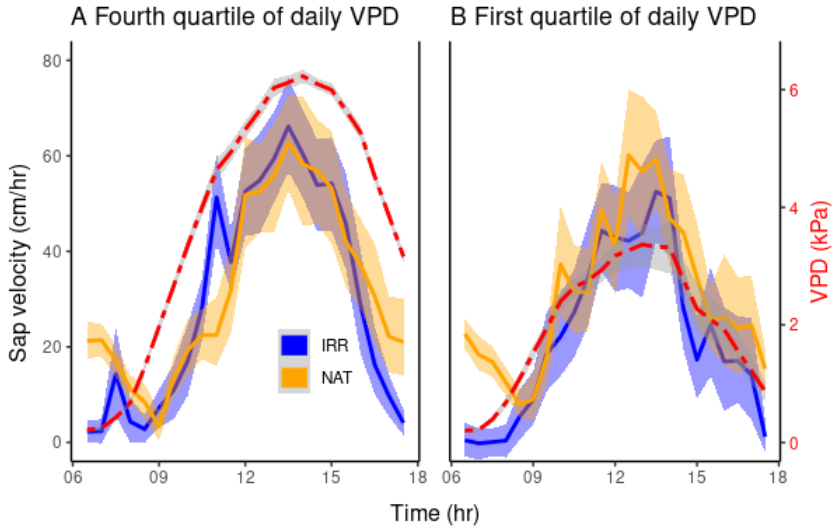

FIGURE 2.5: Sap velocity average daily cycle for cacao trees under high (A) and low (B) VPD conditions. The dashed line represents the average VPD cycle. The average cycles for sap velocity and VPD were obtained using the data from the 25% most and least stressing days of the dry Harmattan season 2019/2020. The shadings depict the the 95% confidence interval.

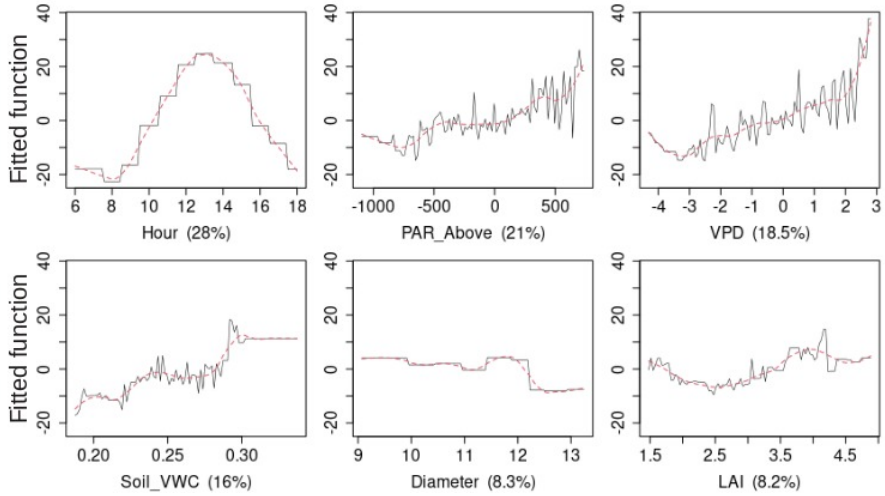

FIGURE 2.6: Overview of daytime sap velocity response to the main environmental drivers as identified with a BRT model (model 1). The responses are calculated on half-hourly data during the entire period of this study. Functional shapes of the response of sap velocity to the environmental variables: VPD, PAR, Soil VWC plus Hour, LAI and tree diameter. PAR and VPD were expressed as variations from the respective daytime cycle. Each variable was presented with the relative weight of its variation in that of sap velocity within parentheses.

The main drivers of half-hourly variations in sap velocity during the day were identified by means of a BRT model (model 1) (Fig. 2.6). The model averted over-fitting and was considered to be stable (training data correlation = 0.885; cross-validation correlation coefficient = 0.741). A regression analysis of predicted against measured values for the test data set showed that model 1, at low values (up to 30 $cm * h^{-1}$), slightly overestimated half-hourly sap velocity, otherwise it underestimated sap velocity (Fig. 2.C.1). Once the effect of the daily cycle (Hour), which has a relative influence of 28.0% in explaining sap velocity, was removed, the prevalent environmental variables explaining the variability in sap velocity were PAR above the canopy (21.0%) and VPD (18.5%), followed by soil VWC (16.0%). The evolution of LAI over the season in the two plots explained 8.2% of the variability, while tree diameter, proxy for the different trees, accounted for 8.3% of the total variability.
Sap velocity responded linearly to the variations of VPD around its mean daily cycle (Δ VPD) up to 2 kPa. Beyond this point, the BRT model suggests an increase in the slope of this relationship. The variability in PAR above the canopy was a key driver of sap velocity. When PAR was above-average compared to its mean daily cycle (Δ PAR >0), sap velocity increased with PAR in a linear fashion. For below-average PAR (Δ PAR <0), sap velocity remained relatively stable until Δ PAR reached -500$\mu mol * s^{-1} * m^{-2}$. Beyond this point, the response of sap flow to PAR declined and then stabilized. Sap velocity increased with soil VWC up to 0.24 $m^3 * m^{-3}$ and plateaued until it reached a threshold value of 0.27 $m^3 * m^{-3}$. Beyond this value, sap velocity increased steeply until VWC reached a value of 0.29 $m^3 * m^{-3}$. At a VWC above 0.29 $m^3 * m^{-3}$ the response of sap velocity flattened out until field capacity (0.34 $m^3 * m^{-3}$)(Figure 2.6). The LAI and tree diameter showed a rather flat relation with sap velocity and were negligible drivers of sap velocity at the sub-daily timescale.

In the sub-daily model, the interactions between VPD and PAR and VPD and LAI were more important than the other interactions (Tab. 2.2) which means that VPD modified the sap velocity response to both LAI and PAR significantly. When VPD and PAR were low compared to the average daily cycle, sap velocity was very low (Fig. 2.7). When VPD was high, the sap velocity was very high, for any value of PAR. Similarly, when PAR was high, sap velocity was high and stable whatever the value of VPD, except when VPD was very high, where

	Hour	Diameter	VPD	PAR_Above	LAI	Soil_VWC
Hour	0	15532.81	43578.24	40167	8701.57	13663.24
Diameter	0	0	23831.45	12599.22	10280.22	25915.23
VPD	0	0	0	**82788.32**	**71754.54**	59080.78
PAR_Above	0	0	0	0	35495.65	23574.91
LAI	0	0	0	0	0	27616.26
Soil_VWC	0	0	0	0	0	0

TABLE 2.2: Interactions between the variables considered in the BRT Model 1 in explaining cacao sap velocity at a sub daily timescale. For each pair of variables it is reported the mean value of the residuals, whose magnitude represents the strength of any interaction effect. In bold are reported the interactions considered strong, thus significant, by the model.

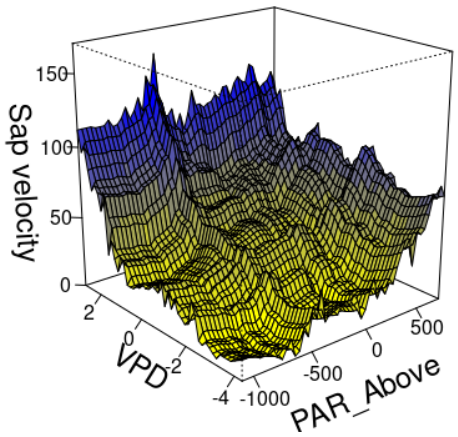

FIGURE 2.7: Three-dimensional partial dependence plots for the interaction between VPD (ΔkPa) and PAR ($\Delta \mu mol * s^{-1} * m^{-2}$) variations from the mean daily cycle in the BRT model 1 for half-hourly sap velocity ($cm * h^{-1}$) in cacao trees. All variables except those plotted are held constant at their mean values.

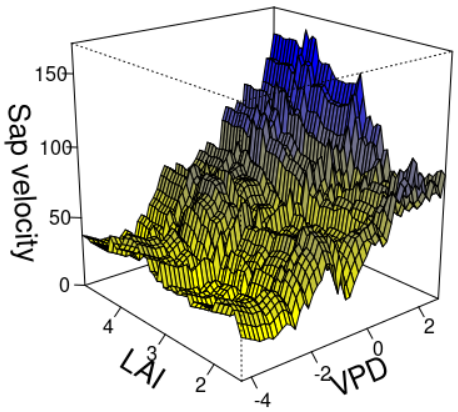

FIGURE 2.8: Three-dimensional partial dependence plots for the interaction between LAI ($m^2[leaf] * m^{-2}[soil]$) and VPD (ΔkPa) variation from the mean daily cycle in the BRT model 1 for half-hourly sap velocity ($cm * h^{-1}$) in cacao trees. All variables except those plotted are held constant at their mean values.

sap velocity was very high. When VPD and LAI were low, the sap flow was also very low (Fig. 2.8). When VPD was low, the sap velocity remained low, whatever the value of LAI. When LAI was low, sap velocity increased with VPD to a high value. But when LAI and VPD were high, sap velocity increased greatly, indicating that there was a clear positive synergistic effect on sap velocity between VPD and LAI. The potentially interesting interaction between VPD and soil VWC was not found strong enough to be considered relevant according to model 1 (Tab. 2.2).

2.3.4 Daily variations of sap velocity in response to climatic drivers

The BRT model based on the daily averages of sap flow velocity rendered a strong training data correlation (0.944), a good cross-validation correlation (0.803). Thus, the model was found to be stable and reliable. An evaluation of predicted against measured values on the test data showed that model 2 predicted well sap velocity despite a slight underestimation at high daily average sap velocities (above 57 $cm * h^{-1}$) (Fig. 2.C.2). Furthermore, when scaling up from the half-hourly to the daily analysis, the weight of the predictors on sap velocity changed (Fig. 2.9). The variability in daily sap velocity was mostly explained by LAI (27.2%) and soil VWC (21.4%). The relative importance of radiation (PAR) and VPD decreased to 18.1% and 17.0% respectively. 16.3% of the variability in sap velocity was explained by variations in trunk diameter.

	PAR_Above	LAI	Soil_VWC	VPD	Diameter
PAR_Above	0	2692.77	340.99	**5507.51**	4970.65
LAI	0	0	**19350.06**	5019.99	5275.63
Soil_VWC	0	0	0	510.93	1408.86
VPD	0	0	0	0	2304.21
Diameter	0	0	0	0	0

TABLE 2.3: Interactions between the variables considered in the BRT Model 2 in explaining cacao sap velocity at the scale of one day. For each pair of variables it is reported the mean value of the residuals, whose magnitude represents the strength of any interaction effect. In bold are reported the interactions considered strong, thus significant, by the model.

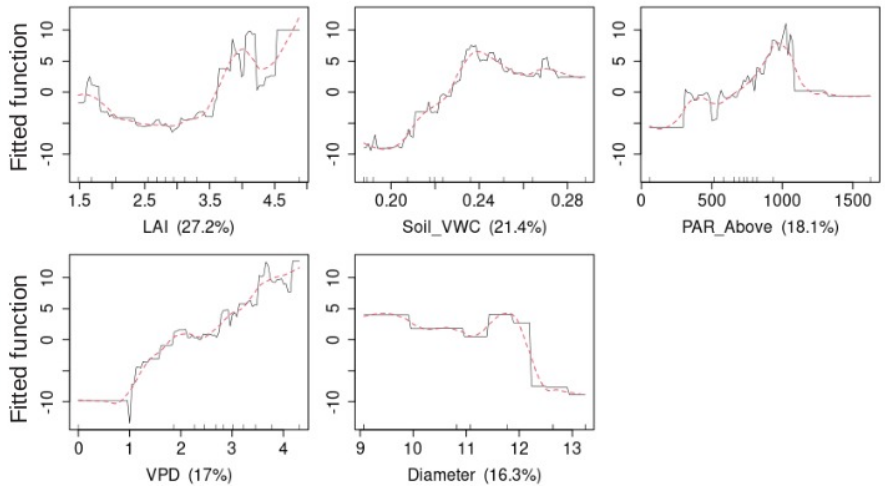

FIGURE 2.9: Overview of cacao's daily sap velocity response to the main environmental drivers according to a BRT model (model 2). The responses are calculated for daily averages during the entire period of this study. Functional shapes of the response of sap velocity to the environmental variables: VPD, PAR, Soil VWC and two not-environmental variables: LAI and tree diameter. Each variable is presented with the relative importance of its variation on that of sap velocity within parentheses.

The shape of the response curves of daily sap velocity to the considered variables was different to that observed for half-hourly values (Fig. 2.6, 2.9). Sap velocity increased nearly linearly with LAI above 3.5 $m^2[leaf] * m^{-2}[soil]$. Sap velocity was insensitive to LAI, for values between 2 and 3.5 $m^2[leaf] * m^{-2}[soil]$. Below $2m^2[leaf] * m^{-2}[soil]$ and down to 1.5 $m^2[leaf] * m^{-2}[soil]$ (minimum value measured in our study), sap flow velocity also responded to changes in LAI, increasing as LAI was lower. Sap flow velocity increased linearly with soil VWC until a threshold level of 0.24 $m^3 * m^{-3}$ (approximately -0.16 MPa for our soil), past which it plateaued. The shape of the response curve of sap velocity to mean daily PAR was almost linear in the range from 0 to 1100 $\mu mol * s^{-1} * m^{-2}$. Beyond this value, the response of sap velocity captured by the BRT model leaned on few points, thus was not considered reliable. Finally, the mean daily sap velocity increased linearly with daily average VPD in a similar fashion to that observed in the half-hourly model 1 (Fig. 2.6, 2.9).

A significant interaction was found between LAI and soil VWC and, to a lesser extent, between VPD and PAR (Tab. 2.3). When LAI was low, sap velocity increased slightly with soil VWC (Fig. 2.10). But when LAI reached the value of 3 $m^2 * m^{-2}$, the increase with soil VWC became much steeperand sap velocity reaches very high values. The interaction between average daily VPD and PAR, although less pronounced, showed that the increase in VPD and PAR have a synergistic effect on sap velocity (Fig. 2.11). Few PAR values were recorded

above 1100 $mumol * s^{-1} * m^{-2}$ and the apparent decrease in sap velocity after this value was not interpretable. At the one-day time scale, no interaction between mean soil VWC and VPD was detected by model 2 (Tab. 2.3), similarly to what was found at the sub-day level (Tab. 2.2).

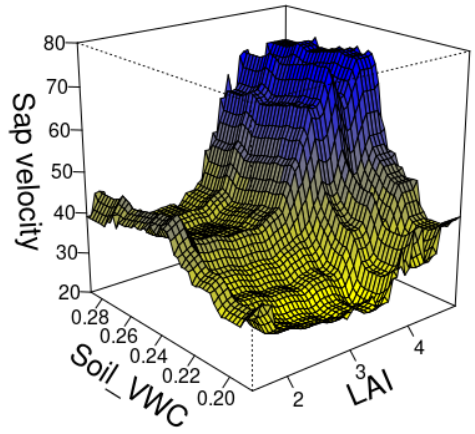

FIGURE 2.10: Three-dimensional partial dependence plots for the interaction between soil VWC ($m^3 * m^{-3}$) and LAI ($m^2[leaf] * m^{-2}[soil]$) in the BRT model 2 for daily average sap velocity ($cm * h^{-1}$) in cacao trees. All variables except those plotted are held constant at their mean values.

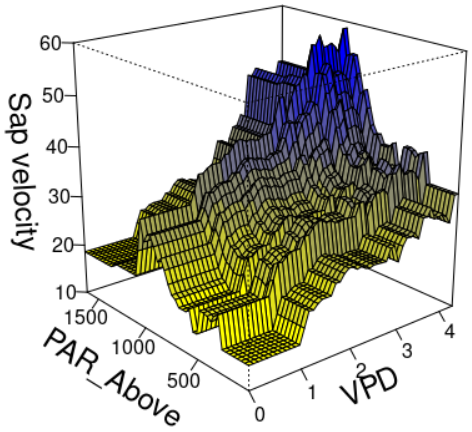

FIGURE 2.11: Three-dimensional partial dependence plots for the interaction between PAR ($\mu mol * s^{-1} * m^{-2}$) and VPD ($kPa$) in the BRT model 2 for daily average sap velocity ($cm * h^{-1}$) in cacao trees. All variables except those plotted are held constant at their mean values.

2.4 Discussion

2.4.1 Climate

The measured climate of the 2019-2020 dry season (Fig. 2.2) was representative for the conditions experienced by cacao during this time of the year in the Eastern region of Ghana. As soil VWC approached the wilting point in the control plot, air humidity dropped even below 20% and temperatures were sub-optimal (Fig. 2.2, Fig. 2.A.1), on a daily basis, the measured conditions were found to be stressful according to the definitions given for soil and atmospheric stresses (see Section 3.1).

2.4.2 Canopy

Despite the occurrence of high temperatures, the trees were able to cope with the climate in December. We argue so because we did not observe any decline in LAI in either watering treatment, in line with previous studies with no atmospheric stress [161, 162]. Leaf shedding is a common response to drought of tropical and subtropical species [31, 70], as it allows trees to reduce transpiration rates and, hence, avoid hydraulic failure. In line with the idea that cacao trees apply this drought-coping strategy, during the more severe part of the dry season (from January onwards), LAI decreased in both watering treatments, although at a faster rate in the control plot (Fig. 2.3), supporting the idea that leaf shedding helps cacao to cope with soil drought. However, given that LAI also decreased in the irrigated plot throughout the experimental period, it is likely that trees in the irrigated plot also suffered from water stress. It could be argued that the irrigation level (60 L/tree on alternate days equivalent to approximately 9.6 mm of rain) was not sufficient to completely mitigate soil drought (Fig. 2.2), despite being in line with the water requirement of a mature tree found in literature [39].

Alternatively, it can be interpreted as the atmospheric drought having contributed to leaf shedding. This latter interpretation is supported by the more abundant litter production observed in December, when the soil VWC was significantly higher in the irrigated plot than in the control but air humidity and temperature reached values above stressful thresholds (Fig. 2.A.1, 2.B.2). The timing of the drop in LAI suggests that the key atmospheric condition impacting the canopy was the extremely low air humidity to which cacao leaves might not be adapted, especially considering that cacao developed under very high relative air humidity [40].

By the end of the dry season, the control plot had lost two thirds of its foliage, twice the loss in the irrigated plot. In light of the lack of interaction between VPD and soil VWC in explaining sap velocity (Tab. 2.2, 2.3) it could be assumed that the effects of atmospheric and soil stress on LAI were independent. If this assumption is accepted, the difference in LAI drop between the two plots must have been driven by the difference in soil VWC (Fig. 2.2, 2.3). The fact that the net loss in LAI in the control relative to that in the irrigated treatment (-62.5% vs. -32.5% over the course of the experiment, respectively) was much larger than the difference in litterfall between the two treatments (309 $g[dry] * m^{-2}$ and 247 $g[dry] * m^{-2}$, respectively - a relative difference of 25%) suggests that some leaf flushing might have occurred in the irrigated treatment. This hypothetical leaf flushing in the irrigated treatment never sufficed to counterbalance the leaf shedding, possibly due to a limitation in carbon to invest in leaf production, resulting in a drop in LAI. Further, more specific, studies to investigate the effects of atmospheric and soil drought on leaf flushing dynamics would be needed in order to properly characterize such effects.

Based on the above reasoning, the loss of canopy density in the irrigated plot was imputable only to the atmospheric stress, while in the control the additional loss was caused by the soil stress and the interaction between the two stresses, if present. Thus, our results on the LAI

evolution and litterfall production show that the impact of atmospheric stress (VPD) on the canopy during the dry Harmattan season may be of similar magnitude, if not greater, than that of soil stress (soil VWC), regardless of the possible interaction between the two stresses (Fig. 2.3). If the two stresses were independent then the depressing effects of soil and atmospheric stress were the same, one third of the initial canopy density each. While the existence of an interaction between the two would mean that the soil stress impacted the canopy less than the atmospheric one. The major role found for the aerial stress is in line with Hutcheon at al. (1973) [112], who concluded that the beneficial effect of irrigation on cacao total biomass production was limited when in presence of atmospheric stress. Other authors reported the same [39, 132] but, to our knowledge, this was the first attempt to quantify the effects under field conditions in West Africa. Our results contrast with those from a study in which LAI did not change in response to a 73% reduction in precipitation over 13 months [162]. It must be noted that the experimental conditions between this experimental site in Sulawesi, Indonesia and ours in Eastern Ghana differ greatly. For the site in Sulawesi, it was suggested that the reduction in incoming precipitation was insufficient to impose stressful conditions due to the high mean annual rainfall (2,844 mm) [90]. Furthermore, at the Indonesian site, daily mean relative air humidity never dropped below 69%, in contrast to our study site, where relative air humidity often fell below 40%, and where we found a significant drop in LAI, irrespective of the irrigation regime.

2.4.3 Sap velocity

The two models developed (half-hourly: BRT model 1, daily: BRT model 2) allowed us to obtain a good estimate of the environmental and climatic drivers of sap velocity on a half-hourly and daily scale. This allowed an effective investigation of the impacts of atmospheric and soil water stress on cacao during Harmattan season. Up to now, in cacao, the response of transpiration to atmospheric drought stress had only been studied under controlled conditions, in young individuals and never in combination with limited water availability [59, 87, 155]. Previous studies addressing the effects of climatic factors (VPD, soil VWC and PAR mainly) on transpiration did not find clear patterns [87, 132]. Fraga et al. 2020 [87] argued that large temporal and spatial heterogeneity, mainly in VPD and soil water, could account for some of the unexplained variability in transpiration. We argue that our approach of separating the instantaneous half-hourly effect from the integrated daily effects allowed us to disentangle some of these patterns. Furthermore, to our knowledge, this is the first study that addressed the effect of the interactions among variables on sap velocity.

Soil VWC and LAI did not change significantly at the time scale of one day. Despite their lack of variation at the sub-daily level, soil VWC and LAI varied over the season, setting different daily conditions for sap velocity variation in response to the variability of the remaining variables (PAR, VPD) (Fig. 2.4,2.5,2.6). The BRT model 1 showed that of these two conditions, soil VWC mattered more than LAI (Fig. 2.6). This suggests that water availability matters more than the total leaf area available for transpiration in determining sap velocity. In cacao the transpiration is largely performed in the outer crown, while the shade leaves are far less active [132, 161]. The loss of foliage probably interested mostly sun leaves [161] but the trees were probably able to adapt the lower strata of the canopy to the new conditions [199, 214], minimizing the direct effect of LAI on sub-daily sap velocity. This was reflected in the flat response of sap velocity to LAI in model 1 (Fig. 2.6). Instead, the different soil VWC over the season appeared to matter more in determining the sub-daily sap velocity possibly hinting that cacao might be more limited by its root water uptake and by the conductivity of the vascular system rather than by the canopy conductance, in line with [125].

Within a day, sap velocity responded mainly to the variation of PAR and VPD and their synergistic effects (Fig. 2.7). At the sub-daily time scale, PAR was the principal driver for sap

velocity, as long as VPD did not exceed the mean daily cycle by more than 2 kPa. Beyond this value for the anomaly, it is possible that for most part of the day stomatal regulation was no longer effective in dealing with the high water demand from the atmosphere. This is supported by the fact that irrigation was not able to limit water loss when VPD was extremely high and the trees ended up transpiring as much as the control plot (Fig. 2.5 A). Moreover, the observed peak in sap velocity up to 20 cm/h in the morning cannot be explained by the extremely low values of VPD and PAR (Fig. 2.5 A, B). However, said peak may be explained as a phenomenon of recovery from embolism [150]. It has been described in other plants that, following embolism due to hydraulic stress, the plant applies a positive root pressure to force the gas to dissolve. Such recovery strategy of embolism removal is often put in place concurrently to the start of transpiration in the morning [96, 150, 207]. The control trees, constantly stressed by the low VWC, may have had to adopt this strategy regardless of the VPD level, as the early morning peak in sap velocity suggests (Fig. 2.5 A,B). The irrigated trees did not present the same peak in the early morning in days with moderate-low average VPD but irrigation might have not prevented embolism when VPD was high, leading to an early morning sap velocity peak compatible with the refilling of vases (Fig. 2.5 A, B). This behaviour is an ulterior element in favour of the fact that irrigation is not sufficient when the atmospheric stress is too strong. Cacao plants naturally occur in the understorey of tropical forests, where light is limited and VPD is rarely high [163]. Hence, we could expect that stomatal behavior is finely-tuned in cacao to respond to variations in light availability, to maximize photosynthesis [16, 199], but it might not be adapted to regulate water loss under increasing VPD, as we observed in our experiment (Fig. 2.4). Before this study, the atmospheric component of water stress had rarely been taken into account because such conditions are seldom met in most of the cacao-growing areas worldwide [90, 210]. Nonetheless, most of the West African cacao belt undergoes atmospheric stress on a quasi-seasonal basis under the influence of the Harmattan winds [2] and the chances of harsher atmospheric stress in the region will increase with climate change [209]. Given that west Africa includes the two leader of cacao production worldwide (Ivory Coast and Ghana) [80], it should be recognized the due importance to the atmospheric stress.

At the seasonal time scale (effects on daily averages), the effects of PAR and VPD, as well as their interaction, were maintained but, at this time scale, soil VWC played a major role as well (Fig. 2.9, 2.11). The response curve of sap velocity to soil VWC in figure 2.9 highlights that, under our experimental conditions, the soil reached a critical soil VWC at which cacao water extraction capacity was challenged (0.24 $m^3 * m^{-3}$, approximately -0.16 MPa for our soil). A significantly lower critical value of soil water potential for water extraction (-0.079 MPa) has previously been reported for young cacao plants under field conditions in Brazil [87]. The difference between the Brazilian study and ours is possibly related to the differences in genetics, age, and rooting depth considered in the two experiments. Here, we studied mature trees subject to water stress on a regular basis every year. These two elements (age and prevailing climate) imply that our trees would have had a more developed rooting system, capable of exploring a larger soil volume.

Contrary to our initial expectations, our results from the BRT models did not clearly show an interactive effect between atmospheric and soil drought on cacao transpiration, represented in the models by VPD and soil VWC (Tab. 2.2, 2.3). Yet, our results cannot completely rule out our initial hypothesis as, for example, Model 1 highlighted a not significant but strong link between VPD and soil VWC (Tab. 2.2). The BRT models could have failed at capturing such interaction because of the paucity of observations when atmospheric and soil drought co-occurred in the control plot, a key requirement to train the model. Furthermore, the provided level of irrigation might have not been sufficient to completely alleviate the soil stress in the irrigated part. If this was the case, the small Δ VWC between plots might have made more complicated for the model to capture an interaction between soil and atmospheric drought

across treatments as well.
At the seasonal time-scale (daily average measurements), we found that the response of sap velocity to both atmospheric and soil drought was modulated by the interaction with LAI. We found that beyond certain threshold values of both VWC (0.24 $m^3 * m^{-3}$) and LAI (3.5 $m^2[leaf] * m^{-2}[soil]$), sap velocity did not respond to further increases in either variable. The daily average sap velocity measured under these conditions, high VWC and LAI (76 $cm * h^{-1}$), could be the maximum supported by the root and vascular system of cacao, although this should be further tested in other climates. When soil VWC was below 0.24 $m^3 * m^{-3}$, sap velocity was strongly responsive to soil VWC variations, regardless of the LAI, whereas for a given soil VWC, the response of sap velocity to changes in LAI was less pronounced (Fig. 2.10). This behaviour is compatible with the higher importance of soil VWC over LAI found in model 1 (Fig. 2.6) and with the more dynamic shape for the response of sap velocity to soil VWC and flatter one for LAI in model 1 (Fig. 2.6) and for most of the range (1.5 to 3.5) in model 2 (Fig. 2.9). Furthermore, the irrigated trees only showed signs of probable embolism recovery in the mornings of days with a high VPD, suggesting that they were not able to uptake enough water from the soil to avoid embolism (Fig. 2.5 A). While in the control the morning peak in sap velocity, that we proposed as a sign of embolism recovery, was present with approximately the same magnitude under high and low VPD (Fig. 2.5 A,B). This suggests that the main limitation for water transportation in the soil-plant-atmosphere continuum was found in the ability of the plant to extract water from the soil. The results discussed in this paragraph sustain the theory that cacao's transpiration is mostly limited by the root water uptake capacity rather than by the conductivity of the vascular system or the total leaf area, in line with [125].

2.5 Conclusions

For the first time, in this study, we assessed the effects of soil and atmospheric water stress on canopy transpiration of adult cocoa trees. We showed that under high soil and atmospheric water stress, irrigation decreased leaf shedding in response to limited water availability in the soil. Nonetheless, under a climate change scenario with harsher conditions experienced by cacao under the influence of the Harmattan winds, irrigation might not suffice to sustain cacao production. In fact, our study highlights that cacao transpiration increases with high VPD, which could further compromise soil water availability and eventually aggravate soil stress. The use of shade nets or of shade trees with a deep rooting system, as previously suggested [174, 225], could be a key requirement for cacao farming in the future to partially alleviate atmospheric drought stress during harsh and stressing periods. This because the seasonal long dry season might worsen with the increasing warming up of the region that would potentially increase the evaporative power of the atmosphere and worsen the water stress, especially the atmospheric one. Deep-rooted vegetation and/or shading nets are also a possible solution as they would diminish the detrimental impact of increased atmospheric drought by buffering temperature and relative air humidity. This prevents stressful values for temperature and relative air humidity without adding competition for water extraction to the list of stresses for cacao trees.

Appendix

2.A Atmospheric stressors

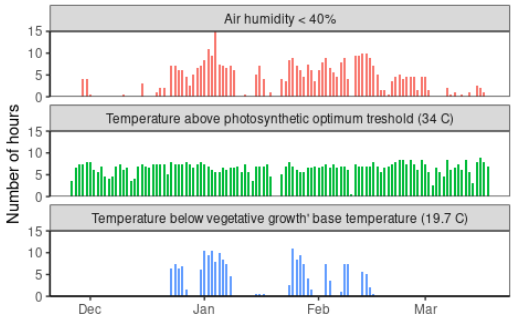

FIGURE 2.A.1: Number of hours per day under stressful climatic conditions for cacao trees according to values reported in [56, 93, 132, 154, 178]; each bar is one day. Top: air humidity below 40%; middle: temperature above photosynthetic optimum threshold (34 °C); bottom: temperature below the base temperature for vegetative growth (19.7 °C).

2.B Leaf area index

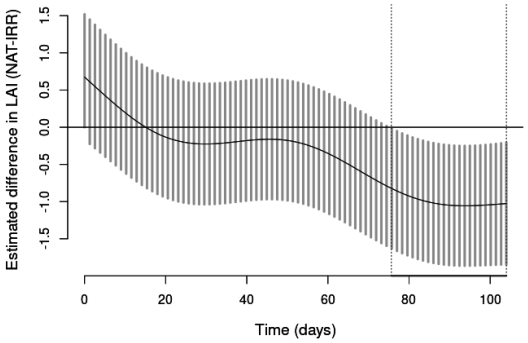

FIGURE 2.B.1: Difference in estimated leaf area index (LAI) between the irrigated and the control plot. The fitted line is a generalized additive model and the shaded area is the 95% prediction interval. A shaded area non-overlapping with the zero-line indicates a significant difference between watering treatments.

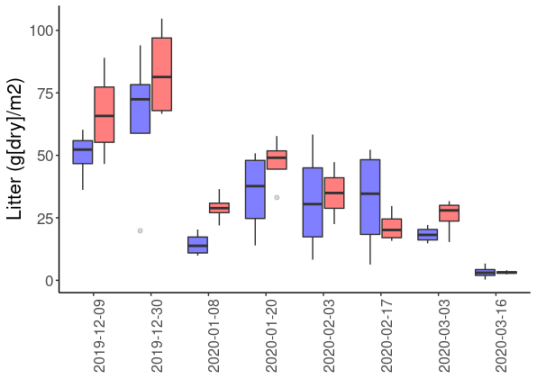

FIGURE 2.B.2: Litter production of cacao trees during the dry Harmattan season, in presence (blue) and absence (red) of irrigation. Box-plots represent variations between the four litter traps per treatment and date. Bold lines represent means per plot and date.

2.C Boosted Regression Trees analysis

2.C.1 parameterization of the models

	Step	Family	tl	bg	nt	tc	lr
Model 1	30 min	Gauss	0.01	0.75	100	3	0.1
Model 2	1 day	Gauss	0.001	0.75	100	3	0.05

TABLE 2.C.1: Parametrization of the BRT models to predict the transpiration during the day at a 30-minute time interval (Model 1) and at a daily time step (Model 2). A BRT model requires the definition of a set of hyperparameters:
family - the type of statistical error distribution characterizing the data, in our case Gaussian;
tolerance (tl) - the threshold in variance change under which to stop the model reiteration;
bag fraction (bg) - the fraction of dataset to use for the training of each tree. The remaining data is used at each step to cross validate the set of relations found;
number of trees (nt) - the number of trees necessary for optimal prediction. It is determined based on tl and bg;
tree complexity (tc) - the maximum level of interaction between variables to consider in a tree;
learning rate (lr) - determines the contribution of each tree to the growing model.
The seed number used was - 210920.

2.C.2 Evaluation of BRT models on the test data

To allow an independent evaluation of the BRT models, 25% of the field data was set aside to be used as a test subset of data and was not used at any point in the training of the BRT models. This section of the appendix presents the evaluation of the models (Model 1, Model 2) on this test data subset.

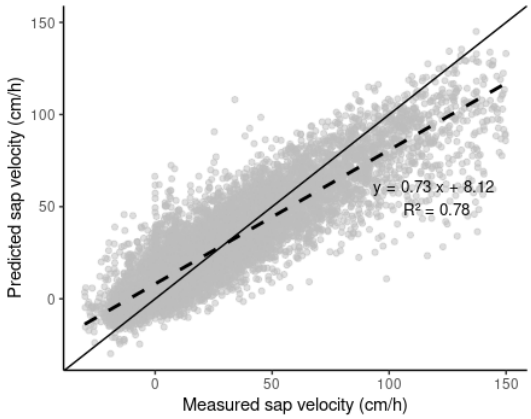

FIGURE 2.C.1: Observed (abscissa) vs. predicted (ordinates) sap velocity, the corresponding linear regression (dashed line) and y=x line (full black line) for the BRT half-hourly model (model 1) test data.

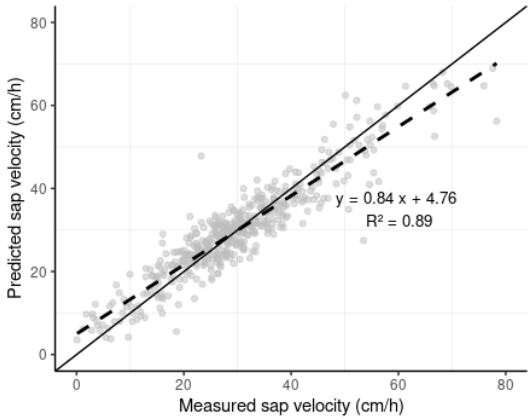

FIGURE 2.C.2: Observed (abscissa) vs. predicted (ordinates) sap velocity, the corresponding linear regression (dashed line) and y=x line (full black line) for the BRT daily model (model 2) test data.

Chapter 3

Influence of different seasonal climate types and their stressing components on the production and yield of *Theobroma cacao* during and after the dry Harmattan period in Eastern Ghana.

The results from the field experiment discussed in Chapter 2 strengthened findings from previous studies in controlled environment about the response of cacao to soil drought [87, 112], quantified the importance of atmospheric drought as a limiting factor for cacao's transpiration and shed light on the canopy deterioration caused by soil and atmospheric water stress. In the context of a mechanistic modelling of cacao, the results from the BRT models discussed in Chapter 2 gave an insight on the shape of the relations describing the response of transpiration to the environment and the existence of interactions between variables. These elements permit the extraction of approximated relations that can inform and guide the modelling exercise (Ch. 5). However, these result rely on data with limited replicates that may limit the possibility of generalizing these relations to other growing systems. Thus, other similar studies are needed to validate and strengthen the drawn conclusions about the short-term effects of drought on cacao's gross transpiration for different stressing situations.
Chapter 2 investigated and clarified the short-term effects of water stress, atmospheric and edaphic, on transpiration and LAI but did not address the short-term repercussions on the cacao plant's reproductive production. In the short-term, a drop in whole-plant transpiration, dependent on the transpiration rate as well as total leaf area, may have led to a lower total carbon assimilation, thus a drop in new biomass production [3, 5, 100, 126, 205]. Furthermore, one strategy that cacao puts in place to cope with water stress is to invest in root biomass to explore more soil volume [39, 162]. Given the lower carbon assimilation and the preferential investment of plant resources toward the roots, allocation to new and old reproductive organs of the plant might be impaired under hydric stress [39, 112]. Consequently, it was crucial to study the short-term consequences of soil and atmospheric water stress on the abundance of flower production, bean filling and cherelle development and wilting rate.

Moreover, the effects of a drought episode may initiate a chain of medium to long-term repercussions on pod formation and development. Chapter 2 discussed how the canopy degrades due to atmospheric and soil hydric stress. As a result, the plant will be inclined to heavily invest in the vegetative part when the rains resume [39]. From this follows that, depending on the severity of canopy degradation, the plant may neglect the reproductive organs to sustain the canopy refurbishing effort. This may translate in practice in trees delaying flowering and subsequent fruit set or being less inclined to fill the existing pods for few weeks after the stressing period. An accurate study to understand the medium to long term effects of drought on production would benefit from a mechanistic model capable of considering all aspects in a holistic way and the ripple effects of each delay and change. Although such a possibility is not viable as long as a model like CASE 2 is duly improved and validated, a first step would be to study the seasonal dynamics of fructification in relation to climate. Such a study will not explain the processes behind a change in seasonal production caused by a drought episode but may be useful for validation and to inform on the importance and nature of the effects on production.
Furthermore, Chapter 2 highlighted the role of irrigation in preserving the canopy and granting the plants more control over stomatal regulation. It remained to be studied how this partial alleviation of stress during a long dry Harmattan season or perhaps a complete alleviation of stress in other moments of the year could impact qualitatively or quantitatively the seasonality of the cacao tree's production. The objective of this chapter is to analyse and evaluate the changes in production that manifest during (short-term) or after (medium to long term) a period of stress contingently to the drought intensity and duration experienced by the plants under irrigation or not.

3.1 Introduction

Climatic parameters such as air relative humidity, temperature and rainfall as well as the occurrence of these under form of aerial or soil drought often shape the inter-annual variability in yield quantity and quality of many crops of the tropics [36, 45, 113, 121, 187]. These oscillations can lead to large year-to-year or even intra-yearly changes in prices of commodities as coffee, rice, oil palm, and cacao on which smallholder farmers across the globe rely for a steady income [79, 113]. Cocoa (*Theobroma cacao* L.) cultivation is a steady source of income for many smallholder farmers in underdeveloped countries, particularly in Ghana and Ivory Coast [8, 216, 230]. These countries account for roughly 60% of the global cacao dry bean production [80, 180], whose export determines a large part of their GDPs and can represent up to 70-100% of the household income of almost two million of smallholder farmers in the region [8, 216, 230, 237]. Furthermore, worldwide cocoa beans market worth is estimated in roughly 7 billion USD [80, 180].
Cacao origins are traced back to the rain-forest ecosystem where air relative humidity and temperatures are stable and water limitation is virtually inexistent, thus the physiological performance of cacao is adapted to its native climatic conditions [59, 87, 245]. Cacao optimum growth temperature range was found to be between 24°C at night and 30°C during the day [167]. The net photosynthetic efficiency and stomatal conductance, both more or less directly influencing biomass production, start declining above 33°C and below 15.8°C [132].
The climate over the west-African cocoa regions differs from the one in the zone of origin. In Ivory Coast and Ghana, climate is characterised by two wet seasons (monthly precipitation $>$ 100 mm) separated by a long main dry season, between mid-November and mid-March, and a shorter, minor dry season in late July until September. During these dry seasons cacao often experiences soil water drought as a consequence of the lack of rainfalls. The alternation of dry and wet seasons shapes cacao's production cycle into a main crop between October and March and a minor crop the rest of the year [46].
The long dry season is characterized by a dry north-easterly trade wind, the Harmattan, that conveys a dry air mass from the Sahara to the northern edge of the sub-Saharian cacao regions where it lingers [208]. When the Harmattan is present, the low air relative humidity allows large daily oscillations in air temperature, which can reach values as high as 44°C [2, 13] and as low as 12-14°C at night [102, 117]. Such extreme temperatures can severely impact cacao's physiology [132] and their wide daily oscillation was proven to inhibit the net growth and physiological performance of cacao [167]. Furthermore, it has been shown that low air relative humidity below 40%, a recurrent condition under the influence of the Harmattan winds, is a major constraint to biomass production in tropical environments, especially in combination with high temperatures [154, 178]. In line with [93] and the study in Ghana previously exposed in Chapter 2 it can be assumed that such conditions would be stressful for cacao as well. Consequently, when the Harmattan is present, in addition to the soil drought induced by the lack of rain, cacao is often exposed to atmospheric stress due to the raw low air relative humidity and the wide daily oscillations between temperature extreme values.
Both soil and atmospheric drought impact negatively on plant growth and productivity [44, 138] because they force the plant to partially or fully close their stomata to reduce transpiration water loss. This causes a reduction in CO_2 uptake to supply photosynthesis that, ultimately, inhibits growth and production of assimilates to feed the reproductive organs, the flowers and pods [153, 247]. For this reason during the dry periods flowering is reduced and, depending on the harshness of the drought event, the bean filling in ripening pods can be slowed down considerably [55, 175]. Besides, cacao presents a self thinning mechanism of cherelles (young pods) that is believed to be greatly linked to the incapability to properly feed all cherelles, for example under stress[155, 226]. As an example, the 2015/16 dry season, the harshest in recent history, led to record low yields for the following mid crop mostly due to

a high wilt rate and a strong reduction of the average bean size, suggesting a problem with bean filling [ICCO2016; personal communication Matthew Stolz, 2018].
It has been reported that the resumption of rain after a dry period is a strong cue for flowering [39, 58]. Nevertheless, after a long main dry season the trees prioritise refurbishing the canopy, lost due to drought, before investing again in reproduction [39, 58, 132] with two hypothetical consequences. First, the fructification for the next crop may be delayed considerably and some pod generations could end up being more or less exposed to the little dry season. Secondly, flushing of new leaves was found to be a strong sink for assimilates out-competing fruits [58, 155], possibly reducing the bean filling capacity of the trees in this phase. It is hypothesised that the specificity of each dry season and the subsequent rains and temperatures can have different ripple effects on cacao's seasonal production profile and volumes. Irrigation has been proposed [39, 112, 200] as a solution to contrast dryness and try to enhance cacao yield volumes and stability for farmers but its effectiveness has to be tested in the field to evaluate the short, mid and long-term beneficial effects on production [87].
Given the high socio-economic relevance of this crop at the regional and global scale, any oscillation in cocoa production in Ghana and Ivory Coast can have worldwide ripple effects. Thus, it is extremely important to better understand and foresee oscillations and changes of trend in production [79] due to climatic stresses and means to improve the stableness of the harvests, therefore the reliability of a steady income for many smallholder farmers. The purposes of this study were to (1) characterize the stressing periods over the season from cacao's perspective based on climate and soil water condition, (2) evaluate the influence of climate and soil water condition on the evolution / shape and abundance of the production cycle and (3) investigate the effectiveness of irrigation in granting higher volumes, better quality or more stable production.

3.2 Materials and methods

3.2.1 Study site and experimental design

The reproductive/productive cycles of two cocoa tree plots, with and without irrigation, were monitored throughout the duration of the experiment (3^{rd} December 2019 to 29^{th} March 2021) with a fortnightly counting of flowers and fruits categorised followed by collection of mature pods for post-harvest analysis. The study was conducted at the Cacao Research Institute of Ghana (CRIG) experimental station located at New Tafo Akyem in the Eastern Region of Ghana (6°13'53.7"N; 0°21'01.6"W; 203 m a.s.l.). The site has a warm and humid climate all year round except for two dry seasons. A long dry season with its centre between December and February, but whose beginning can be as early as mid-November and its end in March. A minor dry season, much less severe, occurs between the second half of July and the beginning of September. The temperature in Tafo fluctuates between an average monthly minimum of 20-22°C and an average monthly maximum of 29-33°C. Annual rainfall varies between 1150 and 1800 mm with an average value of 1565 mm per year [8, 15].
This study used seven-year-old cocoa trees of homogeneous genetic material planted with a spacing of 2.5 x 2.5 m (1600 trees ha^{-1}) in the shade of *Gliricidia sepium* trees with a density of 10 ha^{-1}. The plantation consisted of four blocks with 10 plots each. Each plot contained 40 trees organised in five rows of eight trees. In November 2019, two plots of 40 Amelonado hybrid trees with an average canopy height of 3 m were selected for the study. The plots were selected to be at least 20 m away from the nearest shade tree to be considered as a 'typical West African full sun system'. The two study plots were separated by ten rows of cocoa trees to avoid any edge effect or interaction between the two. From 26^{th} of November 2019 to 29^{th} of March 2021, trees in one plot (irrigation treatment) were irrigated during dry months (< 100 mm/month) with 60 L per tree (equivalent to 9.6 mm) on alternate dates using a hose, while trees in the second plot (control) received only ambient rainfall.

3.2.2 Production and post-harvest data

Every fortnight a team of four technicians went to the field to record the number of flowers and fruit at various stages of development/ripening on each of the 40 trees in both plots, with or without irrigation. Seven categories were considered:

- Open flowers at the time of counting, done in the morning
- Set, the new fruits that appeared between counts (approximately up to 2.5 cm in length).
- Cherelles, i.e. young fruits in the pod's structural expansion phase lasting 6 weeks (approximately between 2.5 and 12 cm in length)
- Pods, all fruits whose length to diameter ratio was stable, a sign that the structural growth phase was finished or almost finished and that the pod filling phase had begun (approximately over 12 cm). Fruits were included in this category on average for 8 weeks.
- Ripe pods, fruits with a stable length to diameter ratio that showed signs of colour change. Fruits remained in this category for about three weeks before harvest.
- Diseased (black pods), all fruits, irrespective of category, showing signs of infection with *Phytophthora spp.*
- Wilted, all fruits (mainly Set or Cherelles) that were wilted.

Two technicians counted tree by tree from different points in the field while the other two recorded the values for each category on a paper form and, at the end of the count, compared the values of the two counts to check for count inconsistencies and, if necessary, the tree in question was checked again. In addition, to keep track of the count over time and check for losses between the two count dates, each new fruit (Set: < 15 days) was recorded with a pin next to the fruit. During the count, it was verified that the number of pins corresponded to the number of fruits at any stage on the floral cushion in question and pins were added where new fruits (Set) were found. In order to simplify and standardize pod counting and marking operations, only the portion of the plant up to 2.5 m was considered. This was considered acceptable because a pod count on the entire high of the trees ($\tilde{3}$.2 m) showed that the upper canopy (above 2.5 m) contained between 0% and 13% of the total pod load. Furthermore, it was decided to remove all the sets one week before the beginning of the experiment (26^{th} of November 2019) and at the same time as the beginning of irrigation in order to verify from the first date, 4^{th} of December, the difference in new fructification with and without irrigation.

Finally, the pods collected at the end of the cycle were collected by tree, grouped by treatment and then processed according to the protocol in use at the CRIG. The protocol dictated that after harvesting all pods from the same plot were weighed and, after two days, opened to obtain the fresh weight of the cocoa beans. Then, keeping the beans separate between the two plots, they were fermented in more or less voluminous containers depending on the quantities involved. The total fermentation time varied between 6 and 8 days depending on the climate, with the heap being turned every two days. Fermentation was followed by drying in the sun until a moisture content of less than 7 % was reached. The mass of dried beans and the number of beans in 100 g were then recorded by treatment.

3.2.3 Environmental data

The daily average soil volumetric water content (VWC) was recorded at four depths (10, 20, 40, and 60 cm) in two locations per plot, equidistant (170 cm) to all surrounding trees and on a flat terrain by means of TEROS 10 capacitance probes (METER group, Pullman,WA, USA) using the manufacturer's calibration for a generic mineral soil. A value of soil VWC per probe was recorded on a CR800 datalogger every 30 minutes from November 26^{th} 2019 to March 29^{th} 2021. In this study these data were then averaged over the day and across all layers and both locations in each plot to obtain a daily value per plot. The latter value was then expressed as a fraction of transpirable soil water (FTSW) based on the laboratory measurements of the average VWC at field capacity (FC) and permanent wilting point (PWP), 34% and 13% respectively [133, 235]. The air relative humidity,temperature, radiation, wind speed and atmospheric pressure were recorded every 5 minutes by an automated ATMOS-41 all-in-one weather station (METER group, Pullman,WA, USA) part of the Trans-African Hydro-Meteorological Observatory (TAHMO) [92] and situated within the premises of CRIG, few hundred meters apart as the crow flies from our field. The atmospheric vapour pressure deficit (VPD) was in accordance to the FAO-56 Penman-Monteith method [6] by means of the Python package *'opencroplib==0.1.5'* [116].

3.2.4 Stress thresholds definition

For the purpose of this study, it was necessary to define stress thresholds in order to be able to objectively define different seasons. In line with what was discussed in the introduction, on the basis of the literature and of a previous study, five stress criteria were identified.

- A temperature of 34°C is reported in the literature as the threshold beyond which the net photosynthetic efficiency of cocoa drops [132]. Any day with more than one occurrence of hourly temperatures above this threshold was considered stressful.

- A temperature of 19.7°C is reported in the literature as the basal temperature for vegetative activity necessary for the development of the Amelonado cacao plant, the most widespread in West Africa. Any day that experienced temperatures below this threshold, even for just one hour, was considered limiting for cacao growth. A lower value of 15.8°C was proposed as the basal temperature for fruiting [56], but this value was so rarely reached in the study environment that it was not considered.
- Air relative humidity below 40% was considered as stressful in line with previous studies in tropical environments [154, 178] because it causes the plant to close its stomata to avoid embolism. Therefore, any day when air relative humidity dropped this low was taken as a stressful day.
- According to a previous study under the same conditions, an air vapour pressure higher than 2 KPa induces a decrease in transpiration and is correlated to a loss of canopy. Consequently, anytime the threshold was passed the entire day was taken as stressful for cacao growth.
- A daily FTSW of less than 0.5, i.e. half of the extractable water availability for transpiration, was considered as the threshold for soil water stress. In the definition of this stress only data from the non-irrigated part were used, of course.

3.2.5 Statistical analysis

All the following statistical analyses were performed in the R environment v3.6.1 [189].

Effect of irrigation on production dynamics

The dynamics of production for all fruits categories and flowering were hypothesised to exhibit a complex non-linear response in time due to the different climate types experienced by the trees over the study period. To study these responses, we used generalized additive models with mixed effects (GAMM), which can incorporate nonlinear dependence. In all cases a negative binomial distribution was used to account for the over dispersion of these data. All models were build using the same explanatory variables. They included the treatment effect (irrigated or control) and a smooth term based on the number of days (time) considered as a continuous variable. The effect of time was fitted by a smooth term using Duchon splines, allowing the predictions to take into account the differential in water availability due to irrigation. A random effect was included to take into consideration the random tree-to-tree variability. To study the phenomenon of wilting it was studied the wilting rate, obtained combining the number of wilted cherelles to the sum of all cherelles (set + cherelles) with the cbind function [20]. The GAM-models for both watering treatments were plotted together to evaluate differences in the seasonal evolution. We interpreted non-overlapping 95% confidence intervals as a significant difference between treatment levels for a given period. The GAMMs were developed using packages: plyr [242], mgcv [246] and itsadug v2.3 [233].

Definition and characterization of the seasons

On the basis of the thresholds for stress defined in the section S. 3.2.4, each given day for each of the stresses was assigned a binary value of 1 if it met the above criteria or a value of zero if that stress was not present. Then, in order to take into account the context and history of each day, the value of each stress was integrated over an interval of +/- 7 days. At the end, for each date and each stress it was obtained a value included in the continuous space between 0 and 1 representing the harshness of the day in light of the past and future climate. This was done to smooth the series and avoid "unrealistic" spikes in stress and allow a better analysis

of the different climate classes experienced during the season. The normalized data on the probability for the five different stresses to occur on a given date were used to find common characteristics and climate types over the study period. The daily probabilities were analysed by mean of a hierarchical agglomerative cluster analysis. Hierarchical agglomerative cluster analysis is an algorithm that groups similar objects into groups called clusters based on their geometric distance. When the raw data are provided, the software will automatically calculate a distance matrix according to the chosen geometry (the default metric is Euclidean) and the method to calculate the distance. The three main families of methods to calculate the distance between two clusters consider their midpoints (average-linkage), their closest data bits (single-linkage) or their farthest data bits (complete-linkage). The result is a set of clusters that are different from each other and whose objects inside are largely similar among them. Hierarchical clustering starts by treating each observation as a separate cluster. It then iteratively identifies the two clusters that are closest to each other, and merges them. This process ends when all clusters are merged together. The main output of hierarchical clustering is a dendrogram, which shows the hierarchical relationship between clusters. The dendrogram can be cut at any height to obtain the input data divided into a number n of clusters corresponding to the number of branches in the dendrogram at the chosen height. In our study, we chose Euclidean geometry and the Ward.D2 method to calculate the distance between points. The Ward.D2 method aims at reducing the sum of squared distances from the average observation in a cluster for each observation [166]. The hierarchical agglomerative cluster analysis used the following R packages: stats v3.5.5 [189]. The choice of method (Ward.D2) and geometry (Euclidean) was dictaxted by the fact that these are the most simple and most widely used in the domain and are suggested for a clustering in a continuous space of data, as in this case. The result from the hierarchical agglomerative cluster analysis was used to determine different classes of climate. The climate classes were used to define a number of homogeneous climate periods over the study period, referred to as seasons in the rest of the document. For each of the stresses defined in S. 3.2.4 a linear model (LM) was constructed in relation to the seasons. From the linear models, pairwise differences between seasons were studied on the basis of their estimated marginal means (EMMs), the average of a factor at one level over all the levels of the other factors. The EMMs analysis was conducted using the emmeans 1.6.0 package [136] in combination with stats v3.5.5 [189] for the linear models.

3.2.6 Combined effect of irrigation and the season on production dynamics

The effects of environmental conditions (seasons and irrigation) on the dynamics of the various production categories defined in S. 3.2.2 were studied by means of a generalised linear mixed model with a negative binomial distribution (GLMM.NB) due to the overdispersion of these data. All models were constructed with the interaction between season and treatment (irrigated or control) as a fixed effect and the tree as a random effect. In the case of wilting, the wilting rate obtained as a fraction of the sum of all categories affected by the phenomenon (sets and cherelles) was studied. In the case of wilting, the number of pods and ripe pods were also considered as fixed effects. The pairwise differences between the seasons and the treatment for each production category were evaluated, once again, with the EMMs. The different GLMM.NBs were created using the package lme4 v1.1-23 [19] and the EMMs with emmeans 1.6.0 package [136].

3.2.7 Combined effect of irrigation and the season on post-harvest

The different seasons and the watering treatment were used as fixed effects in a series of linear models aimed at studying the dynamics of the various post-harvest variables defined in S. 3.2.2.The differences for each variable between the seasons and the treatment were evaluated

with the EMMs. The different GLMM.NBs were created using the package lme4 v1.1-23 [19] and the EMMs with emmeans 1.6.0 package [136].
For all analyses, the differences found by the EMMs were considered significant with a p-value of 0.05 or less and highly significant with a p-value of less than 0.01. The above-mentioned p-values were not taken blindly but taking into account the size of the data for the different seasons as suggested by [123]. With a p-value higher than 0.05 and lower than 0.10 we considered the difference not significant but reported it in the results as a tendency.

3.3 Results

3.3.1 Definition and characterization of the seasons

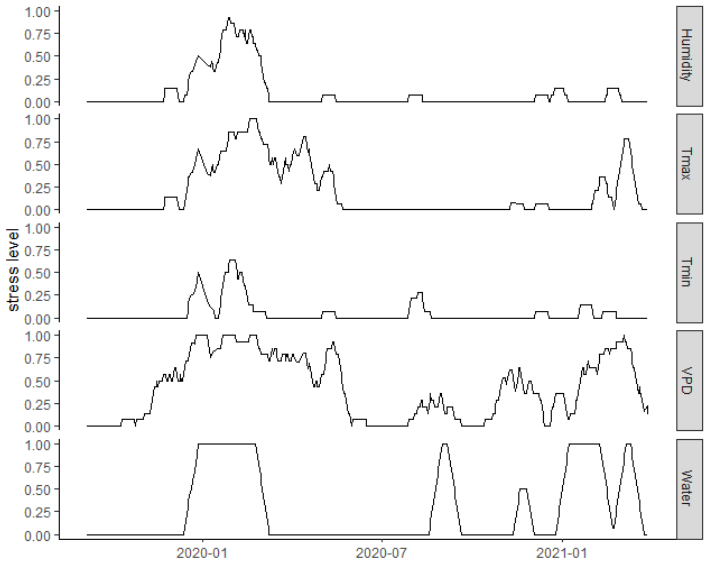

FIGURE 3.3.1: Probability of five stress types (S.3.2.4) to occur over the experimental period (3^{rd} December 2019 to 29^{th} March 2021) at New Tafo Akyem, Ghana (6°13'53.7"N; 0°21'01.6"W; 203 m a.s.l.). The values were calculated for each date as the proportion of stressing days over the period of the date $\pm$ 7 days.

Figure 3.3.1 shows the evolution of the five stresses defined in the methods S. 3.2.4. Soil water stress was stressing the plants from the end of December to the end of February at least both in 2019/2020 and 2020/2021, especially in December 2019 – March 2020. Another short period of soil water stress occurred in August 2020. Aerial drought caused by air relative humidity below 40% occurred around the above-mentioned first episode of soil water drought. Concomitant to the low relative humidity, the threshold for low temperature (19.7°C) was found to be highly probable to be passed in the last week of December 2019 and the first weeks of 2020. A less significant, short period of cold temperatures was in August 2020. Temperatures above 34°C stressed the plants a long period, from December 2019 to mid May 2020, and a much shorter period between the 31st of January 2021 and the end of the experiment on the 16th of March 2021. Aerial drought caused by a VPD above 2 *kPa* was felt by the plants throughout the entire experimental period, from December 2019 to the end of the experiment in March 2021. Only two periods, between the 1^{st} of June and the end of July 2020 and from the 19^{th} of September to the 14^{th} of December 2020, did not show any probability to pass the decided threshold.

The agglomerative hierarchical clustering classification identified four climate classes based on the five types of stress for the cacao tree presented in S. 3.2.4 (Fig. 3.3.1). The four classes highlighted different climates, *class 1* was characterized by the almost complete absence of stress while *class 2* and *class 4* were considered as mildly stressing for the co-occurrence of multiple stresses. Finally, *class 3* was considered highly stressing because all five stresses had a chance to be present. The alternation of the four climate classes allowed us to divide the 16 months of the field trial into seven seasons (Fig. 3.3.2) with homogeneous climate characteristics. In Figure 3.3.2 we have included one month of analysis before the start of the experiment (16^{th} of December 2019) to illustrate that the trees were coming from a not-stressing period. Similarly, the points in Figure 3.3.2 after the 16^{th} of March 2021 are only to highlight that

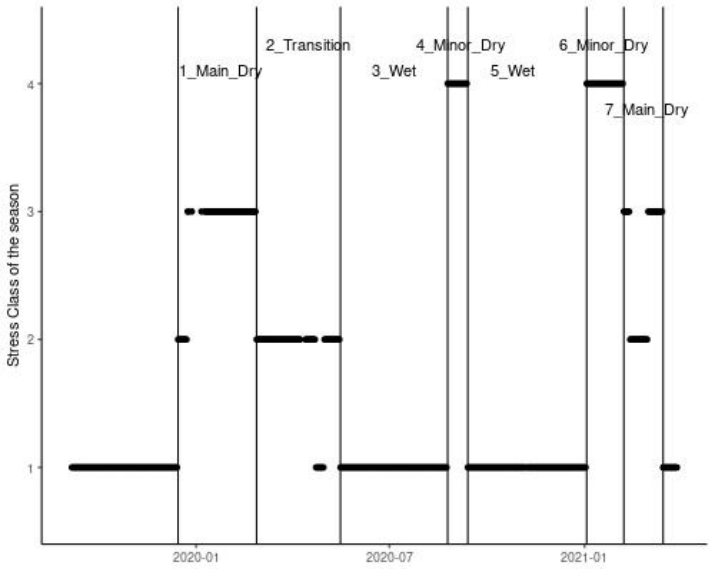

FIGURE 3.3.2: Subdivision of the experimental period into seasons based on climate classes defined through an agglomerative hierarchical clustering.

the experiment was concluded with the end of the second long dry season. The seven seasons included two major dry seasons (1_Main_Dry and 7_Main_Dry), two minor dry seasons (4_Minor_Dry and 6_Minor_Dry) preceded by the same number of wet seasons (3_Wet and 5_Wet) and an intermediate season between the highly stressing 1_Main_Dry and the humid 3_Wet (2_Transition).

3.3.2 Evaluation of the differences between seasons

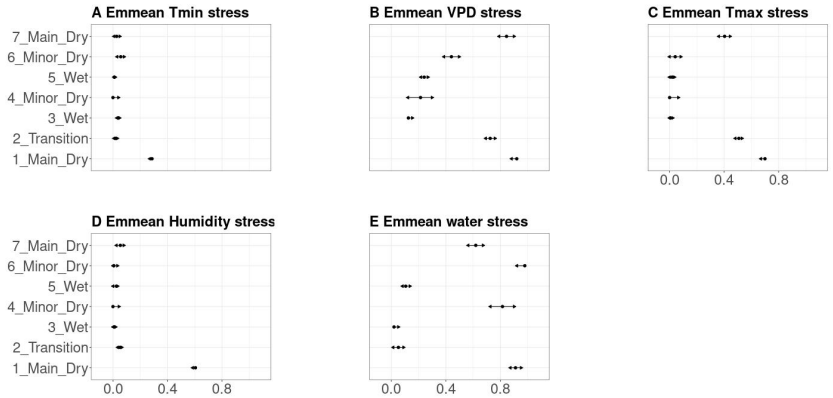

FIGURE 3.3.3: The variability of the 5 stress types across the 7 seasons studied by the estimated marginal means (EMMs). Two seasons with non-touching arrowheads are significantly different from each other. On the x-axis the probability of stress occurrence.

The differences and common characteristics between the seven identified seasons were found through the study of the estimated marginal means of the linear model for the response of each stress type to the seven seasons (Fig. 3.3.3).

1_Main_Dry season differs from all other seasons for the occurrence of temperatures inhibiting vegetative growth and low air relative humidity (Fig. 3.3.3 A and D). These two stresses are almost non-existent during all the other seasons, thus contribute to the characterization of 1_Main_Dry. Furthermore, 1_Main_Dry is characterized by the highest frequency

of extreme high temperatures followed by 2_Transition which is in turn significantly different from the second major dry season, 7_Main_Dry. The other four seasons did not show any significant difference among themselves and with zero, meaning that high temperatures are not a recurrent stress during these seasons (Fig. 3.3.3 C).

The VPD related stress is most frequent during the two major dry seasons but during 2_Transition as well it is high (around 70%), despite being significantly different for the former two (Fig. 3.3.3 B). The vapor pressure was not significantly different from zero only during the first wet season (3_Wet) while the second wet season (5_Wet) had a 25% chance of this stress occurring, not significantly different from 4_Minor_Dry, whose variability makes it not significantly different from 3_Wet as well (Fig. 3.3.3 B). 6_Minor_Dry had an intermediate level of VPD stress higher than 4_Minor_Dry and 5_Wet but lower than 2_Transition. Figure 3.3.3 E shows that soil water stress it is almost non-existent outside of the dry seasons. The two minor dry seasons and the first major one (1_Main_Dry) are dominated by soil moisture limitations while 7_Main_Dry is significantly different from the previous three but still with a high occurrence of soil water stress.

3.3.3 Effect of irrigation on the evolution of the production

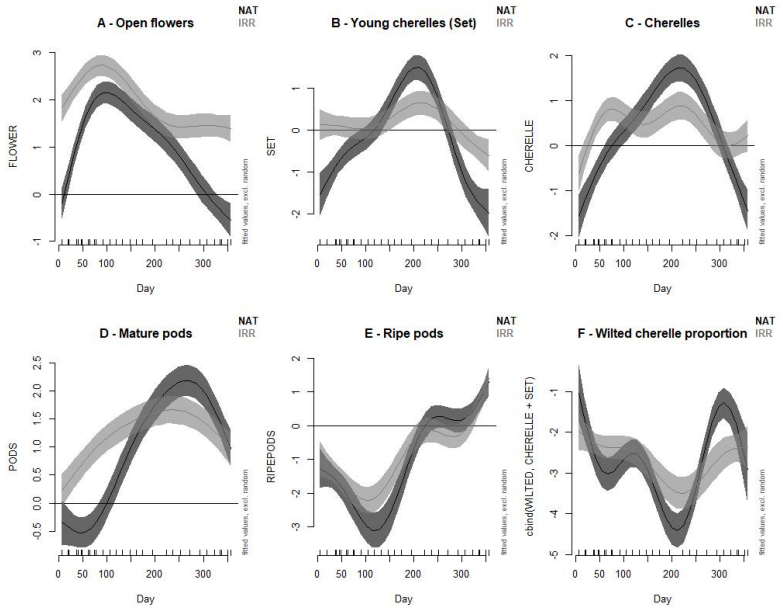

FIGURE 3.3.4: GAM models for the different fruit categories considered in the study and their evolution during the season after a strong Harmattan-induced episode of drought for irrigated trees (light gray) against the not irrigated control (dark gray). On the y-axis is the modelled quantity for each category. The shaded areas represent the 95% confidence interval for each treatemnt. non overlapping segments of the curves denote a significant difference.

Flowering is a parameter believed to react promptly to the environment. Figure 3.3.4 A shows how irrigation favored flowering for the entire season and in particular during the first and last dry periods, when soil water stress was particularly present. During the wet period, the impact of irrigation seemed less significant, even if the plants continued to flower more. After the long and stressing 1_Main_Dry season there was a strong stimulus to flowering in the natural part that led to a narrowing of the gap between control (NAT) and irrigated (IRR) trees. On the contrary, during the dry seasons flowering in the control plot was almost null. In absence of irrigation the cycle of young cherelle setting had a strong unimodal behavior centred around 3_Wet and 4_Minor_Dry (day 200) and with almost no setting of new young

cherelles during the two major dry seasons. Under irrigation the peak on setting remained approximately concomitant to the control's one but significantly lower. Nonetheless, irrigation kept the setting going during the dry periods too, thus maintained a more constant fruit set during the year (Fig. 3.3.4 B).

The behavior of the cherelles is in agreement with the setting (Fig. 3.3.4 B, C), with a unimodal evolution of the control, centered around day 230, and a multi-modal evolution of cherelles under irrigation that kept the curve more stable throughout the season but that was topped by the control's peak. All this agreed and reinforced the previous results on setting (Fig. 3.3.4 C). The wilting rate of young and old cherelles was modeled as not very responsive to climate for the irrigated field while the GAM model for the control showed a bimodal behavior with the two peaks in correspondence of the two wet seasons (Fig. 3.3.4 F). The quantity of mature pods increased in both treatments but the GAM model predicted a higher number of mature pods in the irrigated field for the first part of the season, followed by a higher peak for the control in the second part of the season. At the end of the experiment the two treatments were predicted to have a similar number of mature pods (Fig. 3.3.4 D). Similarly, the ripe pods in the two treatments were predicted to have a similar evolution over the season with just a short period when the irrigated plot is modelled with a higher number of ripe pods (Fig. 3.3.4 E).

3.3.4 Effect of irrigation and seasons on production dynamics

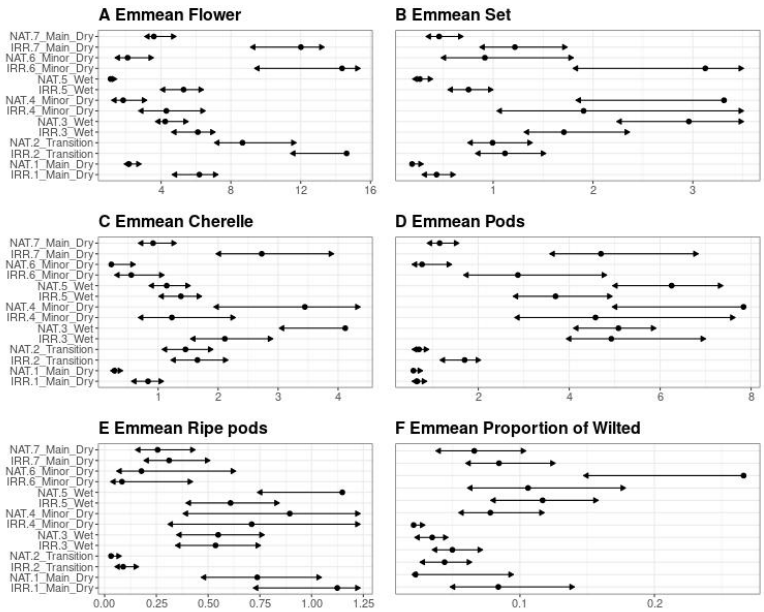

FIGURE 3.3.5: GLM EMM means for the effects of irrigation across the seven seasons for each considered fruit category and the wilt rate. On the y-axis, there are listed the seven seasons for both the control ("NAT") and the irrigated ("IRR") treatments. On the x-axis, is reported the quantification for each category - a number of elements for A, B, C, D, E and a proportion for F.

To verify the differences observed in Figure 3.3.4 and better contextualize them in light of the different seasons identified (Fig. 3.3.2, Fig. 3.3.3) to test the hypotheses put forward earlier, the multiple targeted comparisons (contrasts) highlighted by a GLM of the negative binomial family were studied for each fruit category. Through the study of the contrasts it was possible to evaluate 1) the differences between the two plots during the same season, 2) the differences in behaviour in presence of irrigation or not when switching between two

consecutive seasons and 3) common behaviours during seasons with the same climate class (Fig. 3.3.2).

The analysis found that irrigation kept flowering to significantly higher levels during the whole follow-up period except the first wet season (3_Wet) and the little dry season (4_Minor_Dry). The difference was more marked, a larger difference in the estimated marginal means, for 6_Minor_Dry and 7_Main_Dry while it was just more of a tendency during 2_Transition (p value = 0.058). These results are in accordance with the GAM model (Fig. 3.3.4 A, Fig. 3.3.5 A).

Fig. 3.3.5 A shows that the transition from 1_Main_Dry and 2_Transition saw a significant increase in flowering of similar magnitude in the two plots, regardless of irrigation. The passage from 2_Transition to 3_Wet kept flowering high in both plots but significantly lower in 3_Wet compared with the former season. The arrival of a stressing period (4_Minor_Dry) had a significant depressing effect only on the quantity of open flowers in the control leading to a lower level of flowering that did not significantly change until the end of the experiment (7_Main_Dry). Under irrigation the trees did not significantly change the flower production between 3_Wet, 4_Minor_Dry and 5_Wet. With the passage from 5_Wet to 6_Minor_Dry the trees started producing more flowers, a trend that continued during 7_Main_Dry as well.

The second considered parameter that responds dynamically to climate was setting. Irrigation showed a tendency to boost setting during 1_Main_Dry (p value of 0.06) and in a much more significant way during 5_Wet and 7_Main_Dry. Furthermore, the analysis found a tendency to set more new young cherelles under irrigation during 6_Minor_Dry. The higher peak in setting shown in Fig. 3.3.4 B was supported only by a weak tendency (p value = 0.13) of the control to set more young fruits during 3_Wet (Fig. 3.3.5 B). The transition from 1_Main_Dry to 2_Transition saw a surge in young cherelle production for both treatments, in line with the previous results on flowering (Fig. 3.3.5 A,B). When passing from 2_Transition to 3_Wet, the irrigated plot did not change the quantity of newly set cherelles while the control did see an increase compatible with the pattern evidenced in Fig. 3.3.4 B. When irrigated the trees were able to maintain the same levels of setting as 3_Wet during 4_Minor_Dry and 5_Wet as well to then increase during 6_Minor_Dry until the end of 7_Main_Dry (Fig. 3.3.5 B). In the control plot setting rate did not differ between 3_Wet and 4_Minor_Dry but then it dropped during 5_Wet without significantly changing until the end of the experiment (Fig. 3.3.5 B). Irrespective of irrigation the trees set more young cherelles in 3_Wet than 5_Wet, especially in the control. Similarly, the trees produced more new cherelles during 7_Main_Dry than 1_Main_Dry while no significant difference was found between the two minor dry seasons (Fig. 3.3.5 B).

Under irrigation the trees carried more cherelles than the control during the two major dry seasons and less during 3_Wet. The remaining seasons did not show any significant difference between treatments. In both plots the trees carried more cherelles in 2_Transition compared to the previous season. The positive trend was confirmed for the control trees during 3_Wet as well, while the irrigated plot did not see any significant increase in cherelle numbers. No significant difference was found passing from 3_Wet to 4_Minor_Dry in both treatments while during 5_Wet the control trees tended to carry more cherelles (p value = 0.08). The second minor dry period saw a decrease in the number of cherelles followed by an increase during 7_Main_Dry irrespective of irrigation (Fig. 3.3.5 C). The contrast between seasons of homogeneous type confirmed the same findings as for the previously discussed setting with more fruits during the first wet season and the second major dry season. Furthermore, the analysis highlighted a difference between the two minor dry seasons in favor of the first (4_Minor_Dry) but only for the control (Fig. 3.3.5 C).

Figure 3.3.5 F presents the contrasts in wilt rate, strongly affecting set and cherelle survival, to better understand the dynamics of mature pods over the season and across treatment. Based on the analysis, irrigation does not change the rate of wilting at the level of each

season except for a weak tendency for the wilt rate to be higher in the irrigated plot (p value = 0.12). During the experimental period the control did see a drop in wilt rate from 2_Transition to 3_Wet and between 6_Minor_Dry and 7_Main_Dry. In both treatments the wilt rate was higher during the second wet season compared to the first one (Fig. 3.3.5 F).

The number of pods was greater in the irrigated plot during 2_Transition, 6_Minor_Dry and 7_Main_Dry. Irrigation led to an increase in pods number after 1_Main_Dry that continued until the end of 3_Wet. From then on, the number of pods in the irrigated field was maintained without significant differences. The control, instead showed a significant increase only during the transition from 2_Transition to 3_Wet and a decrease after 5_Wet into 6_Minor_Dry (Fig. 3.3.5 D). More pods were carried during the second major dry season in both treatments and during the first minor dry season only in the control plot. No significant difference was found between the two wet seasons (Fig. 3.3.5 D).

At the end of the fruit cycle, the ripe pods, the analysis did not find any significant effect of irrigation at the level of a single season, thus we looked at the common cycle between the two treatments. The ripe pods' number remained stable over the experimental time except for a lull during 2_Transition and a decrease passing from 5_Wet to 6_Minor_Dry to a level then maintained until the end of the experiment. The first major dry season carried more pods than the second one no matter if irrigated or not and the control ended up having more ripe pods during the first wet season (Fig. 3.3.5 E).

3.3.5 Effect of irrigation and seasons on post-harvest traits

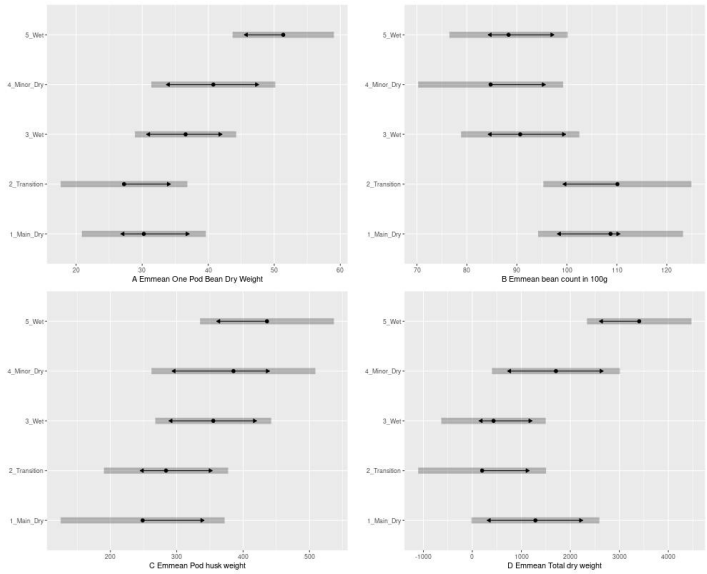

FIGURE 3.3.6: LM EMM means for the post harvest variables in relation to different seasons of four climate types individuated with an agglomerative hierarchical clustering. Not overlapping arrows mark a significant difference.

Due to the complications deriving from the Sars2-Covid-19 related restrictions we have several dates missing, thus the following results should be interpreted with caution. The linear model based on treatment and season did not highlight any difference between irrigated and control trees, consequently in Figure 3.3.6 we only show the effect of the season. The bean dry weight, both for a single average pod and for the total production, did not differ significantly between the seasons except during 5_Wet, when it was higher than during the first three seasons (Fig. 3.3.6 A, D). Similarly, the pod husk fresh weight was higher in 5_Wet compared to 1_Main_Dry and 2_Transition but comparable to 3_Wet and 4_Minor_Dry (Fig.

3.3.6 C). The bean count was significantly higher during the first two seasons respect to 4_Minor_Dry and 5_Wet. 3_Wet was found to be statistically the same as the latter two seasons but also compatible with the former two (1_Main_Dry and 2_Transition) (Fig. 3.3.6 B).

3.4 Discussion

3.4.1 Climate classes and seasons

Based on Figure 3.3.3 it is fair to consider that during 3_Wet and 5_Wet the trees were not stressed, during 4_Minor_Dry and 6_Minor_Dry they felt only soil drought (if not irrigated), during 2_Transition they experienced solely atmospheric stress and during the two major dry periods (1_Main_Dry and 7_Main_Dry) both atmospheric and soil drought were felt by the plants.
The plants underwent two long, major stressing periods corresponding to 1_Main_Dry and 6_Minor_Dry plus 7_Main_Dry. It is known that the southern movement of the inter-tropical front hinders precipitations and brings the dry Harmattan winds upon the cocoa areas [130, 208]. As a consequence of the southern movement of the inter-tropical front, Ghana experiences yearly a dry season between November and March that can be as much as 3 month long [1, 2, 130]. During such period precipitations are almost absent due to the vicinity of the inter-tropical front but it is only when the Harmattan winds pass over the cocoa regions that the dry air leads to violent changes in temperature and to low daytime air relative humidity [130, 208]. When crossing results from the agglomerative hierarchical clustering classification of climate with the occurrence of the five stresses (Fig. 3.3.1), *class 3* is the harshest climate type, with all five stress types potentially occurring(Fig. 3.3.2, 3.3.3). It is fair to assume that the days marked by a *class 3* climate were the most likely to have experienced the Harmattan winds. It was concluded that the long major stressing period in 2019 / 2020 (1_Main_Dry) was harsher than the one in 2020 / 2021 (6_Minor_Dry plus 7_Main_Dry) because of the far higher representation of *class 3* climate, despite in terms of duration they were not very dissimilar. The first half of the major stressing period in 2020/2021 was characterized by *class 4* climate suggesting that during that period the inter-tropical front did not bring extremely dry air over the study site but was close enough to hinder precipitations and cause soil drought (Fig. 3.3.2, 3.3.3). On the contrary, the inter-tropical front must have lingered in a southern-than-average position for longer during the first months of 2020 as even after the resumption of rains the atmospheric conditions remained dryer and warmer than usual for almost three months, the transition period of *class 2* climate (Fig. 3.3.2, 3.3.3).

3.4.2 Effect of climate and irrigation

In evaluating the short-term effects of irrigation and climate on production it was decided to separate highly responsive categories such as flowering and the young fruits (young and old cherelles) from the effects on older pods, whose number was the aftermath of raw setting and survival of cherelles in the previous months.

Among the plant organs fruits are strong sinks, often prioritized by the plant when allocating photosynthates through the phloematic flow [143, 186]. Among fruits the gross sink strength follows a bell-shaped evolution with young cherelles and old pods that pull very little assimilates and the peak in demand around 75-90 days after setting [7, 164]. The young cherelles gross sink strength is low due to their reduced dimension, while the old pods have a very low specific sink strength. A recent review on phloem functionality under drought [201] concluded that phloem loading / unloading is not affected under low or moderate water stress, while a severe drought leads to a fast decline in the source to sink transport of sugars. A clear consequence is the reduction of the plant's capacity to invest in new biomass. In young seedlings of cacao drought has been found to strongly reduce the overall translocation capacity of photosynthates [64] and, when severe enough (below -1.5 MPa at the leaf level), change the assimilates partitioning among organs in favour of the roots [63]. As pointed out by the review [201] many studies, including [63, 64] on cacao, were performed disregarding

the reproductive organs but in this discussion it is assumed that those behaviours remain valid even when fruits appear in adult trees.
Because we had removed all developing fruits except for the old pods and ripe pods, the sinks for assimilates were very low and the trees could have potentially produced a wave of new cherelles. The severity of the first major dry season caused the trees to produce very little new cherelles compared to the rest of the experimental period in both treatments. This confirms the relevance of strong water drought (soil and atmospheric) in inhibiting flowering and setting for the control due to the negative effect on photosynthesis [153, 247] and the lesser phloematic transport of the produced assimilates [201]. Irrigation had a great influence on flower production and fruit set but was not enough to allow a more abundant fruiting during the first major dry season (1_Main_Dry), as was expected due to the lack of strong sinks. In fact, although the amount of open flowers remained higher during all the major dry seasons, the plants did not set significantly more fruits than the control. Furthermore, even with irrigation, the plants responded to the return of the rains with a further increase in flowering and fruit setting after an extreme drought event in line with previous results [39, 132]. This suggests that the irrigated trees reacted as well to an improvement in soil VWC passing from 1_Main_Dry to 2_Transition. A possible explanation is that irrigation, in the recommended and applied quantities, was not sufficient to completely eliminate the production limitations linked to soil drought under concomitant harsh atmospheric conditions. In support of this hypothesis is the fact that, during a period when only soil drought was present (4_Minor_Dry), flowering and fruit set in the control decreased significantly while irrigation allowed to maintain the same levels as during 3_Wet for both categories (Fig. 3.3.4 A, B; 3.3.5 A, B). Moreover, the importance of the atmospheric stress in limiting the investment of the trees in reproduction is highlighted as well by the higher setting seen during the second major dry season (6_Minor_Dry plus 7_Main_Dry) compared to the first (1_Main_Dry) (Fig. 3.3.5 B). The trees in both treatments produced many more fruits when the major dry season was milder and, for the irrigated plot, counterbalanced by irrigation (Fig. 3.3.4 A, B, C; 3.3.5 A, B, C), despite the higher total pod load in the second major dry season. It is proposed that the strong aerial drought during 1_Main_Dry can be considered severe enough to inhibit the transport of assimilates toward the floral cushions, thus the set of new cherelles. The hypothesis that irrigation can only partially help if cacao trees are subject to multiple stresses or excessive stress (1_Main_Dry) has already been put forward by Hutcheon et al. 1973 [112] but only the study presented in Chapter 2 tried to demonstrate it on adult cacao trees in the field under the influence of the Harmattan winds.

Under highly stressing conditions the production was limited mostly by the environment (soil and atmospheric stresses). However, the differences between 3_Wet and 5_Wet may suggest that competition among fruits played an important role in shaping the production profile as well. In both treatments, flowering and setting were significantly higher during the first wet season compared to the second (Fig. 3.3.4 A, B; 3.3.5 A, B) despite the complete lack of stress in both seasons. This can be explained by the higher pod load (sum of all categories) during 4_Minor_Dry and 5_Wet that led to resources competition among fruits as demonstrated for other plants [65, 149, 251].

The higher rate of wilt during the 5_Wet compared to 3_Wet supports as well the fact that, despite the lack of environmental stresses, the trees were limited by their pod load in continuing to set and feed fruits. The same unbalance between the source and the excess of sinks represented by the high total pod load may explain as well why the wilt rate during 6_Minor_Dry was higher than during 7_Main_Dry (Fig. 3.3.4 F; 3.3.5 F). These results suggest that with the setting of 3_Wet and 4_Minor_Dry it was probably reached the fruit carrying capacity for the plants, beyond which the trees inhibited further setting and started to abort some cherelles in line with previous studies on cacao [151, 155, 171] and other species [33, 41, 144, 157].

The wide difference in flowering and setting between plots during 5_Wet suggests that the control required some time to recover from the mild stress of 4_Minor_Dry. If this idea is accepted, then we can conclude that irrigation had a positive effect on limiting the effect of competition (Fig. 3.3.4A, B and 3.3.5A, B). Furthermore, when looking at the number of cocoa fruits a few weeks old (Fig. 3.3.4 C; 3.3.5 C), it can be seen that irrigation kept the production level more constant while in its absence the plants were found to concentrate production when stress was absent (3_Wet) or possibly not too strong (4_Minor_Dry) (Fig. 3.3.4 B,C; 3.3.5 B,C). The different production cycle between control and irrigated plots did not change quantitatively the final production in a significant way (Fig. 3.3.4 D,E; 3.3.5 D, E; 3.3.6). Moreover, irrigation did not significantly influence the rate of cherelle wilt compared to the control (Fig. 3.3.4 F; 3.3.5 F), contrary to what was expected. A recent study across Ghana found that climate played a minor role in shaping the variability of on-farm total cacao yields compared to the current agronomic management and that well managed (ex. irrigated) cacao trees are less impacted by environmental stressors [12]. If we consider irrigation part of an ideal good management, our results seem agree with Asante et al. (2021) [12] on the higher resilience to climate under better watering. Besides, our results from an experimental plantation, as such considered "well managed", suggest that environmental conditions do not impact the overall production but can significantly change its evolution. In a natural situation, without irrigation, the climate probably forces on the plant the most logical behaviour of concentrating production to avoid the stressing periods. This "stress-avoidance" type of seasonal production cycle may be smart for the plant but potentially exposes the total crop to larger intra-annual swings in yields following climate anomalies and outbreaks of pests and diseases. Indeed, the "stress-avoidance" production cycle synchronizes the susceptibility of large parts of the total crop to biotic or abiotic reducing factors. On the other hand, in a less concentrated cropping cycle, as observed under irrigation, any biotic or abiotic stressor would affect a lesser portion of the total production, making the overall production more resilient and stable. The observed cycle under irrigation could be considered a "stress-tolerance" production cycle as the pod generations are less synchronized in terms of susceptibility to biotic or abiotic factors. Even though irrigation did not lead to higher yield nor differences in the post-harvest parameters in the studied situation, it is preferable to irrigate, not only to partially limit the occurrence of severe drought, but as well to reduce the intra-annual variability of the crop, thus of the farmers' income.

In conclusion, irrigation itself was not sufficient to raise the total production level over the study period, both quantitative and qualitative in the post harvest, but it led to a more distributed crop profile, potentially more resilience to extreme events as it minimized the occurrence of concentrated bulk generations that could lead to wider swings. A situation that, instead, was found for the control.

3.5 Conclusions

This study found that, under West African climate, the harsh atmospheric and soil stresses experienced when the Harmattan winds blow over West Africa tended to concentrate production during the not-stressing period irrespective of irrigation. Because the trees concentrated production during the first wet period, they saturated the source-sink capacity and were unable to sustain more setting later in the season, despite the favorable conditions. Irrigation does not nullify the stress when the Harmattan dry season is extremely stressful but helps the trees in spreading more evenly the setting, making the overall production more resilient to extreme events.

Chapter 4

A thorough investigation on the causes and timing of cacao cherelle wilt.

The study in Chapter 3 did not find clear evidence of the influence of different climate types nor irrigation on the wilting rate. In Chapter 3 it was highlighted a similar surge in the wilt rate during the second half of the study period (4_Minor_Dry to 6_Minor_Dry) when the trees carried far more fruits than in the first half of the study period. Such behaviour re-confirmed that competition among and within pod classes is at the root on this phenomenon, regardless of the stress alleviation provided by the irrigation. Cherelle wilt remains a rather unexplored physiological process despite its great importance for cacao production. Despite several studies investigated the abiotic causes for cherelle wilt, to our knowledge there is no clear study quantifying the role of competition and climatic variables on the wilt rate [151, 155, 171, 226].
In the optics of a full modelling of the cacao tree reaction to a changing climate, the wilt rate should have a predominant role. This would also help to better understand whether irrigation, that spreads more the production cycle, can help managing wilting in a future with more frequent stressing conditions. In the only currently available cacao mechanistic model, CASE 2 [257], this process is missing. In order to remedy this weakness of the model and improve our understanding of the complex implications of climate change for future cocoa production in West Africa, it was necessary to break down this process into its basic components. For modelling purposes it was crucial to capture the timing of wilting and to frame the role of competition among fruits even before considering the role of climate.

4.1 Introduction

Between pollination and harvest many processes can reduce the number of fruits bore on a tree. Some fruits may be lost due to visible causes as pests and disease or mechanical damage. While some others may get aborted or dropped for no apparent reason. This cessation of growth is most of the times due to physiological reasons as insufficient pollination [91, 94], extremely low source/sink ratio in the plant. Pre-harvest fruit loss due to physiological reasons is widespread across environments and species, with many orchard species self-thinning their fruits [11, 41, 68, 91, 94, 168, 181]. The self-thinning is often accompanied by a change in the anatomy and chemical characteristics of the fruit that eventually culminates with the fruit drop. In cacao (*Theobroma cacao* L.), fruit drop does not occur but an equivalent process, known as cherelle wilting, reduces the total fruit load. This process sees the young pods (cherelles) wilt and mummify on the tree without being shed [151, 152, 155]. Cherelle wilt due to physiological reasons has been reported to reduce the total fruit set by up to 75% [14, 112, 226] but wilting can even involve 100% of the fruit set [155].
The wilting of cherelles that formed from successful pollinations of incompatible flowers is fairly well understood [128, 155]. However, the factors inducing cherelle wilt when pollen incompatibility is not involved lack clarity. In spite of the great importance of this phenomenon in determining the productivity of a cocoa plantation, hence its profitability, the dedicated scientific literature is scarce and, most of the time, data on wilting can only be extrapolated from studies addressing different questions. In most cases our knowledge of the cherelle wilt is due to the ancillary results of studies focusing on endogenous and exogenous effects affecting cacao. The fact that this process can be caused by a plethora of agents has made it difficult to identify and isolate the relative importance of different triggering factors such as: an insufficient (incomplete) pollination, pollen incompatibility, cherelle sanitary problems or the inherently physiological causes, which are rather related to competition between fruits and, when relevant, climate. A recent review of the current state of the art on cherelle wilt describes the symptoms together with the alleged physiological responses that led to them (Fig. 4.1.1) [155]. However, it does not quantify the importance of each possible cause and it recognizes that some aspects of why and how cherelle wilt occurs are not well comprehended [155]. Moreover, most of the theories on the causes and functioning of cherelle wilt come from single, fairly old sources, which makes it more difficult to formulate solid conclusions.
An important theory that has been advanced in many occasions is that physiological wilting is a way for the plant to autoregulate production when the source/sink ratio is unfavourable. Therefore, it seems that a cherelle is wilted whenever it enters in competition for resources with a stronger sink. Many studies reported that, whenever leaf flushing occurred, the likelihood of cherelle wilt increased greatly [111, 152, 226]. In all cases it was concluded that the trees could not sustain both the increased leaf formation and pod development with their internal energy production. Moreover, whenever the natural pod load was inflated, either by inducing a more abundant flowering with chemical means [222–224] or by manual pollination [151, 152, 226], the final number of harvested pods did not change. Indeed, the more abundant fruit set was followed by a higher wilt rate that levelled the total production. Whenever the fruit load is above the potential production [14], the young cherelles still in the exponential phase of growth, thus with the least competitiveness, are sacrificed [226]. The exponential phase of growth is a period characterized by both cell division and cell expansion that corresponds to the first 70 to 90 days of growth, with cases over 100 days, depending on genetic and climatic factors [128, 151, 226]. Additionally, during the exponential growth phase the xylem bundles are still expanding and can be occluded easily through suberification, effectively "choking" the cherelles condemned to wilt [156, 172]. When pods enter the subsequent linear growth phase, they do not wilt for physiological reasons any more. This because the xylem bundles are more structured and more difficult to obstruct [156, 170]. Furthermore,

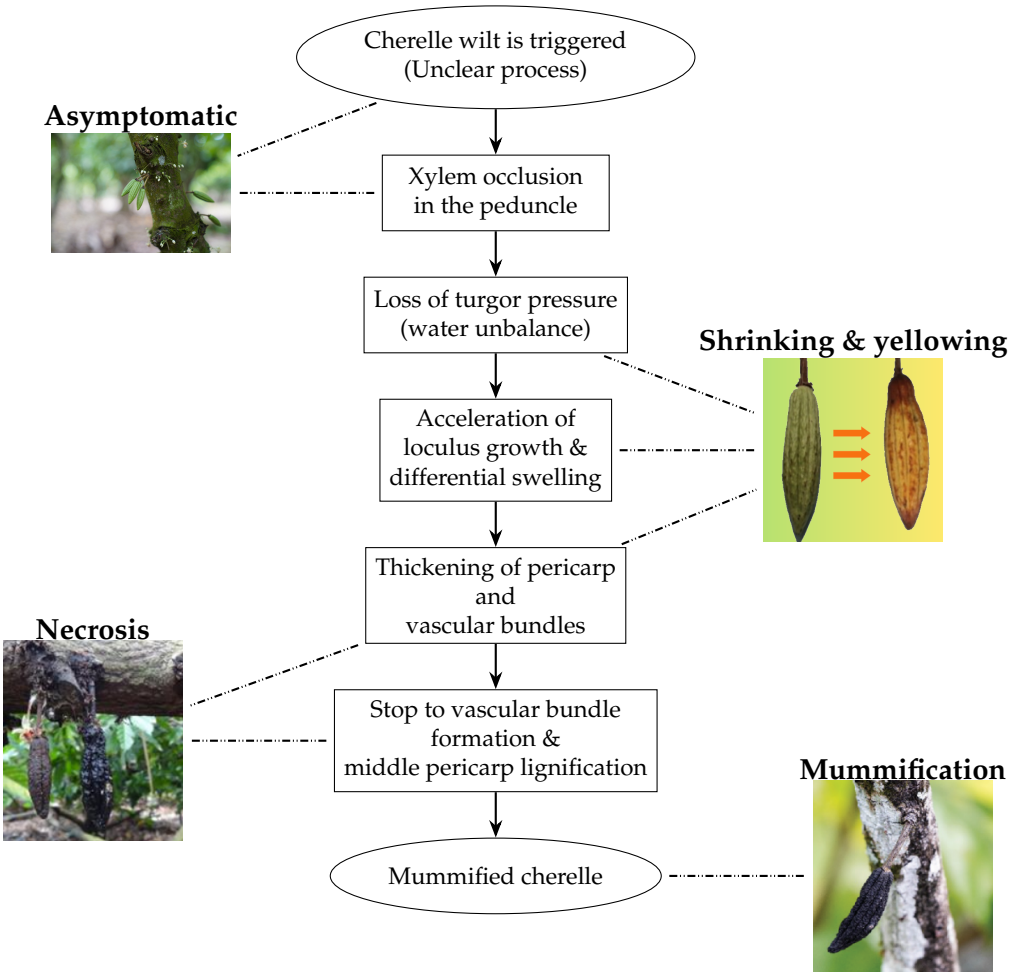

FIGURE 4.1.1: Graphical representation of the physiological steps of cherelle wilt alongside their physical manifestations (symptoms in the pictures) according to Melnick (2016)[155].

by that time they had become a large investment for the tree to throw away, therefore the younger pods are wilted to minimise investment loss as well [155, 226].
It was initially proposed that wilt presented two peaks of occurrence at 50 and 70 days after pollination [151]. The first peak (around 50 days after pollination) coincides with the formation of the cellular endosperm, while the second peak (around 70 days after pollination) should coincides with an accumulation of fat and starch within the pod [103, 151]. The hypothesis of two peaks has been reported to have been challenged in a PhD thesis, which stated the existence of a single peak followed by a progressive decline in incidence [57, 103]). Cherelle wilt is known to be embedded genetically, thus the different patterns proposed in the two studies are not mutually exclusive as the pattern might depend on the genotypes considered.
The first part of the present chapter is aimed at bringing clarity on the timing and development of cherelle wilt for only physiological reasons across several genotypes. This might help advancing and consolidating our understanding of the phenomenon. In order, it investigates:

1. whether the wilted cherelles show a different growth curve than the healthy ones,
2. if different clones present different wilt rate profiles in time (one or two peaks),
3. whether it is possible to predict the wilt of a cherelle from its growth curve.

Once established the sensibility to wilt of cherelles of different ages, another key physiological element worth to study to answer the sub-objective 4 (Ch. 1) is the role of resource competition connected to the total pod load on a tree. It has already been explained that wilting is worse whenever strong sinks compete with the young cherelles for resources [155, 226]. The second part of the chapter wants to explore the influence of pods of different age on cherelle wilting across genotypes. In particular it will be investigated:

1. at which pod age the pods are the strongest competitors for resources,
2. whether the cherelles (or pods) that wilt are influenced differently by the other pods' competition depending on their age
3. if the pod position on the tree (branches or main trunk) has an effect on the susceptibility to wilting.

4.2 Materials and methods

Part one: characterization of cherelle doomed to wilt

4.2.1 Study site

The experiment was carried out at the CIRAD experimental station at Pointe Combi (5°20′N-52°55′W), French Guiana. The annual precipitation in the region is about 3000 mm and is characterised by a drier period from August to November. However, average rainfall only falls below 100 mm per month in September and October. Relative humidity is high all year round with a stable average of over 80%. Temperatures are also stable with an annual average of over 25°C, lows above 20°C and highs of 34°C. The climatic conditions recorded during the study were in line with the general climate model presented for French Guiana: high relative humidity throughout the year, little temperature fluctuation and well-hydrated soil.

4.2.2 Experimental design

A total of 441 pods from ten different clones were followed in the study over three consecutive years (2016-2018). The ten clones studied were: *IMC*97, *PA*121, *B7B*3, *ICS*60, *ICS*95, *CCN*51, *KER*7, *KER*9, *GF*23 and *NA*79. The pollination of these clones was carried out manually with common pollen from the *IFC*5 clone, chosen for its regular flowering throughout the year. Then, the dimensions (length and width) of the cherelles resulting from these pollinations were recorded weekly with a caliper. When a wilt was observed for a cherelle, the dimensions measured the previous week were used as the last reference for the size and the number of days before the observed wilt was calculated considering the pollination day as "day zero".
To evaluate the developmental stage and timing of wilting, two variables were considered: the cherelle's age in days and the cherelle's volume over time. The latter was calculated as the volume of an ellipsoid of revolution using the pod polar and equatorial diameters (p and q respectively) measured weekly with the caliper (Eq. 4.1). The study considered only cherelles up to three months after pollination because after three months wilting becomes an extremely rare event [128, 151, 226].

$$Vol = \frac{\pi * p * q^2}{6} \tag{4.1}$$

4.2.3 Analyses

Which cherelles wilt and when

The shape of the wilting likelihood function in relation to the cherelle age or volume at the time of wilt was evaluated for each clone with a density and acount function in R v3.6.1 [189]. This aimed to verify the presence of peaks in wilting and characterize their occurrence during the development of the cherelles. To test if the wilted cherelles were the weakest (smaller in size at a given age), the evolution of cherelles of the same age that wilted or continued growing were plotted to assess the differences. The clone *ICS*95 was found to have incomplete data on the healthy cherelles that did not wilt so it was excluded. This analysis was performed dividing the cherelle cycle considered (up to 90 days) into three periods of 30 days. Dividing the cycle in three aimed to study if the cherelle size was a predictor for wilting a different growth stages for the different clones. The difference in growth between cherelles doomed to wilt or destined to continue developing was assessed for each clone with a GAMM model using the age as a fixed factor.

Timing of wilting: from trigger to symptoms

Between the moment of wilt triggering a cherelle and when the symptoms make it apparent some time might pass with the cherelle being still perceived as healthy. For each cherelle it was calculated the relative increment in volume between dates in relation to the first date's volume ($\Delta Vol_{relative}$). This was interpreted as the investment of the tree in that cherelle's growth. The differences in the evolution of the slope of $\Delta Vol_{relative}$ of pods that wilted was analysed to pinpoint when wilting of a cherelle was initiated before the symptoms of wilt became evident. Also in this case the growth cycle was split in three periods of 30 days to see if the change in slope of cherelles doomed to wilt is more marked depending on the cherelle developmental stage. This second analysis required to have complete series of wilted cherelles for the entire growth period. Only five clones had enough wilted cherelles for each of the three month-long intervals considered to be used in the analysis: *B7B3*, *ICS60*, *IMC97*, *KER7*, *PA121*. Once more, a GAMM model was used to explain the $\Delta Vol_{relative}$ before the time of wilt as a function of the cherelle age, clone and the state of the cherelle in the previous weeks. Both GAMM models relied on the Gaussian family of models and were carried out and rendered graphically in R v3.6.1 [189] using the packages plyr [242], tidyverse v1.3.0 [243], mgcv [246] and itsadug v2.3 [233].

Part two: the role of competition among fruits

4.2.4 Study site

The study took place at La Lola experimental farm of the CATIE (Centro Agronómico Tropical de Investigación y Enseñanza) in the humid and cloudy tropical forest of Costa Rica (10°06'N 83°23'W, 40 m asl) [134]. At the experimental site the monthly average temperatures are between 20.5°C and 30°C. May and June are the warmest months, whereas December and January are the coldest. At the experimental site, the annual precipitation are around 3,575 mm with a decrease in March - September. According to the FAO/UNESCO soil classification system, the soil is classified as a Eutric Cambisol [134, 165]. Relative humidity is high all year round with a stable average of over 91%. The climatic conditions recorded during the study were in line with the general climatology exposed [134].

4.2.5 Experimental design

For the experiment 91 mature trees (planted in 1998-1999 [134]) of three clones of cacao trees (*CATIER4*, 31; *CC137*, 30; *Pound7*, 30) were considered. The clones were selected for their productivity throughout the year and *Pound7* for its susceptibility to the pod rot (*Moniliophthora roreri*) [134]. Between the 29^{th} of May 2012 (the first generation) and the 12^{th} of June 2013 (the 55^{th} generation) cohorts (generations) of emerging pods under 10 cm were tagged weekly and followed in time until when these were removed either due to harvest or wilting or other causes (i.e. diseases). The total duration of the experiment was of 63 weeks, thus the late generations were followed only partially. In addition, the tag for the pods specified their position on the tree: Branches (H), Main trunk (B). In total the study considered 8796 pods distributed as in Table 4.2.5. The start of the experiment coincided with the minimum in the seasonal pod load, when trees bore no or almost no pods [134]. Every week the state of tagged fruits was recorded using five categories: (1) healthy, (2) infested by pod rot, (3) wilted, (4) harvested and (5) "otro" (spanish for other). The last category comprehended all other possibilities (damaged by rodents, mechanical damage, etc.) but in most occasions it represented pods affected by the black pod disease (*Phythophtora spp.*). Every week, together with the status of the already tagged fruits, were also tagged the new one. It must be noted

	NbTrees	Position	NbPods	TotPods
CATIER4	31	B	275	1837
	31	H	1562	
CC137	30	B	641	3657
	30	H	3016	
Pound7	30	B	1125	3302
	30	H	2177	

TABLE 4.2.1: Distribution among three clones of the 8796 pods tagged and followed in the experiment and their position on the trees. For each clone are reported the number of trees considered (NbTrees), the total number of pods (TotPods) and the number of pods (NbPods) on the trunk (Position = B) or the canopy (Position = H).

that the age of cherelles when first tagged was estimated, based on size, to have varied between 3 and 4 weeks, especially on branches that made the spotting more difficult. For sake of uniformity in the data set, it was assumed that all new cherelles spotted and tagged were 4 weeks old.

4.2.6 Analyses

Wilt distribution in relation to time of the season, age and position on the tree

Since our main interest was cherelle wilt, each weekly pod observation was treated as a binary data. Wilted cherelles were assigned a 1 for the week when wilting was witnessed, all other cherelles or pods were assigned a zero no matter if healthy or infected. The binary data were used to study the difference in wilting behaviour among clones and to verify if the wilt of a cherelle was influenced by its position on the tree.

With the ensemble of binary wilting data it was possible to study the occurrence of cherelle wilt in relation to (1) the moment of the year, (2) cherelle age (in weeks) and (3) cherelle position on the tree.

Predictive factors for wilt

Because virtually all pods on a tree were tagged and followed, for whichever wilted cherelle it was possible to look at the total pod load and its composition both at the moment of wilt and in the weeks before wilt. To this purpose, the pod load was divided into three categories based on the pod age to investigate which pods are the most problematic in terms of competition. The categories were:

1. "Small", corresponding to tagged pods observed for 1 to 7 weeks (i.e. an estimated age since pollination of less than 11 weeks, equivalent to the first two months);

2. "Medium", all tagged pods observed between week 8 and week 13 (i.e. an estimated age since pollination of more than 11 weeks and less than 17 weeks, or the third and fourth months);

3. "Large", all tagged pods from the 14^{th} week onward and until harvest (i.e. an estimated age since pollination of more than 17 weeks).

For the analysis, only pods that wilted up to 13 weeks after the estimated pollination (until the 9^{th} week of recording) were considered. Above this age, wilting was found to be extremely rare. Furthermore, also data for the first week of observation was removed, as only

healthy fruits were tagged. To study the role of competition on wilt rate it was necessary to have the total pod load for each wilted cherelle at any given time. Thus, the late generations, from 48 to 55, had to be removed because the new cherelles were not tagged after the 55^{th} week and the experiment lasted until the 63^{rd} week. This meant that for the late generations from 48 to 55 it was not known the complete pod load at any given time of their cycle. For a given week, wilt was considered as possible for fruits rated healthy or wilted. All other fruits categories (damaged, diseased) had to be removed from the dataset to predict but were kept as predictors. For each healthy or wilted cherelle in time (every week) the total number of fruits of each age group present on the cocoa tree was calculated. This allowed to have the pod load history of the cocoa tree for each wilted cherelle. Four periods previous the moment of wilt were considered: the week (T1), the two weeks (T2), the 3^{rd} and 4^{th} week (T3) and the 5^{th} and 6^{th} week (T4) before the observation. The maximum competition for each age group for any given period was estimated as the maximum number of fruits during the period. The distributions for the count variables for the age categories were highly skewed with a long thin tail of very high values. To avoid the effects of these rare extremes without losing valuable data, the distributions were truncated. All values above the 90% quantile of each category were floored to the category's 90% quantile value.
The binary data of healthy and wilted cherelles per tree per week was used to predict the probability of wilt depending on several predictors. The predictors associated to each binary data point in the dataset were: (1) the clone, (2) age of the pod, (3) position on the tree, (4) the number of "small", "medium" and "large" pods at T1, T2, T3, T4. Because pods from a given period eventually grew into larger ones at later periods, it was decided to only include in the analyses the predictors that were not highly correlated. The threshold for correlation was set at 0.7 [71]. Because of the correlation between variables, 8 explanatory variables were retained: clone, pod age, all pod categories at T1 and the small and large categories at T4. The predictive statistical model was built using the machine learning method known as Boosted Regression Tree analysis (BRT) [62, 71, 72] using the gbm [97] and dismo [107] packages in R v3.6.1 [189]. The BRT analysis used the Bernoulli family of models with a *seed.number* of 146, a *tree complexity* of 4, a *learning rate* of 0.1 and a *bag fraction* of 0.5. The cited parameters for the model are explained in literature [71, 72] and in the caption of Table 2.C.1. The total dataset was randomly divided into a training dataset and a test dataset based on a *seed.number* = 51. The test dataset was built randomly selecting 10% of the initial data (each data item represented one pod in a given week), leaving 90% to the total data to train the model. The model overall skill was evaluated using the AUC coefficient (Area Under the Curve; [88, 217]). Furthermore, it was calculated the confusion matrix with respect to training data for wilted or healthy pods to study the false positives (FP), false negatives (FN), true positives (TP) and true negatives (TN) of the model [219]. In particular, were evaluated the True Positives Rate (TPR) and the False Positive Rate (FPR) (Eq. 4.2). Another step of the validation of the final BRT model, was to evaluate the quality of the model prediction when applied to the test data. The quality of the prediction for the test data was, again, assessed with the TPR and FPR (Eq. 4.2).

$$\begin{cases} TPR = \dfrac{TP}{TP + FN} \\ FPR = \dfrac{FP}{FP + TN} \end{cases} \tag{4.2}$$

4.3 Results

Part one: characterization of cherelles doomed to wilt

4.3.1 Overall developmental stage for wilt

When disregarding the differences among genotypes, the wilting rate profile evolution in time highlighted only one peak between the second and the third week after pollination, followed by a steady decline until 90 days after pollination (Fig. 4.3.1). By means of a logarithmic scale of the volume of the wilted cherelles, it was possible to individuate two different ranges of volumes at which cherelles tended to wilt. The first was between 10 and 300 mm^3, while the second spaced from 1500 to over 10000 mm^3 (Fig. 4.3.2). It is important to note that the second range is far wider than the first on the logarithmic scale in Figure 4.3.2, meaning that on a linear scale the first peak is narrower but taller than the second one, that would appear more less evident.

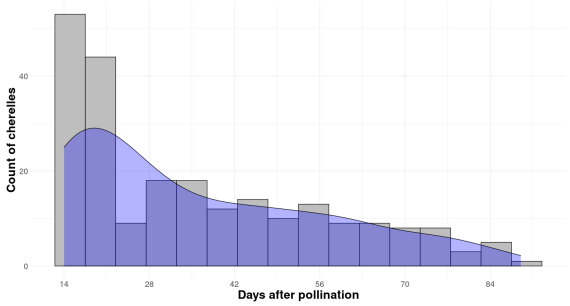

FIGURE 4.3.1: Aggregated density distribution and count for cherelle wilt of ten different clones in the first three months after pollination. Each bar represents a week long interval in age.

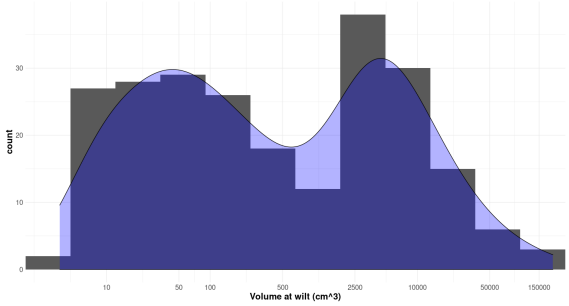

FIGURE 4.3.2: Aggregated density distribution and count for cherelle wilt of ten different clones depending on the wilted cherelle size. The volumes are plotted on a logarithmic scale to reduce the skewness of the data due to the five orders difference in magnitude of the data range (0-150,000).

4.3.2 Clonal variability in the developmental stage for wilt

A preliminary statistical summary of the data found that two weeks after pollination cherelle wilt can start to manifest across most of the considered genotypes. The exceptions being clone *GF*23 (20 days). The average day of wilt varied more across genotypes. In most cases the average wilt day was around one month (between 29.75 and 36.00 days) with only four genotypes with a higher value: *PA*121(40.81 d), *GF*23(48.82 d), *B7B*3(51.09 d), *ICS*95(59.09 d) (Tab. 4.3.1). All clones but *B7B*3 and *GF*23 presented a high wilt count in the first three weeks after pollination, in agreement with Figure 4.3.1. However, the evolution of wilting over time showed to be an intrinsic property of the genotypes with some clones having an early profile of wilt (*CCN*51, *NA*79, *ICS*60) and others a late (*GF*23) or a more evenly distributed one (*ICS*95, *PA*121, *B7B*3, *IMC*97) (Tab. 4.3.1, Fig. 4.3.3). For some clones, there were more than one peak in the wilt count but only *ICS*95, *IMC*97and *NA*79 had peaks of comparable magnitude. The other clones presenting more than one peak had a first peak followed by lower and lower peaks in time (*CCN*51, *ICS*60 and *KER*7) (Fig. 4.3.3).

The minimum volume for wilting was found to be between 3.53 mm^3 and 16.36 mm^3, with the

Clone	mean	min	qs25	qs75	max	n
B7B3	51.09	14.00	33.50	68.00	98.00	22
CCN51	29.75	14.00	14.75	29.00	91.00	36
GF23	48.82	20.00	38.00	60.50	64.00	11
ICS60	34.40	14.00	21.00	48.00	89.00	35
ICS95	59.09	14.00	28.25	84.50	131.00	22
IMC97	35.37	14.00	14.00	51.50	92.00	19
KER7	36.00	14.00	15.00	50.00	79.00	17
KER9	30.57	14.00	14.00	46.00	82.00	14
NA79	30.62	14.00	14.00	41.50	54.00	26
PA121	40.81	14.00	22.00	59.50	78.00	43

TABLE 4.3.1: Days between pollination and the moment of wilt for ten clones of cacao grown in French Guiana (Pointe Combi; 5°20'N-52°55'W). The table reports the mean value per clone along with the minimum, maximum, lower 25% (qs25), upper 25% (qs75) and the number of pods used (n).

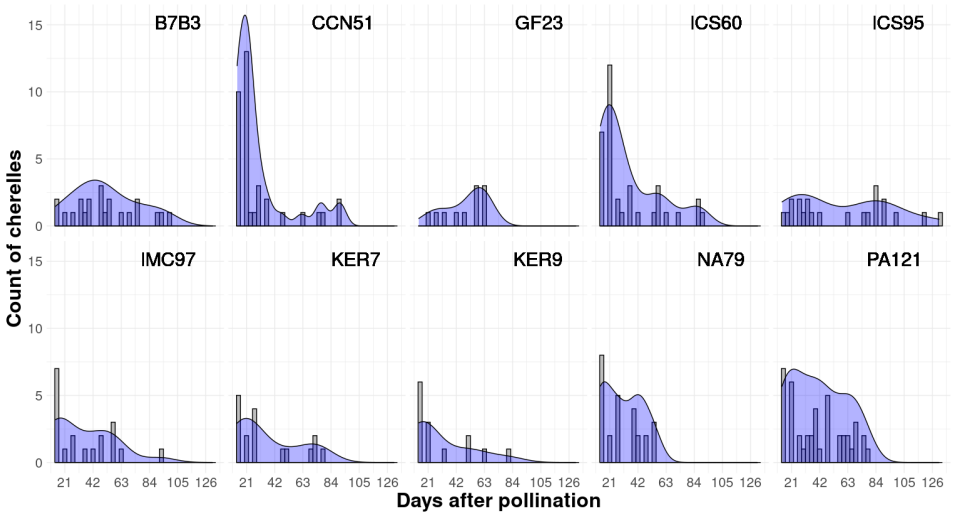

FIGURE 4.3.3: Density distribution and count of cherelle wilt in the first three months after pollination for the same ten cacao clones in Table 4.3.1. Each bar represents a week long interval in age.

only exception of *GF*23 that had a minimum volume of 102.54 mm^3 for wilting. The biggest cherelles that wilted for the different clones ranged between 5182.74 mm^3 and 407439.67 mm^3 in size. The *CCN*51, *ICS*60 and *KER*9 wilted almost exclusively tiny cherelles under 1600 mm^3 (third quartile, qs75 in Tab. 4.3.2), while the *B7B*3 and *GF*23 wilted preferentially bigger cherelles above 1000 mm^3 (data above first quartile, qs25 in Tab. 4.3.2). The volume density distribution of wilted cherelles on a logarithmic scale highlighted that there is a high chance of wilting around 2500 mm^3 for clones *B7B*3 and *GF*23. Contrarily, the *CCN*51 and *ICS*60 wilt almost exclusively cherelles smaller than 500 mm^3. The *NA*79 and *PA*121 present both a tendency to wilt either below 500 mm^3 or larger cherelles around 2500 mm^3. Similarly, the *KER*7 and *IMC*97 appear to have the peaks in wilt around the same values as well but the lower number of data available makes their density distribution less clear. Finally, the *ICS*95 and *KER*9 showed a uniform density distribution, mostly due to the little data available.

Clone	mean	min	qs25	qs75	max	n
B7B3	18837.13	6.28	1254.31	18506.84	134681.99	22
CCN51	5441.33	6.28	23.84	235.31	75755.50	36
GF23	5270.57	102.54	1743.17	7557.43	15946.79	11
ICS60	14148.22	8.38	33.54	1599.41	203767.97	35
ICS95	48243.14	16.36	139.23	30080.97	407439.67	22
IMC97	8505.53	8.38	9.95	4627.64	121457.28	19
KER7	3956.94	4.24	23.56	4214.12	20883.21	17
KER9	4147.63	6.28	7.14	1332.16	44591.11	14
NA79	1382.61	10.47	36.77	3037.85	5182.74	26
PA121	6355.85	3.53	141.90	7655.15	40818.26	43

TABLE 4.3.2: Volume (cm^3) of cherelles at the moment of wilt for ten clones of cacao grown in French Guiana (Pointe Combi; 5°20'N-52°55'W). The table reports the mean value per clone along with the minimum, maximum, lower 25% (qs25), upper 25% (qs75) and the number of pods used (n).

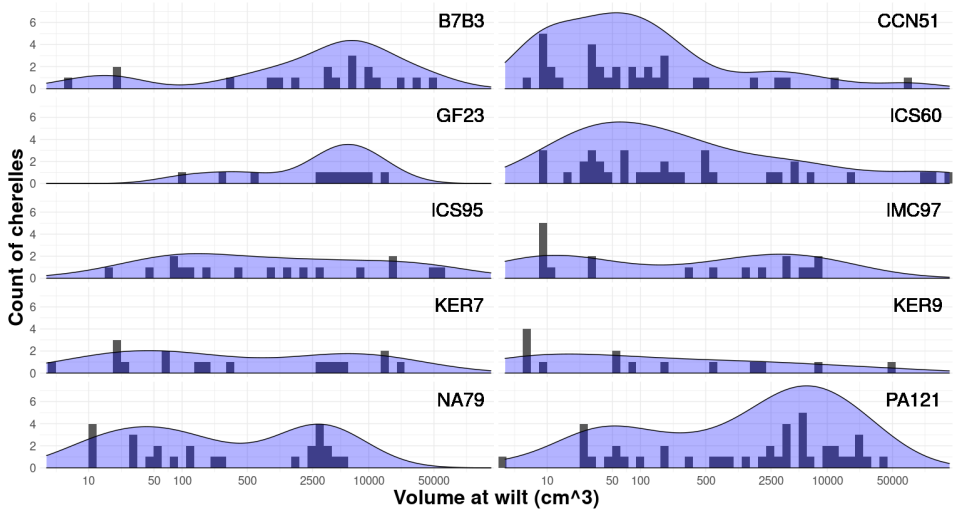

FIGURE 4.3.4: Density distribution and count for cherelle wilt at different volumes for the same ten cacao clones reported in Table 4.3.2. The volumes are plotted on a logarithmic scale to reduce the skewness of the data due to the five orders difference in magnitude of the data range (0-150,000).

4.3.3 Study of wilted cherelles in relation to the healthy ones

In the first 90 days after pollination, when cherelles can wilt, the growth is exponential and differences in volume between healthy and wilted cherelles in the first part of the cycle were

not easily evaluable on a linear scale. Therefore, a logarithmic scale was adopted to avoid data transformation (Figure 4.A.1, 4.A.2, 4.A.3).

Cherelles that wilted in the first month after pollination tended to be perfectly on par in size with the healthy ones for the entire first month in clones *GF*23, *KER*9 and *PA*121. For *B7B*3 the few wilted cherelles in the first two weeks appeared to be sensibly smaller than the healthy ones but the same was not true for the wilted cherelles of the last two weeks. For all other clones the difference in size between wilted and healthy cherelles grew wider in time (mind the logarthmic scale), with the wilted cherelles having a volume often half of the healthy ones from the third week onward (Fig. 4.A.1). The difference in size between wilted and average healthy cherelles continued throughout the second month after pollination for all the clones but *PA*121, *KER*7 (which wilted very little) and the first two weeks for *NA*79. For the latter three clones the wilted cherelles were aligned in size with healthy ones of the same age. Conversely, wilted cherelles for the remaining six clones were either sensibly smaller than the healthy ones (*KER*9, *GF*23 or *CCN*51) or on the lower side of the volume range at the same age (*B7B*3, *ICS*60, *IMC*97) (Fig. 4.A.2). Only five out of nine clones wilted more than one cherelle during the third month after pollination. For the *ICS*60 there were three wilted cherelles, all on par with the pod size at the same age. For the *CCN*51 and *PA*121 the wilted cherelles were significantly smaller than the healthy ones while for *B7B*3 and *KER*7 the wilted cherelles were found at the lower end of the size range of healthy cherelles (Fig. 4.A.3). The

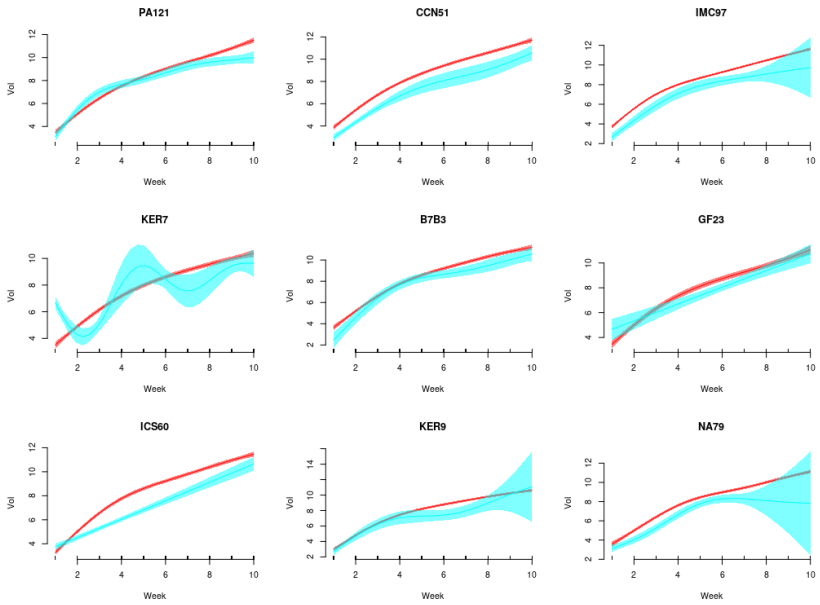

FIGURE 4.3.5: Modelling of the the volumetric growth of healthy (red) and wilted cherelles (blue) for nine cacao clones. The volume (y-axis) is expressed in dm^3. The model was built with as a GAMM with the cherelle age as fixed factor. The shaded areas are the 95% confidence intervals for the two curves and non-overlapping areas were considered as significantly different.

GAMM modelling of the cherelle volumetric growth highlighted significant differences between healthy and destined to wilt (Fig. 4.3.5). According to the GAMM model, the cherelles destined to wilt grow significantly slower than the healthy ones since the beginning for clones *ICS*60, *CCN*51, *IMC*97 and *NA*79. For the latter two clones the late part of the wilted cherelles growth was modelled with an extremely large uncertainty due to insufficient data to train the model (0 or 1 wilted cherelle in Fig. 4.A.3). According to the GAMM model, soon-to-wilt cherelles of the clones *PA*121, *B7B*3 and *KER*7 tend to grow comparably to the healthy ones for the first 4-5 weeks, after that their growth slows down and becomes significantly different the fifth (*KER*7), sixth (*B7B*3) and seventh (*PA*121) week (Fig. 4.3.5). Finally, the modelled

growth of healthy and wilting cherelles for clone *GF*23 was significantly different during the second month after pollination, otherwise the cherelles were modelled to grow at the same volumetric pace. The paucity of wilted cherelles available for clone *KER*7 thoughtout the three months after pollination (Fig. 4.A.1, 4.A.2, 4.A.3) led to an unreliable modelling of the cherelle that wilt by the GAMM model (Fig. 4.3.5). The general result from the GAMM model is that cherelles that are going to wilt eventually experience a slow down in growth.

4.3.4 Timing of wilting: from trigger to symptoms

For the following analyses only five clones were considered (*B*7*B*3, *ICS*60, *IMC*97, *KER*7, *PA*121). The relative volume increase rate in the first 10 weeks after pollination for the wilted cherelles of the five clones dropped between 1 and 3 weeks before the time of appearance of the symptoms (last measured point). The volume increase for the *IMC*97 dropped violently below zero (shrinking cherelles) two weeks before the symptoms were spotted. The other clones were found to decrease the volume increase rate more gradually but all showed a change in slope compared to the healthy ones ahead of the appearance of the symptoms (Fig. 4.3.6). The GAMM model for the relative volume increase rate of wilting cherelles in

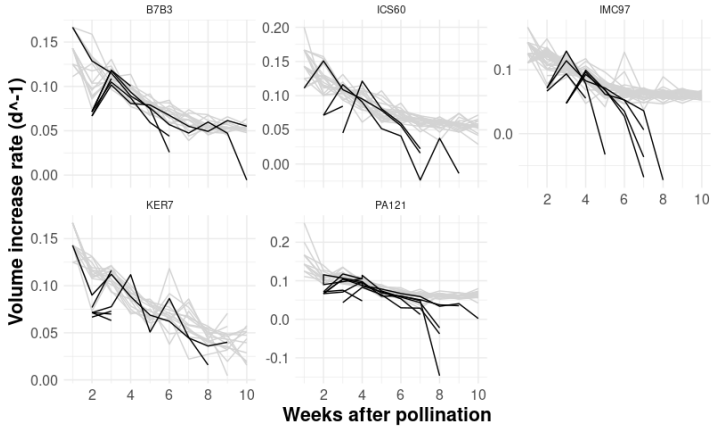

FIGURE 4.3.6: Relative volumetric increase rate in the first ten weeks after pollination for wilted (black) and healthy cherelles (gray) for five cacao clones.

Figure 4.3.7 predicted a sharp reduction across clones starting from the fourth week after pollination. Plotting the modelled data against the measured data yielded a coefficient of correlation of 0.85. The model included as predictor the number of weeks before the wilted cherelle was spotted. The GAMM model showed that in general a wilted cherelle reduces its volumetric increase rate drastically already 3 weeks before the symptoms are spotted (Fig. 4.3.8, in agreement with the previous results (Fig. 4.3.6).

Part two: the role of competition among fruits

4.3.5 Study of the destiny of pods from different generations

First of all, the wilting rate was evaluated in relation to the clone, position on the tree, age group of the cherelle and the cherelle generation ($1^{st} - 55^{th}$). The latter aimed at corroborating the results from Part 1. Out of the 8796 pods followed in the experiment, 1590 pods wilted. This corresponded to an overall wilt rate of 18.1%. The three clones considered had different wilt rates with *CATIER*4 trees wilting 204 of 1837 pods (11.1%), *CC*137 1043 out of 3657 (28.5%) and *Pound*7 343 pods out of 3302 (10.4%). According to the test for equality of proportions *CC*137 trees wilted many more cherelles than the other clones (p-value $< 2.2e^{-16}$).

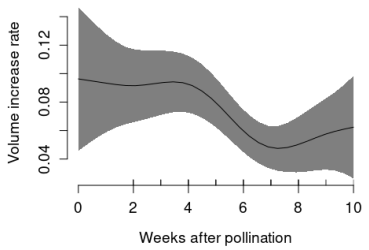

FIGURE 4.3.7: Modelling of the relative volume increase rate of wilting cherelles in the first ten weeks after pollination.The model was built aggregating data from five cacao clones. The model is a GAMM with the month of wilt as fixed factor, the weeks after pollination and the weeks before wilting as smoothing factors. The shaded area represents the 95% confidence interval. The relative volume increase rate (y-axis) is expressed in d^{-1}.

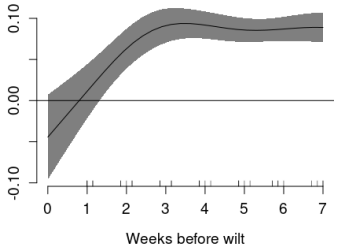

FIGURE 4.3.8: Modelling of the relative volume increase rate in the seven weeks before the moment of wilt for cherelles of five cacao clones. The model is a GAMM with the month of wilt as fixed factor, the weeks after pollination and the weeks before wilting as smoothing factors. The shaded area represents the 95% confidence interval. The relative volume increase rate (y-axis) is expressed in d^{-1}.

On the branches (H), the cherelles had a 18.5% chance of wilting against the 16.8% on the main trunk (B). Although, the test for equality of proportions found no significant difference imputable to the cherelle's position on the tree (p-value = 0.08267). The chance of wilting significantly dropped with progressing age groups. "Small" cherelles had a 14.8% chance of wilting, that dropped to 1.21% for cherelles in the "Medium" category and further dropped to 0.009% for "Large" pods. The significance of the differences was tested with the test for equality of proportions (p-value $< 2.2e^{-16}$ for all couplings).
Cherelles from different generations ($1^{st} - 55^{th}$) did not have the same chances to make it to harvest as they had different probabilities to be removed from the tree for other reasons, moniliosis and wilting mainly (Fig. 4.3.10). In absolute values, the number of harvested pods per generation was a direct consequence of the generation's total number of pods for the *CATIER*4, which had extremely low losses to wilt or moniliosis (Fig. 4.3.9). Nonetheless, the peaks in wilting for *CATIER*4 occurred as well during the development of some of the largest generations (25^{th} and 37^{th}), while losses to moniliosis were much less impactful than the other two clones. Conversely, the clone *Pound*7 tended to produce more abundant generations overall but lost most of the pods to moniliosis and wilting (Fig. 4.3.9 A, B, C). Both moniliosis and wilt surged with the number of pods in a generation (Fig. 4.3.9 A, B, C). The *CC*137 was found to lose several pods due to moniliosis mostly in correspondence of the first group of large generations (15^{th} to 28^{th}), while later large generations (32^{nd}, 45^{th} and 46^{th}) were almost entirely lost due to wilting (Fig. 4.3.9 A, B, C). Overall, the *CC*137 had to an absolute productivity (pods that were harvested) intermediate between the higher yields of *CATIER*4 and the very low yields of *Pound*7 (Fig. 4.3.9 D).
As expected, all processes were more relevant at the field level in absolute values when the generations were more abundant. To test if the probabilities for a pod to be harvested, wilt, be infected by moniliosis or lost for other causes, it was necessary to divide the absolute values for each category by the total number of pods in a generation. The proportion of pods that were harvested tended to decline with the generation's number for all three clones, with the first 5-10 generations being the most efficient in terms of yield (Fig. 4.3.10 A). Disregarding the last ten generations (46^{th} to 55^{th}) that were completely lost for all clones, the most efficient yielder was *CATIER*4 (59% on average), followed by *CC*137 (21.4% on average) and *Pound*7

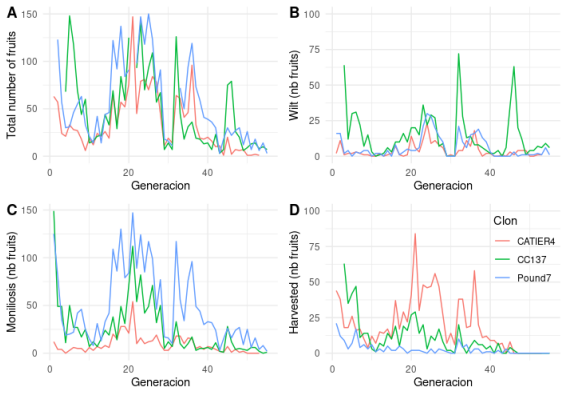

FIGURE 4.3.9: Evolution of the absolute number of cacao pods produced (A) in the field and their destiny for three clones followed for 55 weeks, each corresponding to one different generation of pods. The possible destinies for the pods were to wilt (B), be lost for a moniliosis attack (C) or harvested (D).

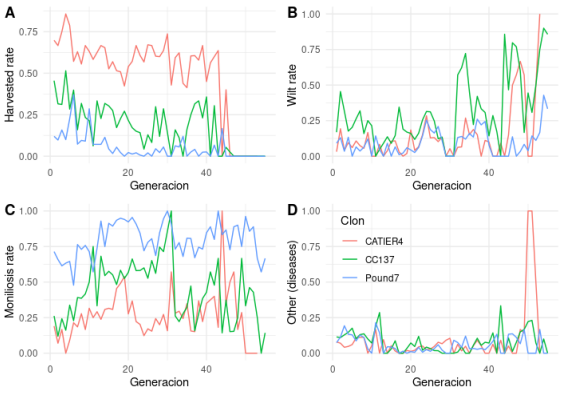

FIGURE 4.3.10: Proportion of cacao pods of three clones to be harvested (A), lost due to cherelle wilting (B), moniliosis (C) or other causes, mostly other diseases (D) for 55 different generations of pods under field conditions. Each generation corresponded to the new fruits registered on a weekly basis.

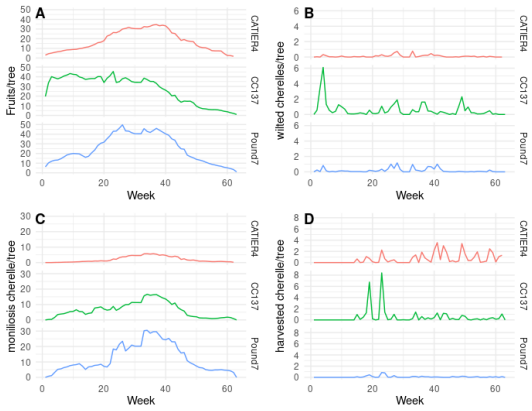

FIGURE 4.3.11: Pod production dynamics at the tree level for three cacao clones under field conditions. Are presented: the total pod load in time (A), the number of wilted (B), moniliosis infectected (C) and harvested (D) cherelles over the 63 weeks of the experiment. The three clones are reported in different colors: *CATIER*4 (red), *CC*137 (green) and *Pound*7 (blue).

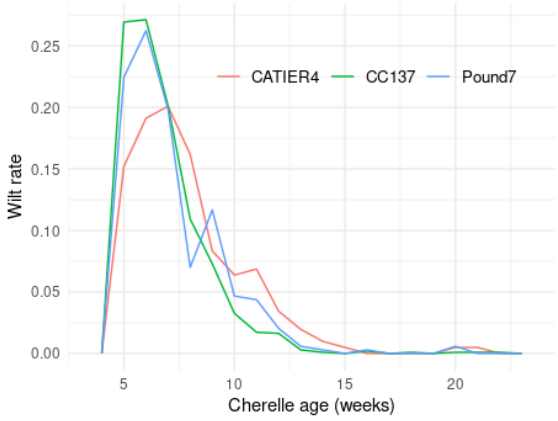

FIGURE 4.3.12: Wilt rate for cacao cherelles of estimated age between 4 and 25 weeks. Each line represents one of the three clones used in the experiment.

(6.5% on average). The probability of wilting varied between generations but tended to be higher for late generations appearing in the second part of the production year, when there are many fruits from different generations on the cocoa tree (Fig. 4.3.10 B). Some peaks in wilting seemed common to all 3 clones (generations 23 and 33-38), while a surge in the wilt rate for the 43^{rd} to 47^{th} generations was common to *CATIER*4 and *CC*137 and went above 50%. The latter clone presented other peaks in wilting up to the 10^{th} generation (22%) and for the 18^{th} generation (35%) (Fig. 4.3.10 B). The generally higher wilt rate of *CC*137 is in agreement with the aforementioned average proportion of wilted fruits. The moniliosis was found to be a major source of pod losses for all clones. The rate of infection for *Pound*7 was steadily above 50% with an average of 79.5%, while the other two clones presented a more irregular rate of infection depending on the generations. The proportion of pods lost for moniliosis for the *CC*137 increased in the first 30 generations up to 100%, then dropped to 25% with two major revamps at generations 38 - 42 and 49 - 52. The average proportion of pods infected by moniliosis for the *CC*137 was 43.6%. The rate of moniliosis infections for *CATIER*4 was the lowest on average (26.6%) and presented peaks at generations 18 - 19, 21, 43 - 45 (Fig. 4.3.10 C). The losses for all other sources were on average 9.3%, 7.7% and 5.9% for *CATIER*4, *CC*137 and *Pound*7 respectively with higher rates for the late generations (43^{rd} - 55^{th}). In particular, the 52^{nd} and 53^{rd} generations for *CATIER*4 were completely lost due to "other" causes (Fig. 4.3.10 D).

4.3.6 Study of the pod load's dynamic at the tree level

Passing from the field level to what happened at the level of an average tree of each clone, it was possible to study the dynamics of wilting, moniliosis and final harvest at the tree level over the 63 weeks of the experiment. The *CC*137 was found to be the fastest to set a large number of pods in the first ten weeks of the experiment and kept the total pod load high until the 32^{nd} week, then declined. The total pod load for the other two clones was built up more gradually until it reached a stable plateau between the 25^{th} and 40^{th} week of the experiment, then declined (Fig. 4.3.11 A). Whenever in Figure 4.3.11 A the slope was flat, it meant that there were no net losses in the pod load. In other words, any loss through harvest, moniliosis or wilt was compensated by the set of new cherelles. The high pod load of *CC*137 in the first weeks was followed by two spikes in wilting during the 3^{rd} and 9^{th} week of the experiment (6 pods/tree and 1 pod/tree respectively), then an average *CC*137 tree wilted between 1 and 2 pods/tree between the 23^{rd} and 28^{th} , 32^{nd} and 35^{th} and 48^{th} and 51^{st} weeks (Fig. 4.3.11 B). *Pound*7 presented a series of peaks of wilt (1 pod/tree) in weeks 4, 26 to 28, 33 and 38 to 41, while *CATIER*4 had at least 1 pod/ tree wilted only in weeks 28 and 33 (Fig. 4.3.11 B). Moniliosis infections were concentrated for all clones between week 20 and 47 and were sensibly more for *Pound*7 (Fig. 4.3.11 C). The *CC*137 had two main harvesting weeks, the 19^{th} (7 pods/tree) and 22^{nd} (8 pods/tree) while the second half of the season was characterized by small weekly harvests of up to 2 pods/tree (Fig. 4.3.11 D). The harvest for clone *CATIER*4 was concentrated in the second half of the season with weekly harvests between 2 and 4 pods/tree, while the *Pound*7, that lost most of the pod load to moniliosis, had a noticeable harvest ($>$ 0.5 pods/tree) only during week 19, 22 and 23, with a maximum of 1 pod/tree (Fig. 4.3.11 D).

4.3.7 Study of wilt rate based on the estimated fruit age

The age in estimated days after pollination of wilted cherelles varied among clones. The age was estimated to be four weeks more than the period that the cherelles were tagged. in estimated days after pollination. *CATIER*4 was estimated to wilt on average at 55 days,

*Pound*7 at 50 and *CC*137 at 47. These results for three clones in Costa Rica are only estimates but are in line with the values found in French Guyana and reported in Table 4.3.1. For all clones the wilt rate is maximum in the first 15 weeks. Clone *CC*137 tends to wilt earlier than the other two clones. It has one peak between 5 and 6 weeks after the estimated pollination, then followed by a steady decline until the 12^{th} week. *Pound*7 presented a surge in wilt rate after 5 weeks from the estimated pollination that peaked at 6 weeks to then generally decline until the 12^{th} week, despite a smaller peak the 9^{th} week. *CATIER*4 presented a later peak at 6-7 weeks followed by a gradual decline slower than the other two clones until the 15^{th} week (Fig. 4.3.12). These results align with those from French Guyana on the presence of a main peak of wilt but not so much on the exact timing (Fig. 4.3.1, 4.3.3). The difference might be due to the different environment and genetic material but could be as well because the age of the pods is not known at the time of their first observation, it is possible that differences in pod size made it easier to detect young pods of one clone than another, leading to over or underestimation of their age.

4.3.8 Predictive factors for wilt: BRT model

The main predictors for cherelle wilt were identified by means of a BRT model (Figure 4.3.13). The eight predictors used to predict the wilted pods on a tree were:

1. Clone: *Clone*,
2. cherelle age: Age_{weeks},
3. position on the tree: *Position*,
4. number of Small pods on the tree one week before: *TreeSmallT*1,
5. number of Small pods on the tree five to six weeks before: *TreeSmallT*4,
6. number of Medium pods on the tree one week before: *TreeMediumT*1,
7. number of Large pods on the tree one week before: *TreeLargeT*1,
8. number of Large pods on the tree five to six weeks before: *TreeLargeT*4

Among the predictors representing competition from other fruits, *TreeSmallT*1 was found to have the highest relative influence in explaining cherelle wilt (31.7%), followed by *TreeSmallT*4 (16.1%) and *TreeLargeT*4 (13.9%). The *TreeLargeT*1 and *TreeMediumT*1 had a marginal influence in explaining cherelle wilt (7.9% and 7.4% respectively). Pods competition aside, the Age_{weeks} was the most important cherelle intrinsic property among the the predictor (14.1%). The importance of the other cherelle intrinsic properties, *Clone* and *Position*, was poor (6.0% and 2.9% respectively) (Figure 4.3.13).

Despite being the most influential predictor by far, an increasing *TreeSmallT*1 did not change the modelled wilting probability, flat functional shape, until around 60 pods/tree. Beyond 60 pods/tree, the probability of wilting appeared to increase but the trend was difficult to verify as the maximum number of *TreeSmallT*1 was around 70 pods/tree and there were few points to build the curve. The probability of wilt increased steeply for *TreeSmallT*4 between 0 and 5 pods/tree, then it tenuously increased until 30 pods/tree, then increased with a steeper slope up to 38 pods/tree and then dropped linearly until reaching at 50 pods/tree roughly the same value as for 10 *TreeSmallT*4. The age of the cherelle (Age_{weeks}) was found by the model to linearly reduce the probability of wilt for cherelles older than 7 weeks after the estimated pollination. The number of *TreeLargeT*4 did not influence the probability of wilt between 0 and 10 pods/tree, then it the probability of wilt linearly increased with the number of *TreeLargeT*4 up to 15. Beyond this threshold, the probability of wilt oscillated around

a stable value. For both *TreeLargeT*1 and *TreeMediumT*1, an increasing number of pods per tree appeared to very slightly reduce the probability of wilt, especially beyond 10 pods/tree. Moreover, the *CC*137 was found to have a higher probability of wilt than the other two clones, in line with the previously presented statistical results for the real data (Fig. 4.3.13, 4.3.10.B) and pods on the trunk were found by the model slightly more susceptible to wilting than on the branches.

The model found that the four most influential predictors were the only ones to present pairwise interactions with a significant strength, even when changing drastically the *seed.number*. This confirmed the lesser importance of *Position*, *Clone*, *TreeMediumT*1 and *TreeLargeT*1 in determining the wilting rate. The importance of the interactions varied with different *seed.number* but the interactions that were stable and strong enough to emerge in all rounds of simulation were among *TreeSmallT*1, *TreeSmallT*4 and *TreeLargeT*4. These interaction were always difficult to interpret because mostly tied to fringe values, thus it was hard to draw meaningful conclusions (Fig. 4.3.14). In general can be stated that:

- if there were only few Small pods the week before as well as 5-6 weeks before, the wilt rate increased considerably Fig. 4.3.14, left);
- the effect of Small pods the week before on wilt rate was boosted by the presence of more than 15 Large pods 5 to 6 weeks before Fig. 4.3.14, centre);
- whenever 5 to 6 weeks before wilt the number of Large pods was high, a decreasing number of Small pods steadily increased the rate of cherelle wilt (Fig. 4.3.14, right).

The model skill in predicting wilted cherelles of the training data was considered good (AUC score for the training data=0.90, AUC score for the cross validation = 0.81) despite the medium training data correlation (0.47) and cross-validation correlation coefficient (0.36). Furthermore, the difference between the AUC score of the training data was close to the AUC of the cross validation data, meaning that the model's over-fitting was acceptable. The soundness of the model, tested by applying it to the training and the test data, not used for model building, was excellent. From the confusion matrix of the training data emerged a True Positives Rate (TPR) of 83.1% and a False Positives Rate (FPR) of 19.8% for the model. Thus, the model provided a good prediction of the wilt dynamics per clone for the training data (Fig. 4.3.15). For the test data, the prediction was less good (TPR of 73.0% and a FPR of 20.5%), especially in the second part of the prediction year (Fig. 4.3.16). The model could find the main peaks in cherelle wilt specific for each clone both for the training and the test data, but their height was, sometimes, underestimated or captured with a week difference (Fig. 4.3.15). Conversely, the minor peaks were often poorly predicted as they corresponded to very few wilted pods. Overall, the BRT model was quite good at predicting the risk of wilt in pods from 5 to 12 weeks. However, it has been already highlighted that there was a tendency to over-fit, which was probably due to relationships between predictors. Despite the model used 8370 different unique pods from 91 trees of three different clones and eliminated the pairwise correlated variables, there may be more global interconnections that remained unknown.

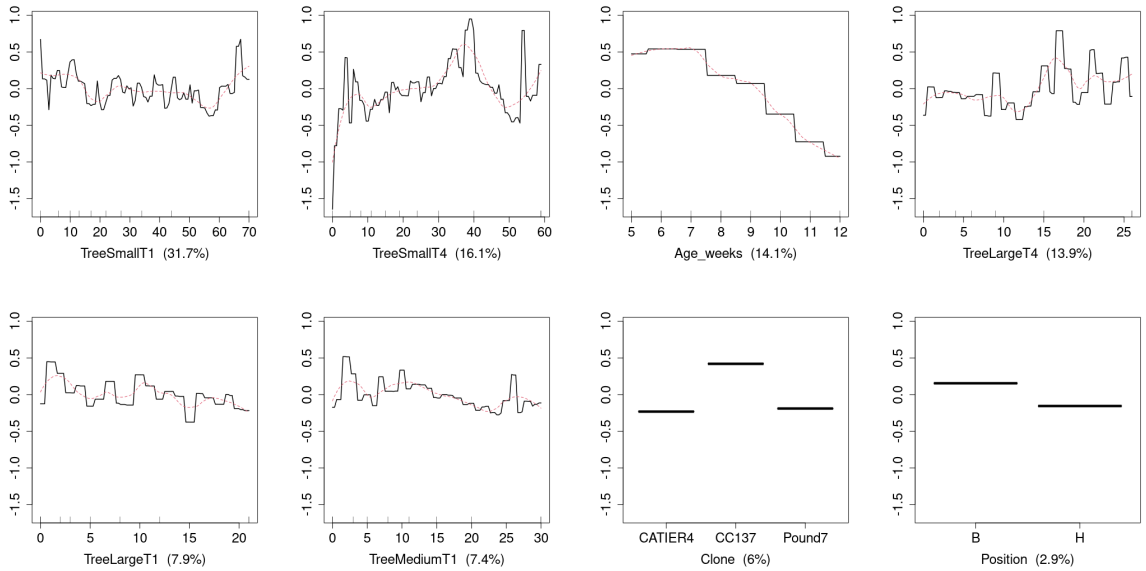

FIGURE 4.3.13: The response of the fitted function identified with a BRT model for cherelle wilt to eight selected predictors. Each variable was presented with the relative weight of its variation on the wilt probability. The variables represent intrinsic properties of the cherelles (Age_{weeks}, *Clone* and *Position*) and competition from pods of different sizes in the weeks before wilting (*TreeSmallT*1, *TreeMediumT*1, *TreeLargeT*1, *TreeSmallT*4, *TreeLargeT*4). T1 = one week earlier, T4 = five to six weeks earlier. In red are presented the smoothed fitted functions.

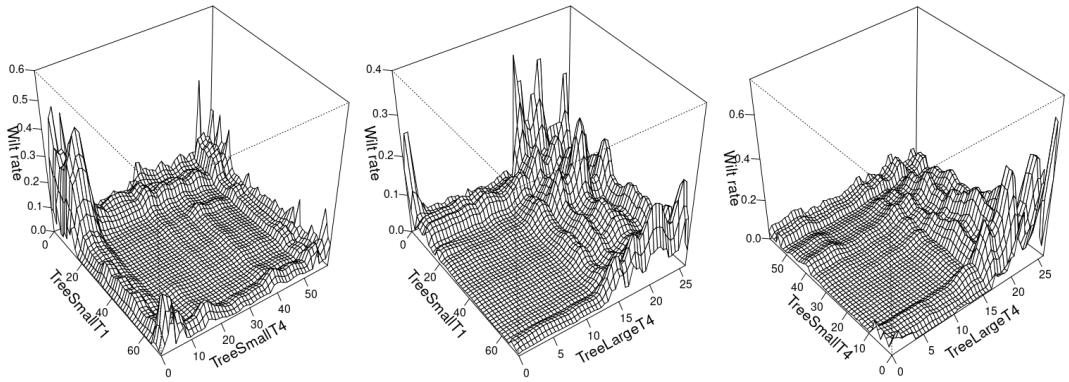

FIGURE 4.3.14: Three-dimensional partial dependency plots for the interaction between *TreeSmallT*1 and *TreeSmallT*4 (left), *TreeSmallT*1 and *TreeLargeT*4 (centre) and *TreeSmallT*4 and *TreeLargeT*4 (right) for the BRT model that predicted cacao cherelle wilt rate. All variables except those plotted are held constant at their mean values.

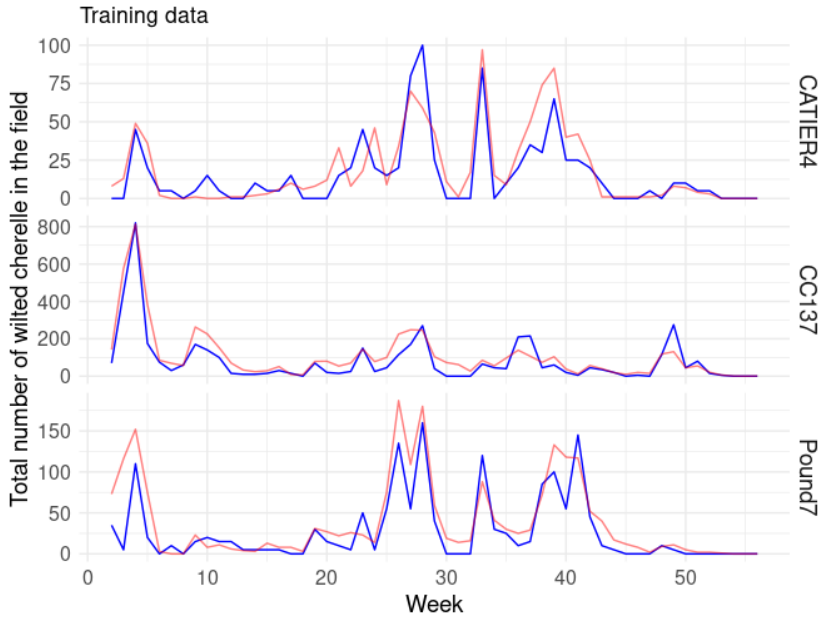

FIGURE 4.3.15: Predicted cherelle wilt dynamics against the measured data at the field level for three cacao clones. The prediction (red) was obtained by applying a BRT model to its training dataset (blue). As the proportion of wilted cherelles in the training data was small, in absolute terms the model produced many more false positives than true positives. Therefore, a coefficient of x5 was applied to the measured data to scale the two curves.

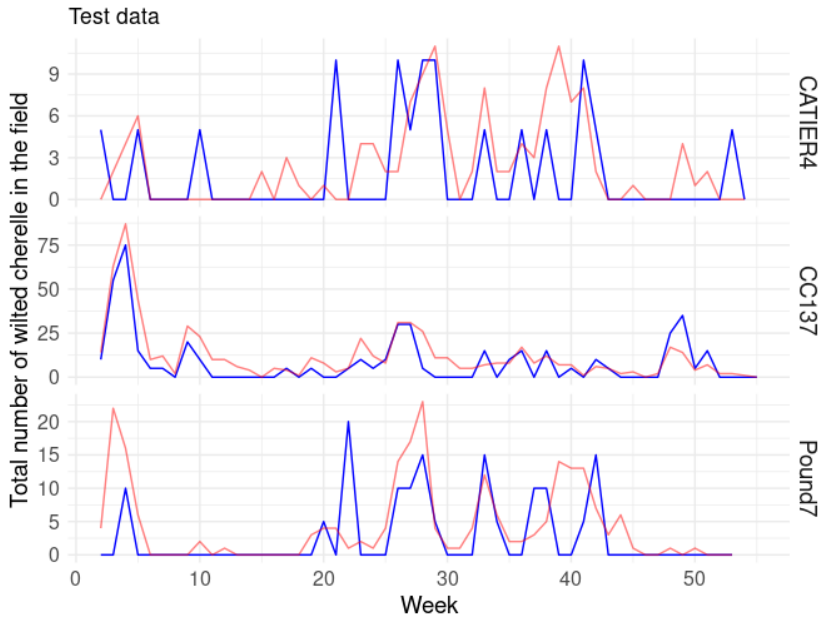

FIGURE 4.3.16: Predicted cherelle wilt dynamics against the measured data at the field level for three cacao clones. The prediction (red) was obtained by applying a BRT model to test dataset not used to train the model (blue). As the proportion of wilted cherelles in the test data was small, in absolute terms the model produced many more false positives than true positives. Therefore, a coefficient of x5 was applied to the measured data to scale the two curves.

4.4 Discussion

4.4.1 Timing: Does cherelle wilt have one or two peaks depending on the clone?

When it comes to cherelle wilt, the genetic component was proven to be key in determining the timing and magnitude of the phenomenon, with clones usually wilting early (i.e. *CCN*51 or *ICS*60 in French Guyana), late (i.e. *GF*23 or *B7B*3 in French Guyana) and more or less abundantly (i.e. *CC*137 in Costa Rica) (Fig. 4.3.3, 4.3.12, 4.3.10). Nonetheless, some common patterns were found in both the experiment in French Guyana and Costa Rica. The major one is that in both cases, regardless of the clone, cherelle wilt presented only one main peak (Fig. 4.3.1, 4.3.3, 4.3.12). For the clones in French Guyana the peak was between 21 and 35 days after pollination. For the clones in Costa Rica the peak was found between 35 and 42 weeks after the estimated pollination. The difference in the timing of the peak in the two studies could have been due to genetics only but the age of wilted cherelles in Costa Rica was estimated and could differ from from the real one by one week. In any case, the presence of only one main peak of wilting, as well as its timing, is in line, and confirms, the results hinted in previous works [57, 103] and with the first of two peaks proposed by Mckelvie (1956) [151]. Although, the latter study proposed the presence of two peaks of wilting of comparable magnitude, a result that was not confirmed by the results of our two experiments. Nevertheless, some clones in French Guiana presented a second minor peak in wilting at around 9-10 weeks after pollination, compatible with Mckelvie (1956) in terms of timing but not magnitude. According to the author, the second peak in wilting might be overlooked whenever hand pollination is not performed [151]. The absence of hand pollination could explain the absence of a second peak in Costa Rica (Fig. 4.3.12) and previous studies [57, 103] but not the results in French Guyana, that were hand pollinated continuously (S. 4.2.2, Fig. 4.3.3).

4.4.2 Fitness: Do wilted cherelles accumulate less biomass than healthy ones?

At parity of age and genetic material, the study in French Guyana (Part 1) concluded that the volumetric growth was slower or among the slowest for cherelles destined to wilt, highlighting a lesser investment by the plant (Fig. 4.3.5). This difference in investment grew in time and became more evident from the third week after pollination onwards. The difference was especially evident in the second month after pollination, when cherelles are almost in the linear part of their growth (Fig. 4.A.2) [7]. According to the GAM model of cherelle growth (Fig. 4.3.5), not all clones had the same evolution of the difference in size between healthy and soon-to-wilt cherelles. Nonetheless, for all clones but *KER7* the most critical month was the second. *KER7* was probably not well captured by the GAM model due to the insufficient number of wilted cherelles observed in the second month (Fig. 4.A.2). The lesser investment by the plant in the cherelles that then wilted was corroborated by the lower volumetric increase rate observed and modelled with a GAM model (Fig. 4.3.6, 4.3.7) and previous studies [156, 172]. In fact, it has been already established that the main mechanism the plant has to wilt cherelles is to occlude the xylematic vases by thickening and suberizing them [156, 170, 172]. The novel contribution of this study was to quantify the time and magnitude of the drop in assimilates. It was documented that the assimilates investment by the plant relative to the volume naturally drops in time. While the healthy ones seem to generally reach an asymptotic value after 6 weeks, the volumetric relative increase of wilting cherelles continued to further drop for all clones but *KER7* (Fig. 4.3.6). Furthermore, it takes around three weeks for the tree to completely shut the assimilates flow of wilting cherelles (Fig. 4.3.8). This was found to be true across clones and progresses our understanding of cherelle wilt. Nevertheless, it would be useful to repeat and confirm these results with a dedicated study in other

environments and with more direct means of measuring the change in the assimilate flow, for example with micro sap flow sensors applied to the peduncule as done for other species with a fragile peduncule as cacao [9, 104, 244].

4.4.3 Fitness: Does the position on the tree matter for cherelle wilt?

It has been proposed in the past that cherelles which set on the thinner branches in the peripheral part of the tree, situated farther from the ground, are more susceptible to wilting than those set on thicker branches nearer the ground or the main trunk. This because of a lesser access to mineral nutrition and assimilates [110, 111, 155]. The statistical analyses from the study in Costa Rica (Part 2 of this chapter) did not find this difference (S. 4.3.5) and the BRT model to predict the probability of cherelle wilt even hinted that the chances are higher on the trunk than on the brances (Fig. 4.3.13). This is a controversial result that goes against what was expected knowing that fruits on lower branches orders have access to more phlolematic flow [60, 251], also in cacao [203]. Although it is relevant, the cited study on cacao fruit dimension based on their position should not constitute a hard proof of the better fitness of pods on the trunk. In fact, their statistical analysis relies on very few pods per category (n=3) [203], it must be confirmed by a larger study. A possible explanation for the irrelevancy of the fruit position might be that the lesser source availability of fruits on the branches might have been compensated by the fact that fruits on the trunk were more packed (more fruits per floral cushion) and felt more the competition by neighbouring fruits. However, the results in part 2 of this chapter cannot advocate for a different wilt rate depending on the cherelle position but cannot completely rule it out either, leaving ground for future dedicated studies to better unravel the subject.

4.4.4 Competition: Which fruits are more susceptible to competition and which others are strong competitors for resources?

If the timing of cherelle wilt was more or less synchronous across clones and locations (Fig. 4.3.1,4.3.12; Tab. 4.3.1), its magnitude changed with the tree's total pod load for the different clones (Fig. 4.3.9,4.3.11). The more abundant generations were always followed by peaks in wilting for all clones, suggesting a high competition within cohorts of cherelle of the same age when still young. The fact that $TreeSmallT1$ (the small cherelles on the tree one week before) was found as the predictor with the largest influence on the wilt rate by the BRT model (Fig. 4.3.13) corroborates as well the idea that intragenerational competition is of great importance. A clear example is the sudden peak in wilting following the early setting of $CC137$ in Figure 4.3.9. More in general, the importance of competition among pods is demonstrated as well by the fact that the major peaks in wilting for all clones occurred not only for the most abundant generations but when the pod load was maximum as well (Fig. 4.3.9, 4.3.11). The spikes in wilt rate were more evident for $CC137$ than for $Pound7$ or $CATIER4$. A simple explanation for $Pound7$ i that it lost many fruits to moniliosis, while $CATIER4$ apparently had a minor tendency to wilt. To summarise, $CC137$ appeared to be a prolific clone that sets many fruits but then wilts a great portion of them. The second most prolific clone was $Pound7$, the wilt rate of which was relatively low and constant mostly due to its high sensibility to moniliosis that slashed its setting down. Finally, $CATIER4$ produced less pods per tree and more spread in time than the other two clones but was characterised by a lower average wilt rate (Fig. 4.3.11, 4.3.10).
The generations in the second part of the season were characterised by a higher average wilt rate than the first half of the generations (Fig. 4.3.10). This is not very likely to be due to a difference in climatic conditions as the climate did not differ much. A better explanation is that

in the end of the production period followed in the experiment, the trees were likely to have exhausted their pool of resources, exacerbating the effects of intergenerational and intragenerational competition (Fig. 4.3.10). Moreover, the low number of new pods set in the second part of the season suggests that there was competition for resources from processes other than fruiting (Fig. 4.3.11). A good example being leaf flushing [58, 226]. Even if it was not possible to verify it, vegetative growth would have contributed to the exhaustion of the pool of assimilates. This would have inhibited setting and increased the competition for resources among the young cherelles. The exhaustion of the tree reserves together with the alleged competition by other organs would explain why the wilt rate went up despite a drop in the total pod load.
According to the BRT model for cherelle wilt prediction, the number of Small cherelles (*TreeSmallT*1, *TreeSmallT*4) is the most important predictor of wilt. The number of Small cherelles a given week do not change the wilting rate the following one but represents the most influential predictor (*TreeSmallT*1 in Fig. 4.3.13). This is because more cherelles there are on the tree at T1, more wilted ones will follow the week after in absolute terms. The number of *TreeSmallT*4 being a strong predictor for wilting that increases the wilt rate with its number means that this category of fruits is largely the most important representative of the intergenerational competition. The *TreeSmallT*4 corresponds to fruits between 10 and 16 weeks old or roughly the young "Medium" pods at the moment of wilt. Oddly, the BRT model reports an opposite trend for *TreeMediumT*1, even though this should largely overlap with *TreeSmallT*4 and convey the same type of information (Fig. 4.3.13). It is possible that the model accounted for the intergenerational competition represented by the "Large" pods only once, thus the effect of the young "Medium" pods (*TreeMediumT*1) overshadowed the role of the entire category (*TreeMediumT*1). The importance of older pods ("Large") relied mostly on their interaction with other categories 5 to 6 weeks before wilting (Fig. 4.3.14). This probably is because a high number of Large pods could correspond to waves of setting that managed to survive in bulk, possibly draining the reserves of assimilates of the plant.
Despite the BRT model did not explain most of the variance in the data (training data coefficient = 0.47, cross-validation correlation coefficient = 0.36), the predictions in Figure 4.3.15 and Figure 4.3.16 as well as the AUC (Area Under the Curve) for the model are proves that the model could at least replicate the clone specific wilting profile over the season. The quality was better when simulating the training data than the test data. Nonetheless, the TPR and FPR for the prediction of the test data was an acceptable result with 73% of wilted cherelles correctly predicted and a fifth of all predicted wilted cherelles not reflected in the real data. This can be considered a first step toward a comprehensive modelling for cherelle wilt.
To increase the explained variance and improve the model predictive power, many other factors should have been factored in. This study focused on the role of competition among fruits but did not consider other forms of competition (i.e. leaf flushing) [155, 226]. Another form of competition not considered here that may play a role is the competition between neighbouring trees. Trees that are more fit might compete better for resources, therefore the wilt rate could have changed between trees based on their vigour. Furthermore, the nutrients availability might have played a role as well. Fertilization has been reported sometimes to contribute reducing the cherelle abortion in cacao [26, 226], while a more recent study in Ghana did not find any effect of increased fertilization on the rate of wilting [98]. Although, the authors from the study expected fertilization to have an impact and proposed that the excellent soil fertility in their case hid the effect of the supplementary fertlization [98]. In this study, it is possible that in the end of the experimental period the nutritional state of the tree and the soil were different and might have decreased the overall tree vigour, thus indirectly increasing the wilt rate. If this ulterior source of uncertainty had been accounted for in the model, it is possible that part of the remaining variance would have been explained. Climate as well was proven to increase fruit abortion in cacao [155], especially rainfall abundance and

temperatures [55, 101, 132]. For our experiment it is probable that climate did not play a major role as the climate was stable and constant throughout the experiment but this element should be factored in in any future attempt to model cherelle wilt. Lastly, because the focus was on competition among fruits, the presence of pests and diseases was disregarded in the BRT model. For example, a study in Asia found that a small percentage of wilted cherelles showed signs of prior insect feeding [26]. Moreover, Melnick (2013) studied the molecular and metabolic changes of cherelle wilt of cacao and its interaction with the presence of moniliosis or frosty pod *Moniliophthora roreri*. The study concluded that cherelle wilt enhances the plant's defences and turns the cherelle in a infertile substrate for moniliosis, effectively disrupting its infection and sporulation [156]. Conversely, there are no clear indications of how certain pathogens affect the wilt rate as wilting has been treated as minor issue for a long time. Scientists are recently making greater efforts to assess the impact of pest management treatments on cherelle wilt but there is still a lot of work to be done [155]. The data used to train the model presented a high proportion of infested pods, especially for the clone *Pound*7 (Fig. 4.3.10) but the moniliosis was not chosen as a predictor in the model. Part of the unexplained variation in the data could have been imputable to the phytosanitary state of the single trees.

4.5 Toward a mechanistic modelling of cherelle wilt: Useful conclusions

In conclusion, this study supports the presence of only one main peak of wilting between the third and fifth week after pollination followed in some clones by one or more considerably lower peaks after the ninth week. Furthermore, the risk of wilting for a cherelle decreases with the age after the first seven weeks of growth (BRT results). Moreover, the process of wilting was found to be initiated three weeks before the symptoms became evident, and in most cases involved cherelles that were already growing slowly compared to others of similar age. During these three weeks the relative growth rate dropped almost linearly. Based on all this, it could be possible to model whether a cherelle will wilt or not based on its biomass accumulation in time compared to the optimal growth. Whenever a certain cherelle is sensed to be growing slowly it could be possible to apply a reduction factor to its relative growth rate. Set aside the fitness of the cherelle, competition for resources was found to be another key predictor for cherelle wilt. Competition for assimilates was proven to be mostly imputable to pods 10 to 16 weeks old, which are in the linear phase of growth and their relative growth rate is maximal [7]. Together with the competition from older pods, the intragenerational competition should be considered as well when modelling cherelle wilt. The general rule supported by our results is that more abundant is a generation, more important will be the magnitude of cherelle wilt for that generation, regardless of the intergenerational competition. Lastly, for the purpose of modelling cherelle wilt the fruit position on the tree appeared to be negligible and anyway requires more investigations to be fully clarified.

Appendix

4.A Chapter 4: Dimension of the wilted cherelles compared to healthy ones

The wilted cherelles from 9 selected clones were plotted month by month with the cherelles of the same age that continued to grow. This was done to have a first, visual understanding of the type of cherelles that wilt.

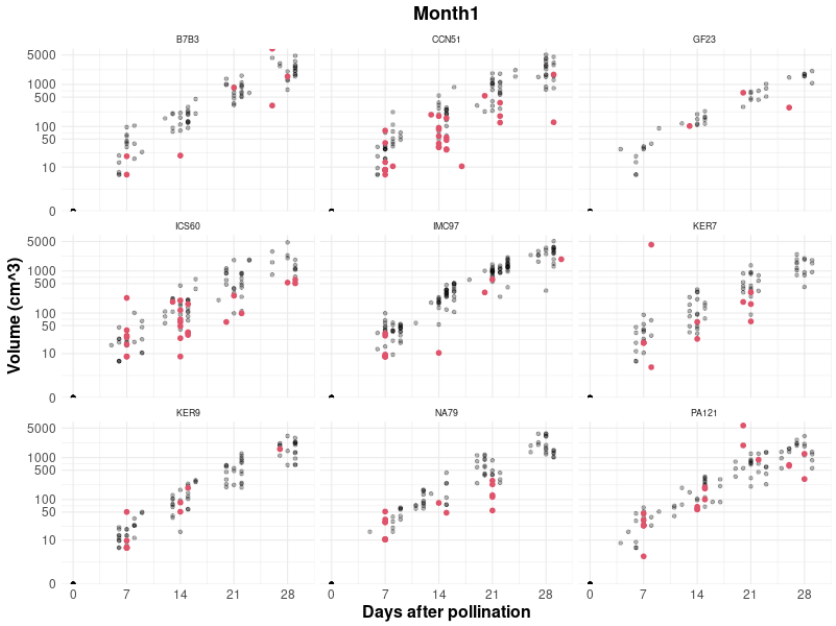

FIGURE 4.A.1: Comparison between the volumetric growth of wilted cherelles (red dots) and healthy cherelles (gray) of the same age during the first month after pollination for 9 cacao clones.

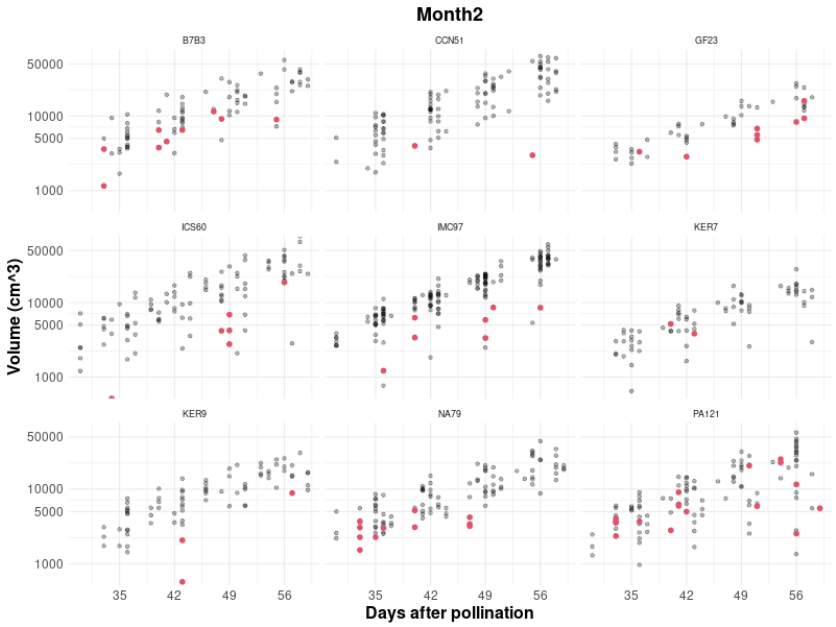

FIGURE 4.A.2: Comparison between the volumetric growth of wilted cherelles (red dots) and healthy cherelles (gray) of the same age during the second month after pollination for 9 cacao clones.

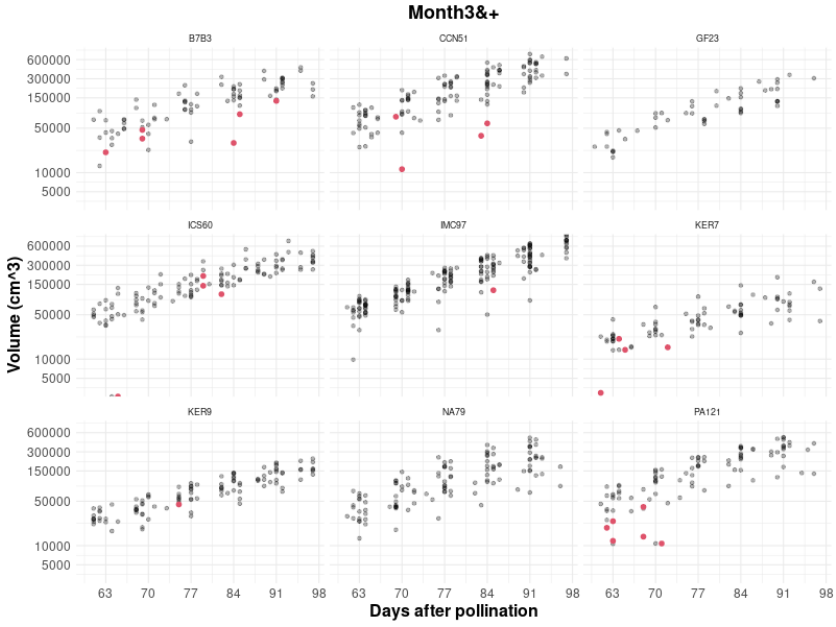

FIGURE 4.A.3: Comparison between the volumetric growth of wilted cherelles (red dots) and healthy cherelles (gray) of the same age during the third month after pollination for 9 cacao clones.

Chapter 5

Towards a comprehensive mechanistic model for cacao

Plant growth modelling allows us to explore, test hypotheses and conduct theoretical experiments on plant growth processes that might otherwise take years of experimentation under field conditions [212]. Time-consuming and costly agronomic field trials to test specific plant traits (genetics) [66, 74, 238], management practices [24, 147, 176] or environmental changes [42, 122, 145, 196] could be evaluated in advance with a much shorter modelling exercise [230]. Furthermore, through simulation, the evolution of whole agroecosystems under different scenarios [183], or the impact on yields that specific episodes may have, can be assessed. Consequently, plant growth modelling has become an essential tool to guide research, particularly in agronomy, forestry and environmental sciences [212].
This dissertation addresses the need for actionable tools that can guide the strategic decisions and investments of a French cocoa trading company, again highlighting the usefulness of models for the private sector as well. From the company's perspective, the objective of this project was to obtain a representation as complete as possible of cocoa physiology in response to climate, to be used for predicting yield variability on a sub-seasonal scale. Therefore, the initial plan was to base the study on CASE 2, the only existing model for cocoa physiology [257]. The idea was to modify the modelling of specific processes, discussed in S. 1.4.2, to tailor the model on the West African cocoa belt growing conditions. Unfortunately, due to intellectual property rights, we had access to the code but not the right to modify it, so we had to change our strategy. We took advantage of this challenge to review the current state of the art in plant modelling and to design a new model for cacao by exploiting (1) the modelling approaches for each plant process best suited to our objective and (2) the incorporation of relevant results from the field experimentation presented earlier in Chapter 2 and 3.

Moreover, during the formulation of the new conceptual model, it was realized that even an unvalidated and not exhaustive modelling of the plant's response to the environment can give an important advantage in operational / commercial decision-making. Examples of how partial descriptions of key plant processes have been applied in a non-scientific environment.

5.1 Conceptual model

The proposed model was conceived with the intent of studying cacao production under a wide array of sub-seasonal climatic scenarios to advance the academic research on cacao physiology and to answer practical question for the industry.
Since the model was intended to be usable not only within a scientific context but by non-scientific users with less data availability as well, it had to be designed in a way that limited the number of inputs needed to run a simulation. On the basis of the typical resolution of climate data easily available to a generic user, the time step of the chosen model was one day. In the same spirit of creating an easily usable model, mainly aimed at studying the influence of climate on the plant and the consequent variation in its productivity, neither the effects of biotic agents nor those of fertilisation were considered. The only limiting factors that influence the plant in the model are radiation, atmospheric conditions (temperature and air relative humidity) and soil water content.
An important characteristic for the model was to be easily upgradable, thus we chose a modular structure with a minimal number of dependencies between modules. The modular structure allows for great independence in the choice for modelling of a process while imposing only the constraint of having the inputs and outputs for each module fixed. The great independence of each module means that in the future it will be easy to make changes, even major ones, to the modelling of a process without undermining the entire structure of the model. Conversely, choosing a more linear but interwoven structure would require more holistic reorganizations. Finally, a modular structure based on the rule "one process, one module" helps

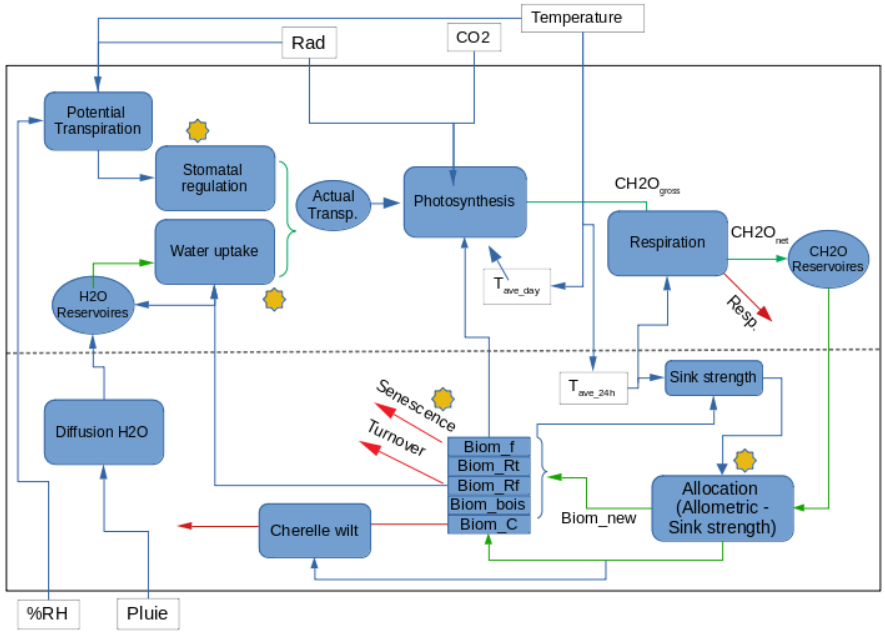

FIGURE 5.1.1: Schematic representation of the conceptual model proposed. Squares are processes (model modules), ellipses are variables used in the model calculation. The yellow "sun" marks the points in the model where water stress modifies the plant processes and relations. These modifications were based on previous knowledge or the experimental results from the previous chapters. Green arrows represent relations between modules which add something to another module (i.e. water, CH_2O), red arrows are net losses, while blue arrows are all other types of connections between modules. Biom_f: leaves, Biom_Rt: primary roots, Biom_Rf: fine roots, Biom_bois: wood, Biom_C: fruits. Graphics by Pietro Della Sala.

with the coding, debugging and validation as well. By separating the processes in modules it is possible to address them one by one and validate them singularly before coupling them. Figure 5.1.1 presents the conceptual scheme of the model, whose core rules/features are:

- a feedback mechanism of transpiration on photosynthetic efficiency. In particular the process of water uptake from the soil, stomatal regulation and photosynthesis are directly coupled;
- a thorough modelling of the soil water content in layers with a feedback mechanism on fine root growth based on the water content of the soil layer where they grow;
- a hybrid allometric - sink strength driven partitioning with a common pool of resources with a "switch" for when the plant is water stressed. This approach is common in many functional structural plant models, which focus on resource allocation among organs. A prominent example is the GREENLAB model [119, 194];
- the novel inclusion of empirical relations to model physiological cherelle wilt due to competition.

In developing the conceptual model 5.1.1 we drew on and combined different approaches found in the literature but the basic structure was largely inspired by the family of crop growth simulation models from the 'School of de Wit'[27, 231] and notably GECROS [248] and CASE2 [257]. While most processes are standardly present in virtually all models (Photosynthesis, Transpiration, Allocation of resources etc.), the main differences compared to past models include:

- a specific module to model stomatal regulation in response to atmospheric stress independent from the soil water uptake. Conversely, previous models like GECROS and CASE2 assumed that stomata regulation perfectly adapted to permit the soil water uptake while in reality, as in our experiment, the plant reduces the stomata opening to avoid or limit embolism at high VPD [148].
- The modelling of cherelle wilt with a dedicated module. In CASE2, that has other goals than our and operated at a seasonal scale, this phenomenon could be neglected. Short-term changes in the pod load, like cherelle wilting, may have bigger influence when considered at a fine timescale. Therefore, in the conceived model to study sub-seasonal changes in production, wilting had to be included.

5.2 Processes and modules

5.2.1 Initialisation

The model is intended for the study of the medium-term effects of climate on a regular cacao plantation. Hence in a default run, a generic average tree would be initialized as mature, healthy, bearing no fruit and with the soil at field capacity. In such case it is recommendable to make the model run for at least a full year before considering the output. This because the model would need to slowly adjust itself to a more realistic pod load. The biomasses for wood, fine and coarse roots and leaves would be initialised from the average total biomass of a cacao tree of 7 to 10 years [185, 256]. The initialised biomasses for each organ type could be calculated either directly with allometric relations, either, when possible, through specific calculations (i.e leaves, Module 5.2.11). All variables, constants and parameters would be initialised as defined by the user. A non-exhaustive list of plant parameters that could be used in the model were retrieved from literature or measured in the field (Tab. 5.2.1).

Table for initialization

Name	Symbol	Value	Unit	Module	Source
Stomatal density		754	stomata$/mm^{-2}$	5	[131]
Stomatal conductance	g_{max}	0.031 (well watered)	$mmol * m^{-2} * s^{-1}$	5	[131]
		0.0465 (well watered)	$mmol * m^{-2} * s^{-1}$		[190]
		0.015 (water deficit)	$mmol * m^{-2} * s^{-1}$		[131, 190]
SLA sun leaf	SLA_{sun}	28	m^2/kg	5, 6	[131]
		12.6	m^2/kg		[125]
		22.5	m^2/kg		measured
SLA shade leaf	SLA_{shade}	28	m^2/kg	5, 6	[131]
		12.6	m^2/kg		[125]
		21.8	m^2/kg		measured
Huber value	HV	$1.34{*}10^{-4}$	m^2/m^2	8	[125]
Light compensation point	LCP	10.2	$\mu mol * m^{-2} * s^{-1}$	6	[131]
Light saturation point	LSP	65	$\mu mol * m^{-2} * s^{-1}$	6	[131]
Wood density	δ_{dry}	351.31	kg/m^{-3}	9	measured
		398	kg/m^{-3}		[125]
Specific fine root area	$SFRA$	229.1	m^2/kg	3	[125]

TABLE 5.2.1: List of variables and constants used to initialize the proposed model. Where more than one value was found in literature, multiple options are presented.

5.2.2 General overview

The conceptual model in Figure 5.1.1 shows the logic flow of the model as well as the main processes modelled. The proposed structure for the model would have a eleven independent modules to represent the main processes described (Fig. 5.1.1) plus one extra module for the model's output, for a total of twelve:

Module. 1 Soil properties: initializes and calculates the physical properties of the soil at each depth based on pre-defined soil types chosen by the user. The soil types are taken from the USDA reference table retrieved from [198]. In alternative the user can define its own parameters for each soil layer.

Module. 2 Soil water level: calculates the water content of the soil for all layers at each time-step. It considers the rainfall and / or irrigation as the input for the first layer, while deeper layers consider percolation from and to other soil layers as the sole input / output mechanism. Water uptake, an additional source of loss of water for a soil layer, is treated in a dedicated module.

Module. 3 Root uptake: here it is calculated the maximum quantity of water that can be depleted by the plant on a certain day from each soil depth depending on the fine root density. The value obtained for the theoretical total possible water absorption is checked against the water demand by the leaves to assess the soil water limitation.

Module. 4 Evapotranspiration: it computes the daily evapotranspiration based on the input climatic variables. By default it uses the Penman-Monteith method [6] with a fixed wind speed as the potential user may not have access to this information and it should play a small role [257]. The value obtained for the theoretical potential evapotranspiration is checked against the water loss allowed by the leaves' stomatal regulation to assess the atmospheric water limitation. The value obtained for the theoretical potential evapotranspiration is checked against the water loss allowed by the leaves' stomatal regulation and the root uptake in Modules 3 and 5 to assess the atmospheric and soil water limitation.

Module. 5 Transpiration: It calculates empirically the stomatal closure based on the potential evapotranspiration (Module 4), then it compares the transpiration value allowed by the leaves with the maximum water uptake allowed by the roots to determine the actual transpiration, limited by one or the other process. It is not included, for now, the effect of the interaction between limitations so the most limiting factor is taken (tipping bucket principle).

Module. 6 Photosynthesis: Based on the transpiration allowed by the roots and stomata, it is here calculated the amount of CO_2 harvested from the atmosphere (Fick's law) and fixed into carbohydrates through photosynthesis.

Module. 7 Senescence: here are calculated the rate of senescence for leaves and fine roots. This module contains a modification factor for leaf senescence under water stress, be it at the soil or atmospheric level, based on the experimental results found and presented earlier in this thesis dissertation (Ch. 2).

Module. 8 Assimilates demand: in this module the potential demand for assimilates by the organs is calculated based on their sink strength. The sink strength is obtained combining some allometric relations, especially for wood and primary roots, with more mechanistic calculations involving the organs' age for leaves, fine roots and

fruits. Moreover, in this module is modelled a switch for more assimilates to be invested in roots under water stress.

Module. 9 Respiration and assimilates allocation: in first instance, this module calculates the loss of carbohydrates consumed to sustain the metabolism of the tissues. Then, it uses the carbohydrates from photosynthesis to replace the lost biomass and allocates the carbohydrates from photosynthesis among the organ classes considering their total demand as a weight. In case the carbohydrates production is superior to the total demand, the extra assimilates are stored inside this module as a "surplus" to be added to the next time-step's photosynthetic production.

Module. 10 Organs' properties update: this module updates the biomass for each organ type and, when necessary other derived properties. The module contains a second assimilates repartition step for fine roots and fruits. The allocation among fine roots depends on the water content of the different soil layers, used as a weight to distribute the new biomass. Similarly, fruits go though a second repartition that uses the sink strength of each fruit age as a weight to determine how resources are invested. For leaves the new biomass is used to calculate the total leaf area at each time-step as well as the portion of leaf area of the outer canopy or inner canopy; each of the two characterized by a different photosynthetic efficiency.

Module. 11 Wilting: With a set of rules aimed at mimicking competition among fruits based on the results from Chapter 4, this module eliminates all cherelles that comply with these rules, if any.

Module. 12 Outputs: here are grouped, shaped and exited the desired outputs for the model. Together with the harvested pods' bean weight, it will be returned a file with the last value for all the variables useful to initialize the model from the last simulation's result. This would for example include all organs' biomasses, water content of all soil layers and the biomass and age distribution for each fruit category. In practice such file can be used to re-initialize the model from the last time step.

These modules can be changed internally but the links among them are fixed and need to be preserved even in future model upgrades. The dependencies of each module on other modules at the same time step are limited to one or maximum two.
Figure 5.1.1 summarizes the dependencies among modules and illustrates the structure of the model. In the following sub-sections, each module is discussed separately, but equations and details are only provided where this project has contributed with something new. For those processes that have not been modified, it has been preferred to refer directly to the source. This to focus only on those aspects that brought any level of novelty.

Soil

5.2.3 Module 1: Soil properties

This module revolves around the rooting structure for cacao and the definition of the soil layers, for each of which it calculates some physical properties.
Cacao has a taproot that reaches 1.5 m for mature trees with a fine root density that decreases with depth [162, 191]. In line with the mentioned rooting characteristics and with the choice already proposed in CASE 2 [257], it is suggested that the taproot is modelled as a cone and that only the portion of soil interested by cacao root exploration is modelled. Consequently, the initialised biomass of the root system (*Biom.roots*) is distributed to create a cone with a fixed basal area dependent on the planting density (NPL) and unknown height [256]. Based

on the biomass the maximal depth exploration is calculated, whose determines the modelled soil depth as well (Eq. 5.1). It is proposed to divide the soil into n layers of thickness z [cm] (Eq. 5.2). The default value for z is 10 cm, but the user can always initialise the model with finer layers. The chosen modelling for water movement in the soil (S.5.2.4) imposes to chose a z superior to 5 cm. The relevant parameters used in Equation 5.1 can be found in Table 5.2.1.

$$Depth_{max} = (\frac{Biom.roots * 1200}{NPL * \delta_{dry} * \pi})^{1/3} \tag{5.1}$$

$$n = \frac{Depth_{max}}{z} \tag{5.2}$$

The fine roots distribution is initialised with a negative exponential evolution that diminishes with the depth (Eq. 5.3). The function to approximate the distribution of fine roots is in line with what other authors [162, 191] and that was already adopted in CASE 2 [257]. To update and improve the quality of the curve, it is proposed to recalibrate it using the recent results from Abou-Rajab et al. 2017 [191] about the fine roots distribution in three different cacao cropping systems. By integrating Equation 5.3 between the values found in Abou-Rajab et al. 2017 [191] for fixed percentages of fine roots it was possible to obtain a value for k of 1.508. The biomass of fine roots in each layer ($Biom.fine.root_l$) is calculates as the product of the total biomass of fine roots ($Biom.fine.root$) and $Fine.root.fraction_l$.

$$Fine.root.fraction_l = e^{-k*(layer*z)} \tag{5.3}$$

Finally, in the model it is suggested to leave the user the possibility to specify the soil type for specific depth intervals or accept the default values based on a typical Ghanaian soil and reported in Section 2.2.2. from the soil type are calculated the main physical soil properties (WP: volumetric water content at permanent wilting point, FC: volumetric water content at field capacity) are calculated for each soil layer (n_{layer}) using the USDA reference table retrieved from [198] in the Mualem - Van Genuchten model [198, 229].

5.2.4 Module 2: Soil water level

In this module, at each time-step (t) the soil water content of each layer (SWC_{layer}) is updated. The first layer receives as input the value for the daily precipitation ($Rain$ in mm), while the other layers receive as input any water content above the field capacity of $layer - 1$ ($Surplus_{l-1}$ in in mm) (Eq. 5.4). The arbitrary assumption that water moves from one layer to the next over a day is only possible if z is above 5 cm because the diffusivity of the soils for cacao cultivation ranges between 6 cm and 10 cm (USDA soil properties [198]). In addition, the root uptake from the previous time step ($Root.up_{l,t-1}$ in mm) is subtracted (Eq. 5.5).

$$SWC_{l,t} = \begin{cases} SWC_{l,t-1} + \dfrac{Rain - Root.up_{l,t-1}}{z}, & \text{if } layer = 1 \\ SWC_{l,t-1} + \dfrac{Surplus_{l-1} - Root.up_{l,t-1}}{z}, & layer \text{ in } [2, n] \end{cases} \tag{5.4}$$

$$Surplus_l = max(0, (SWC_{l,t} \check{} FC_l) * z) \tag{5.5}$$

The idea then is to use the updated $SWC_{l,t}$ to calculate the fraction of transpirable soil water (FTSW, [235]) with an empirical function obtained fitting the FTSW curve from this 2 and a previous study [87] to obtain the soil water potential at which cacao starts reducing transpiration (Fig. 5.2.1 point A) and the one at which there is 50% or complete stomatal closure (Fig. 5.2.1 point B, C). The water potential at which cacao closes stomata can be transformed to SWC ($WP.cacao$) and used in the calculation of a stress coefficient ($Soil.stress.coeff$) to be

multiplied to the potential transpiration and obtain the attainable transpiration allowed by soil limitation. The $Soil.stress.coeff$ will be calculated as a linear decrease between the points A ($FP.cacao$) and C ($WP.cacao$) shown in Figure 5.2.1 following Equation 5.6.

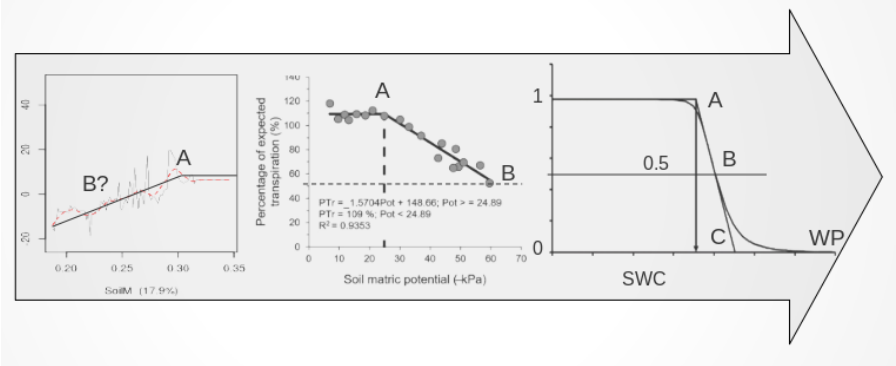

FIGURE 5.2.1: Examples of how to obtain the point of flection ($FP.cacao$, A), the 50% stomatal closure ($WP.cacao$, B) and complete stomatal closure for cacao ($WP.cacao$, C) on a FTSW curve. These may be: extracted from the response of sap velocity to SWC presented in Chapter 2(left) and transformed into a soil water potential based on the soil type, then compared to the value taken from the FTSW curve presented in Fraga et al. (2020) [87] (middle) and finally recalculated as SWC in the model based on the soil type (right).

$$Soil.stress.coeff_{l,t} = \begin{cases} 1, & \text{if } SWC_{l,t} \geqq FP.cacao \\ 0, & \text{if } SWC_{l,t} \leqq WP.cacao \\ \dfrac{SWC_{l,t} - WP.cacao}{FP.cacao - WP.cacao}, & \text{otherwise} \end{cases} \tag{5.6}$$

5.2.5 Module 3: Root uptake

This module depends on both Module 2 and Module 4 but is presented in this section to complete the processes at the soil - root level. From Module 4 (S. 5.2.7) the potential evapotranspiration ($ET.pot$) is fed into this module. The biomass of fine roots for each layer ($Biom.fine.root_{l,t}$) is necessary as well and comes from the calculations of Module 11 (S. 5.2.14) the previous time-step. Finally, it requires the array of $Soil.stress.coeff_{l,t}$ from Module 2 (S. 5.2.4).

For each layer, it is first checked if water uptake is possible at all based on its depth and the presence of fine roots. Then, the maximum root uptake ($Root.up.max_{l,t}$) is calculated as the minimum between the extractable water ($SWC_{l,t} - WP_l$) and the water uptake potentially sustainable by the fine root mass ($Root.up.pot_{l,t}$, Eq. 5.8). To calculate the latter, it is necessary to multiply a fixed root uptake rate (RUR) with the $Soil.stress.coeff_{l,t}$ and the total fine root area of the layer ($Area.fine.root_{l,t}$, Eq. 5.7). The $Area.fine.root_{l,t}$ is obtained as the product of the specific fine root area ($SFRA$ in $cm^2/g[fineroots]$) and $Biom.fine.root_{l,t}$. All these operations are reported in a mathematical form in Equation 5.9.

$$Area.fine.root_{l,t} = SFRA * Biom.fine.root_{l,t} \tag{5.7}$$

$$Root.up.pot_{l,t} = Soil.stress.coeff_{l,t} * RUR * Area.fine.root_{l,t} \tag{5.8}$$

$$Root.up.max_{l,t} = \begin{cases} 0, & \text{if } layer * z > Depth_{max} \\ 0, & \text{if } Biom.fine.root_{l,t} \leqq 0 \\ min(Root.up.pot_{l,t}, SWC_{l,t} - WP_l), & \text{otherwise} \end{cases} \tag{5.9}$$

The total root uptake ($Root.up.max_t$, Eq. 5.10) allowed by the fine roots and the soil moisture is obtained as the sum of $Root.up.max_{l,t}$ for each layer. If the latter is superior to $ET.pot$ (S. 5.2.7), then the transpiration allowed by the roots ($TR.a_{soil}$) is equal to $ET.pot$ and the root uptake from all layers is scaled down proportionally to the total requirement ($\frac{ET.pot}{TR.a_{soil}}$) (Eq. 5.11). This means that when the plant is not water limited, water extraction is evenly performed by all the roots within their possibility. Otherwise, when transpiration is limited ($Root.up.max_t < ET.pot$), $TR.a_{soil}$ is equal to $Root.up.max_t$. In this second case the water extracted from each layer is calculated with a RUR shrunk by a factor $\frac{TR.a_{soil}}{ET.pot}$ (RUR_{red} Eq. 5.11). The chosen modelling assumes that, under soil water stress limitation, the root conductivity and water uptake rate are affected equally in all layers. This is in line with the results by Kotowska et al. (2015) [125].

$$Root.up.max_t = \sum_{l=1}^{n} Root.up.max_{l,t} \tag{5.10}$$

$$Root.up.max_{l,t} = \begin{cases} \begin{cases} TR.a_{soil} = ET.pot \\ Root.up_{l,t} = \dfrac{Root.up.max_{l,t} * ET.pot}{TR.a_{soil}} \end{cases}, & \text{if } Root.up.max_t > ET.pot \\ \begin{cases} TR.a_{soil} = Root.up.max_t \\ RUR_{red} = \dfrac{RUR * TR.a_{soil}}{ET.pot} \\ Root.up_{l,t} = Root.up.max_{l,t} * RUR_{red} \end{cases}, & \text{if } Root.up.max_t < ET.pot \end{cases} \tag{5.11}$$

In Module 5.2.8 it is calculated if the plant is more limited by the soil or by stomatal closure induced by the atmosphere. If the atmospheric conditions cause a reduction in stomatal opening for which $TR.a_{soil}$ results excessive, the final $Root.up_{l,t}$ is calculated as in Equation 5.11 but with the real transpiration ($TR.a$) instead of $ET.pot$ (Eq. 5.12).

$$Root.up_{l,t} = \frac{Root.up.max_{l,t} * TR.a}{TR.a_{soil}} \tag{5.12}$$

5.2.6 Industrial application: the "water resilience model"

Within the frame of my project, I had the chance to apply part of my research and reasoning on the modelling of water uptake to guide strategic decision-making at the service of the cacao trading house Rockwinds in Bordeaux (France). The task at hand was the development of a tool to (1) estimate the number of days left to the cacao trees before experiencing water stress (resilience) ahead or during a dry spell and (2) to quantify the severity of a dry spell. To develop such a tool I took inspiration from the mechanisms described in Sections 5.2.3, 5.2.4, 5.2.5.

The *"water resilience model"* needed to work only with rainfall data as input. Thus, the *"water resilience model"* models a tree with a fixed rooting depth of 100 *cm* in an average West African soil (field capacity fixed at 30% and wilting point at 15%, S.2.2.2) and with a fixed array of transpiration rate choosable by the user. The five transpiration rates defined were:

- Rule of thumb: based on a personal communication, cacao in Ghana needs 100 mm/-month to cover evapotranspiration. From such value is obtained a rule of thumb of: [3.23 mm/day].

- Average rate: the global average of all values reported in literature taking into account the low and high end of given daily transpiration rate intervals ([2, 23, 39, 139, 228]).[2.45 mm/day]
- Max rate: the average maximum daily transpiration rate reported in literature ([2, 23, 39, 139, 228]). [3.25 mm/day]
- Min rate: the average minimum daily transpiration rate reported in literature ([2, 23, 39, 139, 228]). [1.81 mm/day]
- Long dry season: the transpiration rate under prolonged stress was obtained as the 80% of the "Min rate" transpiration rate and was in line with the values from the control experiment we conducted. [1.45 mm/day]

This simple model takes the total precipitations over 30, 60 and 90 days as an input, calculates the monthly useful rainfall by assuming that 15% of rain is lost due to canopy interception [257]. With he corrected values for monthly useful rainfall, it calculates for each day if cacao transpiration, chosen by the user for each month, was covered by the water in the soil. Any surplus during and in the end of a month is carried over to the next simulation step. Whenever the soil water content goes above the total field capacity (150 mm) it is lost in the next simulation step, this simulates loss by percolation. To calculate the number of days of resilience left on a given day, the model imposes no extra precipitation and then counts the number of days before water limitation starts.
A second use for the model is to project the climatological precipitation distribution (1979 - 2019 CPC: [15]) to assess the development of the following months using the present situation as a baseline. This allows as well to create short-term rain scenarios and get an idea of the probable outcome. Recurrent examples of rain scenario may include:

- the average rainfall calculated only with the climatological higher quartile of data for the considered period;
- the average rainfall calculated only with the climatological lower quartile of data for the considered period;
- fixed daily rainfall values (2, 3, 4 mm/day);
- apply a fixed reduction or magnification factor to the climatological average rainfalls ($\pm$ 10%, 20%, 50%)

When simulating future short-term rainfall scenarios, the severity of a dry spell over a given period, is obtained by means of a *severity index*. The latter is calculated as the product between the number of days when trees have to reduce transpiration and the magnitude of the reduction, divided by the length of the period considered. The result is then scaled down by multiplying by 0.1 to simplify the communication. For example, if cacao needs to transpire 20% less for 15 days over a simulated period of 45 days, the *severity index* is $\frac{20 * 15}{45} * 0.1 = 0.67$. Typical values for the *severity index* are between 0 and 5, each with specific expected consequences based on expert knowledge and the study of past seasons:

0. no stress, optimal potential growth;
1. limited stress without consequences appreciable consequences;
2. normal rate of wilting and maybe a little of canopy loss / not detectable bean size effects;
3. higher wilting than usual / partial canopy loss / some visible effects on bean count possible;

4. higher wilting than usual / canopy loss / visible effects on bean count;
5. potential risk of crop failure

This model is routinely ran to monitor the water status (water resilience) and future threats of rainfall scenarios for eight important West African cacao regions. The model lacks a proper validation, for now, and might under or overestimate the value for water resilience. In order to draw operational conclusions from this model, its results are always compared to a reference simulation based only on the climatology. This permits to at least assess the obtained values relatively to the average season (anomalies). Furthermore, the baseline simulation with the climatology allows to contextualize extreme absolute values in light of the normal climatology of the period. For example, the stress value during the long dry Harmattan season is often high and needs to be judged in relation to the norm.

Atmosphere

5.2.7 Module 4: Evapotranspiration

Due to the importance of this key driving process, it was adopted the same choice made by many mechanistic models [28, 248, 257] to calculate evapotranspiration: the Penman-Monteith method [6]. The classic Penman-Monteith formula has been adopted with the simplification of a fixed wind speed by default, of course this can always be an extra input. The choice of a fixed wind speed ($Vwind$) by default was dictated by the fact that the potential user may not have access to this information and it should be an acceptable approximation [257]. It is suggested to adopt the modelling approach of GECROS [248] in particular as it includes a rather useful distinction between shade and sun leaves. Cacao is a perennial used to shaded environments and with a multilayered canopy, thus it is paramount to account for the difference in the radiative component of the Penman-Monteith evapotranspiration formula ($ET0_{rad}$) for different canopy positions and, as a consequence, leaf types. For the set of equations we refer and rely on Yin et al. (2005) [248], in particular to their Section 2 and Appendices B and C. The value obtained with the Penman-Monteith equation adaptation presented in Yin et al. (2005) [248] should then be corrected with the specific crop coefficient (Kc_{cacao}) [6]. Then, it is checked against the water loss allowed by the leaves' stomatal regulation (S. 5.2.8) and the roots' extraction capacity (S. 5.2.5) to assess the atmospheric and soil water limitation.

5.2.8 Module 5: Leaf transpiration and aerial drought

Cacao's transpiration in the model is chosen to be mechanistic with a complete modelling of gas exchange dependent on stomatal opening (Fick's law, [105, 120]). The base approach would be the same chosen in GECROS as well [248] but with an important improvement. A desirable feature of the proposed model was to better capture the stomatal regulation compared with past cacao models that assumed a mathematical optimization of stomatal closure dependent only on soil water limitation [256, 257]. In reality, cacao may limit its transpiration regardless of soil water content to reduce the suction in the xilematic vases and limit the occurrence of cavitation in leaves, branches or even the trunk [31, 125, 215]. Therefore, it is suggested to adopt the set of equations in Section 2 and Appendix C of Yin et al. (2005) [248] to obtain leaf boundary layer resistance to heat (Rbh) and water (Rbw) with which is possible to calculate the leaf stomatal resistance to water in the absence (rsw_p) or presence (rsw_a) of water stress, using $Tr.a_{soil}$ as well. From the previous passages, thoroughly treated and explained in Yin et al. (2005) [248], it is obtained the actual transpiration allowed by the roots and sustained by by the leaves ($Tr.a_{atm}$). To obtain the final value for the transpiration rate it is necessary to include the effect of excessive vapour pressure in inducing stomatal closure.

As a consequence, the proposed method to model stomatal conductance would include a Red_{atm} for stomatal opening decoupled from soil water content. This Red_{atm} would be based on an empirical curve, maybe starting from the experimental study treated in Chapter 2. For example, the sap velocity response to VPD under irrigation or in general during a period when cacao experienced atmospheric stress without a soil water limitation could be used to inform the Red_{atm}. In addition to our study (Ch. 2), it is suggested to draw on other studies that aimed to understand when cacao starts shutting the stomata [2, 87]. Besides, Kotowska et al. (2015) [125] reported on the hydraulic properties of cacao and the maximum flow rate allowed by the stem or leaf vases as a consequence. It is suggested that a set of threshold for avoiding cavitation are included in the model. At these thresholds the modelled cacao tree would drastically reduce stomatal opening. In the end, $Tr.a_{atm}$ must be inferior or equal to a set of thresholds based on the physical conductance of the wood, leaf vases and mesophyll (Eq. 5.13). If this first condition is true, $Tr.a_{atm}$ is corrected with the empirical Red_{atm} (Eq. 5.13) and then compared to $Tr.a_{soil}$ to assess the final transpiration rate net of all limitations. The idea being that the actual evapotranspiration ($Tr.a$) is calculated with the tipping bucket method (the most limiting factor) between $Tr.a_{soil}$ and $Tr.a_{atm}$ (Eq. 5.14).

$$Tr.a_{atm.final} = \begin{cases} min(hydraulic\_thresholds), & \text{if } TR.a_{atm} > min(hydraulic\_thresholds) \\ TR.a_{atm} * Red_{atm}, & \text{otherwise} \end{cases} \tag{5.13}$$

$$Tr.a_t = \begin{cases} TR.a_{soil}, & \text{if } TR.a_{soil} < TR.a_{atm.final} \\ TR.a_{atm.final}, & \text{if } TR.a_{atm.final} < TR.a_{soil} \end{cases} \tag{5.14}$$

5.2.9 Module 6: Photosynthesis

As photosynthesis is the driving process of plant growth, a robust model for this core production process is essential. In order to balance between complexity and accuracy, we chose to adopt the mechanistic modelling of photosynthesis first proposed by Farqhuar et al. (1980) [81] and later improved by Von Caemmerer et al. (2009) [34]. Furthermore, in line with the philosophy adopted in GECROS [248], we have divided the canopy of the cocoa tree into two fractions: "sun" leaves and "shade" leaves ($f.sun$ and $f.shade$), each with its own set of parameters to model photosynthesis. This modellization of photosynthesis is compatible with the chosen way to model transpiration and calculates the total CO_2 harvested by the leaf based on the stomatal conductance for water ($1/rsw_a$) and the total leaf area for "shade" and "sun" leaves. Whenever water stress affects stomatal opening the model applies a reduction factor (Red_{photo}) to the potential photosynthetic activity ($Photo_p$) to obtain the photosynthesis under stress ($Photo_a$). The complete set of equations can be taken, among others, from Yin et al. (2005) [248] in Section 2 and Appendix A. This approach has proved to be extremely accurate but has not always been adopted in physiological models in the past due to the large number of parameters required to parametrise it. It is proposed to adopt it and that the photosynthetic parameters to tune it for cocoa are to be taken from literature [50, 56, 125, 132, 135, 141, 167, 199, 214]. A not-exhaustive list of the selected values for photosynthetic values are reported in Table 5.2.1. The output of Module 6 is the amount of $CH_2O.photo_t$ fixed over the day, then made available to Module 9 for allocation.

5.2.10 Module 7: Senescence

In this module the biomass of leaves and fine roots is updated to account for the biomass turnover. This process precedes the allocation of resources (S. 5.2.11), in this way their demand for assimilates is maximized due to the loss of biomass. The proposed succession of

modules assumes that senescence takes place all at once, in the end of the day (the photosynthesis module precedes this one) and before carbohydrates distribution through the xylem. A base time dependent senescence / turnover rate for fine roots ($Turnover_{fr}$ [d^{-1}]) can be taken from Muñoz and Beer (2001) [165]. For a correct modelling of fine root senescence that responds to climate variability, it is better to transform this value in physiological age ($\circ Cday$). The value proposed for the turnover rate was calculated in Costa Rica (Turrialba) where temperature does not vary throughout the year as in West Africa. Therefore, it is proposed to multiply the rate by the average daily temperature in Turrialba. In this way the model will always module the turnover of fine roots in relation to the daily temperature. To obtain the biomass of fine roots lost it is sufficient to multiply it by the said rate. The new $Biom.fine.root_{l,t}$ is obtained by subtracting the lost biomass from $Biom.fine.root_{l,t-1}$ (Eq. 5.15). On the grounds of the lack of documented proves, it is assumed that the rate of fine root turnover is not modified by the water stress. In Equations 5.15 and 5.19 values for the time step t^* represent transition values that are updated later in other modules.

$$Biom.fine.root_{l,t^*} = Biom.fine.root_{l,t-1} - Biom.fine.root_{l,t-1} * \frac{Turnover_{fr}}{Taverage_{Turrialba}} \tag{5.15}$$

For the leaves, a senescence rate under optimal conditions ($Turnover.0_{lv}$) can be taken as the inverse of the average lifespan of a leaf [160, 161]. Once more, the idea is to express the age of a leaf under unstressed conditions in physiological age ($\circ Cday$) by multiplying the number of days by the average temperature in the state of Bahia, Brazil where the study took place. Fortunately, the temperature is reported alongside the data in the two studies [160, 161]. In addition, for leaves we can adopt a base temperature for vegetative growth for the most widely genetic group in West Africa: Amelonado (19.7; [56]). Thus, $Turnover.0_{lv}$ can be calculated as shown in Equation 5.16.

$$T.base_{veg} = 19.7 \circ C$$

$$Turnover.0_{lv} = \frac{1}{Age.leaf * (Taverage_{Bahia} - T.base_{veg})} \qquad [1/\circ Cday] \tag{5.16}$$

$Turnover.0_{lv}$ can be seen as the base turnover rate dependent only on leaf age. In addition, the model must include the effect of atmospheric and soil water stress too, as observed by us and described in Chapter 2. To achieve that, it is proposed to exploit the slope of the LAI curves in Figure 2.3. In absence of a dedicated study, the slope of the LAI decline for the irrigated plot may be taken almost directly as a senescence rate due to the atmospheric stress. The idea would be to consider the slope of the LAI decline as the sum of $Turnover.0_{lv}$ and the additional rate due to atmospheric stress ($Turnover.atm_{lv}$). The latter could, for example, be expressed in function of the VPD above a certain threshold, in similitude to $Turnover.0_{lv}$ with temperature. The resulting rate would be expressed as a function of VPD above a base threshold (Eq. 5.17). On the ground of the results from Chapter 2 and 3, it is advanced to adopt 2 kPa as base threshold. Similarly, the slope of the LAI decline during the dry season when irrigation was not provided can be seen as the sum of $Turnover.0_{lv}$, $Turnover.atm_{lv}$ and another rate linked to the decline of the $FTSW$ ($Turnover.soil_{lv}$). This would depend on the $FTSW$ on a given day (Eq. 5.18). In the model, the senescence would be computed as the sum of the three turnover rates at each time step and used to calculate the leaf biomass lost (Eq. 5.19).

$$\begin{cases} VPD.base_{veg} = 2kPa \\ \delta VPD = VPD_t - VPD.base_{veg} \\ \delta Temp = Tav_t - T.base_{veg} \\ \delta LAI.IRR_{t0-t} = Turnover.atm_{lv} * min(0, \delta VPD) + Turnover.0_{lv} * (\delta Temp) \\ Turnover.atm_{lv} = \dfrac{\delta LAI.IRR_{t0-t} - Turnover.0_{lv} * (\delta Temp)}{min(0, \delta VPD)} \end{cases} \tag{5.17}$$

$$\begin{cases} \delta LAI.NAT_{t0-t} = Turnover.atm_{lv} * min(0, \delta VPD) + Turnover.0_{lv} * (\delta Temp) + Turnover.soil_{lv} * (1 - FTSW_t) \\ Turnover.soil_{lv} = \dfrac{\delta LAI.NAT_{t0-t} - Turnover.0_{lv} * (\delta Temp) - Turnover.atm_{lv} * min(0, \delta VPD)}{(1 - FTSW_t)} \end{cases} \tag{5.18}$$

$$\begin{cases} Turnover.lv_t = Turnover.0_{lv} * (\delta Temp) + Turnover.atm_{lv} * min(0, \delta VPD) + Turnover.soil_{lv} * (1 - FTSW_t) \\ Biom.lv_{t^*} = Biom.lv_{t-1} - Biom.lv_{t-1} * Turnover.lv_t \\ Biom.sun.lv_{t^*} = Biom.lv_t * f.sun \\ Biom.shade.lv_{t^*} = Biom.lv_t * f.shade \end{cases} \tag{5.19}$$

5.2.11 Module 8: Assimilates demand by the organs

To calculate the theoretical demand for assimilates of each organ class, it is necessary first to calculate the potential biomass of an organ class at each time step. Then, the demand for assimilates is calculated as the gap between the actual and potential biomass of an organ class. To calculate the potential biomass of an organ class, CASE 2 adopted allometric relations for all organs, even when the relationship was not too strong [257]. It is proposed to adopt a different approach than CASE 2 wherever the allometric relations are not solid enough. Hereunder, it is reported the suggested modelling proposed for each organ class potential biomass.

Woody parts

The woody parts of mature trees (branches, trunk, coarse roots) tend to represent a stable fraction of the total biomass of the tree. Consequently, allometric relations of the wood biomass as a function of the total biomass are considered robust and, thus, are widely adopted [43, 51–53]. For cacao as well it is possible to adopt allometric relations for the "branches+trunk" (*Biom.wood.pot*) and "coarse roots" (*Biom.roots.pot*), as the ones proposed in CASE 2, that explain respectively 93% and 87% of the data used to obtain them [256].

Fine roots

The paucity of studies on the belowground development of cacao makes the task of improving the modelling of the potential biomass of fine roots difficult. It is logical to assume that the amount of fine roots depends on the biomass of coarse roots. Consequently, it should have a stable allometric relation with the total tree biomass. This is confirmed as well by the R^2 of the allometric regression function adopted in CASE 2 (R^2: 0.85; [256]). It is proposed to adopt the allometric relation for fine roots, at least until a better approach arises.

Leaves

The plant's total biomass of leaves depends greatly on the canopy state and it is influenced by many factors in the field. For these reasons, it is difficult to extract a solid allometric relationship between the leaves and the total biomass of the plant using field data. For example, the allometric relation adopted in CASE 2 explained just 58% of the field data [256]. Because an empirical relation may not be reliable, the alternative is to model the potential leaf biomass starting from the theory. The Huber value (HV) is a species specific constant that links the sap wood area of the trunk to the total leaf area that it can sustain [22]. The HV for cacao is 1.34 $\pm$0.33 *$10^{-4} m^2/m^2$ [125]. Starting from the sap wood area (*Sap.wood.area*) of the modelled

cacao tree, the HV allows to calculate the maximum total leaf area of the tree ($Area.lv.pot$), transformed then into $Biom.lv.pot_t$ through the specific leaf area (SLA specific for the leaf type; $m^2[leaves]/g[leaves]$). In a mature tree the xylem represents a fixed fraction of the total wood area ($frac.sap$) [35, 99, 140, 188], which in turn is π times the diameter at breast height of the tree (DBH). Therefore, $Area.lv.pot$ can be put in relation with the DBH (Eq. 5.20). The DBH in cacao is strongly related to the total wood aboveground biomass (R^2: 93%; [125]). In conclusion, with a series of passages, it is possible to exploit the strong allometric relation adopted for $Biom.wood.pot_t$ to calculate $Biom.lv.pot_t$ (Eq. 5.20).

$$\begin{cases} DBH_t = \sqrt{\dfrac{e^{\frac{\ln(Biom.wood_t)+2.187}{0.916}}}{\delta * 3}}, & \text{from [43, 125]} \\ Sap.wood.area_t = \pi * DBH_t * frac.sap \\ Area.lv.pot_t = HV * Sap.wood.area_t \\ Biom.lv.pot_t = \dfrac{Area.lv.pot_t * f.sun}{SLA_{sun}} + \dfrac{Area.lv.pot_t * f.shade}{SLA_{shade}} \end{cases} \tag{5.20}$$

For Leaves, roots (fine and coarse) and the woody parts, the demand for assimilates is calculated in the same way. Once the potential biomass for the organ type is calculated, the demand for an organ is equal to the difference between the potential biomass and the actual biomass divided by a fixed conversion factor ($CH_2O.factor_{organ}$) from biomass to units of CH_2O required to form it (Eq. 5.23). The different $CH_2O.factor_{organ}$ can be calculated for all tissue types using Equation 5.21 coupled with the information of different organs' composition [61, 248]. Alternatively, Zuidema et al. (2002) proposes already calculated $CH_2O.factor_{organ}$ for cacao [256]. Moreover, whenever there is soil water stress, the model arbitrarily reduces $Demand.lv$ by a factor $leaf.root.f$ and enhances $Demand.fine.roots$ by the same amount (Eq. 5.23). The factor $leaf.root.f$ depends on the average of the soil stress of each layer weighted by its $Biom.fine.root_{l,t}$ (Eq. 5.22).

$$CH_2O.factor_{organ} = 2.5 * \frac{0.444 * f_{car} + 0.531 * f_{pro} + 0.774 * f_{lip} + 0.667 * f_{lig} + 0.368 * f_{oac}}{1.275 * f_{car} + 1.887 * f_{pro} + 3.189 * f_{lip} + 2.231 * f_{lig} + 0.954 * f_{oac}} \tag{5.21}$$

$$leaf.root.f = \frac{\sum_{l=1}^{n} [Soil.stress.coeff_{l,t} * Biom.fine.root_{l,t}]}{\sum_{l=1}^{n} Biom.fine.root_{l,t}} \tag{5.22}$$

$$\begin{cases} Demand.fine.root_t = \dfrac{(Biom.fine.root.pot_t - Biom.fine.root_{t-1}) * (2 - leaf.root.f)}{CH_2O.factor_{fine.root}} \\ Demand.lv_t = \dfrac{(Biom.lv.pot_t - Biom.lv_{t-1}) * leaf.root.f}{CH_2O.factor_{lv}} \\ Demand.roots_t = \dfrac{Biom.roots.pot_t - Biom.roots_{t-1}}{CH_2O.factor_{roots}} \\ Demand.wood_t = \dfrac{Biom.wood.pot_t - Biom.wood_{t-1}}{CH_2O.factor_{wood}} \end{cases} \tag{5.23}$$

Fruits

For the fruits it is not logical to adopt a potential biomass based on an allometric relation. In first instance, because, it is a process much dependent on several factors (nutrition, age of the tree, the production history of the plant, climate etc.), therefore difficult to assess with

certainty in the field, especially for cacao. As evidence of this, the allometric relation based on several studies adopted in CASE 2 could explain a mere 19% of the data. Secondly, it was preferred a modelling of the fruits as single, independent bodies to ease the integration of cherelle wilt (Ch.4, S. 5.2.14).
Hence, the fruits are modelled as objects (or even a vectors) with three components: structural biomass (*Biom.pod*), the fresh bean biomass (*Biom.bean*) and the physiological age (*Fruit.age*; $\circ Cday$). Depending on the latter, the fruit demand for assimilates is calculated multiplying each of the two fruit biomass components with its corresponding specific sink strength (*SS.pod* and *SS.bean*; $\frac{g[newbiomass]}{\circ Cday * g[fruitbiomass]}$). In Appendix 5.A are presented the results from a study conducted during the PhD aimed at calculating *SS.pod* for different cacao clones (the same as in Chapter 4). This study could not be included in previous chapters because it did not fit any chapter's objectives. Nonetheless, it was decided to present it to provide a clearer picture of the calculations made to inform this part of Module 8.
The *SS.bean* can be taken from literature and, wherever necessary, converted to be a function of $\circ Cday$ [7]. The sum of the demands of *Biom.pod* and *Biom.bean* for each fruit (Eq.5.24) is then taken as the total fruit biomass demanded at a time step t and converted to CH_2O, like the other organs (Eq.5.25).

$$\begin{cases} Demand.pod_{fruitn,t} = Biom.pod_{fruitn,t-1} * SS.pod * Fruit.age_{fruitn,t} \\ Demand.bean_{fruitn,t} = Biom.bean_{fruitn,t-1} * SS.bean * Fruit.age_{fruitn,t} \end{cases} \tag{5.24}$$

$$Demand.fruit_t = \frac{\sum_{n=1}^{nfruits} Demand.pod_{n,t}}{CH_2O.factor_{pod}} + \frac{\sum_{n=1}^{nfruits} Demand.bean_{n,t}}{CH_2O.factor_{bean}} \tag{5.25}$$

Then, the sum of all organs' demands is the output of this module, which informs Module 9.

5.2.12 Module 9: Respiration and assimilates allocation

The first step is for the model to calculate the total amount of CH_2O consumed at time t by the organs for respiration. A purely mechanistic, thorough description of each process consuming carbohydrates in the plant requires an insight on many aspects of the cacao tree that are not considered, above all fertilization. As a reference, in GECROS [248] are individuated and modelled nine respiration processes: growth, symbiotic di-nitrogen (N_2) fixation, root nitrogen uptake, nitrate reduction, not-N ion uptake, phloem loading, protein turnover, maintenance of cell ion concentrations and gradients, and any wasteful respiration. The first six of these are processes that is possible to model separately and that can be quantified, whereas the combination of the remaining three is often represented as a unique "maintenance respiration" and an empirical approach is applied. Because the focus of the envisioned model would be on the plant functioning in relation to climate, fertilization is currently not included. Therefore, it is proposed to ignore most of the nutrient-related processes, at least in first instance. As for transport respiration, the cost of carbon loading/unloading around the plant may be considered negligible in arboriculture, in light of the fact that trees use almost exclusively passive transport [60, 89, 204]. Ultimately, the only respiration types that are considered here are:

- growth respiration: the units of glucose (CH_2O) needed to synthesize an additional unit of tissue's biomass. This type of respiration is included in Module 11, where the new biomasses are calculated. The CH_2O allocated to an organ type is converted to final biomass with fixed conversion rates: $CH_2O.factor_{organ}$;

- maintenance respiration: the sum of protein turnover, maintenance of cell ion concentrations and gradients, and any further respiration that cannot be measured. It proposed to adopt fixed rates ($Resp.rate_{organ}$) for each tissue type and it is suggested to use the specific values calculated for cacao and reported in CASE 2 (Table 4.1; [256]). The values proposed it is suggested for temperatures up to 27 °C, warmer conditions can increase this rate. Thanks to the night-time temperature, daily average temperature does not pass often this threshold so that these values can be taken as fixed in a first moment.

In this module the model takes the maintenance respiration ($Resp.tot_t$) out of the total assimilates available made of: (1) the assimilates produced by photosynthesis in module 6 ($CH_2O.photo_t$) and (2) the surplus from the previous time step ($CH_2O.surplus_{t-1}$) (Eq. 5.27). To do so, it takes the sum of the biomasses after senescence (Module 7) times the respective $Resp.rate_{organ}$. The only exception to this is for the wood biomass, for which only the sapwood is counted. The latter is assumed to be proportional to $Sap.wood.area_t$, thus it is multiplied by $fra.sap$ (Eq. 5.26).

$$\begin{cases} Resp.wood_t = frac.sap * Biom.wood_t * Resp.rate_{wood}, & \text{for wood} \\ Resp.organ_t = Biom.organ_t * Resp.rate_{organ}, & \text{otherwise} \\ Resp.tot_t = \sum Resp.organ_t \end{cases} \tag{5.26}$$

$$CH_2O.tot_t = CH_2O.photo_t + CH_2O.surplus_{t-1} - Resp.tot_t \tag{5.27}$$

If the carbohydrates available to be allocated to the different organs ($CH_2O.tot_t$) cover completely the sum of potential demands from Equations 5.24 and 5.25, then the allocation is quite straightforward and an hypothetical surplus can be carried over to the next time step. Otherwise, the allocation is proposed to be proportional to the organ's demand (Eq. 5.28).

$$\begin{cases} \begin{cases} Allocation.organ_t = Demand.organ_t \\ CH_2O.surplus_t = CH_2O.tot_t - Demand.organ_t \end{cases}, & \text{if } \sum Demand.organ_t < CH_2O.tot_t \\ \begin{cases} Allocation.organ_t = \dfrac{Demand.organ_t * CH_2O.tot_t}{\sum Demand.organ_t} \\ CH_2O.surplus_t = 0 \end{cases}, & \text{otherwise} \end{cases} \tag{5.28}$$

5.2.13 Module 10: Organs' properties update

The allocated assimilates for each organ, $Allocation.organ_t$, are converted to total new biomass by mean of the $CH_2O.factor_{organ}$ and then used to update $Biom.organ_{t-1}$ (Eq. 5.29). This simple multiplication represents the efficiency of conversion from CH_2O to the final tissue type (growth respiration). For coarse roots and wood the new biomass, initialized in the next time step, does not require further manipulations, contrarily to leaves, fine roots and fruits. The total allocation to the leaves is distributed between $Biom.shade.lv_t$ and $Biom.sun.lv_t$ to respect their fixed ratio. Hence, $Allocation.lv_t$ is multiplied by either $f.sun$ or $f.shade$ (Eq. 5.29). When it comes to fine roots, it is important to consider the higher investment in carbohydrates toward the soil strata with more water to extract. On the other hand, it would be unrealistic to arbitrarily assign new biomass to the soil layers where water is available the most as this may be due to a low presence of roots in the previous time steps. The goal is to account for the positive feedback that soil moisture has on fine root growth without forcing the model to strongly invest where there is more water. The proposed way to go is to distribute the assimilates based on the weighted fraction of the biomass that belongs to each soil layer using the $SWC_{l,t}$ as weights (Eq. 5.29). This approach maintains the fine roots presence ($Biom.fine.root_{l,t}$) as the most important factor but corrects it trying to put the modelled tree in the best conditions possible to undergo the next time step. Similarly, the assimilates are

redistributed among fruits based on their weighted fraction of the total fruit demand using their sink strength (Eq. 5.30). After this passage, the assimilates for each fruit are allocated to *Biom.pod* and *Biom.bean* based on the respective demand.

$$\begin{cases} Biom.wood_t = Biom.wood_{t-1} + Allocation.wood_t * CH_2O.factor_{wood} \\ Biom.roots_t = Biom.roots_{t-1} + Allocation.roots_t * CH_2O.factor_{roots} \\ Biom.shade.lv_t = Biom.shade.lv_{t-1} + Allocation.lv_t * CH_2O.factor_{lv} * f.shade \\ Biom.sun.lv_t = Biom.sun.lv_{t-1} + Allocation.lv_t * CH_2O.factor_{lv} * f.sun \\ Biom.fine.root_{l,t} = Biom.fine.root_{l,t-1} + \dfrac{Allocation.fine.root_t * Biom.fine.root_{l,t-1} * SWC_{l,t}}{\sum_{l=1}^{n} (Biom.fine.root_{l,t-1} * SWC_{l,t})} \end{cases} \tag{5.29}$$

$$\begin{cases} Biom.fruit_{n,t-1} = Biom.pod_{n,t-1} + Biom.bean_{n,t-1} \\ Demande.fruit_{n,t} = Demand.pod_{n,t} + Demand.bean_{n,t} \\ Biom.fruit_{n,t} = Biom.fruit_{n,t-1} + \dfrac{Allocation.fruit_t * CH_2O.factor_{fruit}}{Demand.fruit_t} \end{cases} \tag{5.30}$$

In addition, the physiological age of each fruit is updated for the following cycle of calculations at $t+1$ by adding *Tave* to the $Fruit.age_{fruitn,t}$. Whenever a pod reaches maturity in this way, it is immediately "harvested" and outputted as that day's production, divided into pod and bean biomass.
This module would ideally include a proper modelling of fruiting. Since cacao produces plenty of flowers, each with little chance to set a fruit. The most realistic modelling approach might be to make a stochastic Bayesian modelling of flowering in time with a pollination rate to create new fruits. The results in Chapter 3 could be used to guide the statistical description of the seasonality of flowering and setting. This approach is complex and still require to be studied in detail but a recent work has already set the bases to its development [67, 195]. Besides, an additional reason to chose a different approach for the proposed model lays in the fact that a repeatable output is preferable to evaluate the effects of climate on production in different scenarios. The opposite but viable approach is to initiate a fixed amount of biomass / fruits at each time step as it is done in CASE 2 [256]. Ideally, the model itself would take care of "simulating" the seasonality of production by allocating or not resources to the fruits initialized in periods when the tree usually do not set cherelles in reality (i.e. the long dry season Ch. 3). An improvement of this simple approach might be to impose a threshold of minimum $CH_2O.surplus_t$ required for the plant to "decide" to invest in new cherelles (*threshold.set*). The threshold would mimic that when the plant has little resources it invests very little in flowering and the eventual fruits that set would have little chances of survival. Whenever the $CH_2O.surplus_t$ would allow setting, a portion of $CH_2O.surplus_t$ ($frac.set$) could be invested in fruits while the rest would be carried over to the next time step. Hence, the modelled tree would always keep some resources stored to sustain the growth of organs in the future. Moreover, this could be a way to avoid an unrealistic setting pattern in large discrete waves of cherelles, likely to then end up competing among themselves too much, and spread out the setting among subsequent days. The portion of assimilates funnelled into setting could be translated in a number of new cherelles to initialize based on a fixed biomass for a new cherelle ($Biom.fruit_{t0}$; Eq. 5.31). An interesting and useful parameter to be calculated in time by the model is the potential biomass of a fruit as function of its age for each generation ($Biom.fruit.pot_t$). To this purpose, it is proposed that a "dummy" fruit is created for every generation of newly formed fruits ($Number.new.fruits_t$ different from zero) and left to grow to its full potential. The $Biom.fruit.pot_t$ would start from the fixed biomass of a newly set fruit ($Biom.fruit_{t0}$) and always receive the demanded assimilates, effectively skipping the allocation module (S. 5.2.12). The $Biom.fruit.pot_t$ at maturity would be an interesting output for the model to be used as a reference. Furthermore, $Biom.fruit.pot_t$ would be used to in the

module on wilting (S. 5.2.14) as a reference to calculate the fitness of the growing cherelles.

$$\begin{cases} Biom.new.fruits_t = frac.set * CH_2O.surplus_t, & \text{if } CH_2O.surplus_t > threshold.set \\ Number.new.fruits_t = floor(Biom.new.fruits / Biom.fruit_{t0}) \end{cases} \quad (5.31)$$

5.2.14 Module 11: Wilting

This module would attempt to capture wilting in the model for the first time ever. However, many potential sources of wilt would not be considered in the semi-ideal situation that would be simulated. Consequently, the effects of pests, diseases, insufficient pollination, mechanical damage and pollination would not be included. The proposed basic modelling of cherelle wilt would consider only three elements: the timing of susceptibility (age of the fruits), the role of climatic variables such as temperature and soil moisture and competition for resources. The intergenerational and intragenerational competition among fruits, demonstrated to push wilt rate up, is considered embed in the modelling of fruit allocation based on sink strength. In fact, the category of fruits found to strongly compete for resources ("Medium" in Chapter 4, Fig. 4.3.13) corresponds to the fruits in the linear phase of growth, thus with the maximum sink strength. Similarly, it can be assumed that all other fruit categories are competitors proportionally to their sink strength. Similarly, the competition for resources represented by other organs, leaf flush for example, should be an emerging property of the model. Whenever the vegetative growth will drain the plant's resources, the competition will increase and pressure the young cherelles that will start to accumulate less biomass. The competition does not require to be hard coded but its effect on cherelles biomass accumulation still has to be translated into fruit abortion. To this end, it is proposed to impose a probability of wilting (*Base.wilt.rate*) linked to the cherelle's physiological age and then apply it and modify it according to the single cherelle fitness.
The *Base.wilt.rate* curve could be adapted from the evolution of wilting in relation to the time after pollination converted in physiological age by a multiplication for the average temperature in the experiment (Fig. 4.3.1, 4.3.12). The base *wilt.rate* would show only one main peak of susceptibility between, while the secondary peaks observed for some clones (Fig. 4.3.3) would hopefully be captured by the model when modifying the *Base.wilt.rate* according to the cherelle fitness ($wilt.rate_{fruit}$, Eq. 5.32). The cherelle fitness ($fitness$) would be represented by its attained biomass in comparison to its potential biomass at the specific physiological age (Eq. 5.32). A first assumption to be made is that cherelles that attain their potential biomass do not wilt. Contrarily, cherelles far from their potential biomass should see the chances of wilting increasing more than linearly, with cherelles that attained 50% of their potential size ideally having a higher chance of wilting than the base rate. Therefore, it is proposed to define a coefficient of reduction ($coeff.fitness$) as an hyperbolic function of $fitness$. A simple option for the $coeff.fitness$ is reported in Equation 5.32 and complies with all the wanted features. This function was selected among other possible hyperbolic functions passing from (x=1,y=0) in light of the simple form and shape of the curve. A more thorough study investigating the best function would be a welcomed possible improvement. The final wilt rate of a specific fruit ($wilt.rate_{fruit}$, Eq. 5.32) would be capped to one, the certainty of wilting.
At each time step, a given fruit is stochastically wilted, or not, based on its proper $wilt.rate_{fruit}$. This can be achieved by generating a random real number between 0 and 1 and for each fruit and see if it is greater (not wilt) or lesser or equal to (wilt) $wilt.rate_{fruit}$. The stochastic component of this process can be eliminated by fixing a seed number whenever it is required to

have replicable results, i.e. to compare different climatic scenarios.

$$\begin{cases} Base.wilt.rate = f(Fruit.age_{fruitn,t}) \\ fitness = \dfrac{Biom.pod_{fruitn,t}}{Biom.fruit.pot_t} \\ coeff.fitness = \dfrac{2 - fitness}{fitness} - 1 \\ wilt.rate_{fruit} = min(Base.wilt.rate * coeff.fitness, 1) \end{cases} \tag{5.32}$$

Concerning the direct effects of climate, especially temperature, on the rate of wilt [132, 155], the intention was to extrapolate an empirical relation from the analyses in Chapter 3. Unfortunately, the results did not evidence any significant relationship with the climate types considered (Fig. 3.3.4 F, Fig. 3.3.5). It is proposed that the effect of climate on the wilt rate is disregarded in the first version of the module. To better inform a future improvement of this module, an option is to replicate the study of Chapter 4 Part 2 in a West African country where climate changes drastically over the year and could be included among the predictors of a BRT model similar to the one created to explain wilt in Costa Rica (Fig. 4.3.13, 4.3.15, 4.3.16)

5.2.15 Module 12: Outputs

At the end of each time-step a series of parameters and useful information for the user are grouped together, logged in a file and provided as model outputs. The proposed, and non-exhaustive, list of outputs would include:

- the tree age and total biomass ;
- the weight of the harvested pods divided into the two components: husk and beans;
- the biomass for: wood, coarse roots, sun leaves, shade leaves and fine roots;
- the list of fruits with related biomass and physiological age;
- the absolute number of wilted cherelles and the same relative to the total pod load;
- a representation of the water content of the soil at each depth (one can also think of providing values for intervals. e.g. 0-15, 15-30 cm etc.);
- the average temperature, soil moisture and vapour pressure over the day, the last week, past two week etc.;
- a counter for the days of soil and atmospheric water stress over the last 30 days (+0 if no stress, +1 if stress)

The file must be organised in such a way that it can be used to initiate the model from the endpoint of the last simulation, if desired so. This feature is a key requirement for industrial / commercial applications as it simplifies the study of different future scenarios dynamically over the season.

Appendix

5.A Cacao pods sink strength

Analysing a dataset of weekly measurements of the volume of growing pods from seven different clones it was possible to estimate the biomass accumulation rate of the structural phase of growth (pod husk) depending on the physiological age of the cherelle. The data correspond to the "healthy" pods already presented and used in Chapter 4 Part 1 (hand pollinated: M) and additional naturally pollinated pods measured simultaneously (N).
The age of the pods considered in the study was calculated as the sum of useful $^{\circ}Cday$

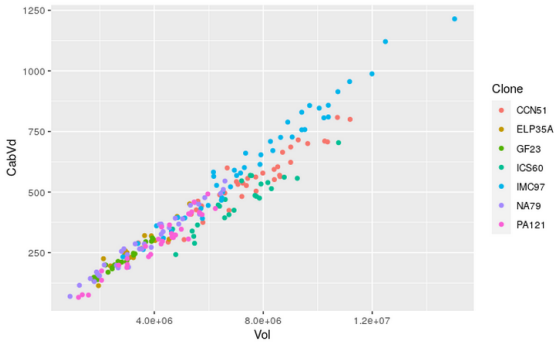

FIGURE 5.A.1: Linear relationship between the volume (x-axis,cm^2) and the weight of the empty pods of seven different cacao clones (y-axis, g). The linear relationship was found useful to convert the volumetric increase of pods in the field into a biomass growth rate.

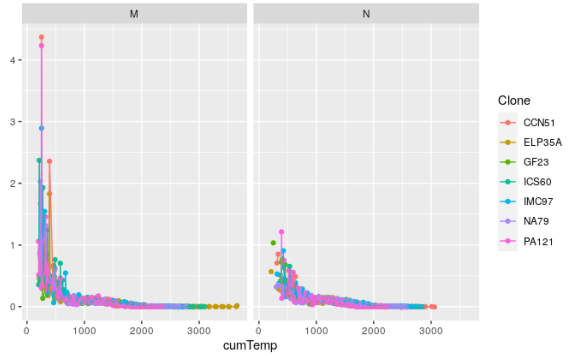

FIGURE 5.A.2: Volumetric increase rate ($cm^3[newbiomass]/cm^3[totalbiomass] * d^{-1}$) of cacao pods across seven cacao clones in relation to their physiological age (sum of °Cday). The relation is reported for hand pollinated pods (left) and naturally pollinated pods (right). The initial difference between the two curves is related to the lack of data for the natural pollination treatment.

accumulated by the pods (Eq. 5.33). This parameter was calculated assuming an average $T.base_{fruit}$ across clones of $10^{\circ}C$ [56]. It was then calculated the volumetric increase rate ($Vol.rate$) for all the 284 pods used in the study (188 from hand pollination and 96 from natural pollination) in relation to the change in physiological age. The volumetric increase rate was calculated as the difference in volume between subsequent dates (t-1, t) divided by the initial volume at $t-1$ and the difference in physiological age (Eq. 5.34). At the same time, it was remarked that there was a solid linear relationship between the pod estimated volume and the husk weight at harvest (Figure 5.A.1). The linear relationship found between the pod volume and husk weight was used to convert the volumetric increase rate into a biomass growth increase rate (Fig. 5.A.2). This rate appeared to be stable across clones and had a similar shape for both hand pollinated and naturally pollinated pods. It is proposed to adopt a regression function of the curve found in this study as a proxy for the sink strength during the structural

phase ($SS.pod$) in Chapter 5.

$$\begin{cases} T.base_{fruit} = 19.7^{\circ}C \\ Fruit.age_{fruitn,t} = \sum_{day=1}^{t} T_{average} - T \end{cases} \tag{5.33}$$

$$Vol.rate = \frac{Volume_t - Volume_{t-1}}{Volume_{t-1} * (Fruit.age_{fruitn,t} - Fruit.age_{fruitn,t-1})} \tag{5.34}$$

Chapter 6

Final conclusions and future research perspectives

This thesis addressed the need for the global cocoa industry to better understand and predict the effects of climate change in West Africa on cocoa production and its seasonal distribution. To answer this necessity, it was crucial to improve the knowledge on cacao physiology under the West African climatic conditions. Taking as reference an existing cacao mechanistic model (CASE 2; [257]), this work proposed a novel, tailored conceptual model to study sub-seasonal climate variations and their effects on the West African cacao production. To understand and properly model the West African production, this project primarily studied the importance of drought stress in cacao, especially the atmospheric drought that is peculiar of the long dry Harmattan season, when rainfalls are absent, the temperature range increases and the relative humidity of the air decreases.

This study indicates that the impact of the atmospheric drought on the tree's canopy and transpiration can be of comparable importance to the more studied soil drought. The importance of atmospheric drought for cacao had been disregarded in the past because it does not occur often in many cacao cultivation zone around the globe. When studying the West African production zone, the atmospheric drought was proven to be a key limiting factor to include in the conceptual model. This study has shown that cacao transpiration strongly responded to high VPD during the stressing long dry Harmattan season (Chapter 2). Moreover, it has found that this eventuality occurred both under constant irrigation or under natural, non irrigated circumstances. The atmospheric drought is not only a source of direct stress that reduces transpiration, leads to leakage of water from the leaf cuticle and can lead to cavitation, but it may further compromise the tree by depleting the soil water reservoirs faster and eventually aggravate soil stress.

Given the demonstrated importance of atmospheric drought, the proposed sub-seasonal model includes atmospheric drought in a simple but effective way (Chapter 5). In conclusion, this study shows the importance of further research towards more experimental evidences and quantification of the effects of harsh atmospheric conditions on cacao - always not ignoring the more studied soil drought. The soil drought has a predominant role at the timescale of the season while the atmospheric drought is responsible for acute peaks of stress over one or few days but with potentially long lasting effects, for example on fructification and production seasonality (Chapter 3). This study did not find any significant interaction between the soil and atmospheric droughts but this should not discourage future research efforts in this direction, both for modeling purposes and to reason about agronomic practices that minimize the overall negative effects of drought. For example, if a synergistic interaction between soil and atmospheric drought was found, it could be interesting to investigate which of the two types of drought should be prioritized and addressed by agronomic techniques to minimize the overall stress.

This study is a first milestone in the direction of connecting the harshness and characteristics of a drought event to the subsequent change in production seasonality, although limited in

its duration (Chapter 3). When replicated over multiple seasons, the study in Chapter 3 may provide insightful information to the industry on which effects on production to expect, depending on well defined climate typologies. Looking at the short-to-medium term, the harsh atmospheric and soil environment experienced when the Harmattan winds blew over West Africa concentrated production during the subsequent cropping season. The concentration of production took place during the first not-stressing period irrespective of irrigation. However, irrigation was found to keep the production profile more distributed over the season, still maintaining a peak in setting during the first favorable wet season. This study advances the hypothesis that the more distributed production profile could make production more resilient to extreme or disruptive events.

Together with the advancement made in understanding the effects of the seasonal occurrence of droughts in West Africa, the project addressed the functioning of cherelle wilt, a self-thinning mechanism of great importance that was missing in the reference model (CASE 2) and needed to be included in any model that aimed at practical applications in the industry world. For far too long the research on cherelle wilt relied on a few, old studies supporting the existence of two peaks of wilting in the development of a cherelle. The risk of wilting for a cherelle was confirmed to be limited by its age, but this study evidenced only one main peak of cherelle wilting for reasons other than incomplete pollination. The peak was found to be centered between the third and fifth week after pollination and steadily decreasing afterwards. Even if cherelles were found to wilt up to 15 weeks after pollination, the risk sensibly decreased after the first seven weeks of growth. The main peak was followed in some clones by one or more considerably lower peaks, starting nine weeks after pollination. The study in Chapter 4 not only brought more clarity about the timing of wilting but, using a novel approach, it quantified the duration of the process of wilting as well. The process of cherelle wilt is initiated three weeks before the symptoms appear on the fruit. During the three weeks between the triggering of wilting and the appearance of the symptoms, the relative growth rate dropped almost linearly. Therefore, the destiny of most wilted cherelles (the aforementioned peak at three to five weeks after pollination) is decided in an early stage of development, precisely in the first two weeks after pollination. This study also confirmed that, in most cases, wilting involved cherelles that had already grown slowly compared to others of similar age demonstrating a lower fitness. The timing of the peak in wilting, the duration of the wilting process and which cherelles of the same generations are more likely to wilt are key pieces of novel information needed to be included in any sub-seasonal model for cacao that includes cherelle wilt, as in the case of the proposed conceptual model in Chapter 5.

To model cherelle wilt, it was vital to, not only, know which cherelles, and at which stage of development, are more susceptible to wilt, but as well what causes this phenomenon. Competition among fruits was a well known but unexplored cause for wilt until, within this project, the importance of intra- and inter-generational competition for resources was investigated. Inter-generational competition for assimilates was proven to be a key predictor for wilting mostly imputable to pods 10 to 16 weeks old. Between 10 and 16 weeks after pollination the fruits are in the linear phase of growth and their relative growth rate is maximized. This result is a great advancement in the understanding of cherelle wilt and, among other things, allowed to conceive a rule for modeling this process based on the fruit's sink strength. On the other hand, the intra-generational competition was found to foster wilting for those fruit cohorts that were very abundant. This result further confirmed the importance of modeling cherelle wilt as dependent of the sink strength of a fruit compared to the overall sink pull of all other organs, especially fruits. Within this project it was not confirmed the expected superior fitness of pods on the lower part of the tree and with higher access to assimilates, especially on the trunk, compared to the periphery of the canopy.

Many of the results of this study represent milestones in understanding better the dynamics of cacao production at the sub-seasonal timescale, particularly under West African climate.

This project has established the importance of atmospheric stress for cacao physiology, proposed a methodology to link production dynamics with different types of drought (Chapter 3) and shed light on the role of competition and cherelle characteristics in the dynamic of cherelle wilt. With these new, precious pieces of information it was possible to advance as well the mechanistic modeling of cacao at a sub-seasonal timescale. Compared to the "reference model", this study proposed innovative solutions to: (1) include the direct effect of atmospheric stress on plant water use, (2) increase the plasticity of the modeled plant in adapting to a soil water stress situation, (3) increase the realism of fruiting and (4) fruit development and growth, and (5) include the fruit abortion mechanism known as "cherelle wilt".

This project has set the basis to model cacao production in West Africa and opens up to further studies on the effect on cocoa physiology of the duration and intensity of soil and atmospheric drought. In particular, an avenue of research arising from this project is to test the same hypotheses in a more extreme environment (such as northern Ghana). This would allow on the one hand to verify the results obtained and on the other hand to investigate how cocoa may be affected by climate change, which should increase the occurrence of extraordinary events, including shorter but much harsher dry seasons. The author, Pietro Della Sala, is of the opinion that many interesting results and theses advanced for cacao modeling, in the past or in this study, require to be replicated before being adopted in a model. The objective of modeling something as complex as cacao interaction with its environment is ambitious and has to be based on established results, thus needs repetition. In particular, repeating the study of the medium- to long-term effects of an extreme climatic event such as the Harmattan over several seasons would help to clarify and quantify the effects of different climate classes on production. Such research should however include the positive effect of irrigation in order to better isolate purely atmospheric effects.

Furthermore, the field studies carried out in West Africa as part of this project (Chapters 2 and 3) focused only on the most common variety family in the production area: Amelonado. Although interesting, the results of this study need to be complemented by future research on drought-sensitive and drought-resistant varieties. In fact, our study can help the industry to better understand the effects of climate on current production, but this may change in the future with varieties developed to adapt West African production to climate change. There is still a lot to be done to better understand the bacterial wilt phenomenon. Our study showed no significant difference in the number of aborted cherelles due to climate or irrigation in a field situation in Ghana. This is probably due to the scarcity of aborted cherelles in general, which did not allow for sufficient numbers to find a statistically significant difference. If the direct effects of climate on abortion rates are to be incorporated into future cocoa modelling, a larger study with a greater number of trees monitored consistently will be required. Apart from this, it would be interesting to monitor the filling of some fruits, for example with xylem sap flow sensors, to improve the accuracy of predicting when a cherelle will abort and the time between abortion induction and visible symptoms in the field.

In this project all analyses were performed for a full-sun system, by far the most common system in West Africa. Thus, the atmospheric drought did not have to account for the shade canopy modification in the micro-climate experienced by cacao and there was no additional water extraction from the soil but by the cacao trees. If, on one hand, this permitted to simplify the studied system, in a future it could be interesting to explore how a certain drought episode, that combines both the soil and atmospheric stress, affects the transpiration rate and production dynamics under increasing levels of shading.

Following the conceptual model designed and presented in Chapter 5, the first step in future research would be to code it and verify its functioning. Firstly, it would be necessary to check the robustness and functioning of each module individually (validation) and, in case of unrealistic outputs, to make the necessary changes. Secondly, the model as a whole needs to be validated. In this respect, a first step would be to simulate the 2019/2020 season used in

chapters 2 and 3. This should then be repeated for other seasons or locations in West Africa. Another interesting research that could result from this study, once the model has been coded and the modules finalised, is an analysis of the sensitivity of each module to the parameters involved in the processes described. In particular, it would be interesting to study how the proposed soil water content feedback mechanism of fine root partitioning would change the distribution of roots over time if soil parameters or root uptake parameters (e.g. RUR) are changed. Another process that would be interesting to study is how the wilt module is impacted by the choice of a different hyperbolic function. More generally, a good avenue for future research is to study the sensitivity of the model as a whole to certain parameters (e.g. baseline temperatures for vegetative and fruit growth).
Finally, the model could be used, hopefully in the near future, for direct applications such as yield predictions in response to known climatic events (of interest to industry). In addition, it could also be used for research purposes. For example, it would ideally be possible to simulate short but frequent drought events as well as long but mild ones. This would answer the question of whether the first or the second option has a greater impact on production in the short, medium and long term.

Bibliography

[1] Abdulai, Issaka, Hoffmann, Munir P., Jassogne, Laurence, Asare, Richard, Graefe, Sophie, Tao, Hsiao Hang, Muilerman, Sander, Vaast, Philippe, Van Asten, Piet, Läderach, Peter, and Rötter, Reimund P. "Variations in yield gaps of smallholder cocoa systems and the main determining factors along a climate gradient in Ghana". In: *Agricultural Systems* 181 (2020). ISSN: 0308521X. DOI: 10.1016/j.agsy.2020.102812.

[2] Abdulai, Issaka, Vaast, Philippe, Hoffmann, Munir P., Asare, Richard, Jassogne, Laurence, Van Asten, Piet, Rötter, Reimund P., and Graefe, Sophie. "Cocoa agroforestry is less resilient to sub-optimal and extreme climate than cocoa in full sun". In: *Global Change Biology* 24.1 (2018), pp. 273–286. ISSN: 13652486. DOI: 10.1111/gcb.13885.

[3] Achten, W. M.J., Maes, W. H., Reubens, B., Mathijs, E., Singh, V. P., Verchot, L., and Muys, B. "Biomass production and allocation in Jatropha curcas L. seedlings under different levels of drought stress". In: *Biomass and Bioenergy* 34.5 (2010), pp. 667–676. ISSN: 0961-9534. DOI: 10.1016/J.BIOMBIOE.2010.01.010.

[4] Adedokun, J. A. "West African precipitation and dominant atmospheric mechanisms". In: *Archiv für Meteorologie, Geophysik und Bioklimatologie Serie A* 27.3-4 (1978), pp. 289–310. ISSN: 00666416. DOI: 10.1007/BF02247952.

[5] Aliche, Ernest B., Theeuwen, Tom P.J.M., Oortwijn, Marian, Visser, Richard G.F., and Linden, C. Gerard van der. "Carbon partitioning mechanisms in POTATO under drought stress". In: *Plant Physiology and Biochemistry* 146 (2020), pp. 211–219. ISSN: 0981-9428. DOI: 10.1016/J.PLAPHY.2019.11.019.

[6] Allen, Richard G, Pereira, Luis S, Raes, Dirk, Smith, Martin, and Ab, W. "Fao,1998". In: *Irrigation and Drainage Paper No. 56, FAO* (1998), p. 300. ISSN: 02545284. DOI: 10.1016/j.eja.2010.12.001.

[7] Almeida, Alex-Alan F. de and Valle, Raúl René. *Análise do crescimento de frutos e sementes de sete genótipos de Theobroma cacao L.* 1995.

[8] Anim-Kwapong, G. J. and Frimpong, E. B. "Vulnerability and Adaptation Assessment Under the Netherlands Climate Change Studies Assistance Programme Phase 2 (NCCSAP2)". In: *Cocoa Research Institute of Ghana* 2 (2008), pp. 1–30.

[9] ARAKI, Takuya, EGUCHI, Toshihiko, WAJIMA, Takahiro, YOSHIDA, Satoshi, and KITANO, Masaharu. "Dynamic analysis of growth, water balance and sap fluxes through phloem and xylem in a tomato fruit: Short-term effect of water stress". In: *Environment Control in Biology* 42.3 (2004), pp. 225–240.

[10] Araque, O., Jaimez, R. E., Tezara, W., Coronel, I., Urich, R., and Espinoza, W. "Comparative photosynthesis, water relations, growth and survival rates in juvenile criollo cacao cultivars (theobroma cacao) during dry and wet seasons". In: *Experimental Agriculture* 48.4 (2012), pp. 513–522. ISSN: 00144797. DOI: 10.1017/S0014479712000427.

[11] Arseneault, Michelle H. and Cline, John A. *A review of apple preharvest fruit drop and practices for horticultural management*. 2016. DOI: 10.1016/j.scienta.2016.08.002.

[12] Asante, Paulina A., Rozendaal, Danaë M.A., Rahn, Eric, Zuidema, Pieter A., Quaye, Amos K., Asare, Richard, Läderach, Peter, and Anten, Niels P.R. "Unravelling drivers of high variability of on-farm cocoa yields across environmental gradients in Ghana". In: *Agricultural Systems* 193.June (2021), p. 103214. ISSN: 0308521X. DOI: 10.1016/j.agsy.2021.103214.

[13] Asare, Rebecca Ashley, Asare, Richard, Asante, Winston Adams, Markussen, Bo, and RÆbild, Anders. "INFLUENCES of SHADING and FERTILIZATION on ON-FARM YIELDS of COCOA in GHANA". In: *Experimental Agriculture* 53.3 (2017), pp. 416–431. ISSN: 14694441. DOI: 10.1017/S0014479716000466.

[14] Ashiru, G.A. and Jacob, V.J. "Potential pod production and pod loss in cacao (Theobroma cacao L.)" In: *Journal of Horticultural Science* 46.1 (1971), pp. 95–102. ISSN: 0022-1589. DOI: 10.1080/00221589.1971.11514387.

[15] Atmospheric Research Staff, (National Center for. *Climate Data Sets: NCAR - Climate Data Guide*. 2015. URL: https://climatedataguide.ucar.edu/climate-data/cpc-unified-gauge-based-analysis-global-daily-precipitation..

[16] Avila-Lovera, Eleinis, Coronel, Ilsa, Jaimez, Ramón, Urich, Rosa, Pereyra, Gabriela, Araque, Osmary, Chacón, Iraima, and Tezara, Wilmer. "ECOPHYSIOLOGICAL TRAITS OF ADULT TREES OF CRIOLLO COCOA CULTIVARS (THEOBROMA CACAO L.) FROM A GERMPLASM BANK IN Venezuela". In: *Experimental Agriculture* 52.1 (2016), pp. 137–153. ISSN: 14694441. DOI: 10.1017/S0014479714000593.

[17] Baligar, V C, Bunce, J A, Machado, R C R, and Elson, M K. "Photosynthetic photon flux density, carbon dioxide concentration, and vapor pressure deficit effects on photosynthesis in cacao seedlings". In: *Photosynthetica* 46.2 (2008), pp. 216–221.

[18] Bartlett, Megan K., Klein, Tamir, Jansen, Steven, Choat, Brendan, and Sack, Lawren. "The correlations and sequence of plant stomatal, hydraulic, and wilting responses to drought". In: *Proceedings of the National Academy of Sciences* 113.46 (2016), pp. 13098–13103. ISSN: 0027-8424. DOI: 10.1073/pnas.1604088113. URL: http://www.pnas.org/lookup/doi/10.1073/pnas.1604088113.

[19] Bates, Douglas, Maechler, Martin, Bolker, Ben, Walker, Steven, Christensen, Rune Haubo Bojesen, Singmann, Henrik, Dai, Bin, and Scheipl, Fabian. *Package 'lme4' - version: 1.1-25*. 2020.

[20] Becker, Richard. *The new S language*. CRC Press, 2018.

[21] Beg, Mohd Shavez, Ahmad, Sameer, Jan, Kulsum, and Bashir, Khalid. "Status, supply chain and processing of cocoa - A review". In: *Trends in Food Science and Technology* 66 (2017), pp. 108–116. ISSN: 09242244. DOI: 10.1016/j.tifs.2017.06.007. URL: http://dx.doi.org/10.1016/j.tifs.2017.06.007.

[22] BERLYN, G. P. "Plant Structures: Xylem Structure and the Ascent of Sap." In: *Science* (1983). ISSN: 0036-8075. DOI: 10.1126/science.222.4623.500-a.

[23] Bertolde, F. Z., Almeida, A. A. F., Pirovani, C. P., Gomes, F. P., Ahnert, D., Baligar, V. C., and Valle, R. R. "Physiological and biochemical responses of Theobroma cacao L. genotypes to flooding". In: *Photosynthetica* 50.3 (2012), pp. 447–457. ISSN: 0300-3604. DOI: 10.1007/s11099-012-0052-4. URL: http://link.springer.com/10.1007/s11099-012-0052-4.

[24] Bizimana, Jean-Claude and Richardson, James W. "Agricultural technology assessment for smallholder farms: An analysis using a farm simulation model (FARMSIM)". In: *Computers and electronics in agriculture* 156 (2019), pp. 406–425.

[25] Bleby, Timothy M., Burgess, Stephen S.O., and Adams, Mark A. "A validation, comparison and error analysis of two heat-pulse methods for measuring sap flow in Eucalyptus marginata saplings". In: *Functional Plant Biology* (2004). ISSN: 14454408. DOI: 10.1071/FP04013.

[26] Bos, Merijn M., Steffan-Dewenter, Ingolf, and Tscharntke, Teja. "Shade tree management affects fruit abortion, insect pests and pathogens of cacao". In: *Agriculture, Ecosystems and Environment* (2007). ISSN: 01678809. DOI: 10.1016/j.agee.2006.09.004.

[27] Bouman, B. A.M., Van Keulen, H., Van Laar, H. H., and Rabbinge, R. "The 'School of de Wit' crop growth simulation models: A pedigree and historical overview". In: *Agricultural Systems* 52.2-3 (1996), pp. 171–198. ISSN: 0308521X. DOI: 10.1016/0308-521X(96)00011-X.

[28] Bouman, BAM. *ORYZA2000: modeling lowland rice*. IRRI, 2001.

[29] Brisson, N., Bona, S., and Bouniols, A. "SOYGRO, un modèle de simulation de la culture du soja; adaptation à des variétés cultivées dans le sud de l'Europe et validation". In: *Agronomie* (1989). ISSN: 0249-5627. DOI: 10.1051/agro:19890103.

[30] Brockwell, Peter J, Davis, Richard A, and Fienberg, Stephen E. *Time series: theory and methods: theory and methods*. Springer Science & Business Media, 1991.

[31] Bucci, Sandra J., Scholz, Fabian G., Campanello, Paula I., Montti, Lia, Jimenez-Castillo, Mylthon, Rockwell, Fulton A., Manna, Ludmila La, Guerra, Pedro, Bernal, Pablo Lopez, Troncoso, Oscar, Enricci, Juan, Holbrook, Michele N., and Goldstein, Guillermo. "Hydraulic differences along the water transport system of South American Nothofagus species: Do leaves protect the stem functionality?" In: *Tree Physiology* 32.7 (2012), pp. 880–893. ISSN: 17584469. DOI: 10.1093/treephys/tps054.

[32] Burgess, S. S.O., Adams, M. A., Turner, N. C., Beverly, C. R., Ong, C. K., Khan, A. A.H., and Bleby, T. M. "An improved heat pulse method to measure low and reverse rates of sap flow in woody plants". In: *Tree Physiology* (2001). ISSN: 0829318X. DOI: 10.1093/treephys/21.9.589.

[33] Byers, Ross E., Costa, Guglielmo, and Vizzotto, Giannina. " Flower and Fruit Thinning of Peach and other Prunus ". In: *Horticultural Reviews*. 2010. DOI: 10.1002/9780470650851.ch7.

[34] Caemmerer, Susanne von, Farquhar, Graham, and Berry, Joseph. "Biochemical model of C 3 photosynthesis". In: *Photosynthesis in silico*. Springer, 2009, pp. 209–230.

[35] Calvo-Alvarado, J. C., McDowell, N. G., and Waring, R. H. "Allometric relationships predicting foliar biomass and leaf area:sapwood area ratio from tree height in five Costa Rican rain forest species". In: *Tree Physiology* 28.11 (2008), pp. 1601–1608. ISSN: 17584469. DOI: 10.1093/treephys/28.11.1601. URL: https://academic.oup.com/treephys/article/28/11/1601/1671280.

[36] Camargo, Marcelo Bento Paes de. "The impact of climatic variability and climate change on Arabic coffee crop in Brazil". In: *Bragantia* (2010). ISSN: 16784499. DOI: 10.1590/s0006-87052010000100030.

[37] Campbell, G. S. "EXTINCTION COEFFICIENTS FOR RADIATION IN PLANT CANOPIES CALCULATED USING AN ELLIPSOIDAL INCLINATION ANGLE DISTRIBUTION". In: 36 (1986), pp. 317–321.

[38] Carimentrand, Aurélie. "Cacao. Etat des lieux sur la déforestation et les standards de durabilité". In: (2020).

[39] Carr, M. K V and Lockwood, G. "The water relations and irrigation requirements of cocoa (Theobroma cacao L.): A review". In: *Experimental Agriculture* 47.4 (2011), pp. 653–676. ISSN: 00144797. DOI: 10.1017/S0014479711000421.

[40] Carvalho, Dália, Torre, Sissel, Kraniotis, Dimitrios, Almeida, Domingos, Heuvelink, E., and Carvalho, Susana. "Elevated air movement enhances stomatal sensitivity to abscisic acid in leaves developed at high relative air humidity". In: *Frontiers in Plant Science* 6 (May 2015). DOI: 10.3389/fpls.2015.00383.

[41] Celton, Jean Marc, Kelner, Jean Jacques, Martinez, Sébastien, Bechti, Abdel, Touhami, Amina Khelifi, James, Marie José, Durel, Charles Eric, Laurens, François, and Costes, Evelyne. "Fruit self-thinning: A trait to consider for genetic improvement of apple tree". In: *PLoS ONE* (2014). ISSN: 19326203. DOI: 10.1371/journal.pone.0091016.

[42] Challinor, Andrew J, Müller, Christoph, Asseng, Senthold, Deva, Chetan, Nicklin, Kathryn Jane, Wallach, Daniel, Vanuytrecht, Eline, Whitfield, Stephen, Ramirez-Villegas, Julian, and Koehler, Ann Kristin. "Improving the use of crop models for risk assessment and climate change adaptation". In: *Agricultural Systems* 159.June 2017 (2018), pp. 296–306. ISSN: 0308521X. DOI: 10.1016/j.agsy.2017.07.010.

[43] Chave, J, Andalo, Ae C, Brown, Ae S, Cairns, Ae M A, Chambers, J Q, Eamus, Ae D, Foïster, Ae H, Fromard, Ae F, Higuchi, N, Kira, Ae T, Lescure, J.-P, Nelson, Ae B W, Ogawa, H, Puig, Ae H, Rie´ra, Ae B, Ae, Rie´ra, Yamakura, T, Brown, S, Cairns, M A, Eamus, D, Foïster, H, Fromard, F, Kira, T, Yamakura, Ae T, and Rie´ra, B Rie´ra. "ECOSYSTEM ECOLOGY Tree allometry and improved estimation of carbon stocks and balance in tropical forests". In: (2005). DOI: 10.1007/s00442-005. URL: http://dx.doi.org/10.1007/s00442-005-.

[44] Chaves, Manuela M., Maroco, João P., and Pereira, João S. "Understanding plant responses to drought - From genes to the whole plant". In: *Functional Plant Biology* 30.3 (2003), pp. 239–264. ISSN: 14454408. DOI: 10.1071/FP02076.

[45] Chung, Nguyen Thi, Jintrawet, Attachai, and Promburom, Panomsak. "Impacts of Seasonal Climate Variability on Rice Production in the Central Highlands of Vietnam". In: *Agriculture and Agricultural Science Procedia* (2015). ISSN: 22107843. DOI: 10.1016/j.aaspro.2015.08.012.

[46] Cocoa Health and Extension Division [CHED] and World Cocoa Foundation [WCF]. "Manual for cocoa extension in Ghana". In: (2016), pp. 1 –104. ISSN: 1098-6596. arXiv: arXiv:1011.1669v3.

[47] COHEN, Y., FUCHS, M., and GREEN, G. C. "Improvement of the heat pulse method for determining sap flow in trees". In: *Plant, Cell & Environment* (1981). ISSN: 13653040. DOI: 10.1111/j.1365-3040.1981.tb02117.x.

[48] Competence, Social and Maturity, Emotional. *Integrating crops and livestock in West Africa*. 2010.

[49] Cuatrecasas, José. *Cacao and its allies: a taxonomic revision of the genus Theobroma*. Vol. 35. 6. Smithsonian Institution, 1964.

[50] da Silva Branco, Márcia Christina, Almeida, Alex Alan Furtado de, Dalmolin, Ândrea Carla, Ahnert, Dário, and Baligar, Virupax C. "Influence of low light intensity and soil flooding on cacao physiology". In: *Scientia Horticulturae* 217.January (2017), pp. 243–257. ISSN: 03044238. DOI: 10.1016/j.scienta.2017.01.038. URL: http://dx.doi.org/10.1016/j.scienta.2017.01.038.

[51] Dahle, Gregory A, Gallagher, Frank J, Gershensond, Dimitry, Schäfer, Karina V R, Grabosky, Jason C, Dahle, G A, Gallagher, F J, Gershensond, D, Schäfer, K V R, and Grabosky, J C. "Allometric and mass relationships of Betula populifolia in a naturally assembled urban brownfield: implications for carbon modeling". In: 17 (2014), pp. 1147–1160. DOI: 10.1007/s11252-014-0377-9.

[52] Dahle, Gregory A. and Grabosky, Jason C. "Allometric patterns in Acer platanoides (Aceraceae) branches". In: *Trees - Structure and Function* 24.2 (2010), pp. 321–326. ISSN: 09311890. DOI: 10.1007/s00468-009-0401-5.

[53] Dahle, Gregory A. and Grabosky, Jason C. "Review of literature on the function and allometric relationships of tree stems and branches". In: *Arboriculture and Urban Forestry* 35.6 (2009), pp. 311–320. ISSN: 02785226.

[54] Das, L, Lohar, D, Sadhukhan, I, Khan, S A, Saha, A, and Sarkar, S. "Evaluation of the performance of ORYZA2000 and assessing the impact of climate change on rice production in Gangetic West Bengal". In: *Journal of Agrometeorology* (2007). ISSN: 0972-1665 ER.

[55] Daymond, A. J. and Hadley, P. "Differential effects of temperature on fruit development and bean quality of contrasting genotypes of cacao (Theobroma cacao)". In: *Annals of Applied Biology* 153.2 (2008), pp. 175–185. ISSN: 00034746. DOI: 10.1111/j.1744-7348.2008.00246.x.

[56] Daymond, A. J. and Hadley, P. "The effects of temperature and light integral on early vegetative growth and chlorophyll fluorescence of four contrasting genotypes of cacao (Theobroma cacao)". In: *Annals of Applied Biology* 145.3 (2004), pp. 257–262. DOI: doi:10.1111/j.1744-7348.2004.tb00381.x.

[57] Daymond, Andrew J. "An investigation into physiological parameters underlying yield variation between different varieties of cocoa." PhD thesis. University of Reading, 2000.

[58] De Almeida, Alex Alan F. and Valle, Raúl R. *Ecophysiology of the cacao tree*. 2007. DOI: 10.1590/S1677-04202007000400011.

[59] De Almeida, Jenny, Tezara, Wilmer, and Herrera, Ana. "Physiological responses to drought and experimental water deficit and waterlogging of four clones of cacao (Theobroma cacao L.) selected for cultivation in Venezuela". In: *Agricultural Water Management* 171 (2016), pp. 80–88. ISSN: 18732283. DOI: 10.1016/j.agwat.2016.03.012.

[60] De Schepper, Veerle, De Swaef, Tom, Bauweraerts, Ingvar, and Steppe, Kathy. "Darwin review Phloem transport: a review of mechanisms and controls". In: (2013). DOI: 10.1093/jxb/ert302. URL: https://academic.oup.com/jxb/article/64/16/4839/593231.

[61] De Vries, F. W.T.Penning, Brunsting, A. H.M., and Van Laar, H. H. "Products, requirements and efficiency of biosynthesis a quantitative approach". In: *Journal of Theoretical Biology* (1974). ISSN: 10958541. DOI: 10.1016/0022-5193(74)90119-2.

[62] De'ath, Glenn and Fabricius, Katharina E. "Classification and regression trees: a powerful yet simple technique for ecological data analysis". In: *Ecology* 81.11 (2000), pp. 3178–3192.

[63] Deng, Ximin, Joly, Robert J., and Hahn, Daniel T. "The Influence of Plant Water Deficit on Distribution of 14C-labelled Assimilates in Cacao Seedlings". In: *Physiologia Plantarum* 78.4 (1990), pp. 623–627. ISSN: 13993054. DOI: 10.1111/j.1399-3054.1990.tb05251.x.

[64] Deng, Ximin, Joly, Robert J., and Hahn, Daniel T. "The influence of plant water deficit on photosynthesis and translocation of 14C-labeled assimilates in cacao seedlings". In: *Physiologia Plantarum* 78.4 (1990), pp. 623–627. ISSN: 13993054. DOI: 10.1111/j.1399-3054.1990.tb05251.x.

[65] Ding, Ning, Chen, Qian, Zhu, Zhanling, Peng, Ling, Ge, Shunfeng, and Jiang, Yuanmao. "Effects of crop load on distribution and utilization of 13C and 15N and fruit quality for dwarf apple trees". In: *Scientific Reports* (2017). ISSN: 20452322. DOI: 10.1038/s41598-017-14509-3.

[66] Ding, Weilong, Xu, Lifeng, Wei, Yang, Wu, Fuli, Zhu, Defeng, Zhang, Yuping, and Max, Nelson. "Genetic algorithm based approach to optimize phenotypical traits of virtual rice". In: *Journal of theoretical biology* 403 (2016), pp. 59–67.

[67] Doaré, Fabien, RIBEYRE, Fabienne, and Cilas, Christian. "Le phénotypage du cacaoyer : comment estimer la granulométrie des fèves de cacao ?" In: *Paper presented at International Symposium on Cocoa Research, 13-17 November 2017, Lima, Peru*. 2017.

[68] Drummon, Francis A. "Wild blueberry fruit drop: A consequence of seed set?" In: *Agronomy* (2020). ISSN: 20734395. DOI: 10.3390/agronomy10070939.

[69] Egea, Gregorio, Verhoef, Anne, and Vidale, Pier Luigi. "Towards an improved and more flexible representation of water stress in coupled photosynthesis-stomatal conductance models". In: *Agricultural and Forest Meteorology* 151.10 (2011), pp. 1370–1384. ISSN: 01681923. DOI: 10.1016/j.agrformet.2011.05.019.

[70] El-Sharkawy, Mabrouk A. "Physiological characteristics of cassava tolerance to prolonged drought in the tropics: implications for breeding cultivars adapted to seasonally dry and semiarid environments". In: *Brazilian Journal of Plant Physiology* 19.4 (2007), pp. 257–286. ISSN: 1677-0420. DOI: 10.1590/S1677-04202007000400003.

[71] Elith, J, Leathwick, J R, and Hastie, T. *A working guide to boosted regression trees*. 2008. DOI: 10.1111/j.1365-2656.2008.01390.x.

[72] Elith, Jane and Leathwick, John. "Boosted Regression Trees for ecological modeling". In: (2011), pp. 1–22.

[73] Elston, J. "Simulation of assimilation, respiration and transpiration of crops". In: *Agricultural Systems* (1982). ISSN: 0308521X. DOI: 10.1016/0308-521x(82)90042-7.

[74] Evers, Jochem B and Vos, Jan. "Modeling branching in cereals". In: *Frontiers in plant science* 4 (2013), p. 399.

[75] Evers, Jochem B., Vos, Jan, Chelle, Michael, Andrieu, Bruno, Fournier, Christian, and Struik, Paul C. "Simulating the effects of localized red : far-red ratio on tillering in spring wheat (Triticum aestivum) using a three-dimensional virtual plant model". In: *New Phytologist* 176.2 (2007), pp. 325–336. ISSN: 0028-646X. DOI: 10.1111/j.1469-8137.2007.02168.x. URL: http://apps.webofknowledge.com/full_record.do?product=WOS&search_mode=Refine&qid=5&SID=N1@joMfhLhkmIb5PkpK&page=2&doc=15&cacheurlFromRightClick=no.

[76] F., Aneani and K., Ofori-Frimpong. "An Analysis of Yield Gap and Some Factors of Cocoa (Theobroma cacao) Yields in Ghana". In: *Sustainable Agriculture Research* (2013). ISSN: 1927-050X. DOI: 10.5539/sar.v2n4p117.

[77] Falque, Matthieu, Vincent, Antoine, Vaissiere, Bernard, and Eskes, Albertus. "Effect of pollination intensity on fruit and seed set in cacao (Theobroma cacao L.)" In: *Sexual Plant Reproduction* 8.6 (1995), pp. 354–360. ISSN: 0934-0882. DOI: 10.1007/BF00243203.

[78] Fang, Yujie and Xiong, Lizhong. *General mechanisms of drought response and their application in drought resistance improvement in plants*. 2015. DOI: 10.1007/s00018-014-1767-0.

[79] FAO. *The State of How does international price volatility affect domestic economies and food security?* 2011. ISBN: 978-92-5-106927-1.

[80] FAOSTAT. *FAOSTAT: Statistical database.* 2019.

[81] Farquhar, Graham D, Caemmerer, S von von, and Berry, Joseph A. "A biochemical model of photosynthetic CO 2 assimilation in leaves of C 3 species". In: *Planta* 149.1 (1980), pp. 78–90.

[82] Fauziah Nur. "The Effect of Harmattan on Cocoa Production in West Africa". PhD thesis. 2018.

[83] Flerchinger, G. N. and Yu, Qiang. "Simplified expressions for radiation scattering in canopies with ellipsoidal leaf angle distributions". In: *Agricultural and Forest Meteorology* 144.3-4 (2007), pp. 230–235. ISSN: 01681923. DOI: 10.1016/j.agrformet.2007.03.002.

[84] Forster, Michael. "The Dual Method Approach (DMA) Resolves Measurement Range Limitations of Heat Pulse Velocity Sap Flow Sensors". In: *Forests* 10.1 (2019), p. 46. ISSN: 1999-4907. DOI: 10.3390/f10010046. URL: http://www.mdpi.com/1999-4907/10/1/46.

[85] Forster, Michael A. "The importance of conduction versus convection in heat pulse sap flow methods". In: *Tree physiology* 40.5 (2020), pp. 683–694. ISSN: 17584469. DOI: 10.1093/treephys/tpaa009.

[86] Fountain Antonie C. y Hütz-Adams, Friedel. *Barometro del Cacao 2020*. 2020.

[87] Fraga Junior, Luciano Sobral, Vellame, Lucas Melo, Oliveira, Aureo Silva de, da Silva Paz, Vital Pedro, Oliveira, Aureo Silva de, and Paz, Vital Pedro da Silva. "Transpiration of young cocoa trees under soil water restriction". In: *Scientia Agricola* 78.2 (2020). ISSN: 1678-992X. DOI: 10.1590/1678-992x-2019-0093.

[88] Friedman, Jerome, Hastie, Trevor, Tibshirani, Robert, et al. *The elements of statistical learning*. Vol. 1. 10. Springer series in statistics New York, 2001.

[89] Fu, Qiushi, Cheng, Lailiang, Guo, Yangdong, and Turgeon, Robert. "Phloem loading strategies and water relations in trees and herbaceous plants". In: *Plant Physiology* 157.3 (2011), pp. 1518–1527. ISSN: 00320889. DOI: 10.1104/pp.111.184820. URL: www.plantphysiol.org/cgi/doi/10.1104/pp.111.184820.

[90] Gateau-Rey, Lauranne, Tanner, Edmund V.J., Rapidel, Bruno, Marelli, Jean Philippe, and Royaert, Stefan. "Climate change could threaten cocoa production: Effects of 2015-16 El Niño-related drought on cocoa agroforests in Bahia, Brazil". In: *PLoS ONE* 13.7 (2018), pp. 1–17. ISSN: 19326203. DOI: 10.1371/journal.pone.0200454.

[91] Gehrke-Vélez, M, Castillo-Vera, A, Ruiz-Bello, C, Moreno-Martinez, J L, and Moreno-Basurto, G. "Delayed self-incompatibility causes morphological alterations and crop reduction in 'Ataúlfo' mango (Mangifera indica L.)" In: *New Zealand Journal of Crop and Horticultural Science* 40.4 (2012), pp. 215–227. ISSN: 01140671. DOI: 10.1080/01140671.2011.632423. URL: https://doi.org/10.1080/01140671.2011.632423.

[92] Giesen, Nick van de, Hut, Rolf, and Selker, John. "The Trans-African Hydro-Meteorological Observatory (TAHMO)". In: *Wiley Interdisciplinary Reviews: Water* (2014). DOI: 10.1002/wat2.1034.

[93] GOMES, A. R.SENA, KOZLOWSKI, T. T., and REICH, P. B. "Some Physiological Responses of Theobroma Cacao Var. Catongo Seedlings To Air Humidity". In: *New Phytologist* 107.3 (1987), pp. 591–602. ISSN: 14698137. DOI: 10.1111/j.1469-8137.1987.tb02929.x.

[94] Goubitz, Shirrinka, Werger, Marinus J.A., Shmida, Avi, and Ne'eman, Gidi. "Cone abortion in Pinus halepensis: The role of pollen quantity, tree size and cone location". In: *Oikos* 97.1 (2002), pp. 125–133. ISSN: 00301299. DOI: 10.1034/j.1600-0706.2002.970113.x.

[95] Goudriaan, Jan and Van Laar, H. H. "Modelling Potential Crop Growth Processes". In: *elsevier science Ltd* 74.4 (1994), p. 238. ISSN: 1750-8460. DOI: 10.1007/978-94-011-0750-1. URL: http://www.ncbi.nlm.nih.gov/pubmed/23589645.

[96] Gouin, Henri. "The watering of tall trees - Embolization and recovery". In: *Journal of Theoretical Biology* 369 (2015), pp. 42–50. ISSN: 10958541. DOI: 10.1016/j.jtbi.2015.01.009.

[97] Greenwell, B, Boehmke, B, Cunningham, J, and GBM, Developers. "gbm: generalized boosted regression models. R package version 2.1. 5". In: *Available at R Core Team https://CRAN. R-project. org/package= gbm [Verified 16 June 2018]* (2018).

[98] Groeneveld, Janna H., Tscharntke, Teja, Moser, Gerald, and Clough, Yann. "Experimental evidence for stronger cacao yield limitation by pollination than by plant resources". In: *Perspectives in Plant Ecology, Evolution and Systematics* 12.3 (2010), pp. 183–191. ISSN: 14338319. DOI: 10.1016/j.ppees.2010.02.005. URL: http://dx.doi.org/10.1016/j.ppees.2010.02.005.

[99] Güney, Aylin. "Sapwood Area Related to Tree Size, Tree Age, and Leaf Area Index in Cedrus libani". In: *Bilge International Journal of Science and Technology Research* 2.1 (2018), pp. 83–91. ISSN: 2587-0742. DOI: 10.30516/bilgesci.389609.

[100] Gutschick, Vincent P. *Photosynthesis, Growth Rate, and Biomass Allocation*. Woodhead Publishing Limited, 1997, pp. 39–78. DOI: 10.1016/b978-012378260-1/50003-8. URL: http://dx.doi.org/10.1016/B978-012378260-1/50003-8.

[101] Hadley, P, Acheampong, K, Pearson, S, End, MJE, and Weis, E. "The effects of environmental factors on cherelle wilt in cocoa grown in controlled environments". In: *Proceedings of the 11th International Cocoa Research Conference, Yamaussoukro, Co^te^ d'Ivoire*. 1994, pp. 661–666.

[102] Hagan, J K, Bosompem, M, and Adjei, I A. "The productive performance of local chickens in three ecological zones of Ghana." In: *Journal of Agricultural and Biological Science* 8.1 (2013), pp. 51–56. ISSN: 1990-6145.

[103] Handley, L R. "The effects of climate change on the reproductive development of Theobroma cacao L." In: September (2016), p. 235. URL: http://centaur.reading.ac.uk/72142/.

[104] Hanssens, Jochen, De Swaef, Tom, Nadezhdina, Nadezhda, and Steppe, Kathy. "Measurement of sap flow dynamics through the tomato peduncle using a non-invasive sensor based on the heat field deformation method". In: *IX International Workshop on Sap Flow 991*. 2013, pp. 409–416.

[105] Hendricks, David W and Hansen, Vaughn E. "Mechanics of Evapo-Transpiration". In: *Transactions of the American Society of Civil Engineers* 128.3 (1963), pp. 422–437.

[106] Hersbach, Hans, Bell, Bill, Berrisford, Paul, Hirahara, Shoji, Horányi, András, Muñoz-Sabater, Joaquín, Nicolas, Julien, Peubey, Carole, Radu, Raluca, Schepers, Dinand, et al. "The ERA5 global reanalysis". In: *Quarterly Journal of the Royal Meteorological Society* 146.730 (2020), pp. 1999–2049.

[107] Hijmans, Robert J, Phillips, Steven, Leathwick, John, Elith, Jane, and Hijmans, Maintainer Robert J. "Package 'dismo'". In: (2017).

[108] Hochberg, Uri, Rockwell, Fulton E., Holbrook, N. Michele, and Cochard, Hervé. "Iso/Anisohydry: A Plant–Environment Interaction Rather Than a Simple Hydraulic Trait". In: *Trends in Plant Science* 23.2 (2018), pp. 112–120. ISSN: 13601385. DOI: 10.1016/j.tplants.2017.11.002. URL: http://dx.doi.org/10.1016/j.tplants.2017.11.002.

[109] Hodges, Harry F., Whisler, Frank D., Bridges, Susan M., Reddy, K. Raja, and McKinion, James M. "Simulation in Crop Management: GOSSYM/COMAX". In: *Agricultural Systems modeting and Simulation*. 2018. DOI: 10.1201/9781482269765-8.

[110] Humphries, E. C. "Wilt of cacao fruits (theobroma cacao): I. An Investigation into the Causes". In: *Annals of Botany* 7.25 (1943). ISSN: 10958290. DOI: 10.1093/oxfordjournals.aob.a088552.

[111] Humphries, E. C. "Wilt of Cacao Fruits (Theobroma Cacao): III. Changes in Mineral Content during Development". In: *Annals of Botany* 8.29 (1944), pp. 57–70. ISSN: 03057364, 10958290. URL: http://www.jstor.org/stable/42908451.

[112] Hutcheon, W V, Smith, R W, and Asomaning, E J A. "Effect of Irrigation on Yield and Physiological Behavior of Mature Amelonado Cocoa in Ghana". In: *Tropical Agriculture* 50.4 (1973), pp. 261–272.

[113] Iizumi, Toshichika, Sakuma, Hirofumi, Yokozawa, Masayuki, Luo, Jing Jia, Challinor, Andrew J., Brown, Molly E., Sakurai, Gen, and Yamagata, Toshio. "Prediction of seasonal climate-induced variations in global food production". In: *Nature Climate Change* (2013). ISSN: 1758678X. DOI: 10.1038/nclimate1945.

[114] Ilyas, Muhammad, Nisar, Mohammad, Khan, Nadeem, Hazrat, Ali, Khan, Aamir Hamid, Hayat, Kashif, Fahad, Shah, Khan, Aziz, and Ullah, Abid. "Drought Tolerance Strategies in Plants: A Mechanistic Approach". In: *Journal of Plant Growth Regulation* 40.3 (2021), pp. 926–944. ISSN: 14358107. DOI: 10.1007/s00344-020-10174-5. URL: https://doi.org/10.1007/s00344-020-10174-5.

[115] (IPCC), Intergovernmental Panel On Climate Change. "The IPCC'S Fifth Assessment Report; What's in it for Africa". In: *Change* (2014). ISSN: 14764687.

[116] J. Berni, Jose A., Zarco-Tejada, Pablo, Sepulcre-Canto, Guadalupe, Fereres, E., and Villalobos, Francisco. "Mapping canopy conductance and CWSI in olive orchards using high resolution thermal remote sensing imagery". In: *Remote Sensing of Environment* 113 (Nov. 2009), pp. 2380–2388. DOI: 10.1016/j.rse.2009.06.018.

[117] Jenik, J. and Hall, J. B. "The Ecological Effects of the Harmattan Wind in the Djebobo Massif (Togo Mountains, Ghana)". In: *The Journal of Ecology* (1966). ISSN: 00220477. DOI: 10.2307/2257816.

[118] Jiménez-Pérez, Alfredo, Cach-Pérez, Manuel J., Valdez-Hernández, Mirna, and Rosa-Manzano, Edilia de la. "Effect of canopy management in the water status of cacao (Theobroma cacao) and the microclimate within the crop area". In: *Botanical Sciences* 97.4 (2019), pp. 701–710. ISSN: 20074476. DOI: 10.17129/botsci.2256.

[119] Jullien, Alexandra, Mathieu, Amélie, Allirand, Jean-Michel, Pinet, Amélie, De Reffye, Philippe, Cournède, Paul-Henry, and Ney, Bertrand. "Characterization of the interactions between architecture and source–sink relationships in winter oilseed rape (Brassica napus) using the GreenLab model". In: *Annals of botany* 107.5 (2011), pp. 765–779.

[120] Kaiser, Hartmut. "The relation between stomatal aperture and gas exchange under consideration of pore geometry and diffusional resistance in the mesophyll". In: *Plant, cell & environment* 32.8 (2009), pp. 1091–1098.

[121] Kath, Jarrod, Mittahalli Byrareddy, Vivekananda, Mushtaq, Shahbaz, Craparo, Alessandro, and Porcel, Mario. "Temperature and rainfall impacts on robusta coffee bean characteristics". In: *Climate Risk Management* (2021). ISSN: 22120963. DOI: 10.1016/j.crm.2021.100281.

[122] Kellner, Juliane, Multsch, Sebastian, Houska, Tobias, Kraft, Philipp, Müller, Christoph, and Breuer, Lutz. "A coupled hydrological-plant growth model for simulating the effect of elevated CO2 on a temperate grassland". In: *Agricultural and Forest Meteorology* 246 (2017), pp. 42–50.

[123] Kim, Jae H and Choi, In. "Choosing the level of significance: A decision-theoretic approach". In: *Abacus* 57.1 (2021), pp. 27–71.

[124] Köhler, Michael, Hanf, Andrea, Barus, Henry, Hendrayanto, and Hölscher, Dirk. "Cacao trees under different shade tree shelter: Effects on water use". In: *Agroforestry Systems* 88.1 (2014), pp. 63–73. ISSN: 01674366. DOI: 10.1007/s10457-013-9656-3.

[125] Kotowska, Martyna M., Hertel, Dietrich, Rajab, Yasmin Abou, Barus, Henry, and Schuldt, Bernhard. "Patterns in hydraulic architecture from roots to branches in six tropical tree species from cacao agroforestry and their relation to wood density and stem growth". In: *Frontiers in Plant Science* 6.March (2015), pp. 1–16. ISSN: 1664-462X. DOI: 10.3389/fpls.2015.00191.

[126] Kumar, R., Sarawgi, A. K., Ramos, C., Amarante, S. T., Ismail, A. M., and Wade, L. J. "Partitioning of dry matter during drought stress in rainfed lowland rice". In: *Field Crops Research* 98.1 (2006), pp. 1–11. ISSN: 0378-4290. DOI: 10.1016/J.FCR.2005.09.015.

[127] Laar, H. H. van, Goudriaan, J., and Van Keulen, H. "SUCROS97: Simulation of crop growth for potential and water-limited production situations". In: *Quantitative approaches in systems analysis* (1997).

[128] LACHENAUD, Philippe. *Facteurs De La Fructification Chez Le Cacaoyer (Theobroma Cacao L.)* 1991.

[129] Läderach, P., Martinez-Valle, A., Schroth, G., and Castro, N. "Predicting the future climatic suitability for cocoa farming of the world's leading producer countries, Ghana and Côte d'Ivoire". In: *Climatic Change* 119.3-4 (2013), pp. 841–854. ISSN: 01650009. DOI: 10.1007/s10584-013-0774-8.

[130] Lafore, J.-P., Flamant, C., Guichard, F., Parker, D. J., Bouniol, D., Fink, a. H., Giraud, V., Gosset, M., Hall, N., Höller, H., Jones, S. C., Protat, A., Roca, R., Roux, F., Saïd, F., and Thorncroft, C. "Progress in understanding of weather systems in West Africa". In: *Atmospheric Science Letters* 12.1 (2011), pp. 7–12. ISSN: 1530261X. DOI: 10.1002/asl.335. URL: http://doi.wiley.com/10.1002/asl.335.

[131] Lahive, F., Hadley, P., and Daymond, A. J. "The impact of elevated CO2and water deficit stress on growth and photosynthesis of juvenile cacao (Theobroma cacao L.)" In: *Photosynthetica* 56.3 (2018), pp. 911–920. ISSN: 03003604. DOI: 10.1007/s11099-017-0743-y.

[132] Lahive, Fiona, Hadley, Paul, and Daymond, Andrew J. "The physiological responses of cacao to the environment and the implications for climate change resilience . A review". In: *Agronomy for Sustainable Development* 39.5 (2019), pp. 1–22. ISSN: 1774-0746. DOI: 10.1007/s13593-018-0552-0.

[133] Lauri, Pierre Éric, Barigah, Têtè Sévérien, Lopez, Gerardo, Martinez, Sébastien, Losciale, Pasquale, Zibordi, Marco, Manfrini, Luigi, Corelli-Grappadelli, Luca, Costes, Evelyne, and Regnard, Jean Luc. "Genetic variability and phenotypic plasticity of apple morphological responses to soil water restriction in relation with leaf functions and stem xylem conductivity". In: *Trees - Structure and Function* 30.5 (2016), pp. 1893–1908. ISSN: 09311890. DOI: 10.1007/s00468-016-1408-3.

[134] Leandro-Muñoz, Mariela E, Tixier, Philippe, Germon, Amandine, Rakotobe, Veromanitra, Phillips-Mora, Wilbert, Maximova, Siela, and Avelino, Jacques. "Effects of microclimatic variables on the symptoms and signs onset of Moniliophthora roreri, causal agent of Moniliophthora pod rot in cacao". In: *PloS one* 12.10 (2017), e0184638.

[135] Lennon, Adrian M, Lewis, Vernessa R, Farrell, Aidan D, and Umaharan, Pathmanathan. "Photochemical responses to light in sun and shade leaves of Theobroma cacao L. (West African Amelonado)". In: *Scientia Horticulturae* 276 (2021), p. 109747. ISSN: 03044238. DOI: 10.1016/j.scienta.2020.109747. URL: https://doi.org/10.1016/j.scienta.2020.109747.

[136] Lenth, Russel V. *Package 'emmeans'*. Tech. rep. 2021.

[137] Limpus, Sarah. "Isohydric and anisohydric characterisation of vegetable crops: The classification of vegetables by their physiological responses to water stress". In: (2009).

[138] Long, S. P. and Bernacchi, C. J. "Gas exchange measurements, what can they tell us about the underlying limitations to photosynthesis? Procedures and sources of error". In: *Journal of Experimental Botany* 54.392 (2003), pp. 2393–2401. ISSN: 00220957. DOI: 10.1093/jxb/erg262.

[139] López-López, Rutilo, Ojeda-Bustamante, Waldo, López Andrade, Alejandro P., and Catalán-Valencia, Ernesto A. "Heat Pulse Method and Sap Flow for Measuring Transpiration in Cacao". In: *Revista Chapingo Serie Zonas Áridas* XII.2 (2013), pp. 85–96. ISSN: 2007526X. DOI: 10.5154/r.rchsza.2012.06.023. URL: http://www.chapingo.mx/revistas/zonas_aridas/contenido.php?id_articulo=1555?id_revistas=8.

[140] Lubczynski, Maciek W, Chavarro-Rincon, Diana C, and Rossiter, David G. "Conductive sapwood area prediction from stem and canopy areas—allometric equations of Kalahari trees, Botswana". In: *Ecohydrology* 10.6 (2017). ISSN: 19360592. DOI: 10.1002/eco.1856. URL: https://doi.org/10.1002/eco.1856.

[141] Machado, Renan, Loram-Lourenço, Lucas, Farnese, Fernanda Santos, Alves, Rauander Douglas Ferreira Barros, Sousa, Letícia Ferreira de, Silva, Fabiano Guimarães, Filho, Sebastião Carvalho Vasconcelos, Torres-Ruiz, José M., Cochard, Hervé, and Menezes-Silva, Paulo Eduardo. "Where do leaf water leaks come from? Trade-offs underlying the variability in minimum conductance across tropical savanna species with contrasting growth strategies". In: *New Phytologist* (2020), pp. 0–3. ISSN: 0028-646X. DOI: 10.1111/nph.16941.

[142] Malhi, Yadvinder and Wright, James. "Spatial patterns and recent trends in the climate of tropical rainforest regions". In: *Philosophical Transactions of the Royal Society B: Biological Sciences*. 2004. DOI: 10.1098/rstb.2003.1433.

[143] Marcelis, L F M and Heuvelink, E. "Concepts of modelling carbon allocation among plant organs". In: *Frontis* 22 (2007), pp. 103–111. DOI: 10.1016/S0167-8892(01)80004-X. URL: http://library.wur.nl/ojs/index.php/frontis/issue/view/241.

[144] Marcelis, L. F.M., Heuvelink, E., Baan Hofman-Eijer, L. R., Den Bakker, J., and Xue, L. B. "Flower and fruit abortion in sweet pepper in relation to source and sink strength". In: *Journal of Experimental Botany* 55.406 (2004), pp. 2261–2268. ISSN: 00220957. DOI: 10.1093/jxb/erh245.

[145] Marin, Fábio R., Ribeiro, Rafael V., and Marchiori, Paulo E.R. "How can crop modeling and plant physiology help to understand the plant responses to climate change? A case study with sugarcane". In: *Theoretical and Experimental Plant Physiology* 26.1 (2014), pp. 49–63. ISSN: 21970025. DOI: 10.1007/s40626-014-0006-2.

[146] Marshall, D. C. "Measurement of Sap Flow in Conifers by Heat Transport." In: *Plant Physiology* (1958). ISSN: 0032-0889. DOI: 10.1104/pp.33.6.385.

[147] Martin, Guillaume, Duru, Michel, Schellberg, Jürgen, and Ewert, Frank. "Simulations of plant productivity are affected by modelling approaches of farm management". In: *Agricultural Systems* 109 (2012), pp. 25–34.

[148] Martin-StPaul, Nicolas, Delzon, Sylvain, and Cochard, Hervé. "Plant resistance to drought depends on timely stomatal closure". In: *Ecology Letters* 20.11 (2017), pp. 1437–1447. ISSN: 14610248. DOI: 10.1111/ele.12851.

[149] Martínez-Fuentes, A., Mesejo, C., Muñoz-Fambuena, N., Reig, C., González-Mas, M. C., Iglesias, D. J., Primo-Millo, E., and Agustí, M. "Fruit load restricts the flowering promotion effect of paclobutrazol in alternate bearing Citrus spp." In: *Scientia Horticulturae* 151 (2013), pp. 122–127. ISSN: 03044238. DOI: 10.1016/j.scienta.2012.12.014.

[150] McCully, M. E., Huang, C. X., and Ling, L. E.C. "Daily embolism and refilling of xylem vessels in the roots of field-grown maize". In: *New Phytologist* 138.2 (1998), pp. 327–342. ISSN: 0028646X. DOI: 10.1046/j.1469-8137.1998.00101.x.

[151] Mckelvie, A. D. "Cherelle wilt of cacao: I. Pod development and its relation to wilt". In: *Journal of Experimental Botany* 7.2 (1956), pp. 252–263. ISSN: 00220957. DOI: 10.1093/jxb/7.2.252. URL: https://academic.oup.com/jxb/article-lookup/doi/10.1093/jxb/7.2.252.

[152] Mckelvie, A. D. "Cherelle wilt of cacao: II. Wilt in relation to yield". In: *Journal of Experimental Botany* 11.3 (1960), pp. 413–424. ISSN: 00220957. DOI: 10.1093/jxb/11.3.413.

[153] Medlyn, Belinda E., Duursma, Remko A., Eamus, Derek, Ellsworth, David S., Prentice, I. Colin, Barton, Craig V.M., Crous, Kristine Y., De Angelis, Paolo, Freeman, Michael, and Wingate, Lisa. "Reconciling the optimal and empirical approaches to modelling stomatal conductance". In: *Global Change Biology* 17.6 (2011), pp. 2134–2144. ISSN: 13541013. DOI: 10.1111/j.1365-2486.2010.02375.x.

[154] Meinzer, Frederick C. "Functional convergence in plant responses to the environment". In: *Oecologia* 134.1 (2003), pp. 1–11. ISSN: 00298549. DOI: 10.1007/s00442-002-1088-0.

[155] Melnick, Rachel L. "Cherelle wilt of cacao: A physiological condition". In: *Cacao Diseases: A History of Old Enemies and New Encounters*. 2016, pp. 483–499. ISBN: 9783319247892. DOI: 10.1007/978-3-319-24789-2_15. eprint: 1011.1669.

[156] Melnick, Rachel L., Strem, Mary D., Crozier, Jayne, Sicher, Richard C., and Bailey, Bryan A. "Molecular and metabolic changes of cherelle wilt of cacao and its effect on Moniliophthora roreri". In: *Physiological and Molecular Plant Pathology* 84.1 (2013), pp. 153–162. ISSN: 08855765. DOI: 10.1016/j.pmpp.2013.09.004. URL: http://dx.doi.org/10.1016/j.pmpp.2013.09.004.

[157] Miranda Jiménez, Carlos and Royo Díaz, J. Bernardo. "Fruit distribution and early thinning intensity influence fruit quality and productivity of peach and nectarine trees". In: *Journal of the American Society for Horticultural Science* (2002). ISSN: 00031062. DOI: 10.21273/jashs.127.6.892.

[158] Mishra, Ashok K. and Singh, Vijay P. *A review of drought concepts*. 2010. DOI: 10.1016/j.jhydrol.2010.07.012.

[159] Mittler, Ron, Vanderauwera, Sandy, Suzuki, Nobuhiro, Miller, Gad, Tognetti, Vanesa B., Vandepoele, Klaas, Gollery, Marty, Shulaev, Vladimir, and Van Breusegem, Frank. "ROS signaling: The new wave?" In: *Trends in Plant Science* 16.6 (2011), pp. 300–309. ISSN: 13601385. DOI: 10.1016/j.tplants.2011.03.007. URL: http://dx.doi.org/10.1016/j.tplants.2011.03.007.

[160] Miyaji, Ken Ichi, Da Silva, Walny S., and De Alvim, Paulo T. "Longevity of leaves of a tropical tree, Theobroma cacao, grown under shading, in relation to position within the canopy and time of emergence". In: *New Phytologist* (1997). ISSN: 0028646X. DOI: 10.1046/j.1469-8137.1997.00667.x.

[161] Miyaji, Ken Ichi, Da Silva, Walny S., and De Alvim, Paulo T. "Productivity of leaves of a tropical tree, Theobroma cacao, grown under shading, in relation to leaf age and light conditions within the canopy". In: *New Phytologist* (1997). ISSN: 0028646X. DOI: 10.1046/j.1469-8137.1997.00841.x.

[162] Moser, G., Leuschner, C., Hertel, D., Hölscher, D., Köhler, M., Leitner, D., Michalzik, B., Prihastanti, E., Tjitrosemito, S., and Schwendenmann, L. "Response of cocoa trees (Theobroma cacao) to a 13-month desiccation period in Sulawesi, Indonesia". In: *Agroforestry Systems* 79.2 (2010), pp. 171–187. ISSN: 01674366. DOI: 10.1007/s10457-010-9303-1.

[163] Motamayor, J. C., Risterucci, A. M., Lopez, P. A., Ortiz, C. F., Moreno, A., and Lanaud, C. "Cacao domestication I: The origin of the cacao cultivated by the Mayas". In: *Heredity* (2002). ISSN: 0018067X. DOI: 10.1038/sj.hdy.6800156.

[164] MUNIZ, JOEL AUGUSTO, NASCIMENTO, MICHERLANIA DA SILVA, FERNANDES, TALES JESUS, MUNIZ, JOEL AUGUSTO, NASCIMENTO, MICHERLANIA DA SILVA, and FERNANDES, TALES JESUS. "Nonlinear Models for Description of Cacao Fruit Growth With Assumption Violations". In: *Revista Caatinga* 30.1 (2017), pp. 250–257. ISSN: 1983-2125. DOI: 10.1590/1983-21252017v30n128rc.

[165] Muñoz, F. and Beer, J. "Fine root dynamics of shaded cacao plantations in Costa Rica". In: *Agroforestry Systems* 51.2 (2001), pp. 119–130. ISSN: 01674366. DOI: 10.1023/A:1010651203815.

[166] Murtagh, Fionn and Legendre, Pierre. "Ward's Hierarchical Agglomerative Clustering Method: Which Algorithms Implement Ward's Criterion?" In: *Journal of Classification* 31.3 (2014), pp. 274–295. ISSN: 1432-1343. DOI: 10.1007/s00357-014-9161-z.

[167] Najihah, Tuan, Ibrahim, Mohd, Hadley, Paul, and Daymond, Andrew. "The Effect of Different Day and Night Temperatures on the Growth and Physiology of Theobroma cacao under Controlled Environment Condition". In: *Annual Research & Review in Biology* 27.2 (2018), pp. 1–15. ISSN: 2347-565X. DOI: 10.9734/arrb/2018/40413.

[168] Nakamura-Yamaguchi, Ayako, Kitahata, Nobutaka, Nishitani, Chikako, Takada, Norio, Terakami, Shingo, Sawamura, Yutaka, Matsuyama, Tomoki, Asami, Tadao, Nakano, Takeshi, Saito, Toshihiro, and Yamamoto, Toshiya. "Pattern and trigger of fruit self-thinning in Japanese pears". In: *Horticulture Journal* 89.4 (2020), pp. 367–374. ISSN: 21890110. DOI: 10.2503/hortj.UTD-177.

[169] Nakicenovic, Nebojsa, Alcamo, Joseph, Grubler, A, Riahi, K, Roehrl, RA, Rogner, H-H, and Victor, N. *Special report on emissions scenarios (SRES), a special report of Working Group III of the intergovernmental panel on climate change*. Cambridge University Press, 2000.

[170] Nichols, R. "Studies of Fruit Development of Cacao (Theobroma cacao) in Relation to Cherelle Wilt : I . Development of the pericarp Author (s): R . NICHOLS Source : Annals of Botany , New Series , Vol . 28 , No . 112 (October 1964), pp . 619-635 Published by : O". In: 28.112 (1964), pp. 619–635.

[171] Nichols, R. "Studies of Fruit Development of Cacao (Theobroma Cacao) in Relation to Cherelle Wilt .2. Auxins and Development of Seeds". In: *Annals of Botany* 29.114 (1965), p. 181.

[172] Nichols, R. "Xylem occlusions in the fruit of cacao (Theobroma cacao) and their relation to cherelle wilt". In: *Annals of Botany* 25.4 (1961), pp. 463–475. ISSN: 03057364. DOI: 10.1093/oxfordjournals.aob.a083765.

[173] Niemenak, N., Cilas, C., Rohsius, C., Bleiholder, H., Meier, U., and Lieberei, R. "Phenological growth stages of cacao plants (Theobroma sp.): Codification and description according to the BBCH scale". In: *Annals of Applied Biology* 156.1 (2010), pp. 13–24. ISSN: 00034746. DOI: 10.1111/j.1744-7348.2009.00356.x.

[174] Niether, Wiebke, Schneidewind, Ulf, Armengot, Laura, Adamtey, Noah, Schneider, Monika, and Gerold, Gerhard. "Spatial-temporal soil moisture dynamics under different cocoa production systems". In: *Catena* 158 (2017), pp. 340–349. ISSN: 03418162. DOI: 10.1016/j.catena.2017.07.011.

[175] Niether, Wiebke, Smit, Inga, Armengot, Laura, Schneider, Monika, Gerold, Gerhard, and Pawelzik, Elke. "Environmental Growing Conditions in Five Production Systems Induce Stress Response and Affect Chemical Composition of Cocoa (Theobroma cacao L.) Beans". In: *Journal of Agricultural and Food Chemistry* 65.47 (2017), pp. 10165–10173. ISSN: 15205118. DOI: 10.1021/acs.jafc.7b04490.

[176] Nyakudya, Innocent Wadzanayi and Stroosnijder, Leo. "Effect of rooting depth, plant density and planting date on maize (Zea mays L.) yield and water use efficiency in semi-arid Zimbabwe: Modelling with AquaCrop". In: *Agricultural Water Management* 146 (2014), pp. 280–296.

[177] Nygren, Pekka, Leblanc, Humberto A., Lu, Miaoer, and Gómez Luciano, Cristino A. "Distribution of coarse and fine roots of Theobroma cacao and shade tree Inga edulis in a cocoa plantation". In: *Annals of Forest Science* 70.3 (2013), pp. 229–239. ISSN: 12864560. DOI: 10.1007/s13595-012-0250-z.

[178] Oguntunde, Philip G. "Whole-plant water use and canopy conductance of cassava under iimited available soil water and varying evaporative demand". In: *Plant and Soil* 278.1-2 (2005), pp. 371–383. ISSN: 0032079X. DOI: 10.1007/s11104-005-0375-z.

[179] Oliver, Melvin J., Wood, Andrew J., and O'Mahony, Patrick. "'To dryness and beyond' - Preparation for the dried state and rehydration in vegetative desiccation-tolerant plants". In: *Plant Growth Regulation* 24.3 (1998), pp. 193–201. ISSN: 01676903. DOI: 10.1023/A:1005863015130.

[180] Organization, International Cocoa. *Quarterly Bulletin of Cocoa Statistics for the Cocoa Year, Volume XLVI, Cocoa Year 2019/20.* 2020.

[181] Othmani, Ahmed, Jemni, Monia, Kadri, Karim, Amel, Sellemi, Artés, Francisco, and Al-Khayri, Jameel M. *Preharvest Fruit Drop of Date Palm (Phoenix dactylifera L.) Cv. Deglet Nour at Kimri Stage: Development, Physico-chemical Characterization, and Functional Properties*. 2020. DOI: 10.1080/15538362.2019.1651241.

[182] Padi, Michael. "Weather Transition Periods in Ghana". In: *Journal of Climatology & Weather Forecasting* 05.02 (2017). DOI: 10.4172/2332-2594.1000211.

[183] Palosuo, Taru, Kersebaum, Kurt Christian, Angulo, Carlos, Hlavinka, Petr, Moriondo, Marco, Olesen, Jørgen E, Patil, Ravi H, Ruget, Françoise, Rumbaur, Christian, Takáč, Jozef, et al. "Simulation of winter wheat yield and its variability in different climates of Europe: A comparison of eight crop growth models". In: *European Journal of Agronomy* 35.3 (2011), pp. 103–114.

[184] Pickering, Nigel B., Jones, James W., and Boote, Kenneth J. "Adapting SOYGRO V5.42 for prediction under climate change conditions". In: *Climate Change and Agriculture: Analysis of Potential International Impacts*. 2015. ISBN: 9780891183259. DOI: 10.2134/asaspecpub59.c4.

[185] Poleuleng, Andi Besse, Agusta, Herdhata, Yahya, Sudirman, Wachjar, Ade, and Tjoa, Aiyen. "The allometric model to estimate biomass and carbon stock in top grafting young cacao plants". In: 26.4 (2020).

[186] Poorter, Hendrik, Niklas, Karl J, Reich, Peter B, Oleksyn, Jacek, Poot, Pieter, and Mommer, Liesje. "Biomass allocation to leaves, stems and roots: meta-analysis of interspecific variation and environmental control". In: *New Phytologist* 193.1 (2011), pp. 30–50. ISSN: 1469-8137. DOI: 10.1111/j.1469-8137.2011.03952.x. URL: http://www.ncbi.nlm.nih.gov/pubmed/22085245.

[187] Prabnakorn, Saowanit, Maskey, Shreedhar, Suryadi, F. X., and Fraiture, Charlotte de. "Rice yield in response to climate trends and drought index in the Mun River Basin, Thailand". In: *Science of the Total Environment* (2018). ISSN: 18791026. DOI: 10.1016/j.scitotenv.2017.11.136.

[188] Quiñonez-Piñón, M. Rebeca and Valeo, Caterina. "Allometry of sapwood depth in five boreal trees". In: *Forests* 8.11 (2017). ISSN: 19994907. DOI: 10.3390/f8110457. URL: www.mdpi.com/journal/forests.

[189] R Core Team. *R: A Language and Environment for Statistical Computing*. R Foundation for Statistical Computing. Vienna, Austria, 2019. URL: https://www.R-project.org/.

[190] Rada, F, Jaimez, R E, García-Nuñez, C, Azócar, a, and Ramírez, M E. "Relaciones hídricas e intercambio de gases en Theobroma cacao var. Guasare bajo períodos de deficit hídrico". In: *Rev. Fac. Agron* 22 (2005), p. 120.

[191] Rajab, Yasmin Abou, Hölscher, Dirk, Leuschner, Christoph, Barus, Henry, Tjoa, Aiyen, and Hertel, Dietrich. "Effects of shade tree cover and diversity on root system structure and dynamics in cacao agroforests: The role of root competition and space partitioning". In: (2017). DOI: 10.1007/s11104-017-3456-x. URL: https://doi.org/10.1007/s11104-017-3456-x.

[192] Rasband, W.S. *ImageJ, U.S. National Institutes of Health, Bethesda, Maryland, USA*. 2014.

[193] Rauff, Kazeem O, Bello, Rasaq, et al. "A review of crop growth simulation models as tools for agricultural meteorology". In: *Agricultural Sciences* 6.09 (2015), p. 1098.

[194] Reffye, Philippe de, Hu, Baogang, Kang, Mengzhen, Letort, Véronique, and Jaeger, Marc. "Two decades of research with the GreenLab model in Agronomy". In: *Annals of botany* 127.3 (2021), pp. 281–295.

[195] Ribeyre, F, Cilas, C, Motisi, N, Reffye, Ph, and Others. "Influence of pollination on the number of beans per cacao pod." In: *International Symposium on Cocoa Research (ISCR), Lima, Peru, 13-17 November 2017*. Vol. 87. 1,2. International Cocoa Organization (ICCO). 2018, pp. 149–200.

[196] Rosenzweig, Cynthia, Elliott, Joshua, Deryng, Delphine, Ruane, Alex C., Müller, Christoph, Arneth, Almut, Boote, Kenneth J., Folberth, Christian, Glotter, Michael, Khabarov, Nikolay, Neumann, Kathleen, Piontek, Franziska, Pugh, Thomas A. M., Schmid, Erwin, Stehfest, Elke, Yang, Hong, and Jones, James W. "Assessing agricultural risks of climate change in the 21st century in a global gridded crop model intercomparison". In: *Proceedings of the National Academy of Sciences* 111.9 (2014), pp. 3268–3273. ISSN: 0027-8424. DOI: 10.1073/pnas.1222463110. URL: http://www.pnas.org/lookup/doi/10.1073/pnas.1222463110.

[197] Ruf, François and Varlet, Frédéric. "The myth of zero deforestation cocoa in Côte d'Ivoire". In: (2017).

[198] Sadeghi, Morteza, Tabatabaeenejad, Alireza, Tuller, Markus, Moghaddam, Mahta, and Jones, Scott B. "Advancing NASA's AirMOSS p-band radar root zone soil moisture retrieval algorithm via incorporation of richards' equation". In: *Remote Sensing* (2017). ISSN: 20724292. DOI: 10.3390/rs9010017.

[199] Salazar, Juan Carlos Suárez, Melgarejo, Luz Marina, Casanoves, Fernando, Di Rienzo, Julio A., DaMatta, Fabio M., and Armas, Cristina. "Photosynthesis limitations in cacao leaves under different agroforestry systems in the Colombian Amazon". In: *PLoS ONE* 13.11 (2018), pp. 1–13. ISSN: 19326203. DOI: 10.1371/journal.pone.0206149.

[200] Sale, P.J.M. "Growth, flowering and fruiting of cacao under controlled soil moisture conditions". In: *Journal of Horticultural Science* 45.2 (1970), pp. 99–118. ISSN: 0022-1589. DOI: 10.1080/00221589.1970.11514337. URL: http://www.tandfonline.com/doi/full/10.1080/00221589.1970.11514337.

[201] Salmon, Yann, Dietrich, Lars, Sevanto, Sanna, Hölttä, Teemu, Dannoura, Masako, and Epron, Daniel. "Drought impacts on tree phloem: From cell-level responses to ecological significance". In: *Tree Physiology* 39.2 (2018), pp. 173–191. ISSN: 17584469. DOI: 10.1093/treephys/tpy153.

[202] Santos, Ronaldo Carvalho, Pires, José Luiz, and Correa, Ronan Xavier. "Morphological characterization of leaf, flower, fruit and seed traits among Brazilian Theobroma L. species". In: *Genetic Resources and Crop Evolution* 59.3 (2012), pp. 327–345. ISSN: 09259864. DOI: 10.1007/s10722-011-9685-6.

[203] Sarawa, Halim, Dirvamena Boer, and Asriningsih. "PHYSICAL QUALITY AND PRODUCTIVITY OF COCOA BEAN (Theobroma cacao L.) BASED ON CANOPY POSITION AND PLANT AGE". In: *EPRA International Journal of Multidisciplinary Research (IJMR)* 2 (2021), pp. 161–168. DOI: 10.36713/epra8091. URL: https://doi.org/10.36713/epra8091.

[204] Savage, Jessica A, Clearwater, Michael J, Haines, Dustin F, Klein, Tamir, Mencuccini, Maurizio, Sevanto, Sanna, Turgeon, Robert, and Zhang, Cankui. "Allocation, stress tolerance and carbon transport in plants: how does phloem physiology affect plant ecology?" In: (2015). DOI: 10.1111/pce.12602.

[205] Schall, Peter, Lödige, Christina, Beck, Michael, and Ammer, Christian. "Biomass allocation to roots and shoots is more sensitive to shade and drought in European beech than in Norway spruce seedlings". In: *Forest Ecology and Management* 266 (2012), pp. 246–253.

[206] Schapire, Robert E. "The boosting approach to machine learning: An overview". In: *Nonlinear estimation and classification*. Springer, 2003, pp. 149–171.

[207] Schenk, H. Jochen, Jansen, Steven, and Hölttä, Teemu. "Positive pressure in xylem and its role in hydraulic function". In: *New Phytologist* 230.1 (2021), pp. 27–45. ISSN: 14698137. DOI: 10.1111/nph.17085.

[208] Schepanski, Kerstin, Heinold, Bernd, and Tegen, Ina. "Harmattan, Saharan heat low, and West African monsoon circulation: Modulations on the Saharan dust outflow towards the North Atlantic". In: *Atmospheric Chemistry and Physics* 17.17 (2017), pp. 10223–10243. ISSN: 16807324. DOI: 10.5194/acp-17-10223-2017.

[209] Schroth, Götz, Läderach, Peter, Martinez-Valle, Armando Isaac, Bunn, Christian, and Jassogne, Laurence. "Vulnerability to climate change of cocoa in West Africa: Patterns, opportunities and limits to adaptation". In: *Science of the Total Environment* 556 (2016), pp. 231–241. ISSN: 18791026. DOI: 10.1016/j.scitotenv.2016.03.024.

[210] Schwendenmann, Luitgard, Veldkamp, Edzo, Moser, Gerald, Hölscher, Dirk, Köhler, Michael, Clough, Yann, Anas, Iswandi, Djajakirana, Gunawan, Erasmi, Stefan, Hertel, Dietrich, Leitner, Daniela, Leuschner, Christoph, Michalzik, Beate, Propastin, Pavel, Tjoa, Aiyen, Tscharntke, Teja, and Straaten, Oliver van. "Effects of an experimental drought on the functioning of a cacao agroforestry system, Sulawesi, Indonesia". In: *Global Change Biology* (2010). ISSN: 13541013. DOI: 10.1111/j.1365-2486.2009.02034.x.

[211] Silva, Anderson Rodrigo da and Lima, Renato Paiva de. "Soilphysics: An R package to determine soil preconsolidation pressure". In: *Computers and Geosciences* (2015). ISSN: 00983004. DOI: 10.1016/j.cageo.2015.08.008.

[212] Silva, João Vasco and Giller, Ken E. *Grand challenges for the 21st century: What crop models can and can't (yet) do*. 2021. DOI: 10.1017/S0021859621000150.

[213] Stoffer, David S. and Bloomfield, Peter. "Fourier Analysis of Time Series: An Introduction". In: *Journal of the American Statistical Association* (2000). ISSN: 01621459. DOI: 10.2307/2669794.

[214] Suárez, Juan Carlos, Casanoves, Fernando, Bieng, Marie Ange Ngo, Melgarejo, Luz Marina, Di Rienzo, Julio A., and Armas, Cristina. "Prediction model for sap flow in cacao trees under different radiation intensities in the western Colombian Amazon". In: *Scientific Reports* 11.1 (2021), pp. 1–14. ISSN: 2045-2322. DOI: 10.1038/s41598-021-89876-z. URL: https://doi.org/10.1038/s41598-021-89876-z.

[215] Sulman, Benjamin N, Roman, D Tyler, Yi, Koong, Wang, Lixin, Phillips, Richard P, and Novick, Kimberly A. "High atmospheric demand for water can limit forest carbon uptake and transpiration as severely as dry soil". In: (2016). DOI: 10.1002/2016GL069416.

[216] Sultan, Benjamin and Gaetani, Marco. *Agriculture in West Africa in the twenty-first century: Climate change and impacts scenarios, and potential for adaptation*. 2016. DOI: 10.3389/fpls.2016.01262.

[217] Termansen, Mette, McClean, Colin J, and Preston, Christopher D. "The use of genetic algorithms and Bayesian classification to model species distributions". In: *Ecological modelling* 192.3-4 (2006), pp. 410–424.

[218] Thomas, Sean C. and Winner, William E. "A rotated ellipsoidal angle density function improves estimation of foliage inclination distributions in forest canopies". In: *Agricultural and Forest Meteorology* 100.1 (2000), pp. 19–24. ISSN: 01681923. DOI: 10.1016/S0168-1923(99)00089-1.

[219] Ting, Kai Ming. "Confusion Matrix". In: *Encyclopedia of Machine Learning and Data Mining*. Ed. by Sammut, Claude and Webb, Geoffrey I. Boston, MA: Springer US, 2017, pp. 260–260. ISBN: 978-1-4899-7687-1. DOI: 10.1007/978-1-4899-7687-1_50. URL: https://doi.org/10.1007/978-1-4899-7687-1_50.

[220] Tondoh, JérÔme Ebagnerin, Kouamé, François N.guessan, Martinez Guéi, Arnauth, Sey, Blandine, Wowo Koné, Armand, and Gnessougou, Noël. "Ecological changes induced by full-sun cocoa farming in CÔte d'Ivoire". In: *Global Ecology and Conservation* (2015). ISSN: 23519894. DOI: 10.1016/j.gecco.2015.02.007.

[221] Ullah, Abid, Sun, Heng, Yang, Xiyan, and Zhang, Xianlong. "Drought coping strategies in cotton: increased crop per drop". In: *Plant biotechnology journal* 15.3 (2017), pp. 271–284.

[222] Uthaiah, BC and Sulladmath, UV. "Effect of growth regulators on cherelle wilt in cacao, Theobroma cacao L." In: *Journal of Plantation Crops (India) v. 9 (1) p. 46-50* (1981).

[223] Uthaiah, BC and Sulladmath, UV. "The possible role of abscisic acid-like and other inhibitors in cherelle wilt of cocoa (Theobroma cacao L.)" In: *Journal of Plantation Crops (India) v. 14 (1) p. 57-64* (1986).

[224] Uthaiah, BC, Sulladmath, UV, et al. "Cytokinin-like substances and cherelle wilt in cacao (Theobroma cacao L." In: *Journal of Plantation Crops* 8.2 (1980), pp. 78–81.

[225] Vaast, Philippe and Somarriba, Eduardo. "Trade-offs between crop intensification and ecosystem services: the role of agroforestry in cocoa cultivation". In: *Agroforestry Systems* 88.6 (2014), pp. 947–956. ISSN: 15729680. DOI: 10.1007/s10457-014-9762-x.

[226] Valle, R. R., De Almeida, A.-A. F., and De O. Leite, R. M. "Energy costs of flowering, fruiting, and cherelle wilt in cacao". In: *Tree Physiology* 6.3 (1990), pp. 329–336. ISSN: 0829-318X. DOI: 10.1093/treephys/6.3.329. URL: https://academic.oup.com/treephys/article-lookup/doi/10.1093/treephys/6.3.329.

[227] Valle RR, Silva WS, and Miranda RAC. "Stomatal resistance and transpiration rates of shaded and unshaded cacao trees". In: *Rev. Theobroma* (1987).

[228] Valle RR, Silva WS, and Miranda RAC. "Stomatal resistance and transpiration rates of shaded and unshaded cacao trees". In: *Rev. Theobroma* (1987).

[229] Van Genuchten, M Th. "A closed-form equation for predicting the hydraulic conductivity of unsaturated soils". In: *Soil science society of America journal* 44.5 (1980), pp. 892–898.

[230] Van Ittersum, Martin K., Van Bussel, Lenny G.J., Wolf, Joost, Grassini, Patricio, Van Wart, Justin, Guilpart, Nicolas, Claessens, Lieven, De Groot, Hugo, Wiebe, Keith, Mason-D'Croz, Daniel, Yang, Haishun, Boogaard, Hendrik, Van Oort, Pepijn A.J., Van Loon, Marloes P., Saito, Kazuki, Adimo, Ochieng, Adjei-Nsiah, Samuel, Agali, Alhassane, Bala, Abdullahi, Chikowo, Regis, Kaizzi, Kayuki, Kouressy, Mamoutou, Makoi, Joachim H.J.R., Ouattara, Korodjouma, Tesfaye, Kindie, and Cassman, Kenneth G. "Can sub-Saharan Africa feed itself?" In: *Proceedings of the National Academy of Sciences of the United States of America* (2016). ISSN: 10916490. DOI: 10.1073/pnas.1610359113.

[231] Van Ittersum, M.K., Leffelaar, P.a., Keulen, H. Van, Kropff, M.J., Bastiaans, L., and Goudriaan, J. "On approaches and applications ofthe Wageningen crop models". In: *European Journal of Agronomy* 13 (2003), pp. 201–234.

[232] Van Keulen, H, De Vries, FWT Penning, and Drees, EM. "A summary model for crop growth". In: *Simulation of plant growth and crop production*. Pudoc, 1982, pp. 87–97.

[233] van Rij, Jacolien, Wieling, Martijn, Baayen, R. Harald, and van Rijn, Hedderik. *itsadug: Interpreting Time Series and Autocorrelated Data Using GAMMs*. R package version 2.3. 2017.

[234] Vandegehuchte, Maurits W., Steppe, Kathy, and Phillips, Nathan. "Improving sap flux density measurements by correctly determining thermal diffusivity, differentiating between bound and unbound water". In: *Tree Physiology* (2012). ISSN: 0829318X. DOI: 10.1093/treephys/tps034.

[235] Verhoef, A. and Egea, G. "Modeling plant transpiration under limited soil water: Comparison of different plant and soil hydraulic parameterizations and preliminary implications for their use in land surface models". In: *Agricultural and Forest Meteorology* 191 (2014), pp. 22–32. ISSN: 01681923. DOI: 10.1016/j.agrformet.2014.02.009.

[236] Vicente-Serrano, Sergio M., Beguería, Santiago, Lorenzo-Lacruz, Jorge, Camarero, Jesús Julio, López-Moreno, Juan I., Azorin-Molina, Cesar, Revuelto, Jesús, Morán-Tejeda, Enrique, and Sanchez-Lorenzo, Arturo. "Performance of drought indices for ecological, agricultural, and hydrological applications". In: *Earth Interactions* 16.10 (2012). ISSN: 00030007. DOI: 10.1175/2012EI000434.1. arXiv: arXiv:1011.1669v3.

[237] Vliet, J. A. van and Giller, K. E. *Mineral Nutrition of Cocoa: A Review*. 1st ed. Vol. 141. Elsevier Inc., 2017, pp. 185–270. ISBN: 9780128124239. DOI: 10.1016/bs.agron.2016.10.017. URL: http://dx.doi.org/10.1016/bs.agron.2016.10.017.

[238] Vos, Jan and Evers, Jochem B. "Plant structure in crop production: considerations on application of FSPM". In: *Proceedings of the 7th International Conference on Functional-Structural Plant Models*. 2013, pp. 301–303.

[239] Wang, Enli, Robertson, M. J., Hammer, G. L., Carberry, P. S., Holzworth, D., Meinke, H., Chapman, S. C., Hargreaves, J. N.G., Huth, N. I., and McLean, G. "Development of a generic crop model template in the cropping system model APSIM". In: *European Journal of Agronomy*. 2002. DOI: 10.1016/S1161-0301(02)00100-4.

[240] Wang, Wen, Ertsen, Maurits W., Svoboda, Mark D., and Hafeez, Mohsin. *Propagation of drought: From meteorological drought to agricultural and hydrological drought*. 2016. DOI: 10.1155/2016/6547209. arXiv: 6547209.

[241] Wessel, Marius and Quist-Wessel, P. M.Foluke. *Cocoa production in West Africa, a review and analysis of recent developments*. 2015. DOI: 10.1016/j.njas.2015.09.001.

[242] Wickham, Hadley. "The Split-Apply-Combine Strategy for Data Analysis". In: *Journal of Statistical Software* 40.1 (2011), pp. 1–29.

[243] Wickham, Hadley, Averick, Mara, Bryan, Jennifer, Chang, Winston, McGowan, Lucy D'Agostino, François, Romain, Grolemund, Garrett, Hayes, Alex, Henry, Lionel, Hester, Jim, Kuhn, Max, Pedersen, Thomas Lin, Miller, Evan, Bache, Stephan Milton, Müller, Kirill, Ooms, Jeroen, Robinson, David, Seidel, Dana Paige, Spinu, Vitalie, Takahashi, Kohske, Vaughan, Davis, Wilke, Claus, Woo, Kara, and Yutani, Hiroaki. "Welcome to the tidyverse". In: *Journal of Open Source Software* 4.43 (2019), p. 1686. DOI: 10.21105/joss.01686.

[244] Winkler, Andreas, Hurtado, Grecia, and Knoche, Moritz. "Xylem, phloem and transpiration flows in developing strawberries". In: *Scientia Horticulturae* 288 (2021), p. 110305.

[245] Wood, G.A.R. and Lass, R.A. *Cocoa*. 2001, p. 620. ISBN: 978-0632063987. DOI: 10.1002/9780470698983.

[246] Wood, S.N. *Generalized Additive Models: An Introduction with R*. 2nd ed. Chapman and Hall/CRC, 2017.

[247] Yang, Jinyan, Duursma, Remko A, De Kauwe, Martin G, Kumarathunge, Dushan, Jiang, Mingkai, Mahmud, Kashif, Gimeno, Teresa E, Crous, Kristine Y, Ellsworth, David S, Peters, J, et al. "Incorporating non-stomatal limitation improves the performance of leaf and canopy models at high vapour pressure deficit". In: *Tree physiology* 39.12 (2019), pp. 1961–1974.

[248] Yin, Xinyou and Laar, H H Van. *Crop Systems Dynamics: An ecophysiological simulation model for genotype-by-environment interactions*. 2005. ISBN: 9789076998558.

[249] Yin, Xinyou and Struik, Paul C. "Can increased leaf photosynthesis be converted into higher crop mass production? A simulation study for rice using the crop model GECROS". In: *Journal of Experimental Botany* (2017). ISSN: 14602431. DOI: 10.1093/jxb/erx085.

[250] Young, Allen M et al. *The chocolate tree: a natural history of cacao.* Smithsonian Institution Press, 1994.

[251] Yuan, Jin H., Dai, Zhan W., Zhao, Jun Y., and Li, Shao H. "Distribution of newly fixed 14C-photoassimilate under deficit irrigation and half-root stress in peach trees". In: *Plant Science* 177.6 (2009), pp. 691–697. ISSN: 01689452. DOI: 10.1016/j.plantsci.2009.09.006.

[252] Zhang, Jingting, Feng, Liping, Zou, Haiping, and Liu, De Li. "Using ORYZA2000 to model cold rice yield response to climate change in the Heilongjiang province, China". In: *Crop Journal* (2015). ISSN: 22145141. DOI: 10.1016/j.cj.2014.09.005.

[253] Zhou, Shuangxi, Duursma, RA Remko a., Medlyn, Belinda E., Kelly, Jeff W G, and Prentice, I. Colin. "How should we model plant responses to drought? An analysis of stomatal and non-stomatal responses to water stress". In: *Agricultural and Forest ...* 182-183 (2013), pp. 204–214. ISSN: 01681923. DOI: http://dx.doi.org/10.1016/j.agrformet.2013.05.009. URL: http://www.sciencedirect.com/science/article/pii/S0168192313001263%5Cnhttp://dx.doi.org/10.1016/j.agrformet.2013.05.009.

[254] Zhu, Junqi, Werf, Wopke van der, Anten, Niels P.R., Vos, Jan, and Evers, Jochem B. "The contribution of phenotypic plasticity to complementary light capture in plant mixtures". In: *New Phytologist* 207.4 (2015), pp. 1213–1222. ISSN: 14698137. DOI: 10.1111/nph.13416.

[255] Zia, Ahmad, Walker, Berkley J., Oung, Hui Min Olivia, Charuvi, Dana, Jahns, Peter, Cousins, Asaph B., Farrant, Jill M., Reich, Ziv, and Kirchhoff, Helmut. "Protection of the photosynthetic apparatus against dehydration stress in the resurrection plant Craterostigma pumilum". In: *The Plant journal : for cell and molecular biology* 87.6 (2016), pp. 664–680. ISSN: 1365313X. DOI: 10.1111/tpj.13227.

[256] Zuidema, Pieter A and Leffelaar, Peter A. "A physiological production model for cacao: User's manual for CASE2 version 2.2 under FSE Windows". In: February (2002).

[257] Zuidema, Pieter A., Leffelaar, Peter A., Gerritsma, Wouter, Mommer, Liesje, and Anten, Niels P.R. "A physiological production model for cocoa (Theobroma cacao): Model presentation, validation and application". In: *Agricultural Systems* 84.2 (2005), pp. 195–225. ISSN: 0308521X. DOI: 10.1016/j.agsy.2004.06.015.